e-ISSN 2667-9973
p-ISSN 1512-1127

საქართველოს გეოფიზიკური საზოგადოების ჟურნალი

მყარი დედამიწის, ატმოსფეროს, ოკეანისა და კოსმოსური პლაზმის ფიზიკა

ტომი 24 , № 2

JOURNAL OF THE GEORGIAN GEOPHYSICAL SOCIETY

Physics of Solid Earth, Atmosphere, Ocean and Space Plasma

Vol. 24 , № 2

Tbilisi

2021

e-ISSN 2667-9973
p-ISSN 1512-1127

საქართველოს გეოფიზიკური საზოგადოების ჟურნალი

მყარი დედამიწის, ატმოსფეროს, ოკეანისა და კოსმოსური პლაზმის ფიზიკა

ტომი 24 , № 2

JOURNAL OF THE GEORGIAN GEOPHYSICAL SOCIETY

Physics of Solid Earth, Atmosphere, Ocean and Space Plasma

Vol. 24 , № 2

Tbilisi
2021

საქართველოს გეოფიზიკური საზოგადოების ჟურნალი

მყარი დედამიწის, ატმოსფეროს, ოკეანისა და კოსმოსური პლაზმის ფიზიკა

მთავარი რედაქტორი: თ. ჭელიძე

ჟურნალის შინაარსი:

ჟურნალი მოიცავს მყარი დედამიწის, ატმოსფეროს, ოკეანისა და კოსმოსური პლაზმის ფიზიკის ყველა მიმართულებას. ჟურნალში ქვეყნდება: კვლევითი წერილები, მიმოხილვები, მოკლე ინფორმაციები, დისკუსიები, წიგნების მიმოხილვები, განცხადებები, კონფერენციების მოხსენებები.

JOURNAL OF THE GEORGIAN GEOPHYSICAL SOCIETY

Physics of Solid Earth, Atmosphere, Ocean and Space Plasma

Editor-in-chief: T. Chelidze

Scope of the Journal:

The Journal is devoted to all branches of the Physics of Solid Earth, Atmosphere, Ocean and Space Plasma. Types of contributions are: research papers, reviews, short communications, discussions, book reviews, announcements, conference reports.

ЖУРНАЛ ГРУЗИНСКОГО ГЕОФИЗИЧЕСКОГО ОБЩЕСТВА

Физика Твердой Земли, Атмосферы, Океана и Космической Плазмы

Главный редактор: Т. Челидзе

Содержание журнала:

Журнал Грузинского геофизического общества охватывает все направления физики твердой Земли, Атмосферы, Океана и Космической Плазмы. В журнале публикуются научные статьи, обзоры, краткие информации, дискуссии, обозрения книг, объявления, доклады конференций.

მისამართი:

საქართველო, 0160, თბილისი, ალექსიძის ქ. 1, მ. ნოდიას სახ. გეოფიზიკის ინსტიტუტი
ტელ.: 233-28-67; ფაქსი; (995 32 2332867); ელ. ფოსტა: tamaz.chelidze@gmail.com; avtandilamiranashvili@gmail.com;
geophysics.journal@tsu.ge

გამოქვეყნების განრიგი და ხელმოწერა:

გამოიცემა წელიწადში ორჯერ. მყარი ვერსიის წლიური ხელმოწერის ფასია: უცხოელი ხელმომწერისათვის - 30 დოლარი, საქართველოში - 10 ლარი. ხელმოწერის მოთხოვნა უნდა გაიგზავნოს რედაქციის მისამართით. შესაძლებელია უფასო ონლაინ წვდომა:
http://openjournals.gela.org.ge/index.php/GGS

ჟურნალი ინდექსირებულა Google Scholar-ში:
https://scholar.google.com/citations?hl=en&user=pdG-bMAAAAAJ

Address:

M. Nodia Institute of Geophysics, 1 Alexidze Str., 0160 Tbilisi, Georgia
Tel.: 233-28-67; Fax: (99532) 2332867; e-mail: tamaz.chelidze@gmail.com; avtandilamiranashvili@gmail.com;
geophysics.journal@tsu.ge

Publication schedule and subscription information:

The journal is issued twice a year. The subscription price for print version is 30 $ in year.
Subscription orders should be sent to editor's address. Free online access is possible:
http://openjournals.gela.org.ge/index.php/GGS

The journal is indexed in the Google Scholar:
https://scholar.google.com/citations?hl=en&user=pdG-bMAAAAAJ

Адрес:

Грузия, 0160, Тбилиси, ул. Алексидзе, 1. Институт геофизики им. М. З. Нодиа
Тел: 233-28-67; 294-35-91; Fax: (99532)2332867; e-mail: tamaz.chelidze@gmail.com; avtandilamiranashvili@gmail.com;
geophysics.journal@tsu.ge

Порядок издания и условия подписки:

Журнал издается дважды в год. Годовая подписная цена для печатной версии - 30 долларов США. Заявка о подписке высылается в адрес редакции. Имеется бесплатный онлайн доступ
http://openjournals.gela.org.ge/index.php/GGS

Журнал индексирован в Google Scholar:
https://scholar.google.com/citations?hl=en&user=pdG-bMAAAAAJ

This journal uses Open Journal Systems 2.4.8.3, which is open source journal management and publishing software developed, supported, and freely distributed by the Public Knowledge Project under the GNU General Public License.

(http://openjournals.gela.org.ge/index.php?journal=GGS&page=about&op=aboutThisPublishingSystem)

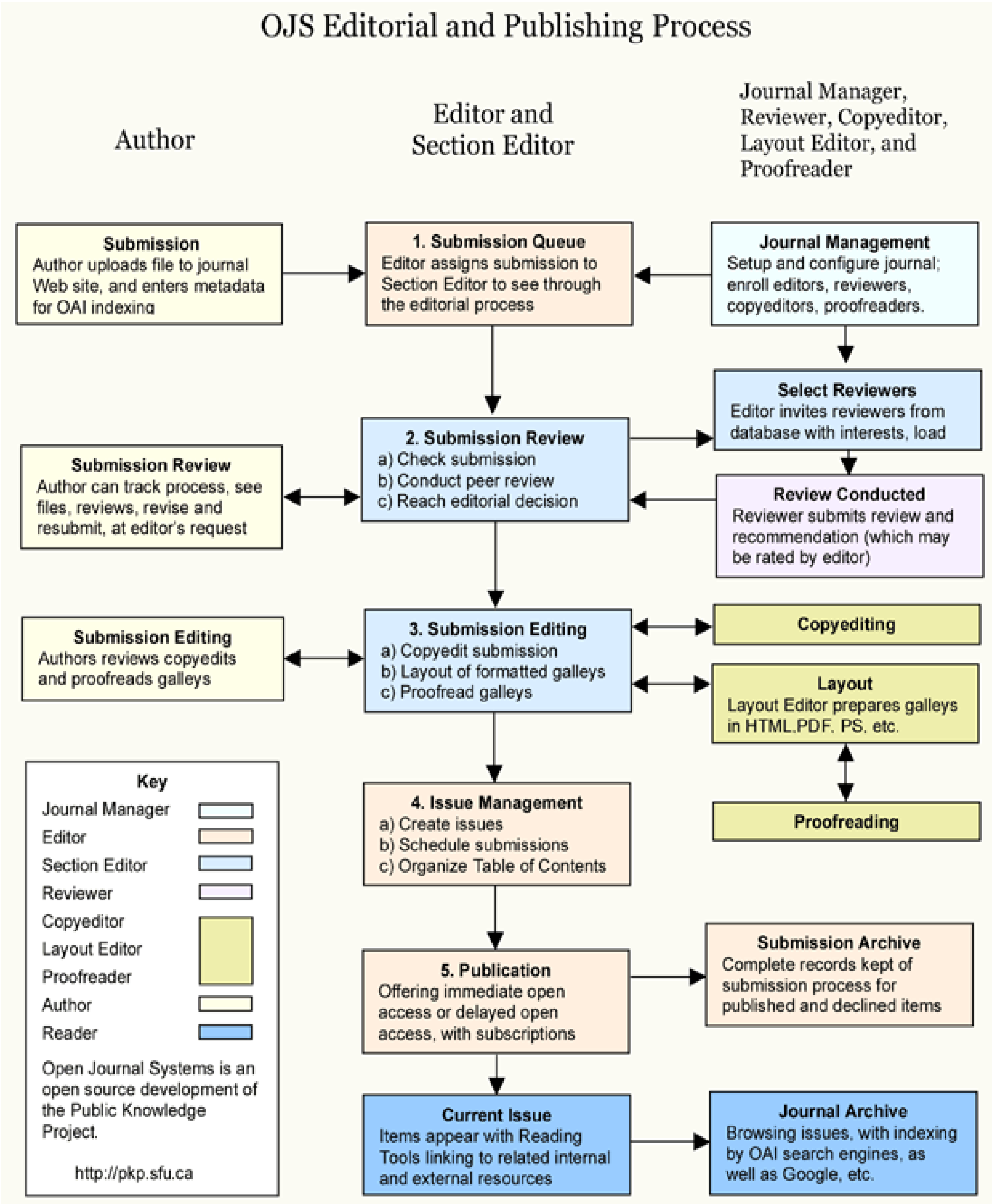

Journal of the Georgian Geophysical Society, e-ISSN: 2667-9973, p-ISSN: 1512-1127
Physics of Solid Earth, Atmosphere, Ocean and Space Plasma, v. 24(2), 2021, pp. 5-21

Development of the Seismic Hazard Zoning Maps and Seismic Building Codes in Georgia (History of Evolution and Critical Analysis)

Otar Sh. Varazanashvili

M. Nodia Institute of Geophysics, Iv. Javakhishvili Tbilisi State University, Georgia
e-mail: otar.varazanashvili@tsu.ge

ABSTRACT

This work reviews the published seismic hazard assessments available for Georgia as well as the seismic loads included in the building code in order to show the state-of-the-art of the seismic hazard assessment studies for the country. The review includes the history and development of seismic hazard assessments and the adoption of seismic building codes in Georgia. All the previous studies were analyzed in order to conclude that a new seismic hazard assessment according to the state-of-the-art is desirable, as well as a change in the hazard description for the actual Georgian building code.

Keywords: *Seismic hazard, seismic zoning, area source model, fault source model, seismic activity, fault slip rates, seismic code.*

1 Introduction

Earthquakes in its destructive effects, fatalities, property damage, take one of the first places among other disasters. Negative consequences of catastrophic earthquakes may be felt for several decades and absorb a significant portion of the national income.

Today scientists and engineers have alot of information about earthquakes, where they are most likely to occur, how deep they originate, and how they affect land. They apply this knowledge to predict where and with what magnitude the next earthquake might occur and for constructing buildings and installations that are considered to be the most resistant to strong earthquakes.

An important step towards reducing human losses and damage caused by strong earthquakes is a reliable seismic hazard zoning, creating seismic norms and the corresponding adequate seismic design. A solution to these and other problems can provide seismic safety of the country.

Reduction of damage in earthquake-prone areas requires modern building codes that should be continuously updated to reflect the improvement in our understanding of the physical effects of earthquake ground shaking on buildings and the increase in the quality and amount of seismological and tectonic studies, among other factors (Sawires et al., [38]).

Seismic zoning (SZ) is a mapping of a seismic hazard at the national level and is based on the study of regional seismicity and major active structures. SZ maps are part of the normative documents providing antiseismic design, land management, economic development, environmental protection and, ultimately, the seismic safety of the country. SZ allocates the homogeneous areas on a map in terms of selected parameters of seismic hazard, it estimates the forecasted maximum seismic impacts in the area in terms of macroseismic intensity, maximum acceleration, etc., the level of which may be exceeded with a given probability over a given time interval.

It should be noted that the current work does not aim at performing seismic hazard analysis in Georgia but rather reviews the history of the development and critical analysis of seismic hazard zoning maps and seismic building codes and main published works regarding this topic.

2 Development of seismic hazard maps in Georgia

Seismic hazard assessment and drawing appropriate zoning maps for Georgia in the past is related with the works on drawing of seismic zoning maps of the former Soviet Union, the part of which was then Georgia.

Historical review of the seismic zoning in former Soviet Union and the methods used are described in many papers (see e.g., Bune et al., [9]; Seismic zoning..., [40]; Mokrushina and Shebalin, [30], [31]; Tsipenyuk, [46]; Gusev, [24]; Gusev, Shumilina, [25]; Ulomov, Shumilina, [47]; ets.).

The first normative map of seismic zoning (Fig. 1) throughout the former Soviet Union (ed. by G. Gorshkov), including the territory of Georgia was published in 1937 (Gorshkov, [19]), and in 1947 was released the new edition of this map (Gorshkov, [20]) and in 1949 was approved as normative (Fig. 2). Both these deterministic seismic zoning maps (SZ-37, SZ-49) in terms of macroseismic intensity were built on the principle of seismic actualism: where have occurred the last strong earthquakes – they will occur in the future.

Fig. 1. SZ-37 map for USSR (editor: G. Gorshkov).

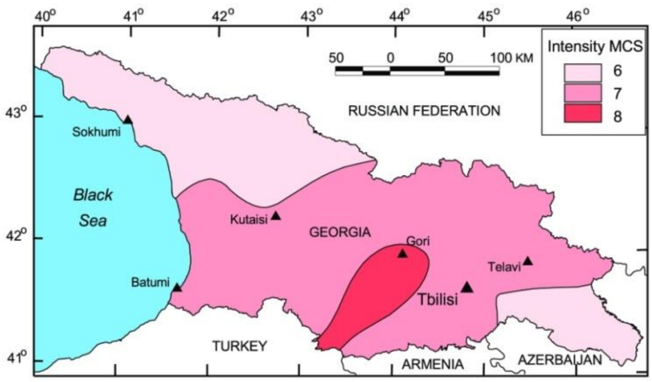

Fig. 2. SZ-49 map for Georgia (editor: G. Gorshkov).

However, in late 40s the foundation of the two-step method had already been laid for estimating seismic hazard with the elements of the prediction (see e.g., Gorshkov, [20]; Medvedev, [28]; Gubin, [22]; Riznichenko, [36]). According to this concept, in the first stage the potential source zones are allocated, and in the second – total shakes generated by them on the earth's surface are calculated. With that, these new methodological approaches have practically not found proper application in all subsequent seismic zoning (SZ) maps - 1957 (eds. by S. Medvedev, B. Petrushevsky, Fig. 3) (Medvedev, [29]), 1968 (ed. C. Medvedev, Fig. 4) (Seismic zoning..., [39]) and 1978 (ed. M. Sadovsky, Fig. 5) (Seismic zoning..., [40]). It should be noted that in the creation of the last two SZ maps the scientists from the former Soviet republics were actively involved (Ulomov, Shumilina, [47]).

The map of 1978 introduced the probabilistic characteristics of recurrence shaking for the first time. In particular indexes 1,2, and 3 near the value of intensity at the same map (e.g., 7_1, 7_2, 7_3) reflect repeatability of seismic shaking once in 100, 1000, and 10 000 years. However, it made a confusion when using maps and seismic risk turned out different in different seismic areas (Gusev, [24]).

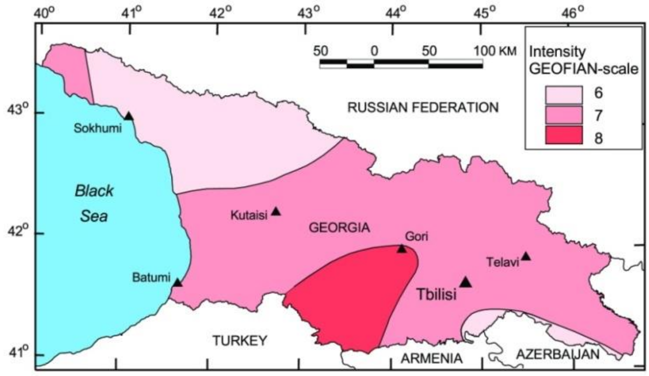

Fig. 3. SZ-57 map for Georgia (editors: S. Medvedev, B. Petrushevsky).

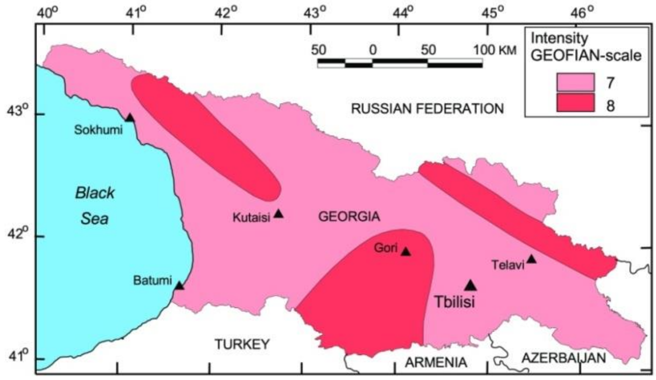

Fig. 4. SZ-68 map for Georgia (authors: Ye. Bius, A. Tskhakaya, M. Rubinshtein)

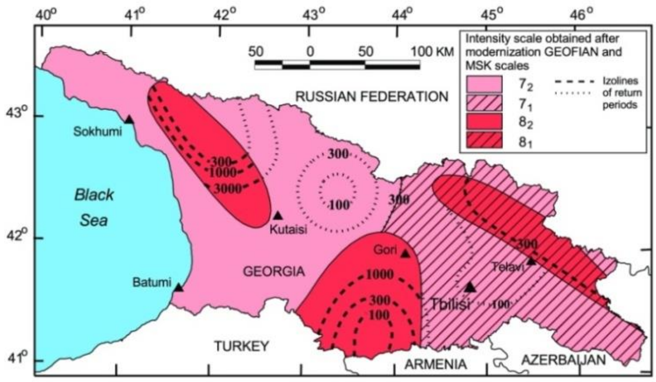

Fig. 5. SZ-78 map for Georgia (authors: I. Aivazishvili, E. Jibladze,
V. Papalashvili, M. Rubinshtein).

With the accumulation of new information about earthquakes and development of the methodology SZ maps periodically have improved, but really they were changed almost after every destructive earthquake, which occurred in zone of SZ map with comparatively lesser predicted intensity. For example, Spitak destructive earthquake in 1988 (in Armenia) with I_o=10 MSK and Racha destructive earthquake in 1991 (in Georgia) with I_o=9 MSK emerged on the SZ-78 map in areas with predictable intensity 7, caused the preparation of a new SZ-91 map for Georgia (ed. M. Aleksidze) (Gotsadze et al., [21]).

SZ-91 map, developed by Georgian scientists (Fig. 6), was the first successful example of the implementation of the two-step method SZ in Georgia. Here the calculation of seismic hazard in terms of macroseismic intensity is really implemented on the basis of constructed seismic sources zones (SSZ) and their parameters. Though this map had some drawbacks: firstly, when editing this small-scale (1:2 500 000) map, under the influence of the recent cases of Spitak and Racha seismic catastrophes, all the zones of expected intensity 7 were removed, which undoubtedly affected its detailing; secondly, the hazard zones were obtained for the events with a mean recurrence of 1000 years, though clear criteria for how this was done was not described; third, these hazard zones, as on all previous SZ maps, were attributed to the average ground conditions, which in its turn, introduced additional uncertainty in the map.

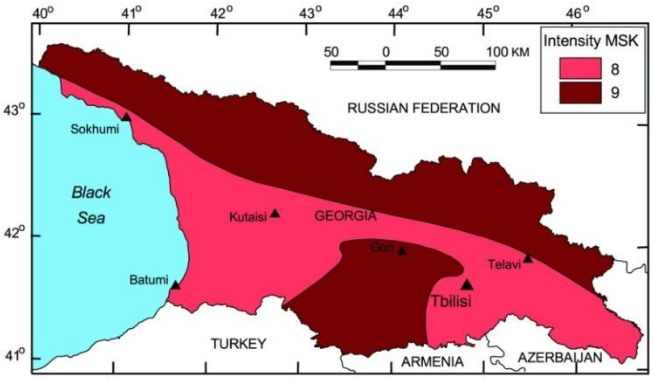

Fig. 6. SZ-91 map for Georgia (authors: O. Varazanashvili, O. Gotsadze, E. Jibladze).

Despite the fact that in the SZ-91 and SZ-78 maps some probabilistic characteristics of shake recurrence were introduced for the first time, they were almost deterministic (as the previous SZ-37, SZ-49, SZ-57, SZ-68 maps). These maps do not give an assessment of seismic hazard in terms of probability of exceedance of a given time interval, the idea of which was most developed in western Europe, the U.S. and Japan, in the works of Cornell,[13] and other scientists (Algermisser, Perkins, [2]; Bender, Perkins, [5]).

Taking into account this and several other reasons (noted above) a set of SZ-99 maps was built in 1999 for Georgia. The maps included 5%, 2% and 1% probability of exceedance in 50 years (ed. I. Gamkrelidze) in terms of macroseismic intensity (scale MSK) and peak ground acceleration (PGA) using well known computer software SEISRISK III (Bender, Perkins, [5]). It was agreed, in terms of macroseismic intensity, to select as normative of the three maps the one that best matched the observed macroseismic data for the entire historical period (Chelidze et al., [10]). Such was SZ-99 map with 2% probability of exceedance, i.e. for the event with a mean recurrence of 2475 years and it, along map with 2% in terms of PGA were presented for approval as a normative (Fig. 7). However, the process of creating new Georgian building codes was stretched in time and approval of SZ-99 map was also postponed. Only 10 years later in 2009, the edited version of this map (SZ-09) was accepted as normative (Fig. 8). Editing mainly touched area of the city Tbilisi where in 2002 there was an earthquake (M_S=4.6, I_o=7.5 MSK) with intensity of at 0.5 MSK higher than it was shown on the SZ-99 map.

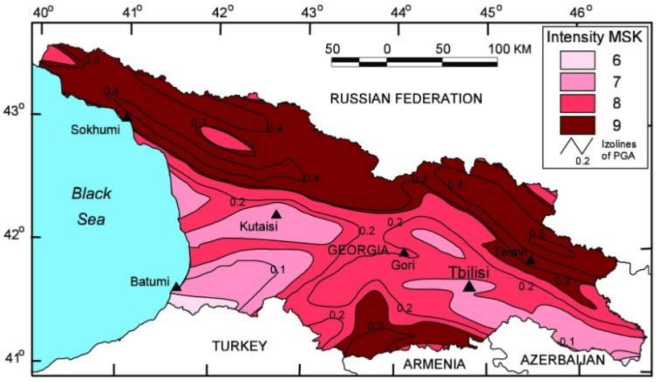

Fig. 7. SZ-99 map for Georgia (authors: T. Chelidze, Z. Javakhishvili et al.)

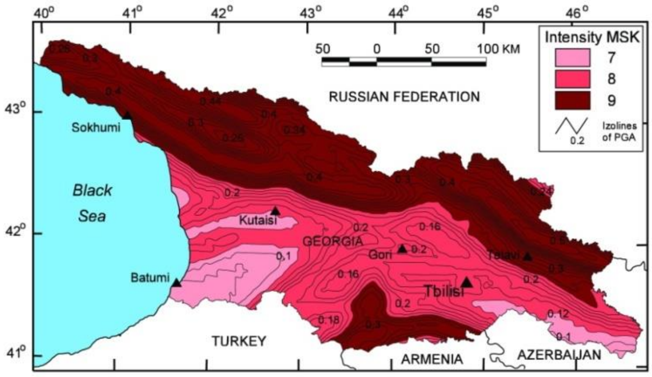

Fig. 8. SZ-09 map for Georgia (editors: I. Gamkrelidze, G. Gabrichidze et al.)

However, further analysis of the SZ-09 map and its comparison with other maps of seismic hazard assessment for Georgia from the international projects and some new works showed significant shortcomings of this map. In particular, a comparison of this map with the maps of seismic hazard calculated in the framework of the project GSHAP (Balassanian et al., [3]), the project EMME,[14] and the work Slejko et al.,[44] showed significant differences in the results of generalization. SZ-09 map shows lower hazard, both on MSK intensity and especially on PGA and these differences are even greater when you consider that the SZ-09 map is built for 2% (average return period of events 2475 years) probability of exceedance in 50 years and the remaining maps for 10% (average return period of events 475 years) probability of exceedance in 50 years. In addition, maps from the GSHAP and Slejko et al.,[44] were calculated by the same software SEISRISK III. These facts suggest that at the time of calculating maps SZ-99 and SZ-09 serious errors were made (Varazanashvili et al., [50]). In addition, the hazard zones on these maps (as in all previous SZ maps), were related to average ground conditions. It became apparent that the present normative seismic hazard map (SZ-09) of Georgia requires urgent recalculation and it is needed to draw a new SZ map in terms of maximum acceleration to rocks.

For the completeness of a historical review of seismic hazard mapping for Georgia below are the maps of seismic hazard (SH), built by individual authors or groups of authors.

Before starting of work on the SZ-78 map, guidelines for seismic zoning were issued (Guidelines..., [23]), where, as an example, a map of the maximum possible shake of southern European part of the former USSR was presented. This map, which also includes the territory of Georgia (Fig. 9), was based on the zones of earthquake source occurrence (ESO) identified through a detailed study of geological, geomorphological and geophysical structural features of the seismogenic zones. Further to move from zones of ESO to shake on the surface, were used data on the average radiuses of isoseists (Guidelines…, [23]; Bune et al., [8]). However, despite widespread use of geological, geomorphological and geophysical data, this deterministic map has turned nonstructural and an obvious tendency to "skip goals" (skip maximum shake with intensity 9).

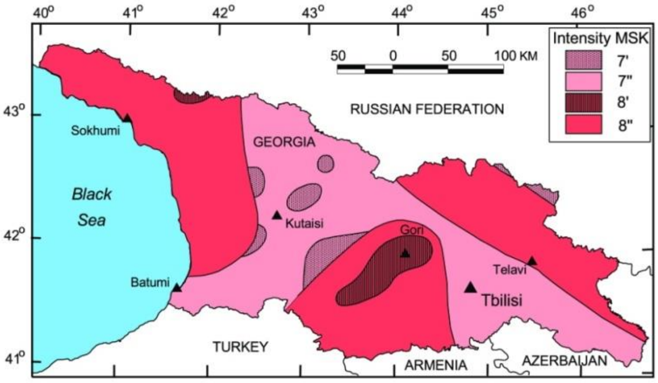

Fig. 9. SH-74 map for Georgia (authors: V. Bune, I. Kirillova et al.).
7´, 8´ – areas intensity seven and eight MSK, where the appropriate intensity shakes in historical time occurred; 7”, 8” – areas of intensity seven and eight MSK with possible manifestation of shakes of appropriate intensity.

In 1995 a paper (Jibladze et al., [26]) was published. It included a SH map for Georgia, built on the basis of the methodology developed in the theory of seismic shakability by Y. Riznichenko (Seismic shakeability..., [41]). The map showed the hazard zones in terms of macroseismic intensity (MSK), indicating in each of them the probability of occurrence in % (or mean return period) 7, 8 and 9 intensity for waiting time 100 years. Difficult-readability was the main drawback of this map. Fig. 10 shows the map of hazard zones in terms of macroseismic intensity only for mean return period T=1000 years.

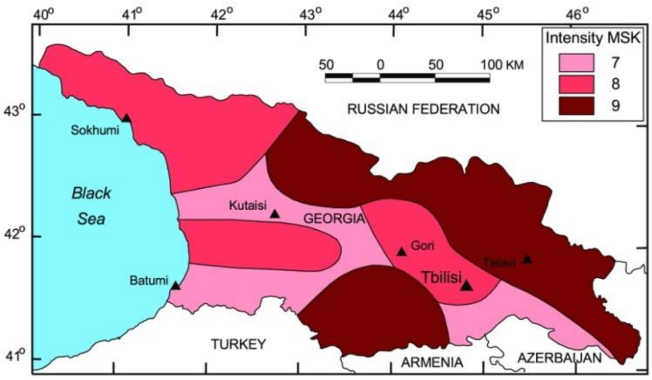

Fig. 10. SH-95 map (for T=1000 years) for Georgia (authors: E. Jibladze, N. Butikashvili et al.)

In 1991-1997, based on the new methodology, a set of probability maps SH-97 (10%, 5%, 1%) of seismic zoning of the Russian Federation and adjacent territory was created. It reflected different degrees of seismic hazard in terms of macroseismic intensity (scale MSK) for average soil conditions (Ulomov, Shumilina, [47]). SH-97 maps have indicated a higher seismic hazard than the one assumed before in many regions of the country and its adjacent areas. However, for the territory of Georgia, this map showed unrealistically large seismic hazard. In particular, as proven (see Varazanashvili et at., [48]), for twenty centuries historical observations of shake with an intensity 9 had covered only 16% of the entire territory of Georgia, where as, for example, on 5% (average return period 1000 years) SH-97 map (Fig. 11) shake with an intensity 9 cover 97% territory of the country, which makes it impossible to consider this set of maps as a normative for Georgia.

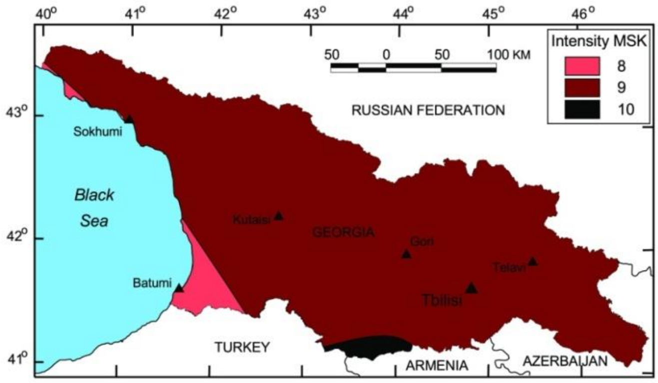

Fig. 11. SH-97 map (5%) for Georgia (authors: V. Ulomov, L. Shumilina et al.).

In 1998 the work on a set of probability (40%, 10%, 5%, 2%, 1%) maps SH-98 (Fig. 12) of seismic hazard for waiting time 50 years in terms of macroseismic intensity (MSK) was completed (Varazanashvili, [48]). Was used the original method of estimating SH, based on models of seismic source zones (SSZ), segments of structural seismic activity and isoseists. Analysis of the obtained maps showed the following: a) The reliability of the results of seismic hazard assessments (both the form and the value of the hazard zones) is more dependent on the reality degree of the SSZ models and their parameters; b) Allocation of segments of structural activity along the SSZ according to data of time interval of 100 years does not give an opportunity to fully reveal the level of seismic activity of SSZ and also solve the problem of calm areas that reduces the value of predicted seismic hazard. Therefore, in the future, instead of seismic activity we should adopt the so-called conditional activity, which besides the number of earthquakes also uses data of modern tectonic movement obtained from GPS network (unfortunately for Georgia full GPS data is not yet available). The main drawback of this work was that the used method was not formalized and published. Moreover SH zones of the set maps were attributed to the average soil conditions.

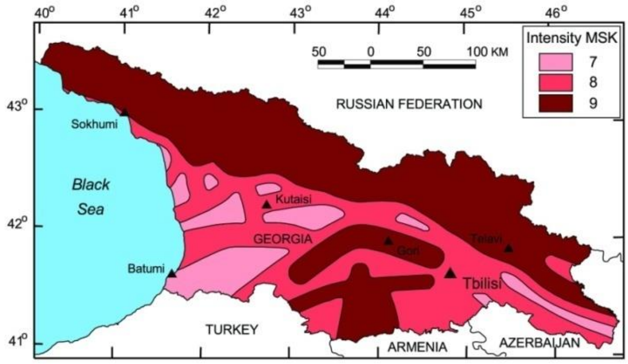

Fig. 12. SH-98 map (2%) for Georgia (author: O. Varazanashvili).

In 1999, SH-99 map of Georgia was published (Fig. 13). It was based on a study of the block structure of the lithosphere of the Caucasus and allocation seismogenic faults (Sikharulidze et al., [43]). Unfortunately, this deterministic SH map for medium soil conditions to a greater extent was committed to the principle of seismic actualism.

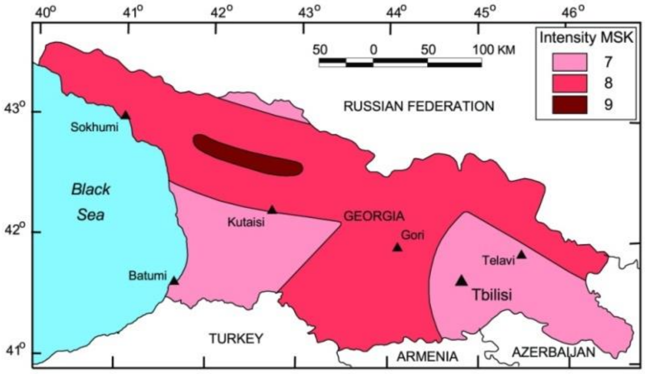

Fig. 13. SH-99 map for Georgia (authors: D. Sikharulidze, V. Papalashvili et al.).

The Global Seismic Hazard Assessment Program (GSHAP) was carried out between 1992-1998. The GSHAP Global Seismic Hazard Map has been compiled by joining the regional maps produced for different GSHAP regions and test areas. It depicted the global seismic hazard as Peak Ground Acceleration (PGA) with a 10% chance of exceedance in 50 years, corresponding to a return period of 475 years (Giardini et al., [18]).

The GSHAP CAUCAS test area was established with the goal of improving global standards in seismic hazard assessment in the Caucasus and included the entire territory of Georgia, Armenia, Azerbaijan, the North Caucasus and Kopetdag. The mapping of probabilistic seismic hazard was implemented on the basis of areal Seismic Source Zones (SSZ) model, compiled according to the lineament model of the region. Maximum magnitudes of SSZs were mainly defined by magnitude of a corresponding seismotectonic structure depending on the magnitude of the strongest earthquake of that zone. In the seismic hazard assessment, the ground motion attenuation model of Joyner and Boore [27] was adopted and calculation of accelerations was done using SElSRlSK III by Bender and Perkins [5], using only the areal homogeneous source zone model. Two seismic hazard maps for rocks and for the reference 475 years return period and for standard logarithm deviation 0.5 and 0.6 were computed (Balassanian et al., [3]). Fig. 14 shows the SO-99 Map for Georgia under the GSHAP project (standard deviation 0.5). As can be seen in Fig. 14, the seismic hazard level in the Greater Caucasus is less than in southern Georgia, which contradicts the observed historical seismicity. In addition, the use of only one ground motion attenuation equation reduces the calculated seismic hazard value and precision of their assessment for the region.

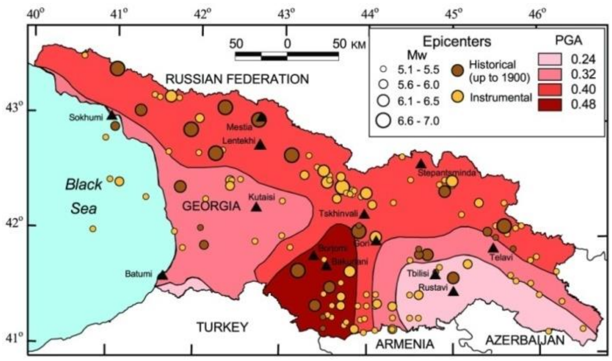

Fig.14. SH-99 map for Georgia from GSHAP project (authors: D. Giardini, G. Gruntal et al.).

The EMME (Earthquake Model of Middle East) Project was established in 2009 and was active until 2015. It was made with the objective of developing a unified framework to evaluate the seismic hazard and the associated risks in one of the most seismically active and vulnerable regions of the world: the Middle East and the Caucasus (Erdik et al., [15], [16]). A comparison of the GSHAP seismic hazard map (representing a previous generation of regional hazard studies (Giardini et al., [18]) with an adequate EMME map (Sesetyan et al., [42]) reveals considerable differences and an increased level of detailing in the resulting seismic hazard distribution on the new generation map. First an enhanced understanding of seismic activity parameters based on the accumulated data in the recent decades and improvement of hazard modelling tools induced changes in the hazard estimate levels and distribution throughout the region and second, an increased level of detail is obtained mainly due to the incorporation of the fault source model in the EMME maps. Active faults provide a longer recurrence interval for the large earthquakes when slip-rates are available. On the other hand one drawback of the present model is that, sliding speeds are sometimes determined very approximately which may result in some cases in hazard levels lower or larger than anticipated. Given the fact that a fault source model cannot be considered fully complete, it is subject to further improvement as more data become available.

OpenQuake hazard engine (Pagani et al. [35]) is the PSHA software used for hazard calculation within the EMME project. The EMME project delivered a reference, homogeneous probabilistic seismic hazard model for the sub-region under study. Being a reference model implies that it can be different than the national seismic hazard models, but may serve as a reference and basis for updating national scale hazard models. Today, the EMME project delivers, fully harmonized datasets and models align with the high-standards adopted and promoted by Global Earthquake Model - GEM (Sesetyan et al., [42]).

Fig. 15 shows the SH-2014 Map for Georgia constructed within the framework of the EMME project. To compare the predicted PGA values with the observed seismicity, the epicenters of strong earthquakes (M_w> 5) for the entire historical period are plotted on the map. As can be seen on the map, almost all epicenters of strong earthquakes are located in the PGA>0.25 g zones, which is a good result for predictive maps and excludes an error such as missing a target.

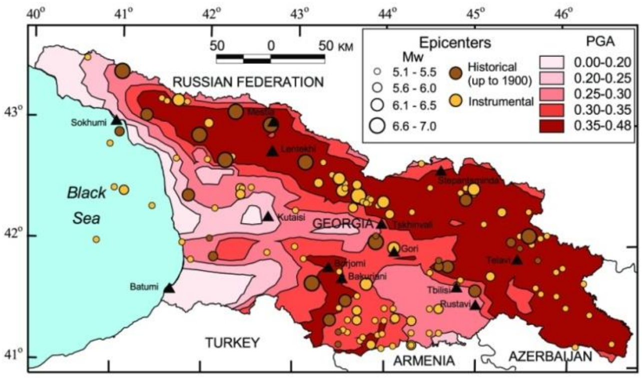

Fig.15. SH-2019 map for Georgia from EMME project (authors: L. Danciu, N. Tsereteli et al.).

In 2019, Lawrence Livermore National Laboratory technical report (Onur et al., [33]) was published, followed by an article (Onur et al., [34]), which outlined the improvements made to the earthquake catalog in Georgia using legacy data and the new hazard assessment based on this improved dataset. Using these improvements in the earthquake catalog in conjunction with new research on active tectonics and hazard analysis concepts, PSHA was conducted to generate new seismic hazard maps for Georgia. PSHA OpenQuake software was used to calculate the hazard (Pagani et al., [35]). According to the authors of these works a subset of active faults with relatively reliable data was selected for the PSHA study, and seismic hazard from the rest of the faults as well as diffuse seismicity were represented using area sources. Maximum magnitudes were assigned to each source zone based on various considerations. Generally, no zone was assigned a maximum magnitude lower than Mw 7.2., and for the study of the recurrence parameters of source zones, preference was given to the non-declustered catalog. Fig. 16 represents the SH-2020 map for Georgia for the peak ground acceleration with a 10% chance of exceedance in 50 years by Onur et al.,[33], [34]. The main drawback of this seismic hazard map (like all other hazard maps by Onur et al.,[33], [34] is that to the west of the meridian passing approximately through the cities of Kutaisi and

Mestia, the seismic hazard fall sharply compared to other parts of the map. The statement that the PSHA results in these works generally reflect the change in rate of seismic activity from west to east is wrong. This is evidenced by the history of the development of SZ in Georgia. In particular, in the first half of the last century, there was an opinion among the scientific community that seismic activity in Western Georgia is lower than in Eastern Georgia, and this was reflected in the corresponding maps of SZ (see SZ-37, SZ-49, SZ-57). Since 1948, after more than ten medium and strong earthquakes with magnitudes Mw 4.5-6.4 occurred within 15 years, the situation changed and this was reflected in subsequent maps of SZ (see SZ-78, SZ-91, etc.). It turned out that the seismicity of Western Georgia is characterized by earthquake swarms and temporarily calm areas (especially in the western part of the Greater Caucasus), and not to low activity compared to the eastern part of the country. This is also evidenced by the historical seismicity (up to 1900) of Georgia (see EMME [14], Varazanashvili et al. [49], [51]), which apparently was not taken into account when carrying out PSHA in the above-mentioned works of Onur et al. [33], [34].The improved catalog of earthquakes in Georgia, which is much talked about in these works, has not been published anywhere and is not available for analysis.

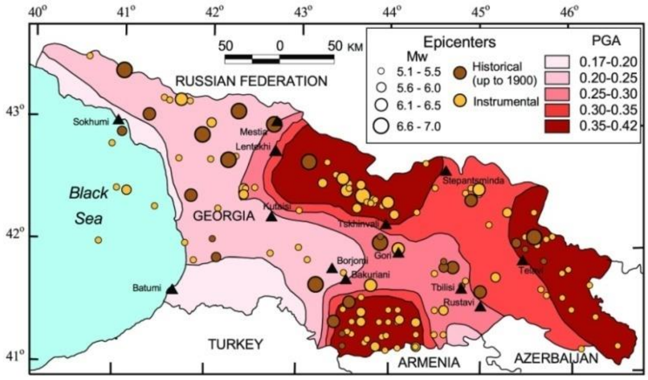

Fig.16. SH-2020 map for Georgia (authors: T. Onur, R. Gok et al.).

As mentioned above, the EMME project delivered a homogeneous probabilistic seismic hazard model for the Middle East and Caucasus sub-region, which may serve as a reference and basis for updating national scale hazard models. The national, updated, probabilistic seismic hazard model for Georgia was presented in 2020 by Tsereteli et al. [45], obtained leveraging from the experience in the EMME project. Input seismic data were homogenised using national data and seismic source models were specified at national level. Georgia Seismic Hazard Model 2020 (SH-2020) reflects the latest scientific findings, i.e. principle of stationary seismicity, active faults and uncertainties quantification and updated datasets i.e. updated earthquake catalogue, revised estimates of the historical catalogue, a homogeneous magnitude scale, improved fault source models and the area source models (for more details see Tsereteli et al. [45]. The drawbacks of this hazard model are related to issues that are common for all modern maps of this type. In particular, a big step forward in the improvement of the PSHA methodology was the use, in conjunction with seismic activity (giving a short-term picture of activity), the sliding velocity of faults (giving a long-term picture of activity). They complement each other well. However, future efforts should be made in the direction of improving estimates the fault slip rates of the region, by incorporating most recent studies. In the process of updating and homogenizing the earthquake catalog, conversion formulas of different magnitudes are used, the effects of their use remains to be studied in future efforts. Limited data on strong ground motion for Georgia and the whole Caucasus have not yet allowed the inclusion of any local model for Georgia in the Logical Tree scheme of ground motion hazard assessments, so the creation of such a model will be one of the subjects of future updates. Fig. 17 shows the SH-2020 map for Georgia by Tsereteli et al. [45], the quality of the forecast pattern of the seismic hazard of a region is determined by how adequate it is to the observed seismicity for the entire historical and modern period. For this, all zones with PGA≥0.32 g from the SO-2020 map (Fig. 17) were compared with the zones with MSK intensity I≥8 from the distribution map of the maximum observed MSK intensity in Georgia (Fig. 18). The results of alignment and comparison of the corresponding zones showed that 75% of the zone with PGA≥0.32 g, 80% -PGA≥0.43 g and 90% - PGA≥0.53 cover zones with I≥8, which is a good result if we take into account the accuracy of delineation the boundaries of zones on these maps and testifies to the adequacy of this hazard forecast map.

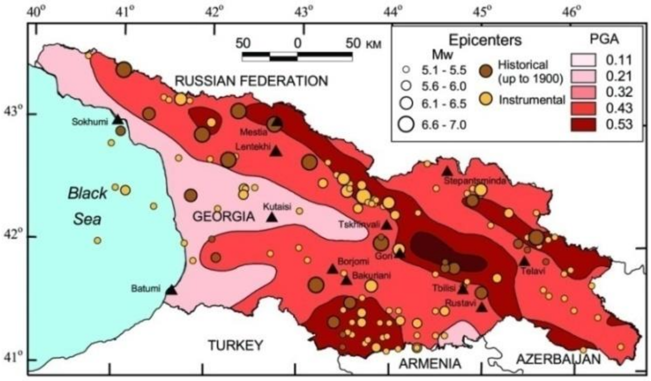

Fig.17. SH-2021 map for Georgia (authors: N. Tsereteli, L. Danciu et al.).

Fig. 18 shows a map of the distribution of maximum MSK intensity (7, 8, and 9 points MSK) from strong earthquake on Georgian territory throughout the historical past. Based on the analysis of these data for twenty centuries it is possible do several important conclusions:

- The area of the region encompassed by intensity 9 MSK for each one out of 19 centuries A.D. the average is ~500 km^2, which practically coincides with the total area of intensity 9 MSK of the well-studied earthquakes of the 20th century. This in its turn means that during 20 centuries only a few of strong (M_S>6.5, I≥9) seismic events have been missed.
- For the area covered by 8 MSK intensity there is quite a different picture. In particular, for each one out of 19 centuries the area of this intensity is on average 1.5 times less than the well-delineated area with an intensity 8 MSK of 20th century, and it means that many historical earthquakes with such intensity are still not detected.
- The area covered by intensity 7 MSK is the background to the whole territory of Georgia and if we take into account the results presented in the previous paragraph, a large part of this area must have intensity 8 MSK.

In addition, on this map, between two large areas of the axial part and the southern slope of the Greater Caucasus thereis clearly visible seismic gap, which was partially filled in 1991 by the strongest Racha earthquake with intensity 9 MSK and its strong aftershocks with an intensity 8 MSK (Varazanashvili et al., [49]).

It should be noted that for Georgia, rigorous statistical validation of probabilistically estimated ground motion is very difficult to take nowadays due to short observational time of the main input datasets (i.e. although the instrumental earthquake catalogue covers about 100 years, strong ground motion data have been recorded only in the last decades, Tsereteli et al., [45]). Therefore, under the conditions of Georgia, the observed maximum macroseismic field shown in Fig. 18 is practically the only controlling factor for predictive assessments of seismic hazard.

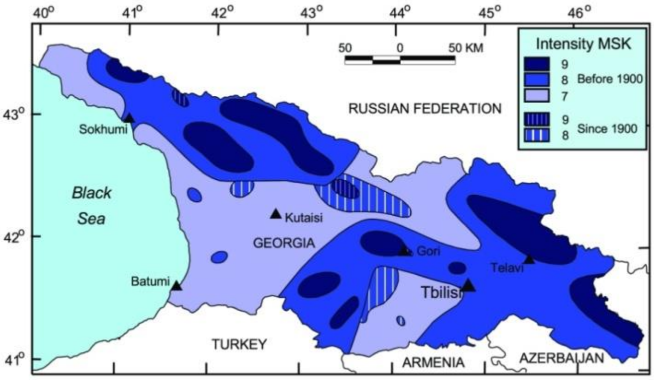

Fig. 18. Map of the total maximum MSK intensity distribution in Georgia during the entire historical past (author: O. Varazanashvili).

3 Development of building codes in Georgia

The history of the creation of building codes in Georgia is closely related to their development from the beginning in the Russian Empire (before 1918), and then in the former Soviet Union (1921-1990), a part of which Georgia was for that time. Since 1991, Georgia has become an independent country and has intensively been developing its national building codes.

More specifically, we can say that in the first quarter of the 20th century in the Russian Empire and in the USSR, the so-called “Established Norm” (Fig. 19), which in modern language is called a collection of construction resource estimates and which represented the construction technologies of the beginning of the last century. In 1927-1930, due to obsolescence, the “Established Norm” was replaced by the "Set of Production Building Codes" drawn up by the USSR Construction Commission (Abramova, [1]). It should be noted that seismic loads did not appear in both of these collections of normative documents.

Fig. 19. Established Norm of the 1918 issue.

In 1937, the first seismic zoning map of the USSR (SZ-37) was prepared, which was included in the official normative publication - “Rules for Anti-seismic Construction” (Rules ..., [37]). The next new seismic zoning map appeared in 1949 (SZ-49), and the first edition of building codes and regulations (SNiP) was put into effect in 1955 (Building codes ..., [6]). Then, in 1957, after the creation of a new map of seismic zoning of the USSR (SZ-57), codes appeared: SN 8-57 (Norms and rules ..., [32]) and SNiP II-A.12-62 (Building codes ..., [7]) (Fig. 20), in which the intensity of the earthquake in the area or at the construction site was taken according to the GEOFIAN intensity scale (Barosh, [4]).

Fig. 20. SNiP II-A.12-62 of the 1963 issue.

Since seismic zoning maps (SZ) are an integral part of regulatory documents that ensure earthquake-resistant construction, updated seismic codes were often published after the appearance of new SZ maps, for example: SZ-68 - SNiP II-A.12-69 * (Construction norms ..., [11]), SZ-78 - SNiP II-7-81 * (Construction norms ..., [12]).It should be noted that in SNiP II-A.12-69 * the seismicity of the construction site was assessed according to the GEOFIAN scale, and in SNiP II-7-81 * - according to the scale obtained after the modernization of the GEOFIAN and MSK-64 scales. The first map of the SZ of independent Georgia was compiled in 1991, but it was included in the structure of the previous codes - SNiP II-7-81*. Only in 2010 it became possible to create new seismic codes for Georgia PN 01.01-09 (Georgian building code,]17]), which included an edited version of the 1999 SZ-99 map (rather outdated), and seismicity was given using the macroseismic intensity on the MSK-64 scale and peak ground accelerations. Today there is a need for a new map of SZ and new seismic code, closest to the European Codes (EC8).

Conclusions

As a result of more than 80 years of research in the field of seismic hazard zoning, the concept of seismic hazard in Georgia has changed significantly and the level of understanding of the hazard model has improved radically. This is evidenced by the entire history of the development of seismic zoning, presented above. Suffice it to say that deterministic assessments in terms of macroseismic intensity for average soil conditions were taken as the calculated hazard for Georgia in the 30s to the beginning of the 90s, and probabilistic hazard estimates are now accepted in terms of peak and spectral ground accelerations for rock.

During this period, the concept and configuration of seismic source models changed significantly, from simple seismically homogeneous are sources to complex “dual” source models: the areal source model and the fault source model, which successfully complement each other. A big step forward in improving the hazard assessment methodology was the combined use of seismic activity and fault slip rates, use of a logic tree scheme in hazard calculations, etc.

As for the ground motion model for Georgia, it was represented by a set of regional or global ground motion prediction models, selected according to the tectonic zoning scheme, as the limited data on strong ground motion for Georgia did not allow them to be included in the hazard assessment logical tree as a local model.

The seismic hazard model and corresponding zoning maps are an integral part of regulatory documents that ensure earthquake-resistant construction, so updated seismic codes are often published after the appearance of new seismic zoning maps. Today there is a need for a new normative map of seismic zoning for Georgia and for new building codes close to the European ones.

Thus, the efforts of researchers in the field of seismology, geology, geophysics and engineering, which created various models of seismic hazard and the corresponding building codes, analyzed the results of their application, studied the properties of earthquake sources and surroundings, as well as the spatial structure of seismicity, led to great progress in understanding the nature of seismic hazard and earthquake-resistant construction on the territory of Georgia. It should be admitted that the degree of knowledge of the danger of Georgian earthquakes is insufficient. Much work remains to be done in order to provide the engineering community and government agencies with a fully reliable performance of potentially destructive ground motion.

References

[1] Abramova M. Yu. Normative and technical documentation: from the sources to the present. Presentation of books from the Fund of FBU "CSTB CIA". Moscow, 2012, 14 p. http://www.cntb-sa.ru/index.php/home/36?task=view

[2] Algermisser S. T., Perkins D. M. A Probabilistic Estimate of Maximum Acceleration in Rock in the Contiguous United States. Open File Report, U.S. Geological Survey, Denver, 1976, pp. 76-416

[3] Balassanian S., Ashirov T., Chelidze T., Gassanov A., Kondorskaya N., Molchan G., Pustovitenko B., Trifonov V., Ulomov V., Giardini D., Erdik M., Ghafory-Ashtiany M., Gru¨nthal G., Mayer-Rosa D., Schenk V., Stucch, M. Seismic hazard assessment for the caucasus test area. Annali di Geof, 42(6), 1999, pp. 1139-1164.

[4] Barosh, P. J. Use of Seismic Intensity data to predict the effects of farthquakes and underground nuclear explosions in various geologic settings. Geological survey bulletin 1279. United States Government Printing Office, Washington, 1969, pp. 1-92.

[5] Bender B., Perkins D. SEISRISK III: a computer program for seismic hazard estimation, U.S. Geol. Surv. Bull., 1772,1987, 48.

[6] Building codes and regulations, part I, II, III, IV. Norms of building design. Gosstroyizdat Publ. House, Moscow, 1954.

[7] Building codes and rules, Part II, Section A. Chapter 12. Construction in seismic regions, design standards SNiP II-A.12-62. Gosstroyizdat Publ. House, Moscow, 1963, 55 p.

[8] Bune V. I., Kirilova I. V., Ananin I. V. et al. Experience of evaluation of seismic hazard in the example of the Caucasus. Seismic investigations for construction. Rroblems of Earthquakes Engineering, 14, 1971, pp. 3-124.

[9] Bune V. I., Medvedev S. V., Risnichenko Yu. V., Shebalin N. V. Successes and hopes seismic zoning of the USSR. Izvestiya, Academy of Sciences, USSR.: Physics of the solid earth, 10, 1974, pp. 95-102.

[10] Chelidze T., Javakhishvili Z., Varazanashvili O., Elashvili M., Kolesnikov Yu., Godoladze T., Butikashvili N., Ghlonti E. Seismic hazard assessment of Georgia (probabilistic approach). Institute of Geophysics, Academy of Sciences of Georgia, 2012, 15 p. http://ebookbrowse.com/seismic-hazard-assessment-of-georgia-pdf-d376754175

[11] Construction norms and rules SNiP II-A.12-69*. Norms of Design, part II. Construction in seismic regions, chapter 12. Stroyizdat Publ. House, Moscow, 1977, 69 p.

[12] Construction norms and rules SNiP II-7-81. Norms of Design, part II. Construction in seismic regions, chapter 7. Stroyizdat Publ. House, Moscow, 1982, 48 p.

[13] Cornell C. A. Engineering seismic risk analysis, Bull. Seism. Soc. Am., 58, 1968, pp. 1583-1606.

[14] EMME. Earthquake Model of Middle East: Hazard, Risk Assessment, Economics and Mitigation. Brochure. Istanbul, 2013, 38 p.

[15] Erdik M., Sesetyan K., Demircioglu M. B,, Tuzun C., Giardini D., Gulen L., Akkar S., Zare M. Assessment of seismic hazard in the Middle East and Caucasus: EMME (Earthquake Model of Middle East) Project. Proc. 15WCEE, 16, 2012a, pp. 12371-12380.

[16] Erdik M., Sesetyan K., Demircioglu M. B., Tuzun C., Giardini D., Mansouri B., Lodi S. H., Al-Nimry H., Tseretelli N., Hovhannisyan G., Chrysostomou C. Z., El-Khoury R., Helou R. Seismic risk assessment

in the Middle East EMME (Earthquake Model of Middle East) Project. Proc. 15WCEE, 16, 2012b, pp. 12557-12566.
[17] Georgian building code (PN 01.01-09). Earthquake Engineering.Tbilisi, 2009, 166 p. https://www.matsne.gov.ge/ka/document/view/86596
[18] Giardini D., Grunthal G., Shedlock K.M., Zhang P. The GSHAP Global Seismic Hazard Map. Annali di Geofisica, vol. 42, n. 6., 4999, pp. 1225-1230.
[19] Gorshkov G. P. On the seismic zoning of Middle Asia. Proceedings of Inst. Seismol. AS USSR, № 79(6), 1938, pp. 67-71.
[20] Gorshkov G. P. Scheme of seismic zoning of the USSR. Jubilee Collection, part I. Publ. by AS USSR, 1947, 454 p.
[21] Gotsadze O., Varazanashvili O., Jibladze E. Engineering analysis of the implications of the 1991 Racha earthquake in Georgia. Metsniereba Publ. House, Tbilisi, 1996, 236 p.
[22] Gubin I. E. Seismotectonic method of seismic zoning. Proceedings of Geophys. Inst. AS USSR, № 13 (140), 1950.
[23] Guidelines for Seismic zoning of the USSR territory. Bune, V. I. (Ed). IPSE of AS USSR, Moscow, 1974, 195 p.
[24] Gusev A. A. About the need to adjust the documents regulating anti-seismic measures in the USSR. Integrated assessment of seismic hazard. Problems of Earthquakes Engineering, 32, 1991, pp. 147-160.
[25] Gusev A. A., Shumilina L. S. Some Problems Concerning the Methods of General Seismic Zoning, Seismichnost i seismicheskoe raionirovanie Severnoi Evrazii (Seismicity and Seismic Zoning of North Eurasia), Moscow: OIFZ RAN, issues 2-3, 1995, pp. 289-300.
[26] Jibladze E., Butikashvil, N., Tsereteli N., Seismic regime, seismic hazard and seismotectonic deformation in the Caucasus, Institute of Geophysics, Georgian Academy of Sciences Press, Tbilisi, 1995, 112 p.
[27] Joyner W.B., Boore D.M. Methods of regression analysis of strong motion data, Bull. Seismol. Soc. Am., 83, 1993, pp. 469-487.
[28] Medvedev S.V. On the problem of accounting of seismic activity of area at construction. Proceedings of Inst. Seismol. AS USSR, №119, 1947.
[29] Medvedev S.V. Seismic zoning map of the USSR territory 1957. Proceedings of Inst. Phys. Solid Earth of Acad. Sci. USSR. №1(158), 1958, pp. 3-28.
[30] Mokrushina N.G., Shebalin N.V. Assessment of the quality of seats strong shakinges on seismic zoning map of the USSR. Rroblems of Earthquakes Engineering, 23, 1982, pp. 97-113.
[31] Mokrushina N.G., Shebalin N.V. Assessment of the quality of seats strong shakinges on seismic zoning map of the USSR. Part II. Map GSZ-78. Integrated assessment of seismic hazard. Rroblems of Earthquakes Engineering, 31, 1991, pp. 122-125.
[32] Norms and rules of construction in seismic regions (SN 8-57). Gosstroyizdat Publ. House, Moscow, 1957, 104 p.
[33] Onur T., Go, R. et al. Probabilistic seismic hazard assessment for Georgia. Technical report LLNL (Lawrence Livermore National Lab.)-TR-771451. OSTI (The Office of Scientific and Technical Information), 2019, Identifier: 963125.
[34] Onur T., Gok R., Godoladze T., Gunia I., Boichenko G., Buzaladze A., Tumanova N., Dzmanashvili M., Sukhishvili L., Javakishvili Z., Cowgill E., Bondár I., Yetirmishli G. Probabilistic Seismic Hazard Assessment Using Legacy Data in Georgia. Seismological Research Letters, 91 (3), 2020, pp. 1500-1517. doi.org/10.1785/0220190331
[35] Pagani M., Monelli D., Weatherill G., Danciu L., Crowley H., Silva V., Henshaw P., Butler L., Nastasi M., Panzeri L., Simionato M., Vigano D. Open Quake Engine: an Open Hazard (and Risk) Software for the Global Earthquake Model, Seismol Res Lett, 85, 2014, pp. 692–702.
[36] Riznichenko Y. V. From the activity of earthquake sources to the shakeability of earth's surface, Izvestiya, Academy of Sciences, USSR.: Physics of the solid earth, №11, 1965, pp. 1-12.

[37] Rules of antiseismic construction. Gosstroyizdat Pub. House, Moscow, 1937, 28 p.
[38] Sawires R.. Peláez J. A., Fat-Helbary R.E., Ibrahim H.A. A review of seismic hazard assessment studies and hazard description in the building codes for Egypt. Acta Geodaetica et Geophysica 51, 2016, pp. 151-180. DOI: 10.1007/s40328-015-0117-5
[39] Seismic Zoning of the USSR. Nauka Publ. House, Moscow, 1968, 476 p.
[40] Seismic Zoning of the USSR Territory: Underlying Methods and Regional Legend of the Map of 1978. Nauka Publ. House, Moscow, 1980, 307 p.
[41] Seismic shakeability of the USSR Territory. Risnichenko, Yu. V. (Ed.). Nauka Publ. House, Moscow, 1979, 192 p.
[42] Sesetyan K., Danciu L., Demircioglu M.B., Giardini D., Erdik M., Akkar S., Gülen L., Zare M., Adamia Sh., Ansar, A., Arakelyan A., Askan A., Avanesyan M., Babayan H., Chelidze T., Durgaryan R., Elias A., Hamzehloo H., Hessami Kh., Kalafat D., Kale Ö., Karakhanyan A., Khan M. A., Mamadli T., Al-Qaryouti M., Sayab M., Tsereteli N., Utkucu M., Varazanashvili O., Waseem M., Yalcin H., Yılmaz M.T. The 2014 Seismic hazard model of the Middle East: overview and results. Bulletin of Earthquake Engineering, 16(8):3535-3566, 2018. https://doi.org/10.1007/s10518-018-0346-4
[43] Sikharulidze D. I., Papalashvili V. G., Tutberidze N. P., Shengelia I. S. Methodological framework for the assessment of seismic hazard and seismic zoning map of the territory of Georgia. Seismic metods and results of investigation the block structure and the dynamic state of the litosphere. Tbilisi,1999, pp. 69-91.
[44] Slejko D., Javakhishvili Z., Rebez A., Santulin M. Elashvili, M, Bragato, P.L. Godoladze T., Garcia J. Seismic hazard assessment for the Tbilisi test area (eastern Georgia). Instituto Nazionale di Oceanografia e di Geofosoca Sperimentale/Triesta (italy), vol. 49, 2008, pp. 37-58.
[45] Tsereteli N., Danciu L., Varazanashvili O., Sesetyan K., Qajaia L., Sharia T., Svanadze D., Khvedelidze I. The 2020 National Seismic Hazard Model for Georgia (Sakartvelo). Building Knowledge for Geohazard Assessment and Management in the Caucasus and other Orogenic Regions (eds. F. L. Bonali, F. P. Mariotto, N.Tsereteli). Springer. Part of the NATO Science for Peace and Security Series C: Environmental Security book series (NAPSC). Chapter 8, 2021, pp. 131-168.
[46] Tsipenyuk I. F. Damageability and reliability of large-panel buildings under seismic actions. Investigations on seismic hazard. Rroblems of Earthquakes Engineering, 29, 1988, pp. 141-153.
[47] Ulomov V.I., Shumilina L.S. Komplekt kart obshchego seismicheskogo raionirovaniya territorii Rossiiskoi Federatsii OSR-97. Masshtab 1:8000000. Obyasnitelnaya zapiska i spisok gorodov i naselennykh punktov, raspolozhennykh v seismoopasnykh raionakh (A Set of 1:8000000 General Seismic Zoning Maps of the Russian Federation (GSZ-97): Explanatory Note and the List of Towns and Settlements Located in Regions of Seismic Hazard), Moscow: OIFZ, 1999.
[48] Varazanashvili O. Seismic hasard assessment of Georgia by deterministic and probabilistic methods. Journal of Georgian Geophysical Society (A), vol. 4, 1999, pp. 35-45.
[49] Varazanashvili O., Tsereteli N., Tsereteli E. Historical earthquakes in Georgia (up to 1900): source analysis and catalogue compilation. Monograph, Pub. Hause MVP, Tbilisi, 2011, 81 p.
[50] Varazanashvili O., Tsereteli N., Amiranashvili A., Tsereteli E., Elizbarashvili E., Dolidze J., Qaldan, L., Saluqvadze M., Adamia Sh., Arevadze N., Gventsadze A. Vulnerability, hazards and multiple risk assessment for Georgia. J. Natural Hazards, vol. 64, Issue 3, 2012, pp. 2021-2056. DOI: 10.1007/s11069-012-0374-3
[51] Varazanashvili O., Tsereteli N., Bonali F.L., Arabidze V., Russo E., Pasquare Mariotto F., Gogoladze Z., Tibaldi A., Kvavadze N., Oppizzi P. GeoInt: the first macroseismic intensity database for the Republic of Georgia. Journal of Seismology, 22(3), 2018, pp. 625-667.

სეისმური საშიშროების ზონირების რუკებისა და სეისმური სამშენებლო კოდების შემუშავება საქართველოში (განვითარების ისტორია და კრიტიკული ანალიზი)

ო. ვარაზანაშვილი

რეზიუმე

ეს ნაშრომი მიმოიხილავს სეისმური საშიშროების გამოქვეყნებულ შეფასებებს, რომლებიც ხელმისაწვდომია საქართველოსთვის, აგრეთვე სამშენებლო კოდებში შეტანილ სეისმურ ზემოქმედებებს, რათა ინახოს ქვეყანაში სეისმური საშიშროების შეფასების კვლევების დონე. მიმოხილვა მოიცავს საქართველოში სეისმური საშიშროების შეფასების ისტორიას და განვითარებას და სამშენებლო კოდების მიღებას. ყველა წინა გამოკვლევის ანალიზის შედეგად გაკეთებულ იქნა დასკვნა, რომ სასურველია სეისმური საშიშროების ახალი შეფასება, რომელიც თანამედროვე მიღწევებს შეესაბამება, აგრეთვე არსებულ ქართულ სამშენებლო კოდებში საშიშროების აღწერილობის შეცვლა.

Разработка карт зонирования сейсмической опасности и сейсмических строительных норм в Грузии (история развития и критический анализ)

О. Ш. Варазанашвили

Резюме

В этой работе рассматриваются опубликованные оценки сейсмической опасности, доступные для Грузии, а также сейсмические воздействия, включенные в строительные нормы, чтобы показать состояние исследований по оценке сейсмической опасности в стране. Обзор включает в себя историю и развитие оценок сейсмической опасности, и принятие строительных норм в Грузии. Все предыдущие исследования были проанализированы, чтобы сделать вывод о том, что желательна новая оценка сейсмической опасности в соответствии с последними достижениями, а также изменение описания опасности для действующих строительных норм Грузии.

Journal of the Georgian Geophysical Society, e-ISSN: 2667-9973, p-ISSN: 1512-1127
Physics of Solid Earth, Atmosphere, Ocean and Space Plasma, v. 24(2), 2021, pp. 22 - 29

Risk of Natural Hazards in Georgia

[1,2] Emil D. Tsereteli, [1]Nana R. Bolashvili, [1,2]George M. Gaprindashvili, [2]Merab V. Gaprindashvili, [1]Nino G. Machavariani

[1]Vakhushti Bagrationi Institute of Geography of Ivane Javakhishvili Tbilisi State University, Tbilisi, Georgia
[2]National Environmental Agency, Department of Geology, Tbilisi, Georgia
gaprindashvili.george@gmail.com

ABSTRACT

Two groups of completely different phenomena and consequences can cause natural hazards. Those are dangerous meteorological processes in the atmosphere and geological processes, which take place on the earth surface and its crust. However, in spite of very different nature and development conditions of these phenomena, there is quite often a synergetic liaison between them, which determines the level of activation/reactivation of the given phenomena.
Natural Hazards become more topical in the beginning of XXI century, as the pressure of them on human environment becomes much heavier. Background of global climate change processes immeasurably increases the risk of uncontrollable disasters.
Taking into account that the South Caucasus region and especially Georgia, belongs to the regions distinguished among the world mountainous areas by natural hazards large scale development processes, frequency recurrence, and negative impact on population and engineering/economic facilities, South Caucasus is recognized as one of the most vulnerable regions.

Key Words: *Natural hazards, landslides, climate change, geology.*

Introduction

Natural hazards become more topical in the beginning of XXI century, as the pressure of them on human environment becomes much heavier. Background of global climate change processes immeasurably increases the risk of uncontrollable disasters.

Taking into account that the South Caucasus region and especially Georgia, belongs to the regions distinguished among the world mountainous areas by natural hazards large scale development processes, frequency recurrence, and negative impact on population and engineering/economic facilities, South Caucasus is recognized as one of the most vulnerable regions. Besides that, the territory of Georgia is located within the limits of 7 – 9-point intensity earthquake risk area. The earthquakes are directly connected with stimulation of landslide-gravitational and debris/mudflow phenomena. Major part of Georgian population, agricultural lands, roads, oil and gas pipe-lines, hydro-technical and irrigation facilities, electric transmitting lines, and mountainous tourism facilities periodically endure the attacks of natural phenomena. Georgia hosts a great variety of morphological and climate conditions - from the humid, subtropical coastlines to highland-alpine-nival areas; whenever natural disasters strike the country, this usually leads to a great number of casualties, also due to very populated human settlements all across Georgia [1 - 5] However, the majority of geo-ecological cataclysms take place in mountain zones, which represent 71% of the country territory and which are occupied by 20% of population. At the same time, the mountainous zones have enormous potential in geopolitical and economic development of the country. 2/3 of landslides observed in the country took place in mountain zones, while debris/mudflows, snow avalanches, rockfalls, rock avalanches took place almost exclusively in mountains. Economical damage caused by natural hazards, as well as casualty and ecological migration in 80% of cases take place in mountain areas followed by devastation of mountain villages and settlements.

Among the multi-spectral geological processes in Georgia the most impressive phenomena are gravitational landslides and debris/mudflows, washing out of marine coasts and river banks within the limits of settlements.

The spatial distribution of landslide and mudflow events over the territory encompasses both the seaside and the highlands. Out of the 70 municipalities regarded as affected by landslide hazards, 29 are included in the average-hazard zone (41%) and 35 (50%) in the high-hazard zone. According to recent data (2011–2018) from 8229 families (Source: Department of Geology of Georgia 2019), as a result of this monitoring activity, 1545 families were given the recommendation to relocate to safer houses/settlements [6].

Risks of geological phenomena

The geological processes developing in mountain regions are characterized by high heterogeneity. Origination or re-activation of them depends on integrated interrelation of multi-spectral factors. Study of development mechanisms of such extremely complex phenomena and determination of that relevant dominant factor (or a group of factors), which can move the geological environment out from homeostatic state and triggers origination/re-activation of this or that kind of processes (or groups of processes), would be impossible without well developed methodology and the well-thought-out systemic approach.

Taking into account that processes are considered as a consequence of interaction of large number of factors (components) in the open equifinal system, where origination/re-activation of geological processes at certain stages of their development should be determined as the final (concluding) action of the whole system. Hence, the assessment of development regularities of contemporary elemental processes and the re-activation trends in the multi-spectral system of triggering factors, should be based on the basic determinative factors.

Presumably, there are certain multi-spectral natural factors triggering processes (some authors define nine different levels [7]), which determine regional and zonal regularities of development of elemental destructive processes and phenomena. The most important factors among them are geological environment (lithologic composition, state, features, tectonic activity, and earth crust movement), relief morphology and its energy potential constant, and the climate, as the unity of meteorological conditions of a given area with the established regime [8]. The scale of development processes and their activation speed depend on sensitivity level of landscape-geological environment of a given space.

Climatic conditions, which in geological past played determinative role in modification processes of the earth surface, as well as in forming of sediments and the landscape-geographic zones, are determining also current correlation of the development time and space of exo-geological processes and the regime of development/re-activation.

However, the role of climate in the relief morphogenesis is quite well investigated. Climate related methodological and theoretical issues are included in a new direction of earth sciences of second half of XX century – “Climatic geo-morphology”. The role of climate factor in engineering geo-dynamics and in the development of contemporary geological processes, especially the issues of forecasting of geological processes in terms of time and space is much less investigated.

Professor A. Shcheko [9,10] who is one of the founders of research methodology on forecasting of elemental geological processes related to the development and activation trends of exogenous geological processes regime, includes the climatic conditions into the main group of changeable factors. This problem is especially important for such complex and vulnerable (in terms of geological processes) mountain regions as

Caucasus and especially Georgia. All zones starting from sea coastal zone and ending with high mountain-nival belt, from humid sub-tropical climate to dry arid climate, are represented in the landscape-ecological environment of Georgia. Each zone is characterized by special type of geological processes, the regime, intensity, and activation level different in accordance with observation conditions of geological environment. Meteorological elements able to provoke certain processes (atmospheric precipitations, humidity, temperature, etc) through deviations from limit values of perennial mean norms can cause changes in the above-mentioned parameters. At the same time, the more syncretic is geological environment, as the receptor and synthesizer of atmospheric precipitations, the higher is activation level of the processes in short time interval.

It should be noted that climate conditions (through increased 'humidity effect') stimulate landslide processes at the slopes which are generally predisposed to such processes and number of which is over 70% among the total number of landslides of different genesis. Climatic factors have decisive role in generation/reactivation of mudflow transformations, erosive processes, floods, snow avalanches, etc.

29% of the whole territory of Georgia is subject to water erosion processes that significantly threaten the environment in general and especially village economy. In 1957-78 the erosive processes damaged 20 000 ha of lands which were excluded from land fund. Area of arable lands by 1980 in Georgia was 673,2 thousand ha, 30,5 % of which were eroded [11]. Soil erosion is especially intensive under the influence of strong anthropogenic factors in mountain regions with scarce plant coverage. About 150-200 tones of fertile soil per 1 ha area is washed out annually in such areas. In case of highly intensive downpours, these figures are increasing up to 300-500 tones per 1 ha, while the soil regeneration processes take centuries in conditions of optimal climate. In this regard the gravest situation is developed in mountainous areas of Ajara, Svaneti, Racha-Lechkhumi, Meskheti, Kazbegi, and Dusheti [12].

Intensive washing out of riverbanks can be observed on big rivers (Rioni, Tskhenistskali, Enguri, Kodori, Mtkvari, Alazani, Iori) in valley and foothill zones, where the annual values of washed out areas fluctuate within 2 – 3,5 m in average. In cases of extreme flooding, this figure increases up to 10 m, especially in the most vulnerable areas. If we take into account that total length of the riverbanks subject to intensive washing out is over 1000 km, and the annual wash out value is approximately 1,5 m, then the annual losses of lands is 150 ha [11].

In lowland areas of Georgia, the washing out of big riverbanks caused by increased water level usually is followed by flooding of significant areas with all negative consequences. According to historical data, around 30-35% of population was affected by extremely intensive floods on river Rioni in 1811-1812. In 1839 water level on this river increased up to 9,6 m, in 1911 – up to 3 m, and in 1922 – up to 2,8. Area of 13 000 ha was flooded in 1982 caused damage of 12 million USA dollars. During the last period, there were not described such catastrophic floods in Kolkheti lowland, except 1987, when 20 000 ha were flooded, 3,2 000 facilities damaged, 2 000 facilities and 16,5 km of railway destroyed. Total damage was calculated about 300 million dollars [13]. Catastrophic floods were described repeatedly in the past years on river Mtkvari, Alazani and lower segments of their tributaries (1839, 1956, 1967, 1968, 1972), which caused damage of several thousands million dollars and took away tens of lives. Some large floods were observed during the last period (2004-2010) on rivers Rioni, Tskhenistskali, and Alazani. Special kind of water erosion is the intensive washing of the Georgian Black Sea coast, which periodically damages high valued recreational areas. From time to time it becomes necessary to provide reconstruction works or moving of highways or railway. In a number of areas of abrasive segments (Musera, New Athoni, Eshera, Ochamchire, Makhinjauri, Gonio-Sarpi, etc) the washing out processes caused by storms coincide with significant activation of landslide processes. By 1980 total area of washed out and degraded coasts was 220 km. In 1967, 1971, and 1978 the direct damage caused by winter storms to Abkhazian coast was estimated up to 27 million dollars [11]. Expenses for coast protection works conducted in Georgian Black Sea coastal areas in 1961-71 were calculated as 45 million dollars, while in 1972-81 – over 81 million dollars. In spite of the measures undertaken for coast protection purposes, the washing speed is catastrophically high, especially on Abkhazian coasts, where beach forming solid sediments today are being taken in a very unacceptable way.

However, the most dangerous/strong natural phenomena among geological processes due to their potential development scale and recurrence frequency, which keep in stress local population and can cause an irreversible economic damage to the country, are <u>landslides and mudflows.</u> <u>Landslides</u> of all kinds and mechanisms known in engineering-geodynamics can be developed in Georgia, starting with the simplest type, deformation of which remains within the aeration zone, and ending by the deep ones (10 meters) of the volume of million cubic meters. However, according to massive development of the landslide processes and the activation intervals, the most distinguishable are those landslides, which can be directly provoked by the regime distribution of atmospheric precipitations. This type of landslides is called climatic (or consistent), dynamic mechanism of which is determined by consistence of water on the slopes and by 'humidity effect'. Changes in 'consistence' features of rocks, as well as critical decreasing of resistance to shifting depend on these parameters. More than 70% of the landslides in Georgia represent this type of landslides and can be found in all landscape-geo-morphological zones [13, 14].

Large development scale and high recurrence frequency of climatic landslides are the main features of almost all landslides in western Georgia. Black Sea coastal undulate zone, Saguramo-Tsivgombori slopes, low mountainous and foothill zone of Shida Kartli, middle segment of river Aragvi basin, and all those areas of the relief of Georgia in general, the slopes of which have an angle over 8% and are built with clay rocks highly sensitive to landslide processes and which are able to accept certain amount of atmospheric precipitation. Dynamics of landslide processes depend on deviation values of atmospheric precipitation in an intra-annual interval from perennial statistic values of a given landscape-geological environment.

According to analysis of geo-monitoring statistic data, activation or attenuation of landslide processes, or their temporary stabilization is in direct correlation with syncretism of geological environment.

Regional perennial engineering-geological research conducted at the territory of Georgia and geo-monitoring data, as well as analysis of regime observation data, show stabilization of exo-geological processes which directly depend on climatic factors, can be reached when the values of atmospheric precipitation and humidity within the given period of time (year, season, month, 24 hours) is below the mean perennial limit value. At the same time, the higher is deficit within the long-time segment, the higher is safety related to limit risks of geological processes. Together with increasing of precipitations to compare with statistic norms, the level and risk of activation of elemental processes increase proportionally.

Taking into consideration all mentioned above, according to space-time development of the exo-geological processes provoked by climatic factors, they can be divided in 5 categories: 1) below the background (stable); 2) background; 3) stressful; 4) extreme; 5) paroxysmal [14].

In a certain geological environment, where amount of precipitations remains within the limits of perennial norm (coincides with statistic climatic regime), exo-geological processes, if there are not any other additional conditions, develop at the background level. In particular, there is a close correlation between dynamics of climatic landslides and alterations of the precipitation regime. A landslide body 'sleeping' in a geological environment of optimal reception features comes out from homeostatic state.

Annual amount of precipitations increased by 100-200 mm to compare with perennial norm, cause activation of landslide processes above the background level. Annual precipitations increased by 200-400 mm provoke activation of the landslide processes and enter the stress state. All landslide bodies which temporarily were in a stable state, as well as new landslides, start activating in those geological environments, deformation horizons of which are characterized by high sensitivity and synthesizing features. Annual precipitations increased by 400-600 mm to compare with the perennial mean value activate the processes entering the extreme stage, when a number of new landslides explode and almost all 'sleeping' landslides start activating. Research data confirm that according to a certain type of macro-circulation regime in atmosphere, extreme activation of elemental processes can gain regional character and later can develop at the global scale. There are number of relevant paradigms in Georgia and in Caucasus in general. For instance, the extreme explosion of landslide processes in West Georgia in 1967-68 which covered area of up to 300 000 ha, damaged and destroyed up to 20 000 living houses. At that time no such extreme activation of the elemental processes was observed in East Georgia. However, in 1987-89 the geological catastrophes of paroxysmal character covered the whole territory of Georgia.

This kind of extreme paroxysms of elemental processes were observed repeatedly all over the country in 1991-1992 and 2004-2005. Total damage caused by these processes was over 12 billion dollars. At the same time, we should take into account that the extreme or paroxysmal elemental processes develop in a very complex way that increases threats to the local population and complicates implementation of the appropriate management measures.

Analysis of perennial data obtained by engineering-geodynamic research and geo-monitoring observation at the territory of Georgia confirm that there is an indisputable correlation between extreme activation of landslide processes and critical deviation from perennial norm of atmospheric precipitations. This correlation is set through ‘humidification effect’ on slopes vulnerable towards landslide processes and because of ability of building rocks to receive atmospheric precipitations, and due to their certain geological features.

During the last period many countries conduct appropriate researches to detect the functional relationship between atmospheric precipitations and those critical values when the landslide, mudflow, and erosion processes, as well as the re-activation extremes start developing. For instance, it is determined for New Zeeland [15], that weak deformation of the slopes takes place in case of daily sum precipitations within the limits 50-55 mm. Mean deformation is observed in case of 60-90 mm and large-scale landslides start developing in case of precipitations over 100 mm. For South-East Asia the critical amount of daily precipitations able to provoke landslides is defined as 100-200 mm [16]. Extreme activation of landslide processes in this region was observed in July of 1996, when during 24 hours 401 mm of precipitations provoked 700 new landsides.

According to the Geology Department of the National Environment Agency, in recent years the quantity and magnitude of landslides and mudflow processes have increased significantly on the territory of the country (Fig. 1). As of 2020, 20% (729 settlements) of Georgia's populated areas were at high risk of geological hazards (Fig. 2-3) – [17, 18].

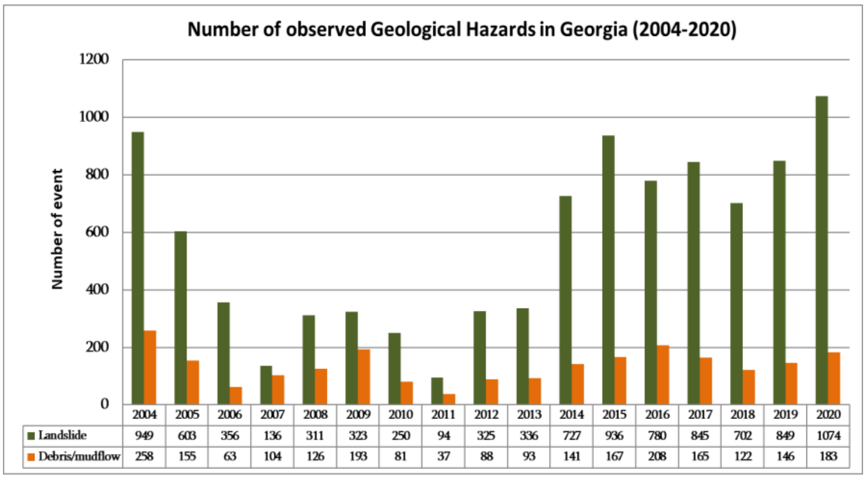

Fig. 1. Number of observed Geological Hazards in Georgia [17, 18].

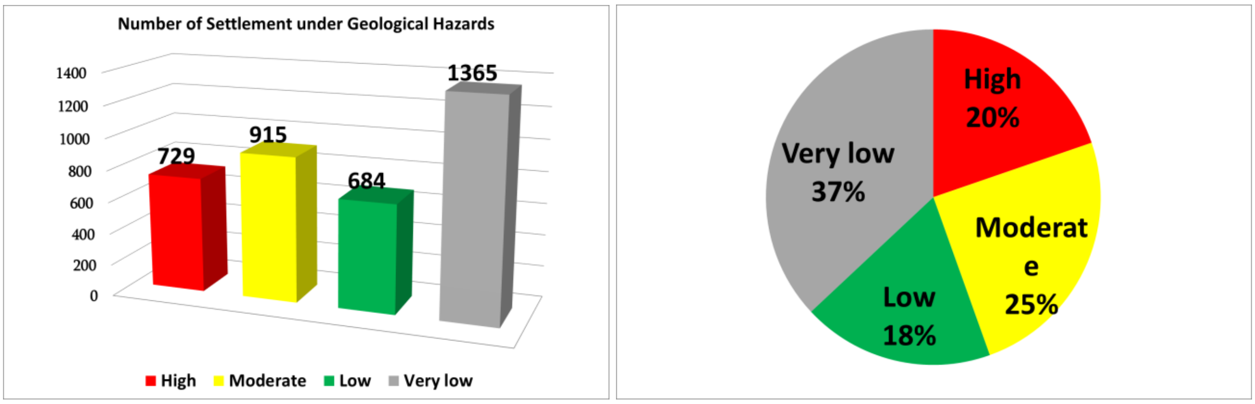

Fig. 2-3. Number of settlements under Geological hazards [17, 18].

Research data confirm that in geological-climatic conditions of Georgia, the humidification level of slopes depend not directly on the amount of daily precipitations, but on the prolonged impact of the same sum amount of precipitations. The exemptions are Mtatusheti low mountainous relief zone of Mtkvari depression built with extremely not-water-proof rocks of molassic rocks, as well as relief forms built with flood-plain and silt facieses, the structure of which can be immediately destroyed by contact with water. Hilly mountainous areas of the Black Sea coastal zone are also characterized by high ability of water penetration and low structural liaison, which in certain conditions can easily loose sustainability.

However, at the territory of Georgia, the landslides which are activating due to certain deviations in amounts of precipitations from maximum permissible values, are the most notable by their development scale. The mentioned deviation has direct effect on humidification level of deformable slopes. Relevant research data show that the maximum value (50-70%) of 'humidity effect' which is able to make move this type of landslides within the limits of deformable horizon is observed in autumn-spring period. It should be noted also, that in summer period the humidity of potentially movable grounds in West Georgia is decreasing by 10-16% in average, while in East Georgia this value is increasing up to 22-30%. Parameters of natural humidity are almost unchangeable below the zone of influence of atmospheric precipitations (below aeration zone) [19, 20].

Activation of landslide processes in accordance with atmospheric precipitation regime clearly indicates the correlation regularities: the intervals between atmospheric precipitations able to provoke landslide processes, fluctuate within 2,5-5 years, while the sequence line between the increase and deficit of precipitations, which represents one cycle of development of the landslide processes, ranges within 3-8 years.

Conclusion

Three main stages, or periods in the dynamics of landslides can be distinguished with regard to regional development of landslides:

1) Maximal re-activation period of landslide processes, which is determined by extreme values of paroxysmal amount of atmospheric precipitations. The intervals between active periods are 4-11 years.
2) Mean activation period of the landslide processes mainly includes intervals of landslide processes between the periods of intensive activation.
3) Background activation period of landslide processes. Number of landslides of this type of dynamics is more than the number of landslide processes performed during previous two activation periods. Usually, the landslide bodies being in this kind of regime, can move to a stress regime, or vice versa, to a stabilization regime, depending on the development of atmospheric precipitation conditions and the connected 'humidification effect' of relevant slopes. The start point of these processes is the moment when 'humidification effect' of slopes vulnerable towards landslide processes does not correspond with the values able to start moving. Analysis of statistic data on atmospheric precipitations in Georgia during last 100 years shows, that the intervals between activation of landslides of the mentioned regime, fluctuate within diapason of 1-5 years.

Note

This article was presented in the form of a report at the International Scientific Conference "Natural Disasters in the 21st Century: Monitoring, Prevention, Mitigation", Tbilisi, December 20-22, 2021.

References

[1] Tsereteli E., Gaprindashvili M., Gaprindashvili G. et al. Problems of natural and anthropogenic disasters in Georgia. J. Georgian Geophys. Soc., Phys. Solid Earth, 15A, 2012, pp.14–22
[2] Tsereteli E., Gobejishvili R., Gaprindashvili G. et al. Challenges of geologic catastrophes in Georgia and ways of their reduction. In: Engineering geology for society and territory, vol 2. Springer, Cham, 2014, pp. 1767–1773. https://doi.org/10.1007/978-3-319-09057-3_313
[3] Gaprindashvili G., Westen C.V. Generation of a national landslide hazard and risk map for the country of Georgia. Nat Hazards, 80(1), 2016, pp. 69–101. https://doi.org/10.1007/s11069-015-19585
[4] Gaprindashvili G., Tsereteli E., Gaprindashvili M. Landslide hazard assessment methodology in Georgia. In: proceedings of the 16th Danube – European conference on. Geotech. Eng., 2(2–3), 2018, pp. 217–222. https://doi.org/10.1002/cepa.674
[5] Gaprindashvili M., Tsereteli E., Gaprindashvili G., Kurtsikidze O. Landslide and Mudflow Hazard Assessment in Georgia. In: Bonali F.L., Pasquaré Mariotto F., Tsereteli N. (eds) Building Knowledge for Geohazard Assessment and Management in the Caucasus and other Orogenic Regions. NATO Science for Peace and Security Series C: Environmental Security. Springer, Dordrecht, 2021 https://doi.org/10.1007/978-94-024-2046-3_14
[6] Department of Geology, National Environmental Agency of Georgia (NEA). Information Geological Bulletins (2000–2019), 2019.
[7] Piotrovskaya T. Types of geodynamic environment and development activity of exogenous geological processes. Engineering-geology today: theory, practice, problems, 1988, pp. 244-253.
[8] Tsereteli E. Natural and catastrophic phenomena and the problem of sustainable development of Georgia and border areas. Tbilisi, Georgia, 2003, 109 pages.
[9] Landslides and Mudflows. Volume 1-2, Center for International Projects UNESCO-UNEP, 1984.
[10] Tsereteli E., Khazaradze R. Natural Disasters, monograph - Geography of Georgia (Part I), "Science", Tbilisi, 2000, pp. 69-90.
[11] State Department of Geology of Georgia. General Scheme of Anti-Erosion Measures (1981-2000), Tbilisi, Georgia, 1988, 725 pages.
[12] Tatashidze Z., Tsereteli E., Bondyrev I., Tsereteli N. Relevance of climatic anomalies in the development of exogeodynamic processes. Vakhushti Bagrationi Institute of Georgraphy, collected papers (new series) # 1 (80) Tbilisi, 2006, pp. 107-120.
[13] Tsereteli E., Gobejishvili R., Gaprindashvili M., Dvalashvili G., Gongadze M. Consumption-gravity surveillance in Georgia and problems of geological structure. Proceedings of the Geographical Society of Azerbaijan, v. XIV, Baku, 2009, pp 1-36.
[14] Eyles R. Triggering rainfalls in Wellington city, New Zealand, 1979, 22 pages;
[15] Ramaswamy S., Aziz M.A. Rain induced landslides in Singapore and their control. Int. Simp. Landslides, proc., V.1, New Delhi, S.A., 1982, pp. 403-406.
[16] Sheko A., Krupaderov V., Malneva M., Dykonova V., Balandin G. Factors of formation factor of landslides and mudflows, monography – landslide and mudflow, Center for International Projects UNESCO-UNEP, 1984, pp. 16-51.
[17] Informational bulletin: Condition of development of geological processes in Georgia, results of activation in 2020 and danger of risk by 2021 - summarizing geological report, Ministry of Environment Protection and Agriculture of Georgia, National Environmental Agency, Department of Geology, Tbilisi, 2021, 502 pages.
[18] Informational bulletin: Condition of development of geological processes in Georgia, results of activation in 2019 and danger of risk by 2020 - summarizing geological report, Ministry of Environment Protection and Agriculture of Georgia, National Environmental Agency, Department of Geology, Tbilisi, 2020, 491 pages, ISBN 978-9941-27-835-8.
[19] Gobechia G., Tsereteli E. Influence of climate on the development of spontaneous exogeological processes and criteria for its assessment. Institute of Water Management of Georgia, 2007, pp. 33-35.

[20] Varazashvili L, Tsereteli E., Kutsnashvili O., Tatashidze Z. Landslide risk in Georgia and their regional classification. Proceedings of Georgian Technical University. # 6 (439), Tbilisi, 2001, pp. 54-60

სტიქიური უბედურების რისკი საქართველოში

ე. წერეთელი, ნ. ბოლაშვილი, გ. გაფრინდაშვილი,
მ. გაფრინდაშვილი, ნ. მაჭავარიანი

რეზიუმე

ბუნების სტიქიური პროცესები ორი ერთმანეთისაგან სრულიად განსხვავებული მოვლენებითა და შედეგებით წარმოგვიდგება: ეს არის ატმოსფეროში ფორმირებული საშიში მეტეოროლოგიური მოვლენები და დედამიწის ზედაპირზე და მის ქერქში წარმოქმნილი სტიქიური გეოლოგიური პროცესები. თუმცა, ხშირად ამ ორი ერთმანეთისაგან დიამეტრიულად განსხვავებული მოვლენის ფორმირების პირობების მიუხედავად, მათ შორის კავშირი სინერგეტიკულია და განსაზღვრავენ ამა თუ იმ მოვლენის წარმოქმნა-რეაქტივაციის ხარისხს.
ბუნებრივი სტიქიით განპირობებული კატაკლიზმები კიდევ უფრო აქტუალური გახდა XXI საუკუნის გარიჟრაჟზე, როდესაც სტიქიური კატასტროფები ადამიანის გარემოზე მიყენებული ფართომასშტაბიანი პრესინგისა და კლიმატის გლობალური ცვლილებების საერთო ფონზე განუზომლად ზრდის მათი საშიშროების რისკს და ხშირად უმართავი ხდება.
სამხრეთ კავკასია და განსაკუთრებით, საქართველო, მიეკუთვნება იმ რეგიონებს, რომლებიც მსოფლიოს მთიან ტერიტორიებს შორის ბუნებრივი საფრთხეების ფართომასშტაბიანი განვითარების პროცესებით გამოირჩევიან. ხშირი განმეორებადობის, მოსახლეობასა და საინჟინრო-ეკონომიკურ ობიექტებზე უარყოფითი ზემოქმედების გამო, სამხრეთ კავკასია ერთ-ერთ ყველაზე მოწყვლად რეგიონადაა აღიარებული.

Риск стихийных бедствий в Грузии

**Э.Д. Церетели, Н.Р. Болашвили, Г.М. Гаприндашвили,
М.В. Гаприндашвили, Н.Г. Мачавариани**

Резюме

Две группы совершенно разных явлений и последствий могут вызвать стихийные бедствия. Это опасные метеорологические процессы в атмосфере и геологические процессы, происходящие на земной поверхности и ее коре. Однако, несмотря на очень различную природу и условия развития этих явлений, нередко между ними существует синергетическая связь, определяющая уровень активации / реактивации данных явлений.
Стихийные бедствия становятся все более актуальными в начале XXI века, поскольку их давление на среду обитания человека становится все более сильным. На фоне глобальных процессов изменения климата неизмеримо возрастает риск неконтролируемых катастроф.
Принимая во внимание, что регион Южного Кавказа, и особенно Грузия, относятся к регионам, выделяющимся среди горных территорий мира крупномасштабными процессами развития природных опасностей, повторяемостью и негативным воздействием на население и инженерно-экономические объекты, Южный Кавказ признан единым целым наиболее уязвимых регионов.

Journal of the Georgian Geophysical Society, e-ISSN: 2667-9973, p-ISSN: 1512-1127
Physics of Solid Earth, Atmosphere, Ocean and Space Plasma, v. 24(2), 2021, pp. 30 - 34

Revealed of Hydrodynamic Anomalies in Boreholes of Georgia Caused by Earthquakes

George I. Melikadze, Tamar J. Jimsheladze, Genadi N. Kobzev, Aleksandre Sh. Tchankvetadze

M. Nodia Institute of Geophysics of I. Javakhishvili Tbilisi State University
melikadze@gmail.com

ABSTRACT

The article contain information about several hydrodynamic anomalies were observed during January 2021 on the multiparametric monitoring network of M. Nodia institute of Geophysics. Data were analyzed by the special program which gives possibility to exclude the influence of geological factors by the common value of tidal variations. Was analyzed reaction of parameters to the earthquake preparation process.

Key words: *hydrodynamic anomalies, seismic event precursors.*

1. Introduction

It is known that variations of water level represent itself an integrated response of aquifer to different periodic as well as non-periodic influences, including earthquake related strain generation in the earth crust [1-2]. Quantitative analysis of impacts of separate components in observed integral dynamics remains one of the main geophysical problems. It is especially important for non-periodic processes related to the earthquake generation, taking into account their possible prognostic value [3-4].
Determination of earthquake precursors is a task of global importance. The article deals about detected anomalies during preparation of average grade earthquake. For this purpose, was developed data of the water level and atmospheric pressure from the Hydrodynamic monitoring network. Has fixed the hydrogeodeformation field variation caused by the earthquake preparation process and reflection of the critical stress in the water level. As a result, have been identified preliminary anomalies and has been confirmed high sensitivity to the geodynamic processes.

2. Data Analysis

Therefore, were analyzing the value of stress field by hydrodynamical parameters [5-6] variations during preparation of several earthquake processes on the territory of Caucasus were calculated and analyzed:

Earthquake in Akhalkalaki area -05.01.2021-25.01.2021 period (Mag=3.4 05.01.2021, Mag=2.9 16.01.2021, Mag=3.0 23.01.2021, Mag=3.2 24.01.2021).

The earthquakes of Akhalkalaki, anomalies were observed on the Chkvishi, Akhalkalaki, Ajameti, Kobuleti, Oni and Gori boreholes.

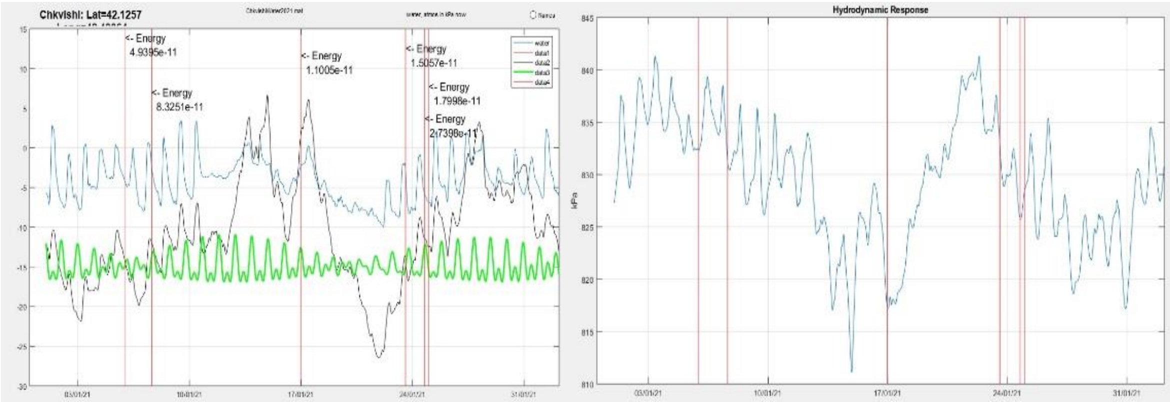

a b

Fig.1. a - Water level, atmospheric pressure and tidal variations at the Chkvishi borehole. Vertical line marks an earthquake. On abscise axis time is in hours. b- Hydrodynamic Response.

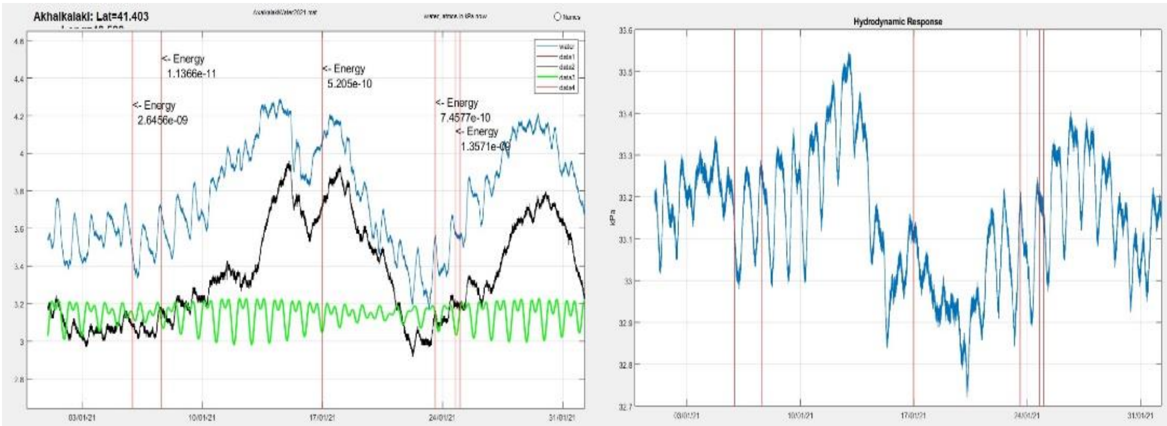

a b

Fig.2. a - Water level, atmospheric pressure and tidal variations at the Akhalkalaki borehole. Vertical line marks an earthquake. On abscise axis time is in hours. b- Hydrodynamic Response.

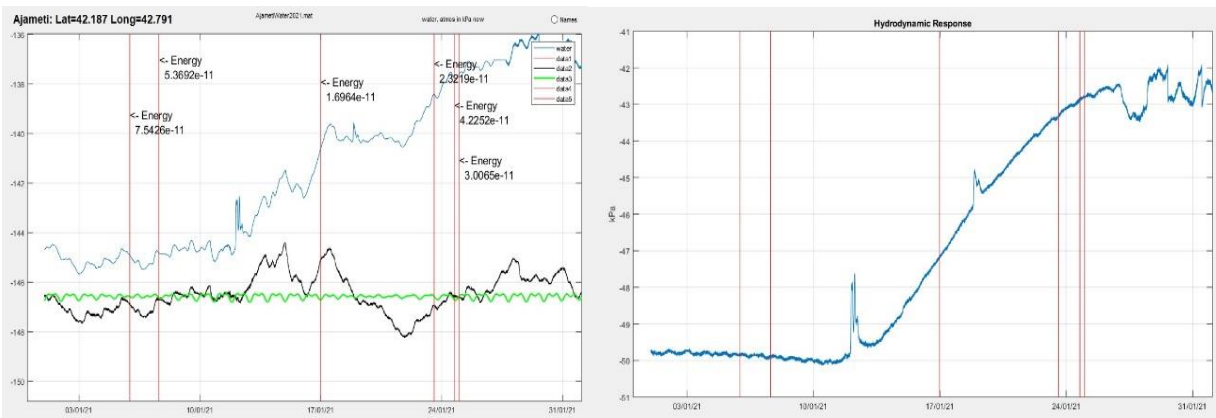

a b

Fig.3. a - Water level, atmospheric pressure and tidal variations at the Ajameti borehole. Vertical line marks an earthquake. On abscise axis time is in hours. b- Hydrodynamic Response.

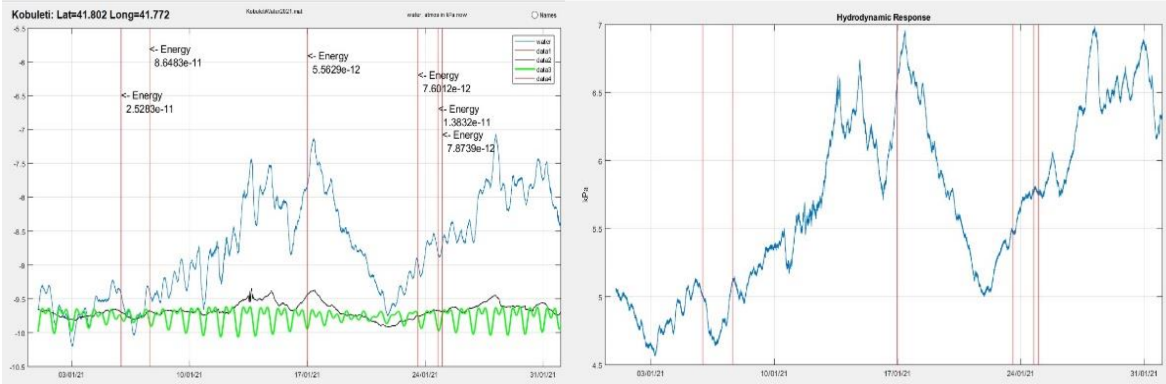

a b

Fig.4. a - Water level, atmospheric pressure and tidal variations at the Kobuleti borehole. Vertical line marks an earthquake. On abscise axis time is in hours. b- Hydrodynamic Response.

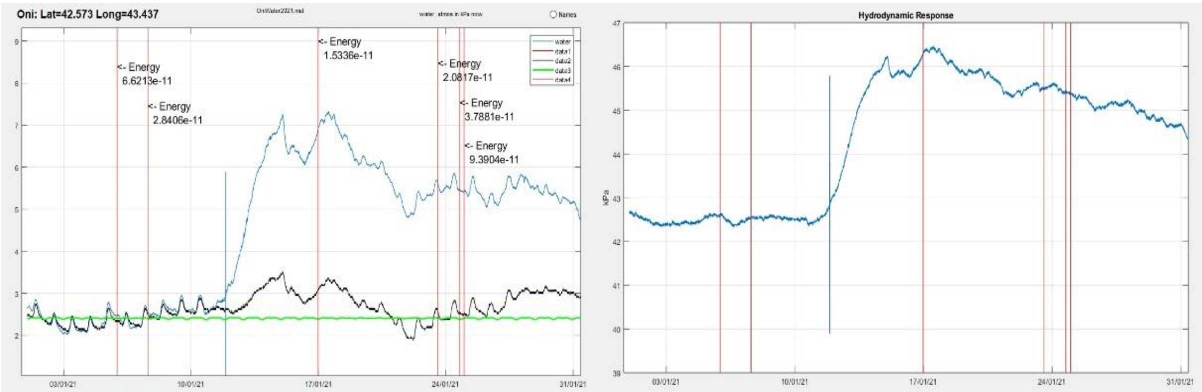

a b

Fig.5. a - Water level, atmospheric pressure and tidal variations at the Oni borehole. Vertical line marks an earthquake. On abscise axis time is in hours. b- Hydrodynamic Response.

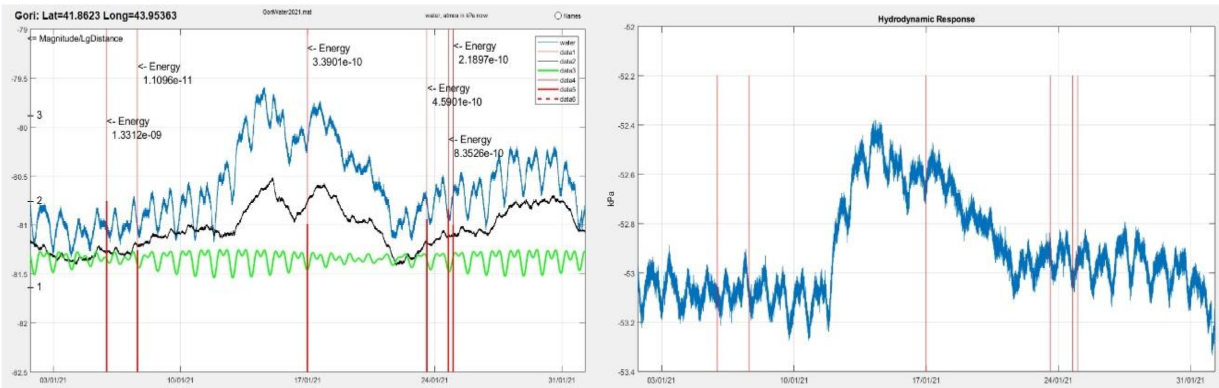

a b

Fig.6. a - Water level, atmospheric pressure and tidal variations at the Gori borehole. Vertical line marks an earthquake. On abscise axis time is in hours. b- Hydrodynamic Response.

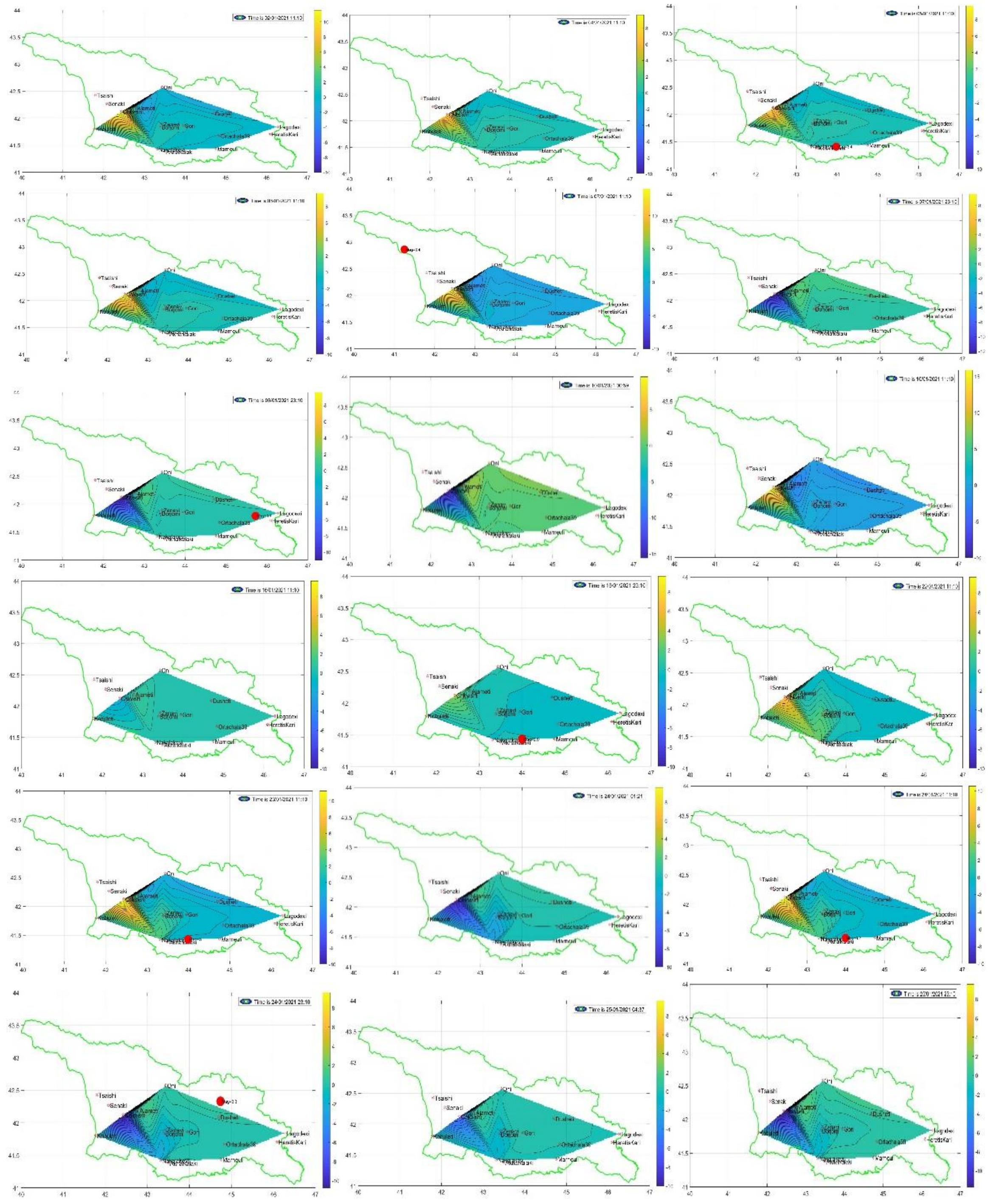

Fig.7. Geodeformation field changes for period 01-25 January 2021.

3. Conclusion

The information content of hydrodynamic boreholes from the earthquake prognostics point of view are ascertained. The recorded anomalies coincide with the preparation period for strong earthquakes. Characteristics of anomalies (amplitude, period, etc) are correlated with earthquake strength. However, in certain cases, high levels of anomalies are recorded in boreholes located relatively far from the epicentre.

References

[1] Varazanashvili O., Tsereteli N., Amiranashvili A., Tsereteli E., Elizbarashvili E., Dolidze J., Qaldani L., Saluqvadze M., Adamia Sh., Arevadze N., Gventcadze A. Vulnerability, Hazards and Multiple Risk Assessment for Georgia. Natural Hazards, v. 64, N. 3, 2012, pp. 2021-2056, DOI: 10.1007/s11069-012-0374-3, http://www.springerlink.com/content/ 9311p18582143662/fulltext.pdf
[2] Melikadze G., Kobzev G., Kapanadze N., Machaidze Z., Jimsheladze T. Analyze of Underground Water Regime Factors for Determine Tectonic Component. LEPT Institute of Hydrogeology and Engineering Geology, Collection articles, vol. XYI. Proceeding of Conference Dedicate to the 100-th Anniversary of Professor Josef Buachidze, Tbilisi, 2007, 20.
[3] Dovgal N., Melikadze G. Methodology of Creation of Multi-Parametrical Network, Workshop materials "Exploration and exploitation of groundwater and thermal water systems in Georgia", Tbilisi, Georgia, 2010, pp. 50-59, http://dspace.nplg.gov.ge/handle/1234/9081
[4] Kartvelishvili K., Melikadze G., Kobzev G. Influence of Atmosphere Pressure and Tidal Variation of Gravity of the Hydrosphere. Trans. of Mikheil Nodia Institute of Geophysics, ISSN 1512-1135, vol. 65, 2010, pp. 169 -173, (in Russian).
[5] Melikadze G., Kobzev G., Jimsheladze T. Some Methods of Analyze Geodynamic Imfuct on the Deep Aquifare. Journal of the Georgian Geophysical Society, Iss. A. Physics of Solid Earth, vol. 17A, 2014, pp.47-52.
[6] Jimsheladze T., Melikadze G., Kobzev G. Construction and Analysis of the Stress State of Environment During the Preparation of the Racha Earthquake 2009. ISSN 1512-1135, vol. 64, 2013, pp. 36-45, (in Russian).

მიწისძვრებით გამოწვეული ჰიდროდინამიური ანომალიების გამოვლენა საქართველოს ჭაბურღილებში

გ. მელიქაძე, თ. ჯიმშელაძე, გ. კობზევი, ა. ჭანკვეტაძე

რეზიუმე

სტატია გადმოგვცემს ინფორმაციას 2021 წლის იანვარში, ახალქალაქის ტერიტორიაზე დაფიქსირებული მიწისძვრების ჯგუფის დროს ნოდიას სახ. გეოფიზიკის ინსტიტუტის მულტიპარამეტრიკულ ქსელზე გამოვლენილ ჰიდროდინამიკურ ანომალიებზე. მონაცემები მუშავდებოდა სპეციალური პროგრამის მეშვეობით, რათა გამორიცხულიყო გეოლოგიური ფაქტორების გავლენა. სხვადასხვა სადგურების მონაცემები კალიბრებოდა მიმოქცევითი ვარიაციებით. გაანალიზდა პარამეტრების ვარიაციები და რეაქციები მიწისძვრის მომზადების პროცესზე.

Выявление гидродинамических аномалии в скважинах Грузии, вызванные землетрясениями

Г.И. Меликадзе, Т. Дж. Джимшеладзе, Г.Н. Кобзев, А. Ш. Чанкветадзе

Резюме

Статья содержит информацию о гидродинамических аномалиях в период групп землетрясений в Ахалкалаки (январь 2021) по данным наблюдений мультипараметрической мониторинговой сети Института геофизики им. М. Нодиа. Данные проанализированы с помощью специальной программы. С целью исключения влияния геологических факторов, данные с различных станций были откалиброваны с помощью значений приливных вариаций. Осуществлен анализ вариаций и реакции параметра на процесс подготовки землетрясения.

Journal of the Georgian Geophysical Society, e-ISSN: 2667-9973, p-ISSN: 1512-1127
Physics of Solid Earth, Atmosphere, Ocean and Space Plasma, v. 24(2), 2021, pp. 35 - 37

Reaction of Georgian Wells to Remote and Nearby Earthquakes. Similarities and Differences

Genadi N. Kobzev, George I. Melikadze, Tamar J. Jimsheladze

M. Nodia Institute of Geophysics of I. Javakhishvili Tbilisi State University
kobzev47@gmail.com

ABSTRACT

The behavior of two wells located in Georgia is compared: Oni and Nakalakevi. A stable relationship (coupling coefficient) between the reactions of water in these wells to earthquakes is found. It is indicated that the coupling coefficients are different for remote and nearby earthquakes.

Key words: *coupling coefficient, resonance period, hydrodynamic anomalies, seismic event precursors.*

1. Introduction

Well coordinates. Oni well: 42.573° N 43.437° E. Nakalakevi well: 41.424° N 43.317° E.
The distance between the wells is 125 km.
Well parameters. Oni well: length 255 m, screen 70-250 m. Confined sub-artesian aquifer; fractured shale and basalts. Nakalakevi well: length 600 m, screen 255-367 m. Confined sub-artesian aquifer; fractured andesite-basalts.
The water level was recorded every 1 minute.

2. Data Analysis

If there is a reaction of water to an earthquake in the Oni and Nakalakevi wells, then:
1. The result of dividing "amplitude of water in Oni" / "amplitude of water in Nakalakevi" is 2.7-2.8 provided: a) remote earthquake (distance ≥1000 km); b) earthquake depth ≤ 40 km.
2. "Amplitude of water in Oni" / "Amplitude of water in Nakalakevi" is 5.7-6.2 if the earthquake is close (distance ≤600 km).

Remote earthquakes

The table and the graph based on it make it possible to assert that under certain conditions the "amplitude of water in Oni" / "amplitude of water in Nakalakevi" is 2.7-2.8.

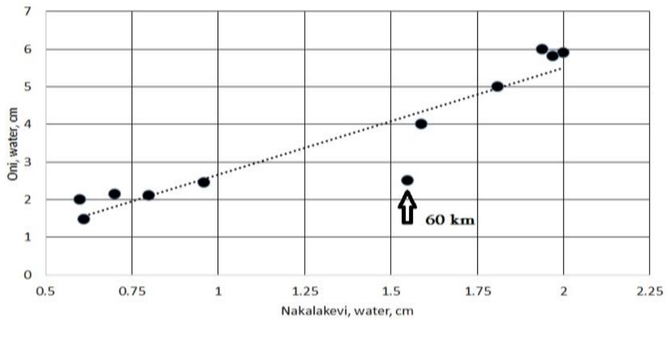

Fig.1. Amplitude ratio of Nakalakevi & Oni water as a reaction to remote earthquakes in 2020-2021.

Table 1. Remote earthquakes

Date	Magnitude	Distance, km	Depth, km	Place	Nakalakevi, water, cm	Oni, water, cm
14/05/2019 12:59	7.5	11876	10	New Britain Region, P.N.G	0.7	2.15
28/01/2020 19:10	7.7	11013	10	Cuba Region	0.6	2
25/03/2020 02:49	7.5	8094	60	East Kuril Islands	1.55	2.5
02/05/2020 12:51	6.6	1742	10	Crete, Greece	0.8	2.1
23/06/2020 15:29	7.4	12368	10	Oaxaca, Mexico	2.0	5.9
22/07/2020 06:12	7.8	9079	30	Alaska, Peninsula	1.94	6
19/10/2020 20:54	7.5	9103	40	South of Alaska	1.59	4
30/10/2020 11:51	7.0	1460	10	Dodecanese Islands, Greece	1.81	5
11/01/2021 21:32	6.7	4326	10	Russia-Mongolia border	0.61	1.48
13/02/2021 14:07	7.1	4866	60	Near East Coast of Honshu, Japan	0.96	2.45
04/03/2021 19:28	8.1	16123	29	Kermades Islands, New Zealand	1.97	5.82

Nearby earthquakes

Water response (or lack thereof) to earthquakes in Turkey at a distance <= 600 km from the well.
Conclusion for close earthquakes at a distance of ≤ 600 km

- If the magnitude is M = 5.0-5.5, then there is no reaction of water to earthquakes.
- If the magnitude is M ≥ 6, then the water reaction is observed and Oni / Nakalakevi is 5.73 or 6.12, which is twice the expected 2.7-2.8.

Remark. In [1, Fig. 1.5], coseismic jumps are noted at a distance from earthquakes ≤ 400 km, if the magnitude is Mw> 6, as well as their absence at a lower magnitude.
Example 1 (distance ≤ 600 km)

1. 24/01/2020 17:55, M=6.8, D=587 km, H=15 km, Eastern Turkey. Oni/Nakalakevi=**5.73**.
2. 25/01/2020 16:30, M=5.1, D=599 km, H=7 km, Eastern Turkey. No water reaction.
3. 23/02/2020 05:53, M=5.7, D=346 km, H=10 km, Turkey-Iran Region,
   Oni=0.22 cm, Nakalakevi=0.0 cm.
4. 23/02/2020 16:00, M=6.0, D=471 km, H=10 km, Turkey-Iran border,
   Oni=3 cm, Nakalakevi=0.49 cm. Oni/Nakalakevi=**6.12**.
5. 15/06/2020 06:51, M=5.5, D=423 km, H=5 km, Eastern Turkey. No water reaction.
6. 25/06/2020 10:03, M=5.4, D=457 km, H=10 km, Turkey-Iran border. No water reaction.
7. 03/12/2020 05:45, M=5.0, D=529 km, H=14 km, Eastern Turkey. No water reaction.
8. 27/12/2020 06:37, M=5.5, D=577 km, H=2 km, Eastern Turkey. No water reaction.

Example 2 (distance ≥ 1000 km)

1 26/06/2017 12:28, M=6.3, D=1498 km, Az=254°, H=9 km, Near the Coast of Turkey,
Oni=1.22 cm, Nakalakevi=0.6 cm. Oni/Nakalakevi=1.22/0.6=**2.03**.

Remark for nearby earthquakes at a distance of ≤ 600 km

When comparing the reaction of wells Oni and Nakalakevi under the condition: distances <= 600 km and Oni/Nakalakevi> 5.5, note that the well Oni, reacting more strongly, is at the same time further down the well Nakalakevi per 100 km for earthquakes in Turkey.

3. Conclusion

Well resonance period as a possible cause of different well response to remote/nearby earthquakes

Let us calculate the resonance period *P* of the well, but previously simplify the calculations.

The formula for the resonance frequency of a pendulum is $f = \frac{1}{2\pi}\sqrt{\frac{g}{H}}$. Since $\frac{\sqrt{g}}{\pi} \approx 0.996 \approx 1$ and period $P = \frac{1}{f}$, then numerically (!) resonance period $P = 2\sqrt{H}$, where *P* is measured in seconds and pendulum's length *H* is in meters. For wells *H*=Hsolid+3/8*Hscreen, [1, p.96].

For well Oni *H*=138 m, for Nakalakevi *H*=530 m. Consequently, Oni have a resonance period *P*=23.5 sec. and for Nakalakevi *P*=46 sec.

For comparison, the sensitive well YuZ-5 located in Kamchatka [1] has a resonance period of 44.6 sec.

The length of the period of the incoming wave from remote earthquakes can be 13-30 sec. Nearby earthquakes have a shorter period of waves. Since the well Oni resonance period is 2 times less than Nakalakevi, then Oni react more noticeably. This difference sharply manifests itself at short distances from earthquakes, but affects differently at distant ones.

Remark. The length of the incoming wave's period was estimated based on the data of the TBLG, Delisi, Georgia seismic station, given in http://ds.iris.edu/wilber3, Station Monitor.

References

1. Копылова Г.Н., Болдина С.В., Гидросейсмические вариации уровня воды в скважинах Камчатки. Монография, 2019, ISBN 978-5-9610-0344-4, Петропавловск-Камчатский: ООО "Камчатпресс", 144 с.

საქართველოს ტერიტორიაზე განლაგებული ჭაბურღილების რეაქცია მახლობელ და შორეულ მიწისძვრებზე. მსგავსება და განსხვავება

გ. კობზევი, გ. მელიქაძე, თ. ჯიმშელაძე

რეზიუმე

ხდება საქართველოს ტერიტორიაზე განლაგებული ორი ჭაბურღილის, ონისა და ახლქალაქის რეაქციის შედარება. ვლინდება მჭიდრო კავშირი, მიწისძვრაზე ამ ორი ჭაბურღილის რეაქციებს შორის. აღმოჩნდა, რომ რომ მათ შორის კორელაციის კოეფიციენტი მახლობელი და შორეული მიწისძვრებისათვის განსხვავებულია.

Реакция скважин Грузии на далекие и близкие землетрясения. Сходства и различия

Г.Н. Кобзев, Г.И. Меликадзе, Т.Дж. Джимшеладзе

Резюме

Сравнивается поведение двух скважин, расположенных в Грузии: Они и Накалакеви. Выявлена устойчивая связь (коэффициент связи) между реакциями воды этих скважин на землетрясения. Указывается, что для дальних и близких землетрясений коэффициенты связи разные.

Journal of the Georgian Geophysical Society, e-ISSN: 2667-9973, p-ISSN: 1512-1127
Physics of Solid Earth, Atmosphere, Ocean and Space Plasma, v. 24(2), 2021, pp. 38 - 42

Identification of the Groundwater Aquifer by Geophysical (Electrical Survey) Methods on the Example of Gudauri Area and Degree of its Hydrogeological Study

[1]George I. Melikadze, [1]Nodar D. Varamashvili, [2]Nana Sh. Khundadze, [2]Tamar J. Razmadze-Brokishvili, [1]Nino A. Kapanadze, [1]Aleksandre Sh. Tchankvetadze, [1]Tornike G. Tchikadze

[1]Iv. Javakhishvili Tbilisi State University. The M. Nodia Institute of Geophysics. melikadze@gmail.com
[2]Georgian Technical University. n.khundadze@gtu.ge; t_razmadze@gtu.ge

ABSTRACT

Gudauri is a mountain ski resort in Georgia in Kazbegi Municipality, at 2196 m asl on the southern slope of the Central Caucasian ridge, 120 km from Tbilisi. As the number of infrastructural facilities and visitors increases in the resort area, the existing water supply systems need additional water outputs to ensure a stable water supply of Gudauri in winter season. This is why, United Water Supply Company of the Ministry of Regional Development and Infrastructure of Georgia starts to build the drinking water and sewerage systems in Gudauri Settlement. The works envisage the construction of the drinking water and sewerage infrastructure of modern standards in Gudauri and nearby villages. Under the Project, within the scope of "Agreement on Hydrogeological Exploration" between Georgian Branch of China Nuclear Industry 23 Construction Co. Ltd. and Georgian Geophysical Society Ltd., from December of 2020 through May of 2021, a group of scientists accomplished the geophysical and hydrogeological surveys on the territory of Gudauri to identify the areas of interest in terms of groundwater extraction.

Keywords*: electrical survey, vertical electrical sounding (VES), hydrogeology, testing.*

1. Introduction

The specific goal of the studies was to identify and isolate the ground aquifers in the study area in Gudauri. The studies aimed to describe the volcanic rocks of different resistance and, finally, to identify the areas of concern in view of groundwater extraction.

In order to study the underground structures, the geophysical surveys were accomplished with vertical electrical sounding (VES) method by using the following geophysical tools: Canadian SARIS and Italian Earth Resistivity Meter 16GL-N. The studies were based accomplished according to the standard vertical electrical sounding (VES) methods [1,2].

2. Data and methods

In the course of the initial surveys, one of the prospective sites was selected on the territory of Gudauri, the "The Panorama District", to conduct the detailed survey. New 24 VES profiles were provided. Following the complex terrain, the lengths of the profiles varied from 500 to 1000 m.

During the field works, for each "VES station", ground resistance was measured along the profile steps of 15 m, 30 m, etc. The field data were calculated by considering the resistances of different layers and their bedding depths using IXID and IPI2WIN softwares.

Then, the boreholes were drilled and the logging surveys and pumping works were accomplished on the alternative locations. The groundwater level was measured at the depth of 87.3 m during the geophysical surveys of borehole #1. Most likely, the aquifer at this depth has several layers. The test results and calculated hydrodynamic parameters are discussed in the present article.

3. Results and discussion

Based on the data of 24 VES points of observation, the possible bedding depth and the strength of the underground water were calculated (Fig. 1,2).

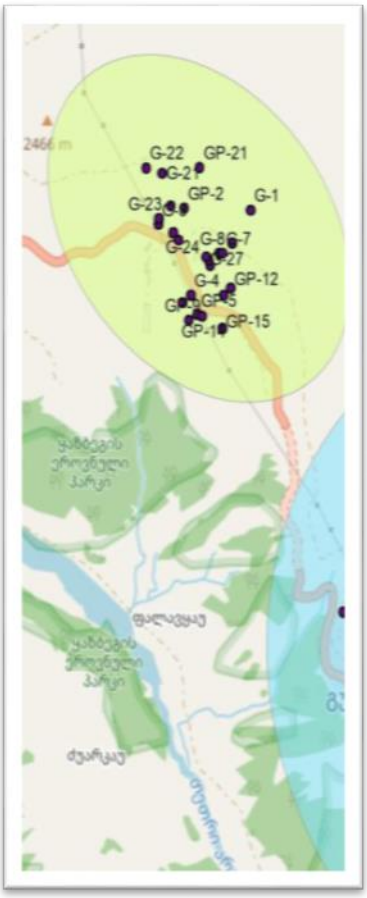

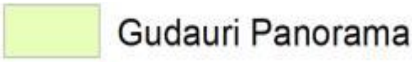

Below are the graphs of resistance distribution for „G-21” and „GP-2” VES points of observation as an example.

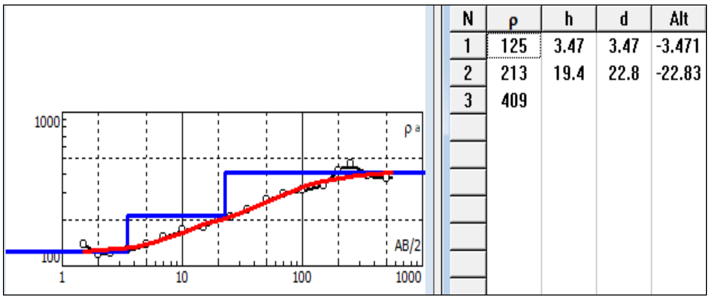

N	ρ	h	d	Alt
1	125	3.47	3.47	-3.471
2	213	19.4	22.8	-22.83
3	409			

G-21

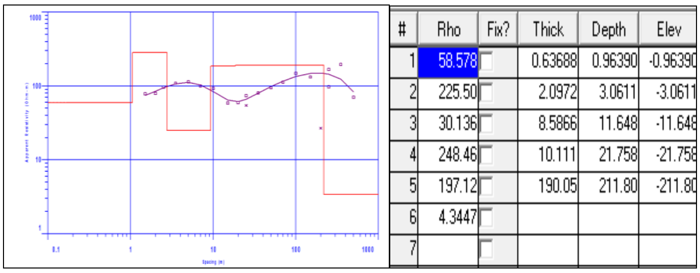

#	Rho	Fix?	Thick	Depth	Elev
1	58.578		0.63688	0.96390	-0.96390
2	225.50		2.0972	3.0611	-3.0611
3	30.136		8.5866	11.648	-11.648
4	248.46		10.111	21.758	-21.758
5	197.12		190.05	211.80	-211.80
6	4.3447				
7					

GP-2

Fig. 1. Location of “VES” profiles

Fig. 2. Profiles VES G-21 and GP-2

Fig. 3 shows the location of the VES points of observation of the auriferous and ‘dry’ layers.

As per the methodology, it is possible to connect short VES profiles and count the data to make long profiles. Fifteen lateral and longitudinal profiles were plotted (Fig. 4). Their lengths vary from 500 to 1000 m. The average distance between the profiles is 250-500 m. A geo-electric section and resistance distribution image are gained along each profile (Fig. 5).

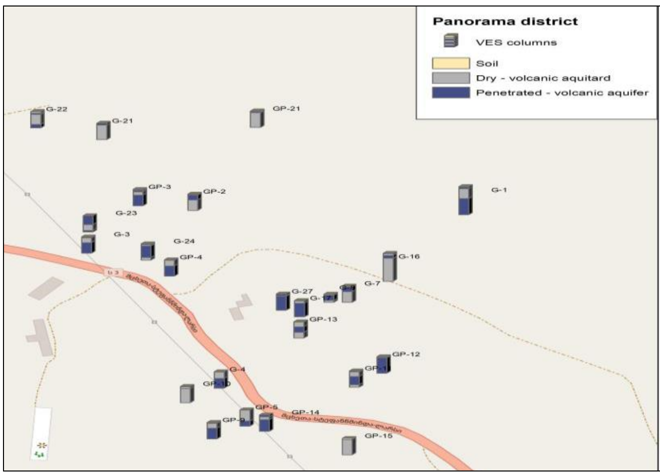

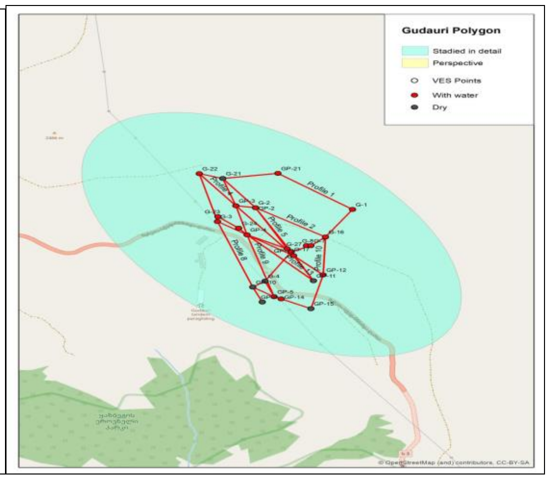

Fig..3. Locations of water-bearing and ‘dry’ VES curves in “Panorama District”

Fig. 4. Plan of location of connected profiles

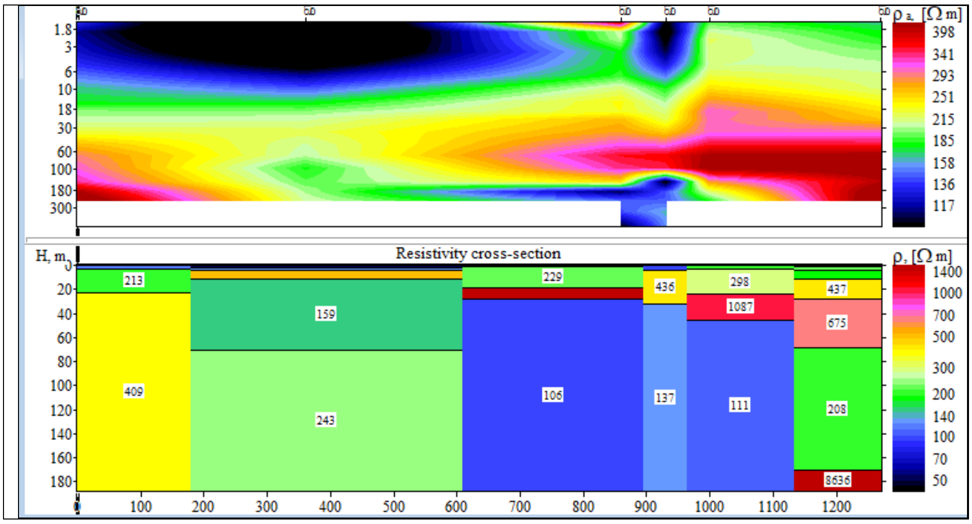

Fig.5. Profile #15 VES Nos. G-21; GP-2; G-27; G-17; GP-13; GP-11

By counting the values of resistance, the types of soil and water-bearing capacities were determined (Table 2).

Table 2. Values of profile resistance and lithology

ID	Lithology	From	To	Strength	X	Y	Z
GP-2	Soil	0	0.75	0.75	456386	4704937	2288
	Water-resistant sand-loamy soil	0.75	4.31	3.56			
	Water-bearing sand-loamy soil	4.31	24.7	20.39			
	Water-resistant sand-loamy soil	24.7	146	121.3			
	Water-bearing sand-loamy soil	146	344	198			

By using the obtained results and "Starter" software, the comparative geological sections were plotted along the geophysical profiles (Fig. 6) to describe the location of the water-bearing horizon in the study area.

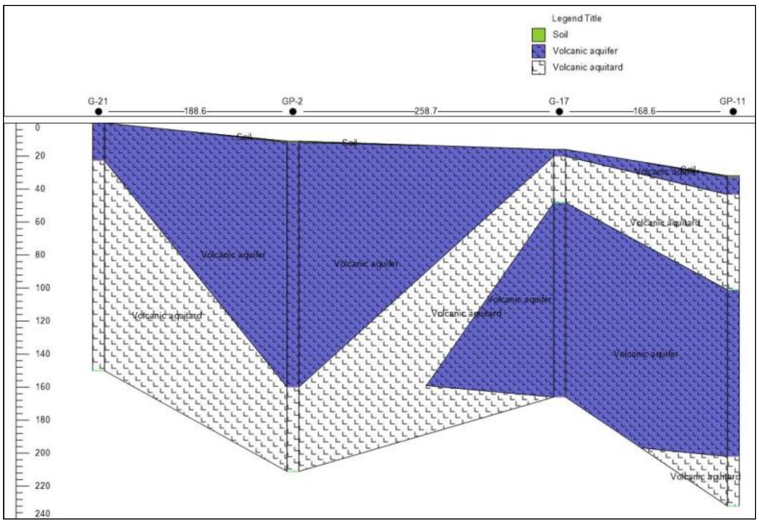

Fig. 6. Profile #5

As the data of profile #5 (which incorporates short profiles G-21; GP-2; G-17; GP-11) suggest, there are two aquifers identified: the former, which is the surface water-bearing layer, is found at the depth of 0-20 m, all along the section from the surface, and another underground water-bearing layer is fixed at the depth of 150 m (under point GP-2), varying between 30 and 150 m (for G-17) and 17 and 170 m (for GP-11).

Total of 11 such profiles were plotted. Based on the obtained results, by using "Voxler-4" software, a 3D model of the study area was developed that established that the aquifers are mostly common in the "lowland" areas built with old alluvial, delluvial and prolluvial layers and covered with a lava layer.

Following the obtained results, two underground water-bearing horizons may be identified: the former is developed in the fissure zones of lava layers at the depth of 2-10 m and the latter is developed in the lava strata of breccias and alluvial-delluvial deposits. Its strength varies between 40 and 60 m. Following the available studies, the perspective areas were identified where the boreholes may be drilled (VES observation points GP-5; GP-14; GP-15; GP-16. Fig. 7).

4. Conclusion

Recommendations given following the exploration and geophysical studies. For the full exposure of the aquifer and study of the hydrodynamic parameters, the boreholes (approximately 200-meter-deep) are to be drilled in the strongest "perspective" sites of the study area.

References

[1] Vertical electrical sounding, practical course "The Basics of Geophysical Methods" for geological students, Moscow, 2007, p. 31.

[2] Kirsch R. Croundwater Geophysics. Springer Berlin Heidelberg, New-York, ISBN 10 3-540-29383-3, 2006, p. 494.

[3] Razmadze-Brokishvili T., Varamashvili N., Melikadze G., Chikadze T., Kajaia G. Investigate Depth of Water Table and Thickness of Aquifer Using Geophysical (Electrometric) Methods, the Case in the Sachkhere Municipality. Transactions of Mikheil Nodia Institute of Geophysics, ISSN 1512-1135, vol. LXXII, 2020.

მიწისქვეშა წყალშემცველი ჰორიზონტის გამოყოფა გეოფიზიკური (ელექტრომიებების) მეთოდით გუდაურის ტერიტორიის მაგალითზე და მისი ჰიდროგეოლოგიური შესწავლილობა

გ. მელიქაძე, ნ. ვარამაშვილი, ნ. ხუნდაძე, თ. რაზმაძე-ბროკიშვილი, ნ. კაპანაძე, ა. ჭანკვეტაძე, თ. ჭიკაძე

რეზიუმე

დაბა გუდაური წარმოადგენს სამთო სათხილამურო კურორტს საქართველოში. მდებარეობს ყაზბეგის მუნიციპალიტეტში, ცენტრალური კავკასიონის სამხრეთ ფერდზე, თბილისიდან 120 კმ-ში და ზღვის დონიდან 2196 მ. სიმაღლეზე. საკურორტო ზონაში მზარდი ინფრასტრუქტურული ობიექტებისა და დამსვენებლების გამო არსებული წყალმომარაგების სისტემები დამატებითი წყლის დებიტის შქმნას საჭიროებს, რათა ზამთრის სეზონზე გუდაურის სტაბილური წყალმომარაგება უზრუნველყოს. ამიტომ, რეგიონული განვითარებისა და ინფრა-

სტრუქტურის სამინისტროს გაერთიანებული წყალმომარაგების კომპანია, დაბა გუდაურში, იწყებს სასმელი წყლისა და კანალიზაციის სისტემების მშენებლობას. სამუშაოები ითვალისწინებს გუდაურსა და მიმდებარე სოფლებში თანამედროვე სტანდარტების შესაბამისი სასმელი წყლისა და კანალიზაციის ინფრასტრუქტურის მოწყობას. პროექტის ფარგლებში, შპს „ჩინურ ბირთვული ინდუსტრიის 23 საკონსტრუქტორო ბირო“-ს საქართველოს ფილიალსა და შპს „საქართველოს გეოფიზიკური ასოციაცია“ - ს შორის არსებული „ჰიდროგეოლოგიური შესწავლის განხორციელებაზე შეთანხმების“ ფარგლებში, მეცნიერთა ჯგუფმა 2020 წლის დეკემბრიდან 2021 წლის მაისის ჩათვლით, გუდაურის ტერიტორიაზე, ჩაატარა გეოფიზიკური და ჰიდროგეოლოგიური კვლევები რათა გამოვლენილიყო ის უბნები, რომლებიც საინტერესოა მიწისქვეშა წყლების მოპოვების თვალსაზრისით.

Выявление водоносного горизонта подземных вод геофизическими (электроразведочными) методами на примере района Гудаури и его гидрогеологическое изучение

Г.И. Меликадзе, Н.Д. Варамашвили, Н.Ш. Хундадзе, Т.Дж. Размадзе-Брокишвили, Н.А. Капанадзе, А.Ш. Чанкветадзе, Т.Г . Чикадзе

Резюме

Гудаури - горнолыжный курорт в Грузии. Он расположен в муниципалитете Казбеги, на южном склоне Центрального Кавказа, в 120 км от Тбилиси и на высоте 2196 м над уровнем моря. По мере увеличения количества инфраструктурных объектов и посетителей в курортной зоне существующие системы водоснабжения нуждаются в дополнительных расходах воды для обеспечения стабильного водоснабжения Гудаури в зимний период. Поэтому Объединенная компания водоснабжения Министерства регионального развития и инфраструктуры Грузии приступает к строительству систем питьевого водоснабжения и канализации в поселке Гудаури. Работы предусматривают строительство современной инфраструктуры питьевой воды и канализации в Гудаури и близлежащих селах. В рамках проекта, в рамках «Соглашения о гидрогеологических исследованиях» между Грузинским филиалом China Nuclear Industry 23 Construction Co. Ltd. и Грузинским геофизическим обществом Ltd., с декабря 2020 года по май 2021 года группа ученых выполнила геофизические исследования и гидрогеологические изыскания на территории Гудаури для выявления территорий, представляющих интерес с точки зрения добычи подземных вод.

Journal of the Georgian Geophysical Society, e-ISSN: 2667-9973, p-ISSN: 1512-1127
Physics of Solid Earth, Atmosphere, Ocean and Space Plasma, v. 24(2), 2021, pp. 43 - 51

Efficiency of Vertical Electrical Sounding in Water Prospecting Problems in Adjara Region (Khelvachauri Municipality)

Nodar D. Varamashvili, Avtandil G. Tarkhan-Mouravi, Nugzar Ya. Ghlonti

Ivane Javakhishvili Tbilisi State University, Mikheil Nodia Institute of Geophysics

ABSTRACT

Different prospecting methods are used in geophysics. The electrical method of prospecting is one of the major fields of applied geophysics. Electrical methods can be divided into two types depending on what source is used, natural or artificial. The first is called natural electric field (NF) methods, and the second is called resistance methods. The vertical electrical sounding method is one of the main resistance methods used in the study of rock watering. The materials presented in our paper are obtained in Khelvachauri district (Georgia), by vertical electro-sounding method to study of rock humidity and research on the possible existence of groundwater at different depths.

Key words: *Vertical electrical sounding (VES), resistivity, groundwater*

Introduction

If the 19th century was dominated by the acquisition and defence of land (territory) and the 20th century was dominated by the acquisition and control of oil and energy resources, then the 21st century will be dominated by the politics of water. Geophysical methods, mainly electroprospecting methods, are used to search and study groundwater. In electroprospecting (resistance method) is used artificial power source. The electricity reaches the ground through the power electrodes and the difference between the arised potentials is measured by the receiving electrodes on the earth surface. If the environment is homogeneous, the resistance method gives us true conductivity, which will not depend on the configuration of electrodes and the position of electrodes on the surface of the earth, since the true conductivity is a constant. In electric resistivity imaging (ERI) electric currents are injected into the ground and the resulting potential differences are measured at the surface, yielding information about the distribution of electrical resistivity below the surface. Finally, this gives an indication of the lithological and structural variation of the subsoil (since resistivity depends on sediment porosity and pore water). In the shallow subsurface, the presence of water controls much of the conductivity variation. Measurement of resistivity is, in general, a measure of water saturation and connectivity of pore space. This is because water has a low resistivity and electric current will follow the path of least resistance. Increasing saturation, increasing salinity of the underground water, increasing porosity of rock (water-filled voids) and increasing number of fractures (water-filled) all tend to *decrease* measured resistivity. Increasing compaction of soils or rock units will expel water and effectively increase resistivity.

In environment ΔV, and therefore impedance ρ should be dependent on the configuration and location of electrodes, as secondary fields influence on the primary field [2]. Therefore, the measured ρ value in nonhomogenous environments is called an apparent resistivity and is signed as ρ_a. The coefficient of reaccount for uneven environment depends on the configuration of electrodes. Different configurations of the electrodes are used according to the type of problem. In our tasks we used the Schumerberger method. Receiver MN electrodes are fixed in the center of the device, while the distance between the current AB electrodes increases gradually [3].

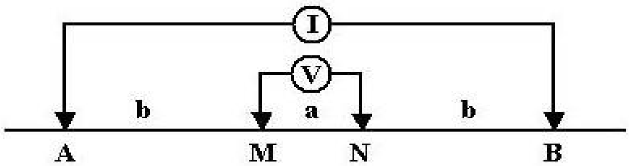

Fig.1. Schlumberger method of vertical electrical sounding

The vertical electrical sounding (VES) method relies on the fact that the greater is the distance between of current electrodes (AB), deeper penetrating the current, than from more deep layers we receivs information by measured potential on the electrode.

Electrical resistance table for some of the rocks

The name of the rock	Electrical resistivity (ohm. m)		
	min	typical	max
clay	5	10	15
loam	10	30	50
sand clay	30	50	80
Water-saturated sands	50	80	200
Sands slightly moist	100	150	500
Dry sands	200	500	10000
Carbonate rocks weakly cracked	500	1000	5000
Intrusive rocks weakly fractured	1000	2000	10000
Bulk	30	50	500
Permafrost rocks of various ice content	500		80000
Ores minerals conductors(in mostly sulphides)	0,001		1-5

As we see from this table [2], the electrical resistance is different for different rocks that allow us to be more confident about the definition of rocks, the water content in them, and to overcome various geophysical tasks.

Study region

Groundwater exploration was carried out in Khelvachauri district by means of electric search (vertical electrical sensing). Khelvachauri municipality is located in the extreme southern part of western Georgia. The territory of the municipality is a hilly foothill zone. The Adjara basin is bordered by Meskheti from the north, Shavsheti from the south, Arsiani ridges from the east, and Guria foothills from the west.

According to E. Gamkrelidze tectonic zones, the territory of Khelvachauri municipality includes the Abastuman-Boshur subzone of the central zone of the Adjara-Trialeti fold system. The tectonic structure of Adjara is not difficult. Only two large folds are established here, which extend over the entire territory of Adjara.

Middle geocene volcanic tuff breccias, breccias, tuffs and volcanic formations of various origins are involved in the geological structure of the municipality. In most cases it is covered with deluvial sediments of the fourth age, clay-clays and inclusions of various coarse-grained materials, and in the river valleys with alluvial sediments. Volcanogenic formations are in most cases chemically depleted and are characterized by sharply reduced physical-mechanical properties. This circumstance creates a favorable environment for the development of natural geological processes.

According to the hydrogeological zones of Georgia, the study area is located in the area of the Adjara-Imereti fissured water pressure system. The following aquifers and complexes are distinguished within it:

1. Aquifer horizon of modern alluvial sediments, which is distributed in the river valleys in the form of strips of different widths (1-1.5 km). Pebbles predominate in the riverbeds, which in lowland conditions turn into rock-sandy and loamy; Total capacity ranges from 2 to 15 m; Nutritional sources are atmospheric precipitation,

filtrates, alluvial, alluvial-deluvial sediments, and downstream water pressure horizons. The use of this precipitate as drinking water is impossible due to its low quality;

2. The aquifer hopping of the undivided alluvial and Old Quaternary marine sediments is particularly widespread along the river. On the right bank of Chorokhi - in Kakhaberi lowland. It is represented by pebbles, clays and sandy compositions. The total precipitation capacity is about 150 m. The lower horizon waters of this complex are suitable for drinking.

3. The aquifer of the Middle Eocene sedimentary aquifer is lithologically represented by alternating andesitic and porphyritic lavas, tuff breccias, tuff sandstones, tuffs, argillites and marls; It is fed at the expense of atmospheric precipitation and river waters and is suitable for drinking.

Results of geophysical survey

It was necessary to investigate the watering of the rocks at different depths in order to subsequently drill wells to obtain drinking water. Electrical prospecting works were carried out in several villages of Khelvachauri district (Fig. 2), based on the appeal of the Khelvachauri Municipality City Hall Ltd. "Khelvachauri Water Channel" administration.

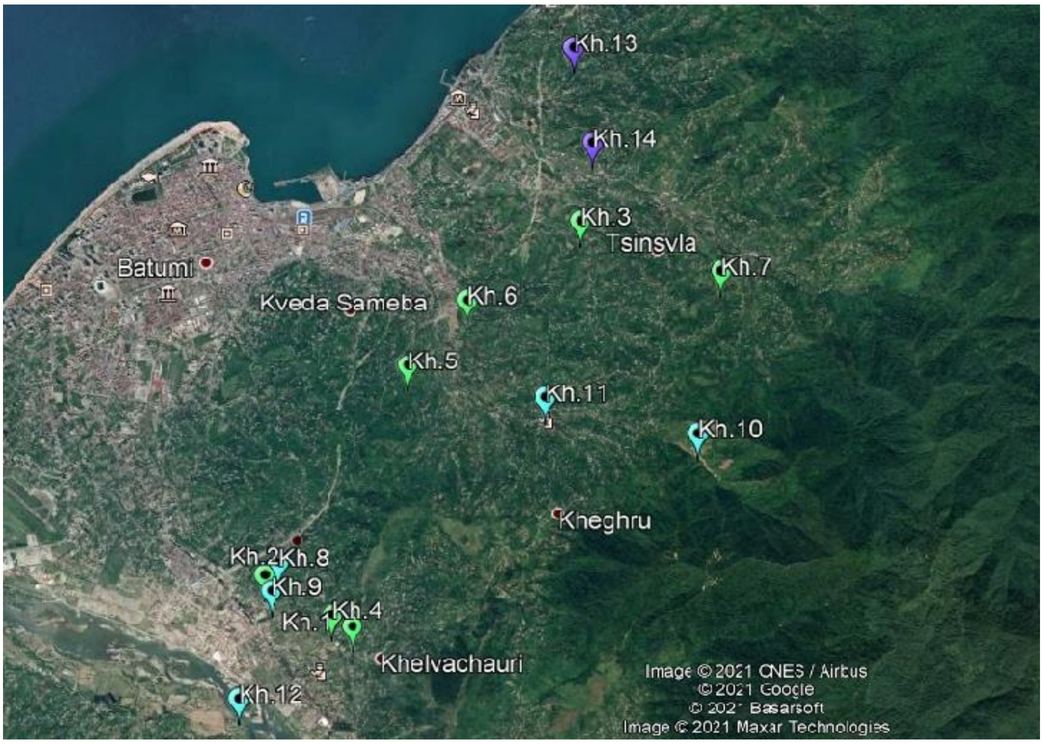

Fig.2. Locations in Khelvachauri district where electrical exploration works were carried out

To solve the given task, geophysical surveys were conducted by the method of vertical electric sensing (VEZ) of the constant current. The method is based on the use of artificially created electromagnetic fields on the diurnal surface, which allows the lithological differentiation of rocks according to the change in the depth of the specific electrical resistance (ρ) of the layers. Due to the specifics of the work, the studies were carried out with a Schlumberger four-electrode symmetrical unit with a maximum expansion of the feeding electrodes AB = 500 m, which allowed electrical sensing to be carried out to a depth of 140-150 m. The works were carried out using an Italian-made electrometric device Earth Resistivity Meter PASI 16GL-N (Fig. 2). Data processing was done through a certified IPI2WIN program.

a. **b.**

Fig.3. a) Earth Resistivity Meter PASI 16GL-N, b) measurement process.

The research was conducted in Khelvachauri district, at 14 different points, which was distributed in almost the entire territory of the district. Based on the obtained results, we can form a certain idea about the depth of groundwater in the area, the thickness of the watered layers, the lithology of the subsurface.

1. The first sounding (Ves-1, Fig. 4.1) was conducted in the village of Zanakidze (Fig. 2, Kh.1). Distribution of current supply electrodes AB = 500 m. A classic type curve is obtained. The first layer with a thickness of h_1 ≈ 1 - 1.5 m and a resistance ρ_1 ≈ 40 - 50 ohm.m-s corresponds to the soil cover. The second layer with a thickness of h_2 ≈ 30 m and a resistnance ρ_2≈ 20 - 22 ohm.m-s should be represented by clay and gravel. The third powerful layer of with electrical resistance ρ_3 ≈ 100 - 150 ohm.m-s, correspond to volcanic formations (breccias, tuff-breccias, tuffs). The aquifer horizon probably starts at the border of the second and third layers, at a depth of about 30-31 m from the surface.
2. Ves-2 (Fig. 4.2) was made in the village of Sharabidze (Fig. 2, Kh.2), behind Medina. Distribution of power electrodes AB = 500 m. The first layer with a thickness of h_1 ≈ 15 - 20 m and with el.resistance ρ_1 ≈ 65 - 70 ohm.m, corresponds to slightly watered quaternary deluvial sediments (clayey, coarse-grained inclusions). This layer is transferred to the Middle Eocene volcanic formations (alternation of andesitic and porphyritic lavas, argillites, marls). This layer's own electrical resistance ρ ≈ 300 ohm.m. From a depth of about 120 - 130 m from the surface will be observed a sharp drop in el.resistance, which in some ways indicates the existence of an aquifer.

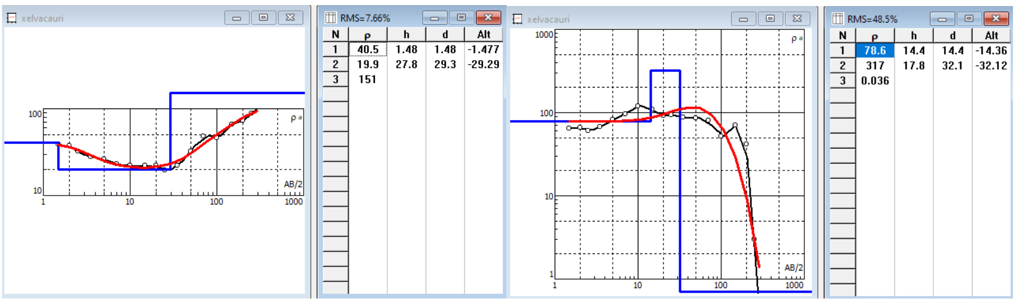

1. 2.

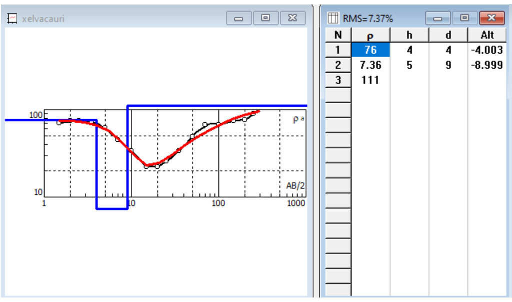

3.

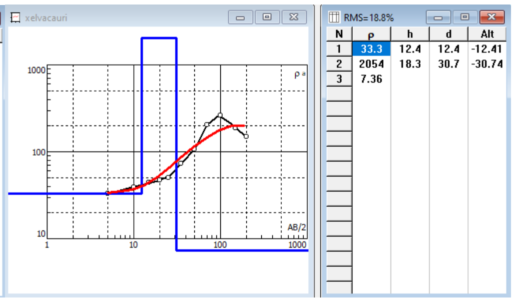

4.

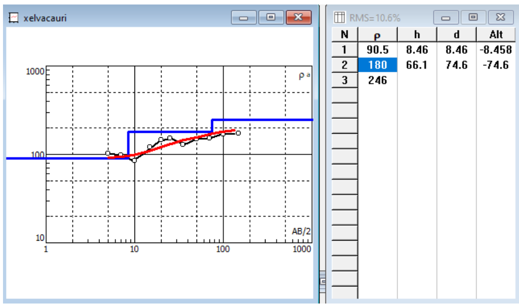

5.

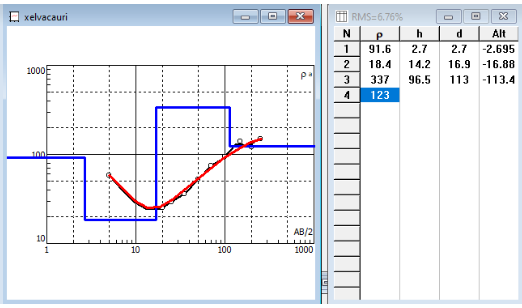

6.

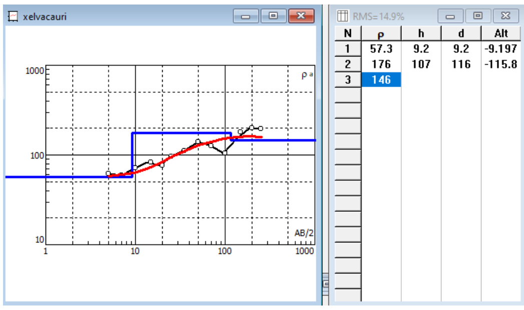

7.

Fig.4. Vertical electrical sounding curves performed in 7 different points in Khelvachauri district: 1. Zanakidzeebi village, **Kh.1**, 2. Sharabidzeebi village, behind Medina, **Kh.2**, 3. Tsinsvla village, Vaneli district, **Kh.3**, 4. Sharabidzeebi village, **Kh.4**, 5. Ganaxleba village, **Kh.5**, 6. Lower Sameba, **Kh.6**, 7. Village Tsinsvla, **Kh.7**.

3. Ves-3 (Fig. 4.3) was made in the village of Tsinsvla (Fig. 2, Kh.3), in the district of Vaneli. Spreading of the power electrodes = 500 m. The first layer with a thickness of $h_1 \approx 2.5$ - 3 m and a specific el.resistance $\rho_1 \approx$ 70 ohm corresponds to deluvial precipitation. The second layer with a thickness of h_2 ≈ 5 - 6 m and the electrical resistance of about 7 - 10 ohms should be represented by clay. The following sequence is volcanic formations with el.resistance ρ ≈ 100 - 110 ohm. The aquifer appears to be separated at a depth of 110 - 120 m, but watering may appear in the higher layers.4.
4. Ves-4 (Fig. 4.4) was made in the village of Sharabidze (Fig. 2, Kh.4). Spreading of current supply electrodes AB = 400 m. The Ves-4 point is located next to the operating well. The first slightly watered layer is at a depth of about 15 m. The drinking water horizon is probably located at a depth of about 130-140 m from the surface and is represented by volcanic formations.
5. Ves-5 (Fig. 4.5) was made in the village Ganaxleba (Fig. 2, Kh.5). Due to the difficult terrain, the maximum spreading of the electrodes is AB = 300 m. The first 15 - 20 m corresponds to the slightly watered sediments of the quaternary (gravel, clayey, coarse-grained inclusions), which then move into volcanic formations. Due to the geometry of the electrode expansion, the probing depth does not exceed 100-110 m. No signs of watering will be observed at this depth.

6. Ves-6 (Fig. 4.6) was made in the village Qveda Sameba (Fig. 2, Kh.6). Maximum spreading of power electrodes AB = 500 m. The first watered horizon corresponding to groundwater ($h_1 \approx 12$ - 15 m, $\rho_1 \approx 20$ - 25 ohm) is represented by alluvial sediments (gravel, sand). The potable aquifer may be located at a depth of approximately 110 - 120 m in the Middle Eocene volcanic rocks (tuff breccias, breccias, sandstones), with resistance ≈ 140 -150 ohm.
7. Ves-7 (Fig. 4.7) was made in the village of Tsinsvla (Fig. 2, Kh.7). Maximum spreading of power electrodes AB = 500 m. The first aquifer is separated at a depth of 22 - 25 m in alluvial-deluvial sediments of the quaternary. The drinking water layer is probably located at a depth of about 110-115 m in the Middle Eocene volcanic rocks.
8. Further research (Ves-8, Fig. 5.1) was conducted in the village of Sharabidzeebi, in the Vaneli district of Medina (Fig. 2, Kh.8). An HK type curve is obtained. The first layer with a thickness of $h_1 \approx 1$ - 1.5 m and a specific impedance $\rho_1 \approx 35$ - 50 ohm.m-s corresponds to the soil cover. The second layer with a thickness of $h_2 \approx$ 10-12 m and a specific resistance $\rho_2 \approx$ 25 - 30 ohm.m-s should be represented by clay. Then comes a powerful layer that matches the pebble with tuff-breccia inserts, with el.resistance $\rho_3 \approx 65$ - 80 ohm.m. Signs of watering should be observed from 15-20 meters, but to get a sufficient amount of water should be drilled to a depth of 130-140 meters.
9. Ves-9 (Fig. 5.2) was also made in the village of Sharabidzeebi, near Medina (Fig. 2, Kh.9). An Q-type curve of specific electrical resistance is obtained. The first watered layer should be located at a depth of 12-15 m from the surface, in the old Quaternary marine sediments. The second aquifer is probably located at a depth of 100-120 meters.

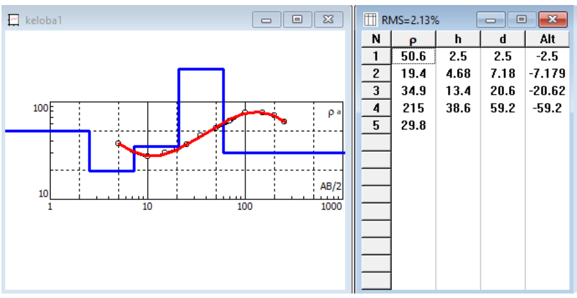

1.

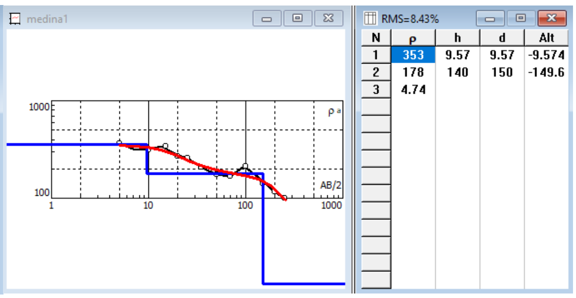

2.

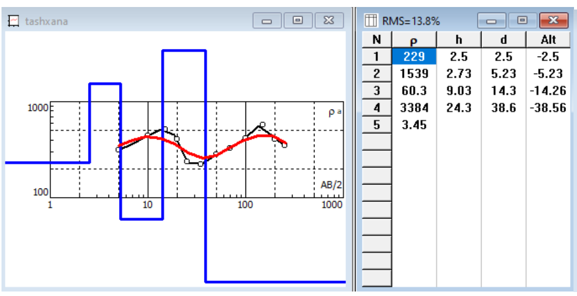

3.

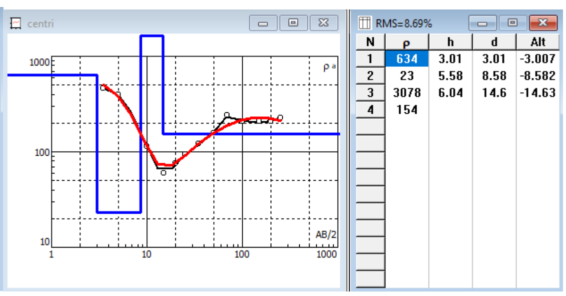

4.

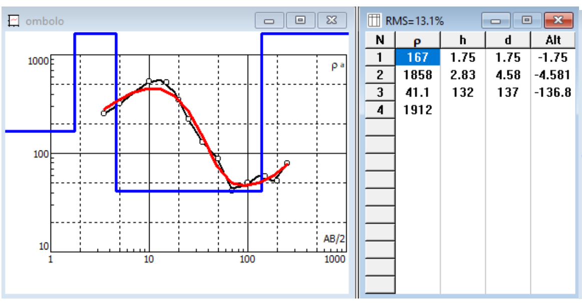

5.

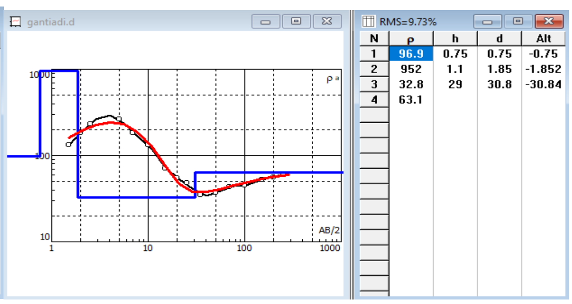

6.

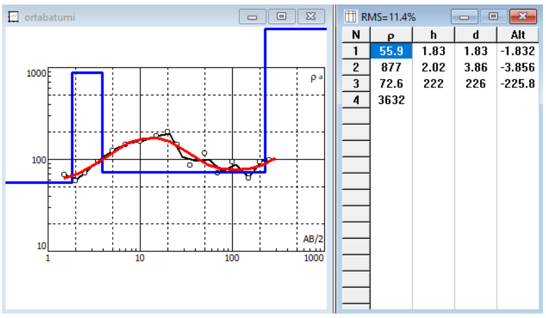

7.

Fig.5. Vertical electrical sounding curves performed in 7 different points in Khelvachauri district: 1. Sharabidzeebi village, Medina1, **Kh.8**, 2. Sharabidzeebi village, Medina2, **Kh.9**, 3. Akhalsheni village, **Kh.10**, 4. Akhalsheni village, center, **Kh.11**, 5. Village Ombolo, **Kh.12**, 6. Village Gantiadi, **Kh.13**, 7. Village Ortabatumi, **Kh.14**.

10. Ves-10 (Fig. 5.3) was made in the village of Akhalsheni, (Fig. 2, Kh.10). The KHK type curve of specific electrical resistance is obtained. The environment is mainly composed of Middle Eocene volcanic formations (tuff breccias, andesites, porphyrites). Increased humidity should be observed from 30-35 meters. The main horizon is probably located at a depth of 130-140 meters, but the presence of water at a depth of 80-90 meters is not ruled out.
11. Ves-11 (Fig. 5.4) was also made in the village of Akhalsheni, in the center (Fig. 2, Kh.11). An HK type curve of specific electrical resistance is obtained. Signs of water should appear from a depth of 18-20 meters in the Quaternary sediments (loamy, gravel). The aquifer is likely to be located at a depth of 100–110 m in volcanic rocks.
12. Ves-12 (Fig. 5.5) was made in the village of Ombolo, (Fig. 2, Kh.12). An KH type curve of specific electrical resistance is obtained. The first aquifer should be opened from 20-25 m into the quaternary sediment. The second aquifer is probably located at a depth of 110-120 meters.
13. Further research (Vez-6, Fig. 3a) was conducted in the village of Gantiadi (Fig. 2, Kh.13). A KH type curve is obtained. The first aquifer should be opened from 8-10 m into the quaternary sediment. The second aquifer is probably located at a depth of 75-80 meters.
14. Vez-7 (Fig. 3b) was made in the village of Ortabatumi (Fig. 2, Kh.14). An KH type curve of specific electrical resistance is obtained. The first watered layer should be located at a depth of 27-30 m from the surface, in the old Quaternary marine sediments. The second aquifer is probably located at a depth of 110-120 meters.

Conclusion

1. The method of geophysical survey (vertical electrical sensing) was found to be effective for these areas to solve the given tasks and well reflects the existence of a geological environment with different subsurface electrical characteristics at the observation points. The reliability of the results is confirmed in some cases by the drilled wells.
2. Based on the surveys conducted at all points of observation, the geophysical characteristics of the studied environments are more or less different from each other. This indicates on the one hand the similarity of the geological environments here and on the other hand the objectivity of the studies conducted.
3. Based on the analysis of the obtained results, the presence of humidity increased layers at the observation points is well expressed. Most of the vertical electrical sounding curves show watered areas. It can be said that Khelvachauri district is quite rich in groundwater. There are places (for example, the area around Kakhaberi Valley) where particularly strong watered layers can be assumed. However, it should also be noted that there are areas where the likelihood of the existence of watered layers is quite low.

4. The results are quite informative, but it is necessary to continue the work to get a more complete picture of the deep distribution of groundwater in the region and their possible capacities. Groundwater micro-zoning through vertical electrical sensing will facilitate the separation of desirable areas for geophysical work.
5. Finally, it should be noted that although the vertical electrical sensing method is a powerful and experienced method for groundwater exploration, it should also be emphasized that at this stage no method can ensure the exact amount of water inflow and the degree of its mineralization. Their real determination can only be done after drilling a well.

References

[1] Varamashvili N., Chelidze T., Devidze M., Chikhladze V. Laboratory and mathematical modeling of landslides triggered by external factors. Field research. Transactions of Mikheil Nodia Institute of Geophysics of Ivane Javakhishvili Tbilisi State University, vol. LXVIII, Monography, Tbilisi, 2017, (in Georgian).
[2] Chelidze T., Varamashvili N., Chelidze Z., Kiria T., Ghlonti N., Kiria J., Tsamalashvili T. Cost effective telemetric monitoring and early warning systems for signaling landslide initiation. Mikheil Nodia Institute of Geophysics of Ivane Javakhishvili Tbilisi State University. Monography. Tbilisi, 2018 (in Georgian).
[3] Varamashvili N., Tefnadze D., Amilaxvari D., Dvali L., Chikadze T., Qajaia G. Vertical electric sounding in water search tasks and for landslide hazards assessment International Scientific Conference „Modern Problems of Ecology“, Kutaisi, Georgia, 21-22 September, 2018
[4] Odilavadze D., Tarkhan-Mouravi A., Varamashvili N., Arziani Z. Prevention of the Danger Triggered by an Earthquake of Exogenous and Endogenous Processes, using a Combination of Geophysical-Geoelectric Methods in Geotechnics. International Scientific Conference Natural Disasters in Georgia: Monitoring, Prevention, Mitigation. Tbilisi 2019.
[5] Varamashvili N.D., Tefnadze D.V., Amilakhvari D.Z., Dvali L.B., Chikadze T.G., Qajaia G.T., Varamashvili D.N.. Water search and landslides study using electroprospecting. Journal of the Georgian Geophysical Society, 22(1), 2019.
[6] Reilly T.E., Dennehy K.F., Alley W.M., Cunningham W.L. Ground-Water Availability in the United States. U.S. Geological Survey, Reston, Virginia: 2008
[7] Groundwater Geophysics, a Tool for Hydrogeology. Reinhard Kirsch (Ed.). Springer-Verlag Berlin Heidelberg, 2009
[8] Vertical electrical sounding, practical course “Basics of geophysical methods” for students of geological specialties, Moscow, 2007 (in Russian)
[9] Electroprospecting: a guide to electrical exploration practice for students of geophysical specialties. Edited by prof. V.K. Khmelevskoy, Assoc. I.N. Modina, Assoc. A.G. Yakovleva – Moscow: 2005 (in Russian)

ვერტიკალური ელექტრული ზონდირების ეფექტურობა აჭარის რეგიონში (ხელვაჩაურის მუნიციპალიტეტში) წყლის ძიების ამოცანებში

ნ. ვარამაშვილი, ა. თარხან-მოურავი, ნ. ღლონტი

რეზიუმე

გეოფიზიკაში გამოიყენება ძიების სხვადასხვა მეთოდები. ძიების ელექტრული მეთოდი (ელექტრომიება) გამოყენებითი გეოფიზიკის ერთ-ერთი ძირითადი დარგია. ელექტრული მეთოდები შეიძლება ორ ტიპად დავყოთ იმის მიხედვით, თუ რა წყარო გამოიყენება, ბუნებრივი

თუ ხელოვნური. პირველ მათგანს ბუნებრივი ელექტრული ველის (ბევ) მეთოდებს უწოდებენ, ხოლო მეორეს -წინააღმდეგობის მეთოდებს. ვერტიკალური ელექტრული ზონდირების მეთოდი ძირითადია წინააღმდეგობის მეთოდებს შორის, რომლებიც გამოიყენება ქანების გაწყლიანების კვლევისას. ჩვენს ნაშრომში წარმოდგენილი მასალები მიღებულია, ხელვაჩაურის რაიონში, ვერტიკალური ელექტრული ზონდირების მეთოდით ქანების გაწყლიანებას და მიწისქვეშა წყლების სხვადასხვა სიღრმეებზე შესაძლო არსებობის კვლევისას.

Эффективность вертикального электрического зондирования в задачах поиска воды в Аджарском регионе (муниципалитет Хелвачаури)

Н. Д. Варамашвили, А.Г. Тархан-Моурави, Н.Я. Глонти

Резюме

В геофизике используются разные поисковые методы. Электроразведка - одно из важнейших направлений прикладной геофизики. Электрические методы можно разделить на два типа в зависимости от того, какой источник используется, естественный или искусственный. Первый называется методом естественного электрического поля (НЭ), а второй - методом сопротивления. Метод вертикального электрического зондирования - один из основных методов сопротивления, используемых при изучении обводненности горных пород. Материалы, представленные в нашей статье, получены в Хелвачаурском районе (Грузия) методом вертикального электрического зондирования с целью изучения влажности горных пород и исследования возможности существования подземных вод на разных глубинах.

Journal of the Georgian Geophysical Society, e-ISSN: 2667-9973, p-ISSN: 1512-1127
Physics of Solid Earth, Atmosphere, Ocean and Space Plasma, v. 24(2), 2021, pp. 52 - 58

Prospects for Mitigating the Effects of the Catastrophic Flood on the Vere River through a Temporary Reservoir

Zurab A. Kereselidze, Tengiz V. Kiria, Jemal K. Kiria, Nodar D. Varamashvili, Manana M. Nikolaishvili

Ivane Javakhishvili Tbilisi State University, Mikheil Nodia Institute of Geophysics

ABSTRACT

The river Vere is a typical mountain river with its gorge of more than 40 km length, range of heights up to 1500 m. This river is considered to be one of the most dangerous rivers in the east Georgia due to its frequent catastrophic overflows. One of the aims of this paper was to estimate the approximate volume of the temporary water reservoir, formed between the Tamarashvili Highway and Gabashvili Street during the catastrophic flood in the Vere River Valley on June 15, 2015. The paper estimates that the temporary water reservoir has a strategic load to manage the catastrophic flood and its consequences, considering the maximum water consumption of the tunnel leading from Svanidze Street and the maximum water permeability of the second tunnel and also taking into account the water flowing from the slopes of temporary water reservoir.

***Key word**: flooding, water reservoir, water flow rate*

Introduction

The catastrophic flood on 13 July, 2015 in the gorge of the river Vere caused many victims and significant material damage. There is an assumption that the catastrophe was the result of torrential rain. However, we suppose that besides abundant precipitations, whose intensity, according to atmospheric radar data, was 70-80 mm, for about 3 hours [1. Banetashvili at all, 2016; 2. Amiranashvili at all, 2018], the flood was caused by the peculiarities of the artificial closed bed of the river Vere, which manifested itself in a critical increase in its hydraulic resistance [3. Kereselidze at all,2018; 4.Kereselidze, Chvedelidze,2018]. Exploitation of the river-bed began in 2010 due to construction of a highway in the last part of the gorge, which in the recent years has been under considerable urban load. The river Vere flows along ≈ 40 km long gorge and joins the main river Mtkvari. The last section of the river gorge (≈5 km) is located in the center of Tbilisi city. The river Vere is characterized with low average yearly water flow rate $Q \approx 1m^3s^{-1}$, though it is considered as one of the most potentially hazardous rivers in Georgia. Quite often, during heavy floods the water flow rate increases by two or more orders. Continuous hydrological observations on the river Vere began from 1962. However, there are quite reliable data on the catastrophic floods, which occurred in the period between 1890-1960 years. So far, the flood, which occurred on 04.07.1960, was considered as the heaviest, when during two and a half of an hour $h \approx 120$ mm precipitation was recorded. During this time, by rough estimates, the water flow rate in the river-bed in the areas of Tbilisi reached enormous value: $Q \approx 320$ $m^3 s^{-1}$. However, it was later considered that the maximum water flow in Vere did not exceed $260\, m^3s^{-1}$ [5.Kereselidze D. at all, 2011]

Thus, according to the experience obtained after the 13.06.2015 disaster it is obvious that the problem of a devastating flood, which was a great threat to Tbilisi in the past, will be actual in the future as well. Therefore, it is necessary to create a forecasting model of negative phenomena in emergency situations.

 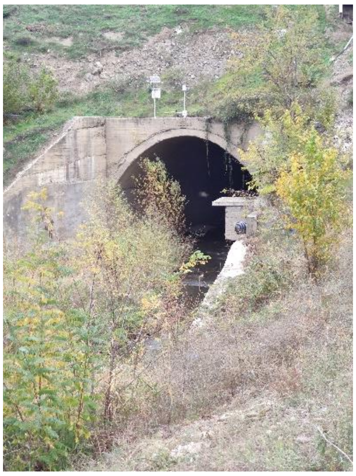

Fig.1. The entrance of the tunnel1 from Svanidze Street

  

Fig 2. The exit of the tunnel1

Constructive feature. In the 30s of the 20-th century in the areas of Tbilisi two tunnels (underground bridge) were built on the river Vere. The first tunnel was ≈ 108 m (Fig1). The old second tunnel (the old second tunnel is now the third tunnel because a new tunnel was built between the first and the old second tunnel and which (new tunnel) in our paper is referred to as the tunnel2) with the length of ≈700 m replaced the last section of the natural river-bed at the area before the confluence of the river Mtkvari. The highways passed over the tunnels. In 2010 after finishing the highway building some part (≈45%) of the natural river-bed between the inlet of the first tunnel and the river Mtkvari appeared covered due to construction of the new artificial (covered) river-bed. As a result it was a construction, a new artificial covered river-bed, consisting of seven tunnels linked to one another with open segments and had the total length of ≈ 2100 m. After the modernization the earlier constructed first tunnel became ≈ 360 m long and the old second tunnel – ≈1200 m. After completion of the construction all the tunnels were semiarch type, had flat concrete basements, compound structure made of reinforced concrete and corrugated steel leaves. It is clear that such an artificial change radically changed the geometry of the river Vere natural bed and, consequently, the hydrological parameters of the valley.

It is well known that any project of potentially vulnerable civil object should include complete assessment of negative consequences of probable disasters. It is natural that such forecasting should have been made also regarding the closed river-bed. However, as the 13.06.2015 disaster showed, seemingly, analysis of the operating mode of the closed river-bed in heavy load conditions had not been done. Supposedly, probability of significant increase of hydraulic resistance in the rather long tunnels with the corrugated inner surfaces was not considered [6. Schlichting,1974; 7.Landau, Lipschitz,1988; 8. Kereselidze

,Shergilashvil, 2016]. After the disaster the river-bed was restored in its original form. Only little corrections were made, namely, walls were built before the two tunnels for guiding the water flow. The inlets of these tunnels are located at the points of maximum bending of the open section of the artificial river-bed (Fig. 3. Tunnel 2). The open section of the ≈30 m long artificial river-bed before Tunnel 2 (Fig.3) bends to that extent that the tunnel is practically located perpendicularly to the river flow. Therefore, supposedly, in the case of increase in the water level the area between the guiding walls will become the problem area of the closed river-bed (water stagnation zone).In this case the effect of the guiding walls can be transformed in hydrodynamic funnel effect and it will additionally reduce the water flow rate in the tunnel.

Fig.3. The entrance of the tunnel 2.

Added to this is the wastewater factor in the area around Kipshidze Street during the 2015 disaster, which were: $Q \approx 30\ m^3 s^{-1}$. [4.Kereselidze at all, 2018]. If we take into account that, according to our rather strict estimation, the throughput of the closed river-bed on the is significantly less than project ($Q \approx 260\ m^3 s^{-1}$and with about 10% inaccuracy is equal to $Q \approx 200\ m^3 s^{-1}$ [4.Kereselidze, Khvedelidze,2018], this section of the Vere river-bed, between the exit of the first tunnel and the entrance of the second tunnel, is a special danger zone.

One of the aims of this paper was toestimate the approximate volume of the temporary water reservoir, formed during the flood between Tamarashvili Highway and Gabashvili Street. It should be noted that the estimated volume of the dam on Svanidze Street in the immediate after math of the disaster was clearly misrepresented. It is possible that the mistake was made by misinterpreting the effect of a power full and slide in the vicinity of Akhaldaba, according to which the Vere gorge was blocked. Consequently, a mound was formed and a large volume of mud mass was accumulated. The dam was then breached, causing the first tunnel to be closed by flood waters. According to the real picture of the catastrophe, such a thing did not happen, otherwise the scale of the destruction would have been even more grandiose. Fortunately, the landslide developed in the last stage of rainfall arrival. In other case, it is obvious that after breaking through Dam, the floodwaters could be crossed Tamarashvili Highway, which turned into a watershed. Fortunately, flooding water level could not reach just 1-1.5 meters to Tamarashvili Highway, otherwise it would have spread to a significant part of the city along with the Vere gorge.

The problem of Kipshidze street section. Thus, in terms of the future danger, we consider the problem of temporary water reservoir between Tamarashvili Highway and Gabashvili Streets to be especially topical. We built a computer model of this section of the gorge in case of its overflowing (Fig. 4). To convincingly calculate the volume of water accumulated in the gorge, we divided this part of the valley, from the exit of the first tunnel (Fig. 2) to the entrance of the second tunnel (Fig. 3), downstream into 34 parts (Fig. 4).

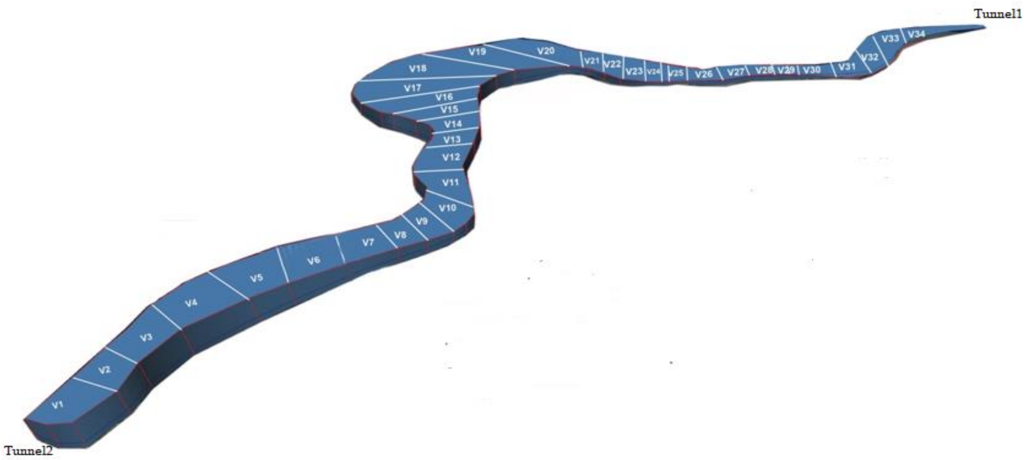

Fig.4. Temporary water reservoir model to calculate its volume

A scan be seen from Fig.4, in order to calculate the volume of the water reservoir, we need to calculate the volume of each sector and summarize them.

$$V = \sum_{i=1}^{34} V_i$$

Volume of each sector

$$V_i = S_i\, h_i,$$

Where S_i is the surface area of the i-th sector, and h_i is the height from the deepest point in the i-th sector to the water surface. The area and corresponding height of each sector are given in Table 1.

Table1

S(i) - m^2	**S(i) - m^2**	**H(i) - m**	**H(i) - m**
S1 = 1119	S18 = 2157	H1 = 8.0	H18 = 4.2
S2 = 959	S19 = 2994	H2 = 8.0	H19 = 4.0
S3 = 1042	S20 = 2447	H3 = 7.5	H20 = 3.7
S4 = 1733	S21 = 2648	H4 = 7.5	H21 = 3.5
S5 = 1312	S22 = 3731	H5 = 7.0	H22 = 3.3
S6 = 1645	S23 = 3930	H6 = 7.0	H23 = 3.0
S7 = 1392	S24 = 2868	H7 = 6.7	H24 = 2.8
S8 = 867	S25 = 1940	H8 = 6.5	H25 = 2.6
S9 = 1226	S26 = 2062	H9 = 6.2	H26 = 2.4
S10 = 970	S27 = 1190	H10 = 6.0	H27 = 2.1
S11 = 1240	S28 = 767	H11 = 5.8	H28 = 1.9
S12 = 1018	S29 = 955	H12 = 5.6	H29 = 1.7
S13 = 779	S30 = 1211	H13 = 5.3	H30 = 1.4
S14 = 859	S31 = 1537	H14 = 5.1	H31 = 1.2
S15 = 904	S32 = 1293	H15 = 4.9	H32 = 1.0
S16 = 1641	S33 = 801	H16 = 4.6	H33 = 0.8
S17 = 1976	S34 = 739	H17 = 4.4	H34 = 0.5

Table1 - the area of each sector (S_i) and the corresponding different between levels (H_i) of the water reservoir.

Table2

V(i) – m^3	**V(i) – m^3**
V1 = 8952	V18 = 9029
V2 = 7672	V19 = 11848
V3 = 7815	V20 = 9124
V4 = 12998	V21 = 9268
V5 = 9184	V22 = 12206
V6 = 11515	V23 = 11958
V7 = 9326	V24 = 8071
V8 = 5611	V25 = 5016
V9 = 7654	V26 = 4860
V10 = 5834	V27 = 2533
V11 = 7174	V28 = 1457
V12 = 5657	V29 = 1596
V13 = 4151	V30 = 1747
V14 = 4381	V31 = 1866
V15 = 4404	V32 = 1275
V16 = 7619	V33 = 606
V17 = 8723	V34 = 391

Table2 – volume of each sector (V_i)

Volume of temporary water reservoir

$$V = \sum_{i=1}^{34} V_i = 221\ 755\ m^3$$

According to our calculations, the volume of the temporary water reservoir is equal to about 225,000 m^3. In the event of a catastrophic flood, it will take approximately 75 minutes to fill the temporary water reservoir, roughly calculation. It envisages a reduction in the conductivity of the second tunnel due to the corrugated walls, a reduction in its cross-section due to a 40 cm concrete cover on the floor and, most importantly during catastrophic flood, about 50 $m^3 s^{-1}$ water flow from Kipshidze Street and from opposite slope. Catastrophic precipitation mayl ast longer, butt his time (75 min) will be sufficient for safety-related measures.

Conclusion

1. The cross-section of the second tunnel does not envisage runoff from Kipshidze Street. Also, runoff from the opposite slope should probably be considered. In our estimation, the catastrophic flooding in front of the second tunnel was significantly due to these factors. It is estimated that the runoff from Kipshidze Street was $Q_1 \approx$ (30 – 40) $m^3 s^{-1}$, which was added to the water consumption from the first tunnel.
2. According to our water reservoir model, it is likely to act as a dempher that can protect the rest of the river Vere bed from water overflow. For example, if we consider that the water flow in the first and second tunnels is $Q_2 \approx$ 225 $m^3 s^{-1}$, which is considered as a measure of the flow of June 13, 2015 (Kereselidze, Khvedelidze), in case of runoff $Q_1 \approx$ 50 $m^3 s^{-1}$from the slope, it will take T ≈ 75 min to fill the spontaneous reservoir. Even if the catastrophic rainfall continues for a longer period of time, it is likely that this time will be sufficient to implement necessary flood control measures in the lower part of the Vere Valley.
3. In our opinion, it is an urgent task to build a protective wall along the entire length of Kipshidze slope. We also note that the small, previously built wall here has already been amortized. It is therefore necessary to construct the new wall in such a way that the entire slope before the entrance to the second tunnel was protected.

References

[1] Banetashvili V.G., Gelovani G.T., Grebencova A.B., Javakhishvili N.P., Iobadze K.V., Mitin M.N., SaginashviliN.M., Samkharadze I.N.,Khurtsidze G.T., Tsereteli A.G., Tskhvediashvili G.N., Chkhaidze B.D. Some examples of heavy rainfall in eastern Georgia based on 2015 radiolocation data. Proceedings of the M. Nodia Institute of Geophysics, v. 66, 2016, pp. 75-83, (in Russian).
[2] Amiranashvili A.G., Kereselidze Z.A., Mitin M.N., Khvedelidze I.B., Chikhladze V.A. Alarming Factors of the Microclimate of the Vere River Valley and Their Influence on the Intensity of Floods. Proceedings of the Michael Nodia Institute of Geophysics, v. 69, 2018, pp. 196-210, (in Georgian).
[3] Kereselidze Z., Khvedelidze I., Shergilashvili G. On the Probable Technical Reasons of the Devastating Flood in 2015 in Tbilisi. Journal of the Georgian Geophysical Society, ISSN: 1512-1127, Physics of Solid Earth, Atmosphere, Ocean and Space Plasma, v.21(2), 2018, pp. 5 -16.
[4] Kereselidze Z, Khvedelidze I. Evaluation of water flow at Vera during the flood of 13.06.2015. Proceedings of the Michael Nodia Institute of Geophysics, v. 68, 2017, pp.100-117, (in Georgian).
[5] Kereselidze D., Alaverdashvili G., Kiknadze D., Cincadze N., Kokaia N. Catastrophic flooding on river Vere and its calculation methodic. TSU proceedings, geography, N 8-9, 2011, (in Georgian).

[6] Schlichting H. Boundary-Layer Theory. Chapt. XX , M., Nauka, 1974, (in Russian)
[7] Landau L.D., Lipschitz E.M. Hydrodynamic. Chapt. 4, M., Nauka, 1988, (in Russian).
[8] Kereselidze Z., Shergilashvil G. Overflow of Vere River on 13 June 2015 and Hydrodynamic Problem of Closed Channel. Proceedings of the Michael Nodia Institute of Geophysics, v. 66, 2016, pp. 196-221, 2016, (in Georgian).

მდინარე ვერეზე კატასტროფული წყალმოვარდნის შედეგების შერბილების პერსპექტივები დროებითი საგუბარის მეშვეობით

ზ. კერესელიძე, თ. ქირია, ჯ. ქირია, ნ. ვარამაშვილი, მ. ნიკოლაიშვილი

რეზიუმე

მდინარე ვერე წარმოადგენს ტიპიურ მთის მდინარეს, რომლის ხეობის სიგრძე 40 კილომეტრზე მეტია, სიმაღლეთა სხვაობა თითქმის კილომეტრნახევარი. ხშირი კატასტროფული წყალმოვარდნების გამო ეს მდინარე ითვლება ერთ-ერთ ყველაზე სახიფათოდ აღმოსავლეთ საქართველოში. აღნიშნული ნაშრომის ერთ-ერთი მიზანი იყო 2015 წლის 15 ივნისს, მდინარე ვერეს ხეობაში განვითარებული კატასტროფული წყალმოვარდნის დროს თამარაშვილის მაგისტრალსა და გაბაშვილის ქუჩებს შორის წარმოქნილი დროებითი საგუბარის მიახლოებითი მოცულობის შეფასება. ჩვენი აზრით, სვანიძის ქუჩიდან გამომავალი გვირაბის მაქსიმალური წყლის ხარჯის და მდინარე ვერეს ე.წ. მეორე გვირაბის წყლის მაქსიმალური გამტარობის გათვალისწინებით და ასევე საგუბარის ფერდობებიდან ჩამონადენი წყლის გათვალისწინებით. დროებით საგუბარს აქვს სტრატეგიული დატვირთვა კატასტროფული წყალმოვარდნის და მისი შედეგების მართვისათვის.

Перспективы смягчения последствий катастрофического наводнения на реке Вере за счет временного водохранилища

З.А. Кереселидзе, Т.В. Кирия, Дж.К. Кирия, Н.Д. Варамашвили, М.М. Николаишвили

Резюме

Река Вере - типичная горная река с протяженностью долины более 40 километров с перепадом высот почти в полтора километра. Из-за частых катастрофических наводнений эта река считается одной из самых опасных в Восточной Грузии. Одна из целей данной статьи - оценить приблизительный объем временной плотины, образовавшейся между шоссе Тамарашвили и улицами Габашвили во время катастрофического наводнения в долине реки Вере 15 июня 2015 года. На наш взгляд, учитывая максимальную пропускную способность тоннеля, ведущего от улицы Сванидзе и также, принимая во внимание максимальную водопроницаемость так называемого второго туннеля реки Вере, и учитывая потоки воды, текущие со склонов водохранилища, временное водохранилище несет стратегическую нагрузку по управлению катастрофического наводнения и его последствий.

Journal of the Georgian Geophysical Society, e-ISSN: 2667-9973, p-ISSN: 1512-1127
Physics of Solid Earth, Atmosphere, Ocean and Space Plasma, v. 24(2), 2021, pp. 59 - 65

Studies of the Influence of Galactic Cosmic Rays on the Cloud Cover of the Earth.
Review of Research in Recent Decades

Irina P. Mkurnalidze, Naili I. Kapanadze

Institute of Hydrometeorology at the Georgian Technical University, 150-a D. Agmashenebeli Ave, 0112
i.mkurnalidze@gmail.com

ABSTRACT

A review of scientific studies of the existence of the influence of galactic cosmic rays on cloudiness on Earth and, accordingly, on climatic fluctuations is given. Corresponding illustrations are presented. Describes the work on this topic, carried out in the international center CERN (project "CLOUD"). The article examines the research of the last decades.
Key Words: *Galactic cosmic rays, cloud cover, temperature anomaly, global temperature.*

It is known that clouds form in the troposphere, under different conditions of distribution of moisture, temperature, aerosols. Cosmic rays have a definite influence on these parameters [1]. Consequently, cloud cover caused by changes in cosmic factors may affect the radiation balance of the Earth's surface and, consequently, climate change.

In the last decade of the twentieth century, during a satellite observation led by Henry Svensmark, Danish scientists discovered that cloudy areas change with changes in the intensity of cosmic rays. Svensmark put forward a hypothesis that cosmic rays contribute to the development of low cloud cover and thus influence the Earth's climate. He later used a special camera to experimentally prove that cosmic rays ionize water vapor molecules, thereby ensuring the formation of cloud droplets. According to his theory, the sun's magnetic field (especially during periods of solar activity) deflects galactic cosmic rays and lowers the ionization potential of clouds. Therefore, the increased magnetic field of the sun can indirectly reduce the Earth's albedo and cause climate warming [2].

The following four conditions must be met to prove the validity of Svensmark's theory:

1. The magnetic field of the sun should have a long-term positive trend of change;
2. The flow of galactic cosmic rays should have a long-term negative trend;
3. Cosmic rays should intensively ionize low-tier clouds;
4. Low cloud cover should have a long-term negative trend.

Studies have shown that neither the magnetic field nor its other characteristics of the sun have changed significantly in the last 30 years [3]. Observations of cosmic ray fluxes have also shown that no significant change has been observed since the mid-twentieth century. According to Benestad [4], galactic cosmic rays undergo a change, but not in the direction that explained the increase in temperature on Earth (Fig. 1). According to studies by American scientist Richard Meweldt [5], the intensity of cosmic rays has increased by 19% over the last 50 years.

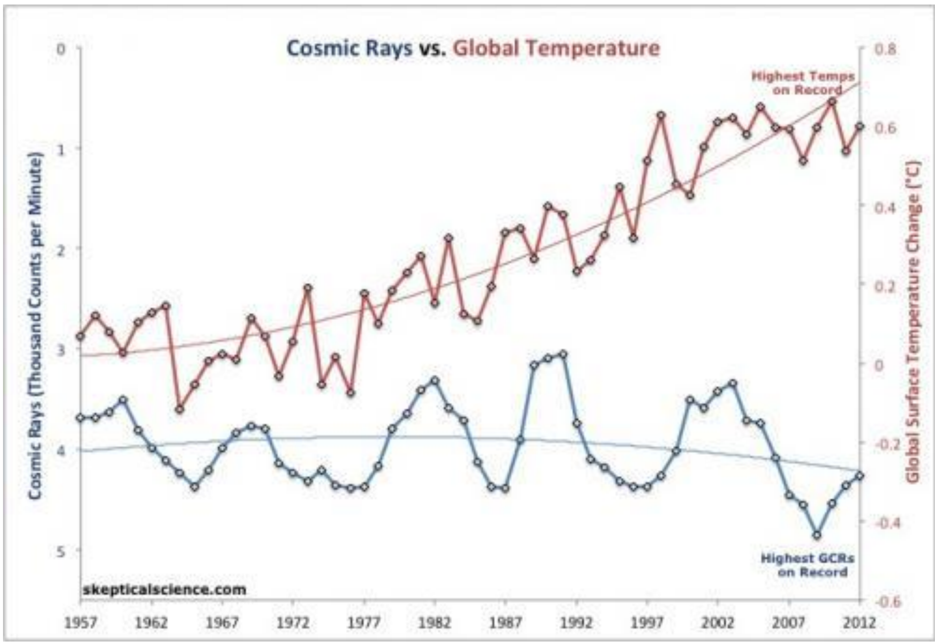

Fig. 1. Comparison of average annual values of galactic rays taken from the Neutron Monitor database (bottom chart) with average annual global temperature data (top chart) NOAA NCD.

GCK record values were observed, which should have caused an increase in cloudiness and cooling, but 2009 and 2010 were the hottest (NASA GISS)

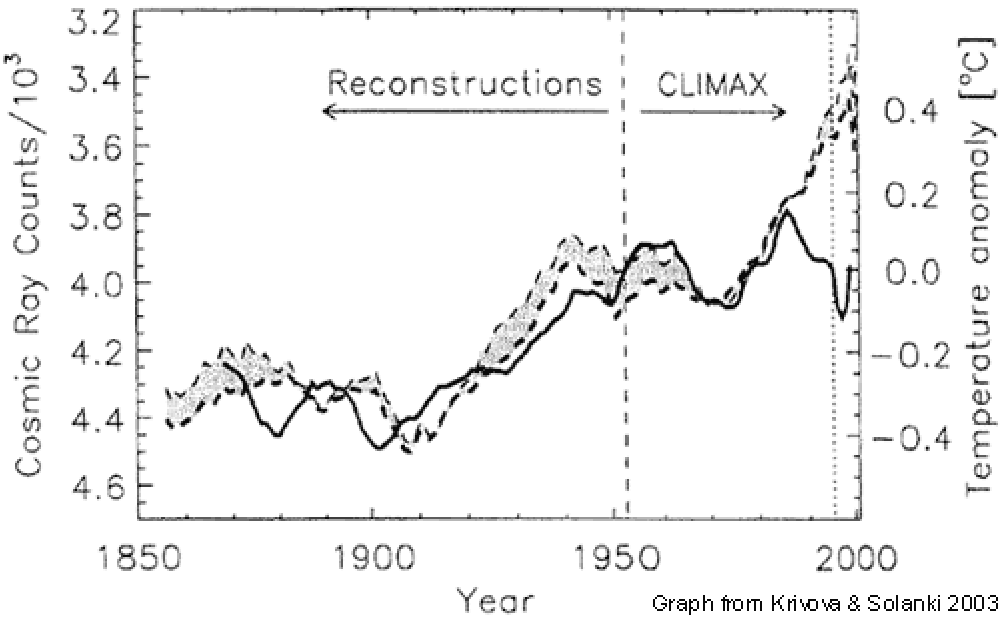

Fig. 2. Comparison of cosmic radiation (whole line) recovered before 1952 and observed after 1952 with global temperature (point) [6].

The flux of cosmic rays varies almost uniformly with respect to temperature between 1970 and 1985 (Fig. 2), although by 2000 the course of these two parameters is quite different from each other and does not allow us to prove that the cause of the 15% increase in temperature is cosmic rays. In order for the clouds to be successfully sown with GCR, the following must be performed:

GCR should cause the formation of aerosols; these newly formed aerosols must be large enough to form condensation nuclei; condensation nuclei must form clouds intensively.

Fulfillment of the first condition is doubtful. Relevant studies are conducted at CERN. Pierce and Adams [6] used a model with online microphysics to estimate the growth rate of ionized aerosols and found that the growth rate is very small and cannot play a significant role in cloud formation, and therefore in climate change. Numerous studies [7-11] have shown that no statistically significant correlation was found between the galactic cosmic rays and the four characteristics of the cloud.

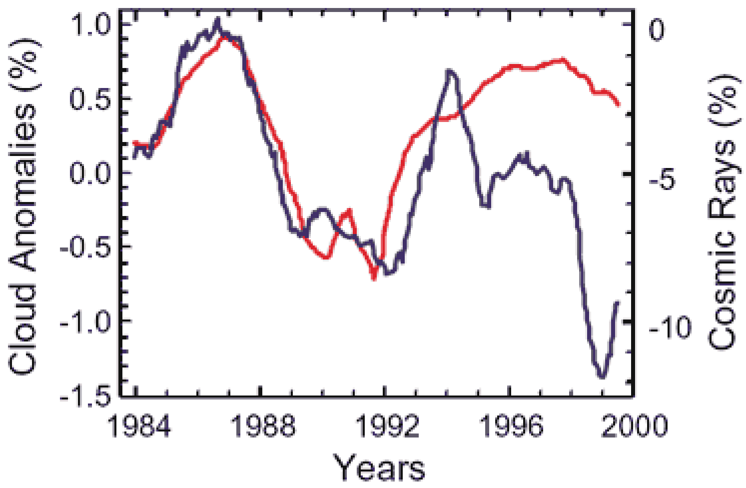

Fig. 3. Comparing the lower tier cloudiness (lower curve) and the intensity of the galactic cosmic rays (upper curve).

According to Fig. 3, the correlation between cosmic radiation and low tier cloudiness existed only until 1991, after which the picture was reversed, cloudiness is 6 months behind cosmic radiation, while cloud formation occurs in a few days.

Analysis of satellite and other terrestrial observations has shown that there are large differences in the mean time period between low-lying cloudiness and total cloudiness, although artefacts are also present. Observed low-cloud cover averages suspicion over the average ocean around the world, as cloud cover is fairly high and reduced solar energy absorption between 1952 and 1997, according to these data. This fact must have led to a drop in global temperature on Earth, which is not true.

Sloel and Wolfendal [10] studied the effects of cosmic rays on the climate over the last billion years and found that variations in galactic cosmic rays were small and could not have a significant impact on Earth's climate.

In addition to the papers mentioned above, there are many other papers that prove that at the turn of the last centuries, the correlation between cosmic rays and the cloud on Earth was broken. There are relatively few papers that cite the probable causes of this event. One such paper is presented by a group of scientists from the Joffe Institute of Physics and Technology in St. Petersburg. The above studies were performed within the framework of the international project "Satellite Climatology". This paper states:

„The question of cloud-GCR links remains controversial and requires new studies, both experimental and theoretical, to evaluate a real contribution of galactic cosmic rays to solar activity influence on the Earth's climate [12]. The data presented in this chapter show that possible links between clouds and GCR variations on the decadal and longer time scales could involve not only direct (microphysical) effects, but mostly indirect ones mediated by circulation changes. This should be taken into account when considering long-term GCR effects on the cloudiness state.

The stratospheric polar vortex plays an important role in the formation of long-term impacts GCR on cloudiness at mid-latitudes (30º-60º). This hurricane controls the confluence of the stratosphere and the troposphere, which contributes to the GCS influencing extratropical cyclonic activity and, consequently, cloudiness under strong hurricane conditions.

This may explain the high correlations between GCR and cloud cover in the 1980s and 1990s, when there was a strong hurricane period.

The sharp weakening of the polar vortex in 2000 in both the northern and southern hemispheres changed the nature of the GCR impact on cyclone evolution and led to the disappearance of the correlation between GCR and “cloud cover“.

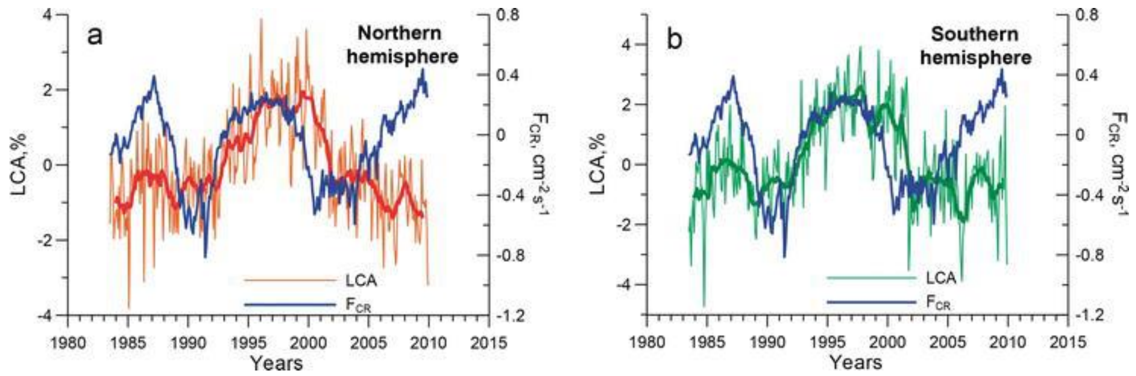

Fig. 4. Temporal variations of the monthly values of cloudiness (LCA) and GCR (FCR) in the northern (a) and southern (b) hemispheres. A thick line shows the 12-month values of cloudiness.

An interesting opinion was published by Kh. Abdusamatov (ГАА (Пулково) РАН), which follows, he writes [13], that the so-called The Sversmark hypothesis does not take into account the variations of nearly 200 years of solar radiation, and the fact that an increase in GCS flux at a large minimum of solar activity causes cloud formation and heat energy to be reflected back into space. Because of this, the Earth's heat balance takes on negative values, i.e. the climate cools down. The authors of the hypothesis do not take into account the variability of physical processes in the atmosphere - increasing reflection and absorption of heat energy from the Earth's surface, reflection of solar radiation from the Earth's surface, narrowing of atmospheric transparency windows and enhancing the thermal effect. These processes compensate for the cooling.

According to Abdusamatov and his group, the difference in the average global energy balance between Earth and space during a 2% increase or decrease in low cloud cover is almost zero: $E1-E0\approx0$ The potential increase in cloud cover will practically not cause a change in the average global energy balance between Earth and space, nor will it affect climate change. The potential increase in cloud cover will have virtually no change in the average global energy balance between Earth and space, nor will it affect climate change.

As you know, the grandiose CLOUD project is being carried out at CERN. For scientific research, the project uses a super clean chamber made of super pure materials, in which real atmospheric processes are simulated - the growth of aerosol particles and their transformation into cloud droplets. Atmospheric parameters are monitored - gas concentration, ultraviolet radiation, cosmic ray intensity measured by a proton synchrotron [14].

Despite the fact that aerosol processes are not well understood, from a climatic point of view, it is possible to assume that 50% of their amount turns into cloud droplets.

Specialists in aerosols and elementary particle physics from 22 research institutes, both in Europe and the United States, are working on the project.

The data are processed by combining statistics and optimized software, in which elementary particle physics plays a leading role compared to climate models.

The main goal of the project is to investigate the impact of cosmic rays on climate and cloud cover. The great uncertainty is not the study of greenhouse gases, but the understanding of how much the number of aerosols and clouds has increased as a result of human action since the beginning of the industrialization period. This raises the question - what part of aerosols is compensated by greenhouse gases? Numerous experiments are aimed at elucidating the role of aerosols in anthropogenic climate change.

Experiments are carried out under different ionization conditions, which allow quantifying the impact of GCR on the research processes. Significantly studies on smog generation in megacities Experiments have shown that ammonia and nitric acid grow newly formed particles 100 times faster than previously known. The process is interrupted as it takes place in a much polluted atmosphere of cities. The layer where this happens becomes under the inversion layer.

To assess anthropogenic impacts, the baseline state of the atmosphere is considered to be the era before industrialization. The fact that biogenic gases form large amounts of aerosols and cloud droplets suggests that cloudiness and temperature do not differ much between now and before. An important result of the research is that it has been experimentally established that only trees can form large numbers of condensing nuclei. Previously it was thought that sulfuric acid was necessary for the formation of aerosols. Since sulfuric acid was 5 times less in the atmosphere before industrialization, according to climate models, clouds were also less.

Under the influence of GCR, the rate of production of biogenic particles increases 100 times. Therefore, before the industrialization period, the atmosphere was more sensitive to cosmic rays than in the current polluted atmosphere. It turned out that sulfuric acid itself is not a nuclide, it needs ammonia. Before the CLOUD project, particles were measured, not molecular composition, so the experiments were not pure, many

The results obtained with CLOUD are used in the models of the so-called IPCC– Intergovernmental Panel on Climate Change. The project established a link between theory, experimentation and modeling. Several institutes are working on regional and global aerosol cloud models. New experimental zones should be developed in the future. The project will last for another 10 years. But, according to the press secretary of the project, it takes more than 80 years to answer all the questions.

In Georgia studies of the effects on cosmic rays on cloudiness also began recently. In particular, in the works [14-16] the effects of cosmic radiation on the formation in the atmosphere of the secondary aerosols, which have an effect on cloudiness, are studied. In the works [17,18] the inter-annual distributions of cloudless days and cloudless nights in Abastumani Astrophysical Observatory, at various helio-geophysical conditions, and their coupling with cosmic factors were studied. In the work [19], a study of the relationship between the annual variations in the intensity of galactic cosmic rays and the variability of cloudiness and air temperature in Tbilisi was carried out according to the data of 1963-1990. In the work [20] results of the study of the connection between annual variations of intensity of galactic cosmic rays and the changeability of the total cloudiness, atmospheric precipitation and air temperature in 1966-2015 in Tbilisi. The statistical characteristics of the indicated parameters (trends, random component, linear correlations between real and random components, etc.) are studied. In particular, it was found that, within the variation range, the contribution to total cloudiness variability from cosmic ray intensity is 5.3%, and random components of cosmic ray intensity - 7.4%.

And here is how Jasper Kirkby [21] answers the question; will humanity be able to survive catastrophic climate change?

“The Earth has undergone much greater natural fluctuations in climate. Earth's climate is fundamentally stable. The oceans occupy 2/3 of the earth's surface, and the latent heat of their evaporation is the greatest stabilizer of the climate. The oceans never evaporated and never froze. In addition only 2% of CO2 is in the atmosphere, the rest is diluted in the ocean. So for several hundred years the amount of CO2 in the atmosphere will be almost the same as it was before the industrialization period. Some scientists have suggested that in the current conditions there may be some turning point in the climate, but many things have happened and life has not disappeared. And in general, the problem of environmental pollution should not be equated with the problem of climate. It should be considered separately” Advises us to be more optimistic.

References

[1] Mkurnalidze I., Kapanadze N. Cosmic Rays and their Influence on the Earth's Atmosphere (Contemporary Achievements). Int. Sc. Conf. „Modern Problems of Ecology“, Proc., ISSN 1512-1976, v. 7, Tbilisi-Telavi, Georgia, 26-28 September, 2020, pp. 279-283, (in Georgian)
[2] Svensmark H. et.al. Variation cosmic ray flux and global cloud coverage a missing link in solar-climate relationship, Journal at Atmospheric and Solar-Terrestrial Physics, vol.59, issue 11, 1997, pp. 1125-1132.
[3] Krivova N.A., Vieira L.E.A., Solanki S.K. Reconstruction of Solar spectral irradiance since the Maunder minimum, Journal of Geophysical Research Spice physics, vol. 115, issue A12, 2010.
[4] Benestad R.E. et.al. Learning from mistakes in climate research, Theoretical and applied climatology, 126, 2016, pp. 699-703.
[5] Meweldt R. Cosmic rays Hit Spare Age High Solar Eruptions and Energetic Particles, (Geophysical Monograph Series) 1st Edition, ISBN-13:978-0875904306, ISBN-10:0875904300, 365p.
[6] Pierce P.J, Adams C. Cosmic rays affect cloud condensation nuclei by altering new particle formation rates? Geophysical Research Letters, vol.36, issue 9, 2009.
[7] Kazil J., Lovejing E.R.L. et.al. Aerosol nucleation over ocean and the role of galactic cosmic rays. Atmos. Chem. Phys.,6, 4905-4924-2006, 1006.
[8] Sloan T., Wolfendale A.W. Cosmic rays, solar activity and the climate. Environmental Research Letters, Vol.8, Num.4, 2013.
[9] Calogovic J. et. al Sudden cosmic ray decreases: No change of global cloud cover. Geophysical Research Letters, Vol.37, issue 3, 2010.
[10] Kristjansson J.E. et. al. Cosmic Rays, CCN and Clouds-reassessment using MODIS data. Atmos. Chem. Phys. Discuss., 8, 13265-13299, 2008.
[11] Krissansen-Totton J., Davies R. Investigation of cosmic ray-cloud connections using MISR. Department of Physics the University of Oucklend, New Zeland, 2013.
[12] Veretenenko S., Ogurtsov M., Lindholm M., Jolkenen R. Galactic Cosmic Rays and Low Clouds: Possible Reasons for Correlation Reversal. Submitted: December 12th 2017 Reviewed:February 14th 2018 Published: August 22nd 2018, DOI:10.5772/intechopen. 75428
[13] Abdussamatov H.I. Earth’s Climate Does Not Depend on Variations in Cosmic Rays and Cloud Coverage. Geomagnetism and Aeronomy, 59, Publish 11 March 2020, pp. 935-941.
[14] Amiranashvili A., Bliadze T., Chikhladze V. Photochemical smog in Tbilisi. Monograph, Trans. of Mikheil Nodia institute of Geophysics, ISSN 1512-1135, v. 63, Tb., 2012, 160 p., (in Georgian).
[15] Amiranashvili A.G. On the Role of Cosmic and Radioactive Radiation on the Formation of the Secondary Aerosols in Atmosphere. Int. Conference “Near-Earth Astronomy 2007”, Abstract, Terskol, Russia, September 3-7, 2007, p. 85.
[16] Amiranashvili A.G., Amiranashvili V.A., Bakradze T.S., Chikhladze V.A., Glonti N. Ya., Kharchilava J.F., Tuskia I.I On the Influence of Cosmic Rays on the Secondary Aerosols Formation in the Atmosphere. 7th Int. Conference "Problems of Geocosmos", Abstract, St. Petersburg, Russia, May 26 - 30, 2008.
[17] Todua M., Didebulidze G. G. Cosmic factors influence on the inter-annual variations of the green 557.7 Nm line and red 630.0 Nm line nightglow intensities and their possible coupling with cloud covering at Abastumani (41.75°N, 42.82°E). Acta Geophysica, v. 62, iss. 2, 2014, pp.381-399.
[18] Didebulidze G.G., Todua M. Investigation of presence of cosmic factors in the inter-annual distributions of cloudless days and nights in Abastumani. Sun and Geosphere, v.10, No.1, 2015, pp. 59-63.
[19] Amiranashvili A.G., Bakradze T.S., Ghlonti N.Ya., Khurodze T.V., Tuskia I.I. On the Connection Between Annual Variations of the Intensity of Galactic Cosmic Rays and the Changeability of Cloudiness and Air Temperature in Tbilisi. Journal of the Georgian Geophysical Society, Issue B. Physics of Atmosphere, Ocean and Space Plasma, v.19B, Tbilisi, 2016, pp. 128-134.
[20] Amiranashvili A., Bakradze T., Erkomaishvili T., Ghlonti N., Tuskia I. On the Relationship of Annual Variations of the Intensity of Galactic Cosmic Rays with the Variability of Total Cloudiness, Atmospheric

Precipitation and Air Temperature in Tbilisi in 1966-2015. Journal of the Georgian Geophysical Society, ISSN: 1512-1127, Physics of Solid Earth, Atmosphere, Ocean and Space Plasma, v. 23(2), 2020, pp. 64 – 71.
[21] Kirkby J. Interview by Paola Catapano and Matthew Chalmers. CERN, May 2020.

გალაქტიკური კოსმოსური სხივების დედამიწის ღრუბლიანობაზე გავლენის გამოკვლევა.
ბოლო ათწლეულების სამეცნიერო კვლევების მიმოხილვა

ი. მკურნალიძე, ნ. კაპანაძე

რეზიუმე

განხილულია მთელი რიგი სამეცნიერო ნაშრომებისა, რომლებიც ეხება გალაქტიკური კოსმოსური სხივების დედამიწის ღრუბლიანობასა და კლიმატზე შესაძლო გავლენის არსებობას. მოყვანილია შესაბამისი გრაფიკები. გაანალიზებულია საერთაშორისო ცენტრში CERN (პროექტი “CLOUD”), ბოლო ათწლეულში ჩატარებული, აღნიშნულ თემატიკისადმი მიძღვნილი კვლევები. მოყვანილია პროექტის წამყვანი სპეციალისტის მოსაზრება დედამიწის კლიმატის შესაძლო კატასტროფული ცვლილების შესახებ.

Исследования влияния галактических космических лучей на облачный покров Земли.
Обзор исследований последних десятилетий

И.П. Мкурналидзе, Н.И. Капанадзе

Резюме

В данной статье дан обзор ряда научных работ, в которых представлены исследования существования влияния галактических космических лучей на облачный покров Земли и её климат. Представлены соответствующие графики. Описаны работы, проводимые в международном центре CERN, посвященные данной тематике (проект «CLOUD»). Приведено мнение ведущего специалиста проекта по поводу возможности катастрофического изменения климата на Земле. Рассмотренные в данной статье исследования проведены в последние десятилетия.

Journal of the Georgian Geophysical Society, e-ISSN: 2667-9973, p-ISSN: 1512-1127
Physics of Solid Earth, Atmosphere, Ocean and Space Plasma, v. 24(2), 2021, pp. 66 - 72

On Some Considerations of Cloud Particles and Photons Interaction

Marika R. Tatishvili

Institute of Hydrometeorology of Georgian Technical University, Tbilisi, Georgia
m.tatishvili@gtu.ge

ABSTRACT

The interaction of light (photon) and cloud particles according main quantum assumption that system internal energy is composed by bound microparticles (cluster) under certain conditions can obtain allowed discrete significances has been discussed in the article. The objective is to calculate the transition probability from one state into another caused by inner forces or any internal processes. The cluster may be presented as multipole system. The some peculiarities of microstructure of cloud formations have been discussed using quantum disperse forces or Van-Der-Vaals forces that are typical for water particles. To obtain the expression for interaction potential the wave functions of basic and exited states of clusters and dispersion matrix have been introduced describing by virtual photon. It has been turned out that virtual photon interaction causes potential holes and barriers that are decreased by height and width. The isolated long wave quant may be the radiation that is generated throughout observed microphysical processes.

Key Words: *Water molecule, photon exchange, interaction potential, probability amplitude, wave function.*

Introduction

Water is a compound and polar molecule, which is liquid at standard temperature and pressure. It has the chemical formula H_2O, meaning that one molecule of water is composed of two hydrogen atoms and one oxygen atom. Water is found almost everywhere on earth and is required by all known life. About 70% of the Earth's surface is covered by water. The important feature of the water molecule is its polar nature. The water molecule forms an angle with hydrogen atoms at the tips and oxygen at the vertex. Since oxygen has a higher electronegativity than hydrogen, the side of the molecule with the oxygen atom has a partial negative charge. Usually the molecule with such charge difference is called a dipole. The charge differences cause water molecules to be attracted to each other and to other polar molecules. This attraction is known as hydrogen bonding. This bonding gives water unusual properties. Many studies and experiments with HT equipments are made to understand water properties [1].

The interaction of light (photon) and cloud particles according main quantum assumption that system internal energy is composed by bound microparticles (cluster) under certain conditions can obtain allowed discrete significances has been discussed in the article. The objective is to calculate the transition probability from one state into another caused by inner forces or any internal processes. The cluster may be presented as multipole system. The multipole is the system composed by couple opposite charges that have definite symmetry type. The simplest is the dipole. If the transition is forbidden in dipole approach it may happen in higher approaches – quadrupole (electric) or magnetic dipole. Their probability is approximately 10^6 times less than dipole. To search out transition probability of cluster from basic state into exciting or virtual one interacting with electromagnetic field the identification of Einstein factors have to be needed [2,3].

The some peculiarities of microstructure of cloud formations have been discussed using quantum disperse forces or Van-Der-Vaals forces that are typical for water particles. To obtain the expression for interaction potential the wave functions of basic and exited states of clusters and dispersion matrix have been introduced describing by virtual photon. It has been turned out that virtual photon interaction causes potential holes and barriers that are decreased by height and width. The isolated long wave quant may be the radiation that is generated throughout observed microphysical processes.

Methods

The water H_2O is the molecule everybody knows and life is impossible without it. But for all its familiarity and import for life, aspects of water's behavior have been hard to understand, including its transformation in cloud medium.

Meteorology is an extraordinarily interdisciplinary subject, with quantitative links to many of the applied sciences and now in presented paper cloud medium is discussed using quantum theory.

Microparticles are described using wave function in quantum mechanics. The quantum system state is considered defined if its wave function (Schrödinger) or ket-vector (Dirac) is given.

The system energy change comes with quantum transportation from one energetic level into another. If $E_1>E_2$ than system emits energy equal to E_1-E_2 and if $E_1>E_2$ then absorbs. Such transportations happen while interaction with electromagnetic radiation. Emitted or absorbed photon energy is defined by Bohr frequency law:

$$\hbar w_{12} = |E_2 - E_1| \qquad (1)$$

Molecules full energy may be presented by the kinetic energy sum connected with mass center and by internal energy sum. Molecules energy may be considered as compound from three parts:

1. Electron energy connected with their rotation around nuclei
2. E_{os} – oscillation energy connected with nuclear vibration towards mass center
3. E_{rot} –rotation energy connected with molecules rotation towards mass center

Diatomic molecule rotates around mass center located on symmetry axis of molecule. Rotation energy is defined as:

$$E_{rot} = \hbar^2 \frac{K(K+1)}{2I} = BK(K+1) \qquad (2)$$

where $I=MR_o^2$ inertial moment;
B- rotation constant;
K=0, 1, 2, 3 rotation quantum number
$|M_{rot}| = \sqrt{K(K+1)\hbar}$ - impulse momentum of rotation

Vibration energy may be defined as following

$$E_{os} = \hbar w_0 (q+\tfrac{1}{2}) - \hbar w_0 \kappa (q+\tfrac{1}{2})^2 \qquad (3)$$

where $\kappa = \frac{\hbar w_0}{4D} << 1$ –is nonharmonic constant.

Characterization of electric terms doesn’t differ from diatomic molecule terms. In molecule nucleus electic field have no central symmetry thus the full orbital moment haven’t been kept. In diatomic molecule the electric field has axial symmetry and in this case the component on the axis passing through the nucleus of orbital momentum has been kept. It is called molecule orbital quantum number and gets discrete values 0,1,2,...

Molecule state is also chracterized by full electron spin S and it has internal quantum number $\Omega = \Lambda + S$

The light is considerd as the combination of photons with ka state and $-\hbar w$, $\hbar k$ impulses. Photon or molecular system interaction happens by forming or disappearance of light quants. During this process energy and impulse are keeping. Quantum trasformation is system trasportation from one energetic state into another. The task is to identify transformation probability from one energetic state into another. Clusters may be presented as multipole systems. Multipole is the system compound from couple of opposite charges, obtaining definite symmetry. The simpliest is dipole. If transpostation is prohebitated in dipole approach it may happen in higher approach – quadropole (electric) or magnetic dipolic.

Their probability is 10^6 time less than dipole. To identify transportation probability the Einstein members have to be defined according clusters properties. Spontaneous and forced motion members may be identifies.

Quantum transition combination is characterized by D_{mn} numbers two dimensional unity and is infinite matrix:

$$\begin{Vmatrix} D_{11,} D_{12}, \ldots\ldots D_{1n} \ldots \\ D_{21}, D_{22}, \ldots D_{2n} \ldots \\ \ldots\ldots\ldots\ldots\ldots\ldots\ldots \\ D_{n1}, D_{n2}, \ldots D_{nn} \ldots \\ \ldots\ldots\ldots\ldots\ldots\ldots\ldots \end{Vmatrix}$$

where $D^0_{mn} = e\int\limits_v \psi^*_m \vec{r}\, \psi_n dv$

is dipole transition matrix element

The nondiagonal matrix elements are time functions and corresponds light absorption or emitting by those frequencies defined from Bohr frequency selection low.

And Einstein members can be defined as for spontaneous and forced transition probabilities:

$A_{mn} = \frac{w^3_{mn}}{3q_0\pi\hbar c^3}\left(D_{mn}\right)^2$ - spontaneous transition probability

$B_{mn} = \frac{\pi}{12q_0\hbar^2}\left(D_{mn}\right)^2$ -forced transition probability

Amn is approximately 10^8 sec $^{-1}$

If some matrix element equals 0 it is called prohibited then this transition doesn't happens in dipole approach and happens in magnetic. If transitions are prohibited or banned for clusters higher energetic level the lower energetic level is called metastable and clusters life duration is 10^{-3} sec. or more.

If transition is allowed in dipole approach then system life duration is of spontaneous transition probability order. If transition is banned in dipole approach or $D_{mn}=0$ it doesn't mean that it haven't happen generally as cluster has electric quadruple or magnetic dipole moment. If transition is banned for clusters high energetic level than lower level in electric dipole interactions is called as metastable level. In this clusters life duration is 10^{-3} sec or more. In first quantum transition approach there acts Bohr prohibition principle. If such transition still happens it would be on the second or higher approach order and probability will be also less. Such are light scattering in viscous medium, mist, aerosols and etc.

This process on molecular level happens as follows: if outer emitting frequency differs from absorption frequency energy quant is anyway transmitted to the cluster which transforms into virtual state with short life period and will be defined from the uncertainty principle. Then it emits same frequency photon and returns at initial state. I definite conditions cluster may transform into final state from virtual. I simple case the falling wave is flat and emitted spherical. Energy and impulse are kept as usual except virtual state, when energy isn't keeping. For those transitions it is necessary that the electron-photon interaction matrix element have to be differs from 0.

In definite conditions cluster may transform from virtual into final state that will be differ from initial. Also emitted photon has different polarization and frequency.

In second approach it is possible the existence of two photon absorption process. After absorbing photon system transits into virtual state where it absorbs another photon and then transports into stationary state

In classical mechanics, the possible states of system S are all positive normalised functions (Distribution function) on the phase space P and possible observables are all real function on P. P is fixed and uniquely associated with the system alone and forms the basis of this kinematic description. Hence, transitions between different sets of observables similar to those described above would be impossible in classical mechanics. They are only enabled in quantum mechanics by the non-objective character of observables: not only their values cannot be ascribed to microsystem S alone but some of them are not even registrable in principle due to external conditions in which S is. It is assumed that the quantum kinematics of a microsystem is defined mathematically by the possible states represented by all positive normalised (trace one) operators, and possible observables represented by some self-adjoint operators, on the Hilbert space associated with the system. Then the transitions of states and observables that go with changes of separation status cannot be viewed as a part of a dynamical trajectory due to some new version of the dynamics of S, but as a change of its kinematic description. Thus, although the change of separation status is similar to the collapse of the wave function (the non-local character included), it is both more radical and better understood.

On Earth the dimpliest and common is water molecule that has essential significance in existence of organ and nonorganic life. The most of its properties are preconditioned by the fact that three component atoms aren't placed on one line. Negative charge prevailed on oxygen atoms part and positive on hydrogen. Thus water molecule is electrically polarized. The cloud properties and their stability may be explain from water molecules properties and characterizing forces that reach maximum for 1micro-meter particles and are separated from each other on 50km distance

The comparison between the experimental and calculated molecular dipole moments is difficult, as the experiments are measuring the dipole moment in the vibrational ground state $\mu 0$, whereas the calculations are carried out for the equilibrium dipole moment μe, and thus we would have to carry out a vibrational averaging in order to speak of the same quantity. However, there are a few experimental values for μe. However it is estimated as H_2O= 1.8473(10) [6,7].

For the total molecular energy, i.e., E in the molecular SchrÄodinger equation, there is no experimental counterpart. and we examine it in order to establish a feeling on the severity of the approximations involved in the calculation. We should recall that there were a third class of approximations in addition to the truncation of one- and N-electron spaces: approximations in the molecular Hamiltonian ^H . To investigate the validity of the use of the non-relativistic Hamiltonian, we include the leading-order one-electron relativistic corrections that include the spin-orbit interaction (SO), mass-velocity (MV), and the Darwin (Dar) corrections. The leading-order two-electron contributions, such as the two-electron Darwin contribution and the spin-spin contact interaction, are smaller by at least one order of magnitude. The MV and Dar corrections are always of opposite sign. The calculation is carried out using the CCSDT model for the water molecule in the cc-pCV*X*Z bases, at a CCSD(T)/cc-pCVQZ geometry [6,7].

Total energy [*Eh*]

	CCSDT	HF
DZ	-76.24121	-76.02680
TZ	-76.33228	-76.05716
QZ	-76.35981	-76.06482
5Z	-76.36899	-76.06708

Among atoms and molecules acts force that always has attractive character. It is intermolecular dispersive or Van-Deer-Vaalse force. It is only one of the expressions of electromagnetic force. It acts among electrically neutral systems such as dipole or quadruple. In dipoles force reduces by r^4 inverse proportional and in quadrupole by r^{-6}. It is not temperature dependent and it s nature is quantum [8,9]. By increasing dipole number their interaction increases. But its interaction is limited by the matter that light speed is finite

For cluster stable and exiting states wave function $\Psi = \Psi(x,y,z,t)$ have been used. Its physical essence is that it is particle detection probability in d_v volume for t time moment.
Probability is defined as

$$W = |\Psi(x,y,z,t)|^2 = \Psi^* \Psi \qquad (4)$$

Ψ^* is complex conjugated quantity of Ψ .

$\int_v |\Psi(x,y,z,t)|^2 dv = 1$ - is rationing condition and Ψ function that assure this condition standardized.

For cluster stable and exiting states wave function $\Psi = \Psi(x, y, z, t)$ have been used. Its physical essence is that it is particle detection probability in d_v volume for t time moment.

Probability is defined as

$$W = \left|\Psi(x, y, z, t)\right|^2 = \Psi^* \Psi$$

Ψ^* is complex conjugated quantity of Ψ .

$\int\limits_v \left|\Psi(x, y, z, t)\right|^2 dv = 1$ - is rationing condition and Ψ function that assure this condition standardized.

Generally it is expressed as:

$$\Psi(x, y, z, t) = \iiint \varphi\left(P_x, P_y, P_z, t\right) \exp(i \tfrac{px+py+pz}{h}) \tfrac{dp_x dp_y dp_z}{(2\Pi\hbar)^{3/2}}, \tag{5}$$

Suppose φ_1, φ_2 are clusters basic and exited states wave functions. Their interaction in lower approach is descriped by so called scattering matrix

$$\varphi(x,t) = \widehat{S}(t, t_0)\varphi(x, t_0), \tag{6}$$

where

$$\widehat{S}(t, t_0) = \exp(-\tfrac{i}{h}\widehat{H}(t - t_0)).$$

$\widehat{H}$ is system Hamiltonian. The matrix elements of scattering operator define transition probability from initial quantum state into another.

$$S_{if} = -i\int d\vec{r}_1 d\vec{r}_2 dt \varphi_1^* \varphi_2^{\cdot} U(r)\varphi_2\varphi_1 \exp(-i(E_{1i} + E_{2i} - E_{1f} - E_{2f})t),$$

where $E_i E_f$ is clusters basic and final states kinetic energies.

The interaction potential may be connected with averaged scattering matrix that is described by one-photon resonant exchange Hamiltonian

$$H = -\vec{d}_1\vec{E}_1(r) - \vec{d}_2\vec{E}_2(r)$$

where $\vec{d}, \vec{E}$ are dipole moment and field tension operators. Then for potential the following is obatained:

$$U(\vec{r}) = \tfrac{i}{4\Pi}\int\limits_{-\infty}^{\infty} d\omega\omega^2 \alpha_{ik}(\omega) D_{ik}(\omega, \vec{r}), \tag{7}$$

Where D_{ik} is photon Green function and

$$\alpha_{ik} = \tfrac{1}{3}\delta_{ik}\sum_n |d_n|^2 \left[(\omega_n - \omega - i\Gamma_n)^{-1} + (\omega_n + \omega - i\Gamma_n)^{-1}\right], \tag{8}$$

is the polarization tensor.

After integration (7) considering (8) the following expression is obtained for potential

$$U(r) = -\tfrac{2}{3c^2}\sum_n r_n^{-1}\left|d_n\right|^2 \omega_n^2 \exp(\tfrac{\Gamma_n r}{c})\cos\tfrac{\omega_n r}{c}. \tag{9}$$

In equation summarization occurs for all levels.

Conclusion

The century long of theoretical research and the on-going revolution in computer technology have made quantum mechanics applicable to small molecules, where quantum-mechanical calculations have reached the accuracy that challenges experimental results. However, limitations of existing quantum mechanical methods to describe the large molecular systems, that modern molecular science often deals with, is real obstacle to forth going. The extremely different approaches must be taken to describe such systems [10,11, 12].

Thus one photon resonance exchange creates decreasing potential holes by height and depth. From this expression may be obtaied solution for isolated long-wave radiation potentials. isolated long-wave quants may be the radiation which happens when on cluster surface or cristallyne lattice additional molecule enters or in drop while molecule difussion [12.13].

During cristalization and condensation the some portion of latent heat may be trasformed in characterized radiation. The transformation energy is distributed between existed and new energetic levels. They are called as phase radiation and is depended on medium optical properties. The cloud medium may be imagined as unity of clusters that are on different energetic levels, interacting through energy emition-absorbtion. According to this Earth surrounding environment is one of possible renewable energy source [14], the use of which gives chanse on transition into new energy transportation means.

References

[1] Direct observation of ultrafast hydrogen bond strengthening in liquid water". Jie Yang, Riccardo Dettori, J. Pedro F. Nunes, Nanna H. List, etc. Nature, 2021, DOI: 10.1038/s41586-021-03793-9

[2] Landau L.D., Lifshic E.M. Quantum Mechanics. v.3. 1989

[3] Perelman M.E., Badinov I.Ia. Model of cloud formations. Bulletin of Georgian Acedemy of Sciences, v.131, N2, 1988

[4] Hasted D. Physics of atomic collisions. 1965

[5] Tatishvili M. Some peculiarities of mathematical simulation of cloud microstructure. Transactions of the Institute of Hydrometeorology, v.114, 2009.

[6] Baur G. et al. Nuclear Physics, A 729, 2003, pp. 787–808

[7] Pekka Manninen. manninen@chem.helsinki.fi http://www.chem.helsinki.fi/»manninen/mqm06.html

[8] Tatishvili M. Energy transformation in clouds according quantum principles. International Scientific Journal. Journal of Environmental Science, vol. 3, 2014, pp. 7-9.

[9] Tatishvili M. Developing Weather Forecasting System in Georgia. Ecology & Environmental Sciences, 2 (7), 2017, DOI:10.15406/mojes.2017.02.00046

[10] Selvam A. M. A General Systems Theory for Chaos, Quantum Mechanics and Gravity. Apeiron 11, 134-146, http://redshift.vif.com/JournalFiles/V11NO3PDF/V11N3SEL.PDF http://arxiv.org/html/physics/0211066, 2004

[11] Palmer T.N. Quantum Reality, Complex Numbers and the Meteorological Butterfly Effect. European Centre for Medium-Range Weather Forecasts Shinfield Park, RG2 9AX, Reading .UK. Bulletin of the American Meteorological Society", April 2005

[12] Hajcek P. A new approach to quantum measurement problem: cluster separability. Journal of Physics: Conference, Series 306**,** 2011, 012035 doi:10.1088/1742-6596/306/1/012035

[13] Tatishvili M.R., Palavandishvili A.M. Impact of Short-Term Geomagnetic Activity on Weather and Climate Formation in Georgian Region. Journal of the Georgian Geophysical Society,Physics of Solid Earth, Atmosphere, Ocean and Space Plasma, ISSN: 1512-1127, v. 23(2), 2020.

[14] Tatishvili M.R., Khvedelidze Z.V., Demetrashvili D.I. On some weather forecasting models in Georgia. Journal of the Georgian Geophysical Society, Physics of Solid Earth, Atmosphere, Ocean and Space Plasma, . ISSN: 1512-1127, v. 23(2), 2020.

ღრუბლის ნაწილაკების და ფოტონების ურთიერთქმედების ზოგიერთი მოსაზრების შესახებ

მ. ტატიშვილი

რეზიუმე

სინათლის (ფოტონის) და ღრუბლის ნაწილაკების ურთიერთქმედება ძირითადი კვანტური დაშვების მიხედვით, რომ სისტემის შიდა ენერგია შედგება ბმული მიკრონაწილაკებით (კლასტერი) გარკვეულ პირობებში, რომლითაც შესაძლებელია მათთვის დაშვებული დისკრეტული მნიშვნელობების მიღება, განხილულია სტატიაში. კვლევის მიზანია გამოვთვალოთ ერთი მდგომარეობიდან მეორეში გადასვლის ალბათობა, რომელიც გამოწვეულია შინაგანი ძალებით ან რაიმე შინაგანი პროცესებით. კლასტერი შეიძლება წარმოდგენილი იყოს როგორც მრავალპოლუსიანი სისტემა. ღრუბლოვანი წარმონაქმნების მიკროსტრუქტურის ზოგიერთი თავისებურება განხილულია წყლის ნაწილაკებისათვის დამახასიათებელი კვანტური დისპერსიული ძალების ან ვან-დერ-ვაალსის ძალების გამოყენებით. ურთიერთქმედების პოტენციალის ფორმულის მისაღებად შემოტანილია კლასტერის ძირითადი და ბოლო მდგომარეობების ტალღური ფუნქციები და დისპერსიული მატრიცა, რომელიც აღწერს ვირტუალურ ფოტონს. აღმოჩნდა, რომ ვირტუალური ფოტონის ურთიერთქმედება იწვევს პოტენციურ ხვრელებსა და ბარიერებს, რომლებიც სიმაღლის და სიგანის მიხედვით მცირდება. იზოლირებული გრძელი ტალღის რაოდენობა შეიძლება იყოს რადიაცია, რომელიც წარმოიქმნება დაკვირვებადი მიკროფიზიკური პროცესების განმავლობაში.

О некоторых соображениях взаимодействия облачных частиц и фотонов

М.Р. Татишвили

Резюме

В статье обсуждается взаимодействие света (фотона) и облачных частиц в соответствие с основным квантовым предположением о том, что внутренняя энергия системы состоит из связанных микрочастиц (кластера), которые при определенных условиях могут принимать разрешенные дискретные значения. Цель состоит в том, чтобы рассчитать вероятность перехода из одного состояния в другое, вызванное внутренними силами или какими-либо внутренними процессами. Кластер можно представить как многополюсную систему. Некоторые особенности микроструктуры облачных образований обсуждались с использованием квантово-дисперсных сил или сил Ван-дер-Ваальса, характерных для частиц воды. Для получения выражения для потенциала взаимодействия введены волновые функции основного и возбужденного состояний кластеров и дисперсионной матрицы, описываемые виртуальным фотоном. Оказалось, что взаимодействие виртуальных фотонов вызывает потенциальные ямы и барьеры, которые уменьшаются по высоте и ширине. Изолированный длинноволновый квант может быть излучением, генерируемым во время наблюдаемых микрофизических процессов.

Journal of the Georgian Geophysical Society, e-ISSN: 2667-9973, p-ISSN: 1512-1127
Physics of Solid Earth, Atmosphere, Ocean and Space Plasma, v. 24(2), 2021, pp. 73 - 77

Study of the Mean and Extreme Values, Intensity and Recurrence Variability of Meteorological Elements Based on the 1956-2015 Observation Data

[1]Marika R. Tatishvili, [2]Lia D. Megrelidze, [1,2]Ana M. Palavandishvili

[1]*Institute of Hydrometeorology of Georgian Technical University, Tbilisi, Georgia*
[2]*National Environmental Agency*
m.tatishvili@gtu.ge

ABSTRACT

Based on the data of the last 60 years (1956-2015) of 39 stations of the Georgian Meteorological Network, the nature of the change in the intensity and recurrence of the mean and extreme values of the meteorological elements was studied. The mentioned 39 stations were selected in order to optimally take into account the climatic features of the territory of Georgia. The trends of temperature and precipitation were evaluated. For the indices (35 indices) the change trends according to the average annual value were studied. The R-based software package ClimPact2 was used to calculate the sector climate indexes. The R-based software RHtestV4 and RHtests_dlyPrcp4 were used to check the homogeneity of the discussed time series.

Key Words: *Mean and extreme value, average annual value, climatic indices, homogeneity check, warming and cooling centers.*

Introduction

Georgian relief may be characterized by three sharply expressed orographic elements: in north Caucasus, in south – Georgian south uplands and lowland or intermountain depression located between those two risings. This one begins from The Black Sea shore by triangular Colchis Lowland and spreads up to eastern Georgia like narrow strip. Between those two uplands small scaled orographic elements are allocated. Such complicated relief has definite influence on air masses motion in atmosphere lower layers. Mainly west and eastern atmospheric processes prevailed over Georgian territory. Due to complex orographic conditions and influence of the black Sea in Georgia exist most of Earths climatic types, from marine wet subtropical climate in west Georgia and steppe continental climate in east Georgia up to eternal snow and glaciers in high mountain zone of Great Caucasus, and 40% of existed landscapes [1]. Thus those climatic zones uphold the formation of different dangerous hydrometeorological phenomena, namely: hailstone, heavy showers, flooding, thunderstorm, draughts, sea storms. The economical losses and casualties caused by those catastrophic events are impressive [2].

Here exist most of Earths climatic types, from marine wet subtropical climate of west Georgia and steppe continental climate of east Georgia up to eternal snow and glaciers of high mountain zone of Great Caucasus, and also approximately 40% of observed landscapes. The complexity of the orographic structure of Georgian territory, along with other physical -geographical factors is the cause of wide variety of climates and landscapes. There are almost all types of climates observed on the Globe, from the climate of eternal snows of high mountains and glaciers to steppe continental climate of eastern Georgia and humid climate of the Black Sea coast subtropical

Current geodynamics and orographic properties of Georgia play an important role in the formation of various weather patterns. Such complex relief conditions the formation and evolution of various scaled circulation systems and heterogeneous spatial distribution of meteorological elements. This is verified by the fact, that precipitation annual distribution has diverse type, with sharply expressed spatial inhomogeneities.

The local circulation systems developed on the background of synoptical processes play significant role in the spatial-temporal distribution of weather determining parameters. The study of all those phenomena needs the processing of long-term observation series of those climatic parameters.

Data and methods

Based on the 39 stations data of the Georgian Meteorological Network of last 60 years (1956-2015), the change nature of the intensity and recurrence of the mean and extreme values of the meteorological elements was studied. These 39 stations were selected in order to optimally take into account the climatic characteristics of the territory of Georgia; the temperature and precipitation change trends, as well as wind speed was assessed.

Extreme values of climate parameters are more sensitive to climate change than their mean values, however, medium values often make it impossible to assess socio-economic impacts on different sectors of climate change. In addition to the mean values of climate parameters, various types of climate characteristics / indices (such as heat waves, extremely rainy / rainless periods, etc.) are calculated to assess climate change., the calculation methodology of which is developed according to the recommendations of the IPCC and by which the change regularities of the magnitude, frequency and intensity of extreme climate parameters are determined.

In order to increase the reliability of the obtained results, these parameters were evaluated by two methods: for each parameter to detect change trends in 1956-2015 and to assess the statistical reliability of these trends (Mann-Kendall method) and for two 30-year periods (1956-1985 & 1986-2015) the comparison of mean / extreme values.

The R-based software package ClimPact2, developed by the IMO Climate Commission's Sector Climate Index Expert Group (https://github.com/ARCCSS-extremes/climpact2), was used to calculate sectoral climate indices [3].

R-based software RHtestV4 and RHtests_dlyPrcp4 (http://etccdi.pacificclimate.org/software.shtml) were used to test the homogeneity of the time series under consideration [4].

Between the two 30-year periods (1956-1985 & 1986-2015), the average annual atmosphere surface layer temperature in the country has risen almost everywhere, within 1 degree, with an average increase of 0.5^0C in the territory.

The warming process is relatively intense in Samegrelo-Zemo Svaneti, Kakheti and Samtskhe-Javakheti. The most significant warming was revealed in Dedoplistskaro district.

Discussion

The precipitation regime changes are unstable in time and are also spatially heterogeneous, although they are still characterized by some regularity. In particular, the annual rainfall in western Georgia is mainly increased, while in some eastern regions - decreased, although the nature of the change in annual rainfall is mostly unreliable and there are no obvious trends. Trends were revealed only on a number of curves. Trends in the change in the average annual rainfall in the West are almost everywhere positive, with the largest deviation between the two periods (up to 15%) and, consequently, the most stable growth trend was observed in Poti and Khulo (60-75 mm / 10 years). The only exceptions are significant tendencies of precipitation decrease (60-120 mm / 10 years) in Guria and high mountains of Adjara (Goderdzi Pass). In the east, the annual growth is maximal and the corresponding trends are significant in Lagodekhi (17%, 75 mm / 10 years), while the decrease in precipitation is most intense in Tianeti (-18%, 39 mm / 10 years).

The average wind speed change tends seems to be decreased for almost all study stations. The average wind speed between the two 30-year periods decreases by an average of 1-2 m / s. Exceptions in this regard are Kobuleti and Bakhmaro, where the wind speed is unstable, but increases with each passing season. It should be noted, however, that these trends are based solely on observations prior to 2010. Most of the trends in average wind speed change across the country are reliable for both annual values and seasonal average speeds. Only at Tbilisi station the trend is not stable in any season of the year, in Zugdidi - in autumn (September-October) and in Kutaisi - in summer. The picture of the most intense decrease in average wind speed in the whole area was revealed in Mta-Sabueti and Poti, where the average annual speeds decrease by 0.5 m / s every 10 years, and in the east - in Shida Kartli (Gori). Such a decrease in wind speeds is due to the intense decline detected in the spring of this parameter, most notably in April.

The number of strong windy days (maximum wind speed ≥15 m / s, ≥25 m / s) was selected to characterize the maximum wind speed regime. Since maximum speed wind data are available only from 1970, the change trends were built on 1970-2015. For the period, while the comparison of the numbers of strong winds was carried out in 1971-1985, 1986-2000 and 2001-2015for 15-year periods.
Tendencies to decrease the number of strong winds (≥15 m / s) are predominant in the West, while in Eastern Georgia, their frequency will be observed. It is noteworthy that the number of such days is decreasing in western Georgia - Kutaisi and especially on the western slopes of the Likhi Range (Mta-Sabueti), where trends were revealed in the summer-autumn seasons, and in the east, in the Mtkvari gorge, a significant increase is observed. Frequency of strong winds in Gori will be observed in all seasons, while in Tbilisi their annual number increases mainly at the expense of March. The trend changes maximum in Mta-. Sabueti and Gori and are 1.7 days / 10 years. The frequency of extremely strong winds (≥25 m / s) changes with a similar regularity. In particular, a significant decrease in such days was observed in Kutaisi and Mta-Sabueti, while the steady increase is observed in Gori, as well as in Poti.

Conclusion

The following may be stated based on the analysis of observation data:

- The average annual temperature has risen everywhere, up to 1 degree.
- Warming is taking place in June-October (0.7-1.3 degrees), especially in August (0.9-1.8 degrees).
- Spring-winter warming is unreliable.
- Cooling trends are also predominant in some months (May, November-December).
- In western Georgia it is mainly conditioned by the increase of night temperatures, and in the east - by daytime temperatures.
- Annual precipitation is mainly increased in western Georgia, while it is reduced in some eastern regions.
- The increase in the West is mainly observed in January, in the East - in October-November, while the decrease is everywhere at the expense of July-September.

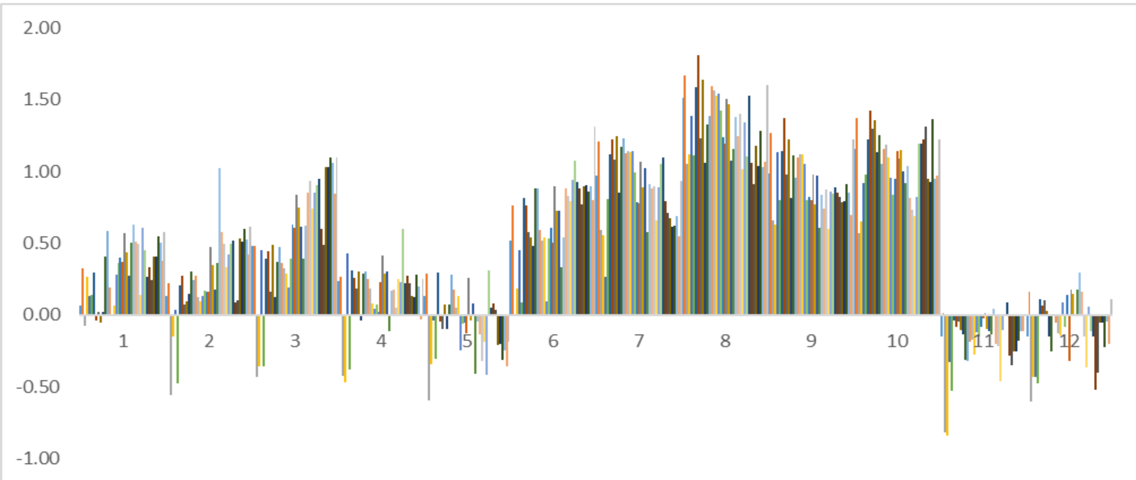

Fig.1. The monthly mean temperature change based on the1956-2015 observation data.

The conducted research gives possibility to conclude regarding precipitation change:

- Annual precipitation is mostly increased in western Georgia, while it is reduced in a number of eastern regions.
- The increase in the West is mainly observed in January, in the East - in October-November, while the decrease is everywhere mainly due to July-September.

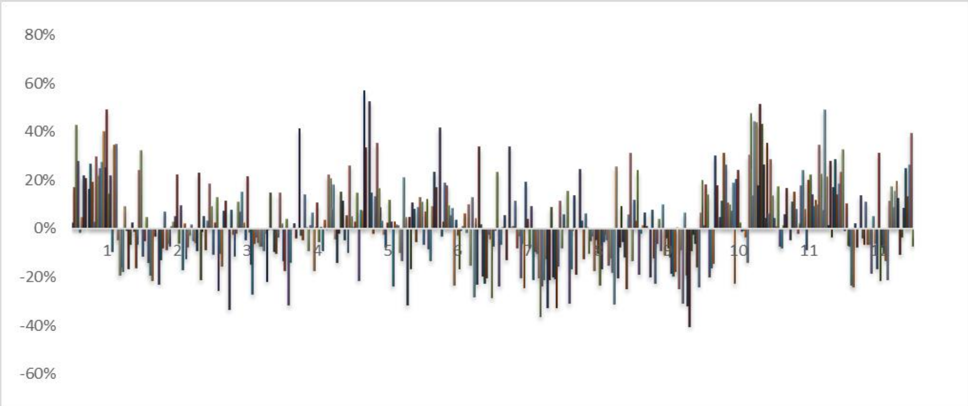

Fig.2. Precipitation change based on the1956-2015 observation data.

The linear trends for Poti and Tianeti stations are presented below.

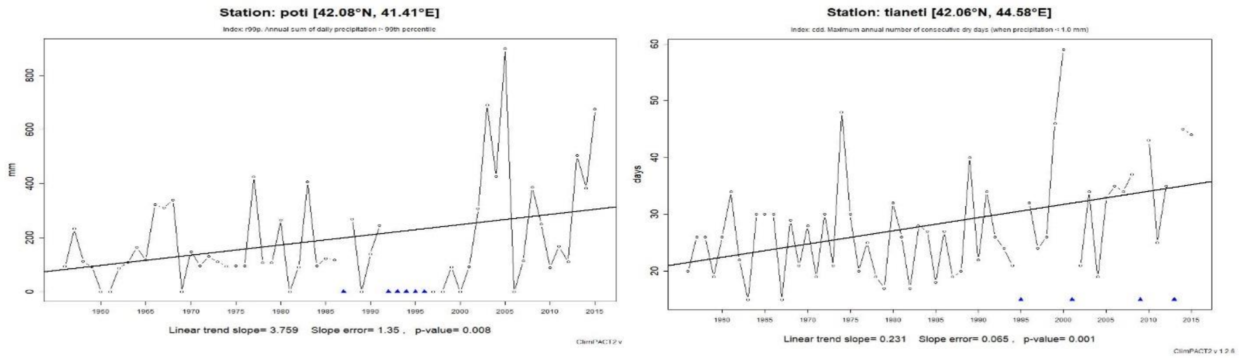

Fig.3. Precipitation linear trends for Poti and Tianeti.

In Samegrelo and Adjara-Guria precipitation tendency has increased character, which is due to the frequency of heavy rainfall (R95pTOT, R99pTOT r95p, r99p, r30mm, r50mm). In addition, a significant increase in the maximum daily precipitation (Rx1D, Rx5D) was observed in these areas.

In the south and east of the country, precipitation indices for most stations (especially in Kakheti and Mtskheta-Mtianeti) indicate precipitation decrease due to the prolonged precipitation periods (CDD). At the same time, there are increased tendencies in Tbilisi, Telavi and Lagodekhi, as well as the increasing number of cases of extreme rainfall.

Therefore, it is likely that droughts, floods and natural geological processes will increase in frequency.

References

[1] Climate and climatic resources of Georgia, 1971.

[2]Tatishvili M., Elizbarashvili E., Meskhia R., Elizbarashvili Sh. Natural hydrometeorological disasters, their causes and prevention measures. The Macrotheme Review. A multidisciplinary journal of global macro trends, 148-154, A Macrotheme Capital Management, LLC Academic Publication, Volume 2, Issue 1, Winter 2013 (January). ISSN 1848-4735, France

[3] https://github.com/ARCCSS-extremes/climpact2

[4] http://etccdi.pacificclimate.org/software.shtml

მეტეოროლოგიური ელემენტების საშუალო და ექსტრემალური მნიშვნელობების, ინტენსივობისა და განმეორებადობის ცვალებადობის შესწავლა ბოლო 60-წლიანი პერიოდის (1956-2015 წ.წ.) დაკვირვებათა მონაცემების საფუძველზე

მ. ტატიშვილი, ლ.მეგრელიძე, ა.ფალავანდიშვილი

რეზიუმე

საქართველოს მეტეოროლოგიური ქსელის 39 სადგურის უკანასკნელი 60-წლიანი პერიოდის (1956-2015 წ.წ.) მონაცემებზე დაყრდნობით შესწავლილი იქნა მეტეოროლოგიური ელემენტების საშუალო და ექსტრემალური მნიშვნელობების ინტენსივობისა და განმეორებადობის ცვლილების ხასიათი. აღნიშნული 39 სადგური შერჩეული იქნა საქართველოს ტერიტორიის კლიმატური თავისებურებების ოპტიმალურად გათვალისწინების მიზნით. შეფასებული იქნა, როგორც ტემპერატურისა და ნალექების, ცვლილების ტენდენციები. სექტორული კლიმატური ინდექსების გაანგარიშებისთვის გამოყენებული იქნა **R-**დაფუძნებული პროგრამული პაკეტი ClimPact2.განსახილველი დროითი სერიების ჰომოგენურობის შემოწმების მიზნით გამოყენებული იქნა **R-**დაფუძნებული პროგრამული უზრუნველყოფები RHtestV4 და RHtests_dlyPrcp4

Изучение средних и экстремальных значений, интенсивности и повторяемости метеорологических элементов на основе данных наблюдений за 1956-2015 гг.

М.Р. Татишвили, Л.Д. Мегрелидзе, А. М. Палавандишвили

Резюме

По данным 39 станций Грузинской метеорологической сети за последние 60 лет (1956-2015 гг.) изучен характер изменения интенсивности и повторяемости средних и экстремальных значений метеорологических элементов. Указанные 39 станций выбраны с целью оптимального учета климатических особенностей территории Грузии. Были оценены тенденции изменения температуры и осадков. Для расчета климатических индексов использовался программный пакет ClimPact2 на базе R. Программное обеспечение на основе R RHtestV4 и RHtests_dlyPrcp4 использовалось для проверки однородности рассматриваемого временного ряда.

Journal of the Georgian Geophysical Society, e-ISSN: 2667-9973, p-ISSN: 1512-1127
Physics of Solid Earth, Atmosphere, Ocean and Space Plasma, v. 24(2), 2021, pp. 78 - 91

Changeability of the Meteorological Parameters Associated with Holiday Climate Index in Different Mountainous Regions of Georgia in 1956-2015

[1]Avtandil G. Amiranashvili, [2]Liana G. Kartvelishvili, [2]Nato B. Kutaladze, [2]Lia D. Megrelidze, [3]Marika R. Tatishvili

[1]Mikheil Nodia Institute of Geophysics of Ivane Javakhishvili Tbilisi State University, Tbilisi, Georgia
*1, M. Alexidze Str., 0160, Tbilisi, Georgia, e-mail:*avtandilamiranashvili@gmail.com
[2]National Environmental Agency of Georgia
[3]Institute of Hydrometeorology of Georgian Technical University, Tbilisi, Georgia

ABSTRACT

Statistical data on meteorological parameters associated with the Holiday Climate Index (monthly mean maximum air temperature, monthly mean relative air humidity, cloud cover, monthly precipitation, wind speed) in thirteen mountainous regions of Georgia (Bakhmaro, Bakuriani, Borjomi, Goderdzi, Gudauri, Khaishi, Khulo, Lentekhi, Mestia, Pasanauri, Shovi, Stepantsminda, Tianeti) from 1956 to 2015 are presented. In particular, the changeability of the indicated meteorological parameters during 1986÷2015 in comparison with 1956÷1985 for above enumerated points is studied.

Key Words: *Meteorological parameters, Holiday Climate Index.*

Introduction

In recent decades, the problem of global climate change has acquired special significance [1,2]. At the same time, the air temperature and other climatic elements changing has considerable spatial and temporal inhomogeneities both in the global (Global Land, Global Land of the Northern and Southern Hemisphere, Zonal territories, etc.) [1-6], and regional scales (even the territory of small countries with complex terrain) scales [7-9].

This problem is also of great importance in Georgia due to the diversity of climatic regions on its territory [10-17].

Sustainable development of various spheres of the national economy, including resort and tourism industry is largely determined by climate change, which is of vital importance.

The resort and tourist potential of the area is especially preconditioned by its bioclimatic conditions. Therefore, it is important to identify existing and future changes of these conditions under the impact of climate change.

In particular, information on the changeability of the different simple thermal indices as well as the Tourism Climate Index (TCI) [18] and the Holiday Climate Index (HCI) [19] in the recent decades in different countries (including some locations of Georgia) is represented in [8,20-30].

Simple thermal indices include more than one meteorological parameter and consider the combined action of the air temperature, humidity, wind speed and etc. on the human organism [31-34]. For example, to determine the monthly mean values of TCI following data are necessary: mean and maximum mean air temperature, mean and mean minimum relative humidity, precipitation, sunshine duration and wind speed [18].

Primarily, in the work [35] the investigating results of changeability of the mean monthly values of meteorological parameters, used to determine TCI values and different simple thermal indices on the two regions of Georgia (Adjarian Autonomous Republic and Kakheti) during the period from 1961 through 2010 are presented.

This work is the continuation of the previous research. Results of statistical analysis of meteorological parameters data associated with the Holiday Climate Index in thirteen mountainous regions of Georgia (Bakhmaro, Bakuriani, Borjomi, Goderdzi, Gudauri, Khaishi, Khulo, Lentekhi, Mestia, Pasanauri, Shovi, Stepantsminda, Tianeti) from 1956 to 2015 are presented below.

Study Area, material and methods

The research for thirteen mountainous regions of Georgia (Bakhmaro, Bakuriani, Borjomi, Goderdzi, Gudauri, Khaishi, Khulo, Lentekhi, Mestia, Pasanauri, Shovi, Stepantsminda, Tianeti) is carried out. Table 1 presents the information on the coordinates and heights of the location of those13 meteorological stations whose data were used in the work.

Table 1. Coordinates and heights of the 13 mountainous meteorological stations in Georgia.

Location (Abbreviation)	Latitude, N°	Longitude, E°	Height, m, a.s.l.
Bakhmaro (Bakh)	42.32	41.85	1926
Bakuriani (Bak)	43.52	41.73	1665
Borjomi (Borj)	43.40	41.83	789
Goderdzi (God)	42.52	41.63	2025
Gudauri (Gud)	44.48	42.47	2194
Khaishi (Kha)	42.18	42.95	730
Khulo (Khu)	42.32	41.65	914
Lentekhi (Lent)	42.73	42.78	760
Mestia (Mest)	42.75	43.05	1441
Pasanauri (Pas)	44.70	42.35	1070
Shovi (Sho)	43.68	42.70	1507
Stepantsminda (Step)	44.65	42.67	1744
Tianeti (Tian)	44.97	42.12	1099

In the work Georgian National Environmental Agency on monthly mean meteorological parameters data associated with the Holiday Climate Index [19, 36-38] (max air temperature, air relative humidity, total cloud cover, precipitation sum and wind speed) in the period from 1956 through 2015 are used.

For the data analysis the standard statistical methods of the studies were used [39]. The difference between the mean values of the meteorological parameters into 1986-2015 and 1956-1985 with the use of Student's criterion was determined (level of significance not worse than 0.15).

The following designations are used below: T_{max} - mean maximum air temperature (°C), RH- mean relative humidity (%), CC – mean total cloud cover (amount); P - sum precipitation - (mm), V - mean wind speed (m/sec). ΔT_{max}. ΔV - the difference between the mean values of the meteorological parameters during 1986-2015 and 1956-1985 periods.

Results and discussion

The obtained Results are available on the Tables 2-6 and Fig. 1-10.

Mean max air temperature

The mean annual, half year and monthly min and max air temperature (T_{max}) data are presented in Table 2 and Fig. 1. The range of variability of the mean values of T_{max} for the indicated stations is as follows:

Mean Year - from 6.6 °C (Goderdzi) to 16.4 °C (Borjomi); Mean Cold - from 0.0 °C (Goderdzi) to 9.7 °C (Khulo); Mean Warm - from 13.3 °C (Goderdzi) to 23.9 °C (Khaishi); Min - from -11.8 °C (Goderdzi) to -0.5 °C (Borjomi); Max - from 23.4 °C (Goderdzi) to 35.0 °C (Borjomi).

Table 2. The mean min, monthly mean, max and mean seasonal values of T_{max} (°C) in thirteen locations of Georgia in 1956-2015.

Location	Mean Year	Mean Cold	Mean Warm	Min	Max
Bakhmaro	8.6	3.0	14.2	-8.2	24.2
Bakuriani	11.3	5.1	17.5	-5.7	27.7
Borjomi	16.4	9.4	23.5	-0.5	35.0
Goderdzi	6.6	0.0	13.3	-11.8	23.4
Gudauri	7.8	2.0	13.7	-8.8	25.4
Khaishi	16.3	8.7	23.9	-1.3	33.7
Khulo	15.8	9.7	22.0	-1.6	31.4
Lentekhi	15.8	7.9	23.7	-1.9	34.5
Mestia	13.4	5.9	20.9	-6.4	30.2
Pasanauri	14.5	7.4	21.6	-2.9	33.0
Shovi	12.6	5.7	19.5	-5.5	30.8
Stepantsminda	10.6	4.5	16.7	-5.7	27.4
Tianeti	14.4	7.6	21.2	-1.7	31.6

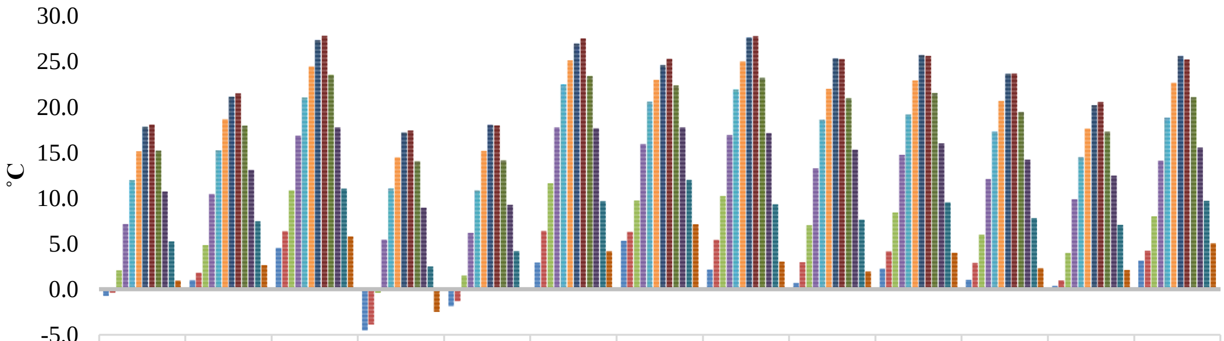

	Bakh	Bak	Borj	God	Gud	Kha	Khu	Lent	Mest	Pas	Sho	Step	Tian
Jan	-0.7	1.0	4.5	-4.5	-1.9	2.9	5.3	2.1	0.7	2.2	1.0	0.3	3.1
Feb	-0.4	1.8	6.4	-3.9	-1.3	6.4	6.3	5.4	2.9	4.1	2.9	1.0	4.2
Mar	2.1	4.8	10.8	-0.4	1.5	11.6	9.7	10.2	7.0	8.4	6.0	4.0	8.0
Apr	7.2	10.4	16.9	5.5	6.2	17.8	15.9	16.9	13.3	14.8	12.1	9.9	14.1
May	12.0	15.2	21.0	11.0	10.9	22.5	20.6	21.9	18.6	19.2	17.3	14.5	18.8
Jun	15.1	18.6	24.4	14.5	15.2	25.1	23.0	25.0	22.0	22.9	20.6	17.6	22.6
Jul	17.8	21.1	27.3	17.2	18.0	26.9	24.6	27.6	25.3	25.7	23.6	20.2	25.6
Aug	18.1	21.5	27.8	17.4	18.0	27.5	25.3	27.8	25.2	25.6	23.7	20.5	25.2
Sep	15.2	18.0	23.5	14.1	14.2	23.4	22.4	23.2	21.0	21.5	19.4	17.3	21.1
Oct	10.7	13.1	17.8	9.0	9.3	17.7	17.8	17.1	15.3	16.0	14.2	12.5	15.6
Nov	5.2	7.5	11.0	2.5	4.2	9.6	12.0	9.3	7.6	9.5	7.8	7.1	9.7
Dec	1.0	2.7	5.8	-2.5	0.0	4.2	7.1	3.0	2.0	4.0	2.3	2.1	5.1

Fig. 1. T_{max} monthly mean values of in thirteen locations of Georgia in 1956-2015.

The intra-annual distribution of T_{max} values for all 13 investigations points of Georgia are presented on Fig. 1. The smallest T_{max} values for all points during January are detected. The T_{max} greatest values for Bakhmaro, Bakuriani, Borjomi, Goderdzi, Khaishi, Khulo, Lentekhi, Shovi and Stepantsminda during August are fixed; for Mestia, Pasanauri and Tianeti – during July, and for Gudauri – during July and August (Fig. 1).

The information onthe changeability of the ΔT_{max} values of in separate points is presented below (Fig. 2).

The variability of the mean monthly max air temperature is observed for 13 points of Georgia in 69 cases (including 66 cases - an increase and only for 3 cases - a decrease in ΔT_{max} values).

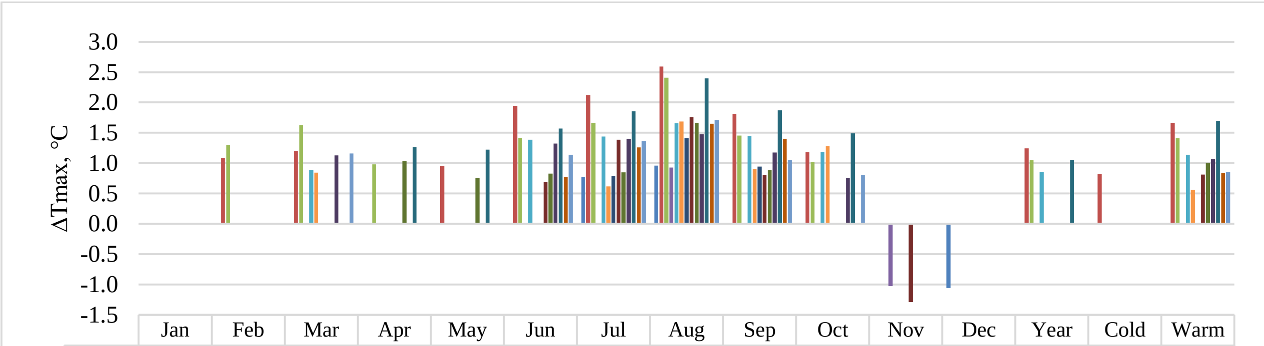

	Jan	Feb	Mar	Apr	May	Jun	Jul	Aug	Sep	Oct	Nov	Dec	Year	Cold	Warm
Bakh							0.8	1.0				-1.1			
Bak		1.1	1.2		1.0	1.9	2.1	2.6	1.8	1.2			1.2	0.8	1.7
Borj		1.3	1.6	1.0		1.4	1.7	2.4	1.5	1.0			1.0		1.4
God								0.9			-1.0				
Gud			0.9			1.4	1.4	1.7	1.5	1.2			0.9		1.1
Kha			0.8				0.6	1.7	0.9	1.3					0.6
Khu							0.8	1.4	0.9						
Lent						0.7	1.4	1.8	0.8		-1.3				0.8
Mest				1.0	0.8	0.8	0.9	1.7	0.9						1.0
Pas			1.1			1.3	1.4	1.5	1.2	0.8					1.1
Sho				1.3	1.2	1.6	1.9	2.4	1.9	1.5			1.1		1.7
Step						0.8	1.3	1.6	1.4						0.8
Tian			1.2			1.1	1.4	1.7	1.1	0.8					0.9

Fig. 2. Difference between the T_{max} mean values for 1986-2015 and 1956-1985 in thirteen locations of Georgia

The variations of the ΔT_{max} values in the separate points are the following: Bakhmaro - increase of the values of ΔT_{max} (July, August), decrease (-1.1 °C, December); Bakuriani - increase (February, March, May-October, mean annual, cold and warm seasons mean); Borjomi - increase (February-April, June-October, mean annual and warm season mean); Goderdzi - increase (August), decrease (-1.0 °C, November); Gudauri - increase (March, June-October, mean annual and warm season mean); Khaishi - increase (March, July-October, warm season mean); Khulo - increase (July-September); Lentekhi - increase (July-September, warm season mean), decrease (-1.3 °C, November); Mestia - increase (April-September, warm season mean); Pasanauri - increase (March, June-October, warm season mean); Shovi - increase (April-October, mean annual and warm season mean); Stepantsminda - increase (June-September, warm season mean); Tianeti - increase (March, June-October, warm season mean).

Totally, the ΔT_{max} values change from -1.3°C (Khulo, November) to 2.6 °C (Baruriani, August), amplitude - 3.9 °C.

Air mean relative humidity

The mean annual, half year and monthly min and max air relative humidity (RH) data are available in Table 3 and on Fig. 3.

The range of variability of the RH mean values for the indicated stations is as follows: Mean Year - from 69.4 % (Stepantsminda) to 86.9 % (Goderdzi); Mean Cold - from 65.7 % (Stepantsminda) to 88.4 % (Goderdzi); Mean Warm - from 72.2 % (Mestia) to 85.4 (Goderdzi); Min - from 38.2 % (Khulo) to 61.3 % (Goderdzi); Max - from 91.0 % (Bakhmaro, Bakuriani) to 100 % (Goderdzi, Lentekhi).

The intra-annual distribution of RH values for all indicated investigations points of Georgia are presented in Fig. 3. The RH smallest values for all points during January are observed (62.8 %, Stepantsminda). The RH greatest values for Goderdzi (91.1 %) in February are fixed (Fig. 3).

Table 3. The mean monthly min, mean monthly max and mean seasonal RH (%) values in thirteen locations of Georgia in 1956-2015.

Location	Mean Year	Mean Cold	Mean Warm	Min	Max
Bakhmaro	74.1	73.3	74.8	50.0	91.0
Bakuriani	78.4	78.9	78.0	56.0	91.0
Borjomi	77.9	80.4	75.5	55.3	94.2
Goderdzi	86.9	88.4	85.4	61.3	100
Gudauri	74.2	71.4	76.9	47.2	91.7
Khaishi	77.8	81.2	74.4	48.0	97.0
Khulo	71.4	69.8	73.0	38.2	92.0
Lentekhi	80.2	85.2	75.2	48.6	100
Mestia	75.8	79.5	72.2	53.0	97.9
Pasanauri	75.2	75.9	74.5	56.0	92.0
Shovi	78.3	80.0	76.5	57.3	92.6
Stepantsminda	69.4	65.7	73.2	43.0	96.0
Tianeti	80.8	83.1	78.5	61.0	98.7

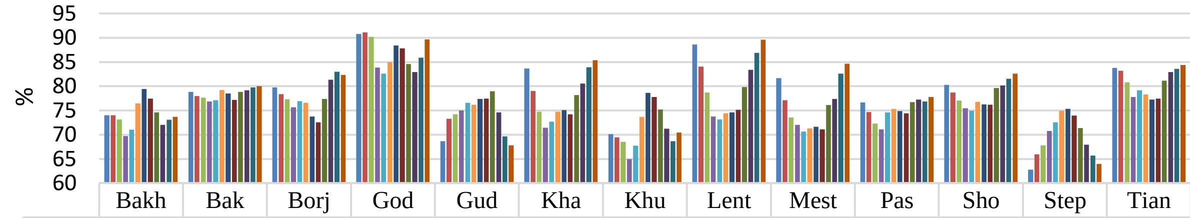

	Bakh	Bak	Borj	God	Gud	Kha	Khu	Lent	Mest	Pas	Sho	Step	Tian
Jan	74.0	78.8	79.7	90.8	68.6	83.6	70.1	88.6	81.7	76.6	80.3	62.8	83.8
Feb	74.0	78.0	78.4	91.1	73.3	79.0	69.5	84.0	77.1	74.7	78.7	66.0	83.2
Mar	73.2	77.7	77.3	90.2	74.2	74.7	68.5	78.7	73.5	72.3	77.0	67.8	80.8
Apr	69.7	76.9	75.6	83.8	75.0	71.4	65.0	73.8	72.1	71.1	75.5	70.8	77.8
May	71.0	77.1	76.9	82.6	76.6	72.7	67.8	73.2	70.7	74.6	75.0	72.6	79.2
Jun	76.4	79.3	76.6	85.0	76.2	74.8	73.7	74.4	71.3	75.3	76.8	74.9	78.3
Jul	79.4	78.5	73.8	88.4	77.4	75.0	78.6	74.6	71.7	74.9	76.3	75.4	77.3
Aug	77.4	77.2	72.6	87.8	77.5	74.2	77.8	75.2	71.1	74.4	76.2	73.9	77.5
Sep	74.6	78.9	77.4	84.6	79.0	78.2	75.2	79.8	76.1	76.7	79.6	71.4	81.1
Oct	72.0	79.2	81.4	82.9	74.6	80.6	71.3	83.4	77.4	77.3	80.1	67.9	83.0
Nov	73.1	79.8	83.0	85.9	69.7	83.9	68.7	86.9	82.6	76.9	81.5	65.7	83.6
Dec	73.7	80.0	82.4	89.7	67.8	85.4	70.4	89.6	84.6	77.8	82.6	64.0	84.4

Fig. 3. The monthly mean values of relative humidity in thirteen locations of Georgia in 1956-2015.

The changeability of the ΔRH values of in separate points is presented on the Fig. 4.

The variability of the monthly mean air relative humidity is detected for all investigated points in 86 cases (including 79 cases - an increase and only for 7 cases - a decreaseof ΔRH values).

The changeability of the ΔRH values in the separate points is the following: Bakhmaro - increase of the ΔRH values (January-June, October-December, mean annual and cold season mean), decrease (-2.5 %, August); Bakuriani - increase (January, February, April-June, October, December, mean annual, cold and warm seasons mean); Borjomi - increase (all month and seasons, except July, August and November); Goderdzi - increase (all month and seasons, except September); Gudauri - increase (January, February, mean annual and cold season mean); Khaishi - increase (January, March-June, November, December, mean annual and cold season mean); Khulo - increase (January, June, October, mean annual and cold season mean); Lentekhi - increase (January, November, cold season mean); Mestia - increase (January, November, December) decrease (March, April, August, September, mean annual and warm season mean); Pasanauri - increase (January, February, mean annual and cold season mean); Shovi - increase (January, February, October, mean annual and cold season mean), decrease (August and September); Stepantsminda - increase (all month and seasons, except July, August and September); Tianeti - increase (all month and seasons).

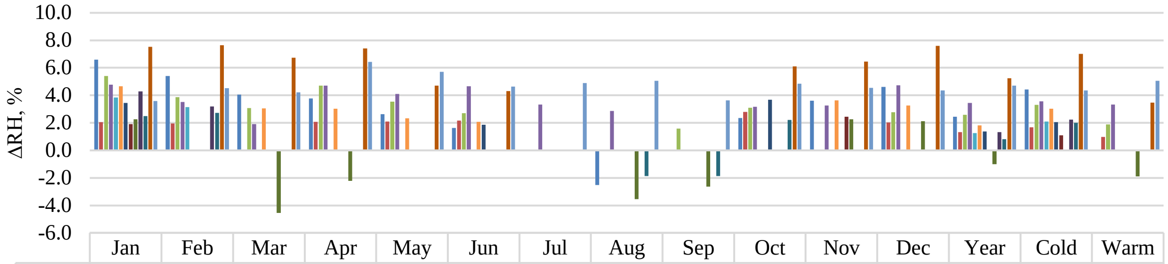

	Jan	Feb	Mar	Apr	May	Jun	Jul	Aug	Sep	Oct	Nov	Dec	Year	Cold	Warm
Bakh	6.6	5.4	4.0	3.8	2.6	1.6		-2.5		2.4	3.6	4.6	2.4	4.4	
Bak	2.1	1.9		2.1	2.1	2.2				2.8		2.0	1.3	1.7	1.0
Borj	5.4	3.9	3.1	4.7	3.5	2.7			1.6	3.1		2.8	2.6	3.3	1.9
God	4.8	3.5	1.9	4.7	4.1	4.7	3.3	2.9		3.2	3.3	4.7	3.4	3.6	3.3
Gud	3.8	3.1											1.3	2.1	
Kha	4.7		3.1	3.0	2.3	2.1					3.6	3.3	1.8	3.0	
Khu	3.4					1.9				3.7			1.4	2.0	
Lent	1.9										2.4			1.1	
Mest	2.3		-4.5	-2.2				-3.5	-2.6		2.3	2.1	-1.0		-1.9
Pas	4.3	3.2											1.3	2.2	
Sho	2.5	2.7						-1.9	-1.9	2.2			0.8	2.0	
Step	7.5	7.6	6.7	7.4	4.7	4.3				6.1	6.4	7.6	5.2	7.0	3.5
Tian	3.6	4.5	4.2	6.4	5.7	4.6	4.9	5.1	3.6	4.8	4.5	4.4	4.7	4.3	5.1

Fig. 4. Difference between the RH mean values for 1986-2015 and 1956-1985 in thirteen locations of Georgia

Completely, the ΔRH values change from -4.5 % (Mestia, March) to 7.6 % (Stepantsminda, February, December), and the amplitude is 12.1 %.

Total Cloud Cover

The mean annual, half year and monthly min and max total cloud cover amount (CC) data in are available from Table 4 and Fig. 5.

Table 4. The mean monthly min, mean monthly max and mean seasonal values of total cloud cover amount in thirteen locations of Georgia in 1956-2015.

Location	Mean Year	Mean Cold	Mean Warm	Min	Max
Bakhmaro	6.0	6.1	6.0	2.2	9.0
Bakuriani	6.1	6.1	6.1	2.0	9.1
Borjomi	6.2	6.4	6.0	2.3	9.1
Goderdzi	6.8	6.9	6.8	3.0	10
Gudauri	5.4	5.1	5.7	1.8	8.5
Khaishi	5.5	5.8	5.1	1.6	9.0
Khulo	6.1	6.1	6.0	2.0	9.0
Lentekhi	6.3	6.3	6.3	3.0	9.1
Mestia	6.1	6.3	5.9	2.0	9.1
Pasanauri	5.4	5.3	5.6	1.8	9.0
Shovi	6.4	6.5	6.4	2.0	10
Stepantsminda	5.4	4.9	5.9	1.8	9.0
Tianeti	5.7	5.8	5.6	2.0	9.0

The range of variability of the CC mean values for the indicated stations is as follows: Mean Year - from 5.4 (Gudauri, Pasanauri, Stepantsminda) to 6.8 (Goderdzi); Mean Cold - from 4.9 (Stepantsminda) to 6.9 (Goderdzi); Mean Warm - from 5.1 (Khaishi) to 6.8 (Goderdzi); Min - from 1.6 (Khaishi) to 3.0 (Goderdzi, Lentekhi); Max - from 8.5 (Gudauri) to 10 (Goderdzi, Shovi).

The intra-annual distribution of CC values for all indicated investigations points of Georgia is presented on Fig. 5 d. The smallest CC values for all points during August are fixed (4.4, Khaishi).

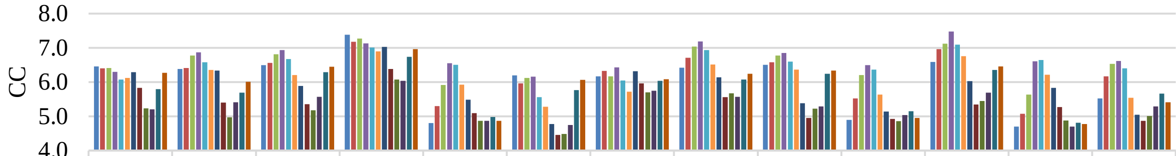

	Bakh	Bak	Borj	God	Gud	Kha	Khu	Lent	Mest	Pas	Sho	Step	Tian
Jan	6.5	6.4	6.5	7.4	4.8	6.2	6.2	6.4	6.5	4.9	6.6	4.7	5.5
Feb	6.4	6.4	6.6	7.2	5.3	6.0	6.3	6.7	6.6	5.5	7.0	5.1	6.2
Mar	6.4	6.8	6.8	7.3	5.9	6.1	6.2	7.0	6.8	6.2	7.1	5.6	6.5
Apr	6.3	6.9	6.9	7.1	6.5	6.2	6.4	7.2	6.9	6.5	7.5	6.6	6.6
May	6.1	6.6	6.7	7.0	6.5	5.6	6.0	6.9	6.6	6.4	7.1	6.6	6.4
Jun	6.1	6.4	6.2	6.9	5.9	5.3	5.7	6.5	6.4	5.6	6.8	6.2	5.5
Jul	6.3	6.3	5.9	7.0	5.5	4.8	6.3	6.1	5.4	5.1	6.0	5.8	5.0
Aug	5.8	5.4	5.3	6.4	5.1	4.4	6.0	5.6	4.9	4.9	5.3	5.3	4.9
Sep	5.2	5.0	5.2	6.1	4.9	4.5	5.7	5.7	5.2	4.9	5.4	4.9	5.0
Oct	5.2	5.4	5.6	6.0	4.9	4.7	5.7	5.6	5.3	5.0	5.7	4.7	5.3
Nov	5.8	5.7	6.3	6.7	5.0	5.8	6.0	6.1	6.2	5.1	6.4	4.8	5.7
Dec	6.3	6.0	6.4	7.0	4.9	6.1	6.1	6.2	6.3	5.0	6.5	4.8	5.4

Fig. 5. Total cloud cover monthly mean values of in thirteen locations of Georgia in 1956-2015.

The CC greatest values for Shovi (7.5) are detected in April (Fig. 5).

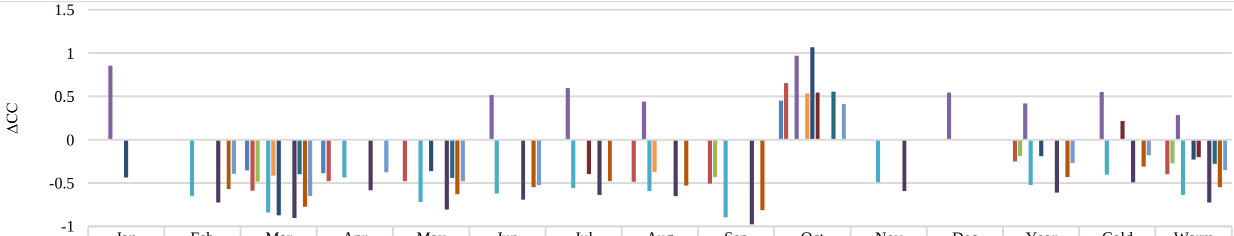

	Jan	Feb	Mar	Apr	May	Jun	Jul	Aug	Sep	Oct	Nov	Dec	Year	Cold	Warm
Bakh			-0.4	-0.4						0.5					
Bak			-0.6	-0.5	-0.5			-0.5	-0.5	0.7			-0.3		-0.4
Borj			-0.5						-0.4				-0.2		-0.3
God	0.9					0.5	0.6	0.4		1.0		0.5	0.4	0.6	0.3
Gud		-0.6	-0.8	-0.4	-0.7	-0.6	-0.6	-0.6	-0.9		-0.5		-0.5	-0.4	-0.6
Kha			-0.4					-0.4		0.5					
Khu	-0.4		-0.9		-0.4					1.1			-0.2		-0.2
Lent							-0.4			0.5				0.2	-0.2
Mest															
Pas		-0.7	-0.9	-0.6	-0.8	-0.7	-0.6	-0.7	-1.0		-0.6		-0.6	-0.5	-0.7
Sho			-0.4		-0.4					0.6					-0.3
Step		-0.6	-0.8		-0.6	-0.5	-0.5	-0.5	-0.8				-0.4	-0.3	-0.5
Tian		-0.4	-0.6	-0.4	-0.5	-0.5				0.4			-0.3	-0.2	-0.3

Fig. 6. Difference between the mean values of total cloud cover for 1986-2015 and 1956-1985 in thirteen locations of Georgia

The ΔCC values variation in separate points is presented on Fig. 6. The variability of the mean monthly total cloud cover is detected for 12 investigated points (except Mestia) in 60 cases (including 48 cases - a decrease and for 12 cases - an increase in ΔCC values).

The changeability of the ΔRH values in the separate points is the following: Bakhmaro - decrease of the ΔCC values (March, April), increase (October); Bakuriani - decrease (March-May, August, September, mean annual and warm seasons mean), increase (October); Borjomi - decrease (March, September, mean annual and warm season mean); Goderdzi - increase (all month and seasons, except February-May, September and November); Gudauri - decrease (all month and seasons, except January, October and December); Khaishi - decrease (March, August), increase (October); Khulo - decrease (January, March, May, mean annual and warm season mean), increase (October); Lentekhi - decrease (July and warm season mean), increase (October and cold season mean); Mestia – no changes; Pasanauri - decrease (all month and seasons, except January, October and December); Shovi - decrease (March, May and warm season mean), increase (October); Stepantsminda - decrease (all month and seasons, except January, April, October-December); Tianeti - decrease (February-June, mean annual, cold and warm seasons mean), increase (October).

Atmospheric precipitation sum

The mean monthly annual, half year and monthly min and max P values are available in Table 5 and Fig. 7.

Table 5. monthly min, monthly max and mean monthly seasonal P (mm) values in thirteen locations of Georgia in 1956-2015.

Location	Mean Year	Mean Cold	Mean Warm	Min	Max
Bakhmaro	130	154	107	9.8	554
Bakuriani	70	59	82	0.5	283
Borjomi	55	48	62	1.5	181
Goderdzi	110	115	104	7.7	361
Gudauri	128	106	151	0	536
Khaishi	102	108	96	1.0	670
Khulo	117	149	84	0.5	628
Lentekhi	107	110	104	1.3	556
Mestia	82	76	88	1.0	284
Pasanauri	82	59	105	0	353
Shovi	98	85	111	3.4	444
Stepantsminda	62	34	89	0	252
Tianeti	64	42	85	0	277

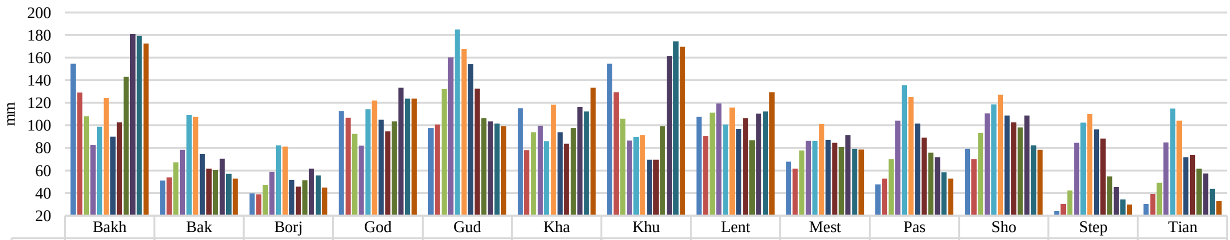

	Bakh	Bak	Borj	God	Gud	Kha	Khu	Lent	Mest	Pas	Sho	Step	Tian
Jan	155	51	40	113	98	115	155	107	68	48	79	24	31
Feb	129	54	39	107	101	78	129	90	62	53	70	30	39
Mar	108	67	47	93	132	94	106	111	78	70	93	42	49
Apr	82	78	59	82	160	100	87	120	86	104	111	85	85
May	99	109	82	114	185	86	90	101	86	135	119	102	115
Jun	124	108	81	122	168	118	91	116	101	125	127	110	104
Jul	90	74	52	105	154	94	70	97	87	102	109	96	72
Aug	103	61	46	95	132	84	69	106	84	89	103	88	74
Sep	143	60	51	104	106	98	99	87	81	76	98	55	62
Oct	181	70	62	133	104	116	161	110	91	72	109	46	57
Nov	179	57	56	124	101	112	174	112	79	58	82	34	44
Dec	172	53	45	124	99	133	170	129	79	53	78	30	33

Fig. 7. Precipitation monthly mean values of in thirteen locations of Georgia in 1956-2015.

The variability range of the P mean values for the indicated stations is as follows: Mean Year - from 55 mm (Borjomi) to 130 mm (Bakhmaro); Mean Cold - from 34 mm (Stepantsminda) to 154 mm (Bakhmaro); Mean Warm - from 62 mm (Borjomi) to 151 mm (Gudauri); Min - from 0 mm (Gudauri, Pasanauri, Stepantsminda and Tianeti) to 9.8 mm (Bakhmaro); Max - from 181 mm (Borjomi) to 670 mm (Khaishi).

The intra-annual distribution of P values for all indicated investigations points of Georgia are presented in Fig. 7. The P smallest values for Stepantsminda during January are observed (24 mm). The P greatest values for Gudauri (185 mm) in May are observed (Fig. 7).

The changeability data of the ΔP values in separate points is presented in Fig. 8. The variability of the atmospheric precipitation monthly mean sum is observed for 11 investigated points (except Bakhmaro, and Bakuriani) in 25 cases (including for 12 cases - an increase and for 13 cases - a decrease of ΔP values).

The changeability of the ΔP values in the separate points is the following: Bakhmaro and Bakuriani (no changes); Borjomi - decrease (June and December); Goderdzi - decrease (March, April mean annual and warm season mean); Gudauri - increase (August, October and cold season mean), decrease (September); Khaishi - increase (April and May); Khulo - increase (January, September, mean annual, cold and warm seasons mean); Lentekhi - increase (May and June), decrease (September); Mestia – increase (mean annual and cold season mean); Pasanauri - increase (August, October and cold season mean); Shovi - increase (October); Stepantsminda - decrease (July, September), increase (October); Tianeti - decrease (March, May-July, September, mean annual and warm seasons mean).

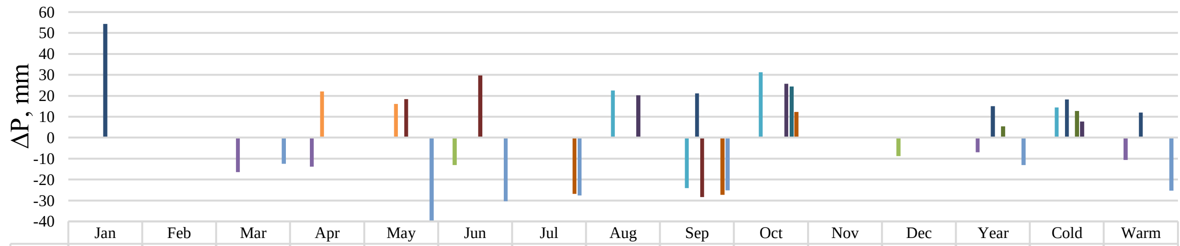

	Jan	Feb	Mar	Apr	May	Jun	Jul	Aug	Sep	Oct	Nov	Dec	Year	Cold	Warm
Bakh															
Bak															
Borj						-13						-9			
God			-16	-14									-7		-11
Gud								23	-24	31				14	
Kha				22	16										
Khu	54								21				15	18	12
Lent					18	30			-28						
Mest													5	13	
Pas								20		26				8	
Sho										24					
Step							-27		-27	12					
Tian			-12		-40	-30	-28		-25				-13		-25

Fig. 8. Difference between the P mean values during 1986-2015 and 1956-1985 in thirteen locations of Georgia

Mean wind speed

The mean annual, half year and monthly min and max wind speed (V) data are available in Table 6 and also on Fig. 9.

The range of variability of the V mean values for the indicated stations is as follows: Mean Year - from 0.3 m/sec (Lentekhi) to 4.8 m/sec (Goderdzi); Mean Cold - from 0.2 m/sec (Lentekhi) to 5.4 m/sec (Goderdzi); Mean Warm - from 0.4 m/sec (Lentekhi) to 4.2 m/sec (Goderdzi); Min - 0 m/sec (for all stations); Max - from 2.1 m/sec (Lentekhi) to 10.7 m/sec (Goderdzi).

The intra-annual distribution of V values for all indicated investigations points of Georgia are presented on Fig. 9. The smallest V values for all points during January and December are observed (0.1 m/sec, Lentekhi). The greatest values of V for Goderdzi (6.1 m/sec) in January are also fixed (Fig. 9).

Table 6. The monthly mean min, monthly mean max and mean seasonal V (m/s) values in thirteen locations of Georgia in 1956-2015.

Location	Mean Year	Mean Cold	Mean Warm	Min	Max
Bakhmaro	1.7	2.2	1.3		5.7
Bakuriani	1.3	1.1	1.5		5.2
Borjomi	0.7	0.5	0.8		2.2
Goderdzi	4.8	5.4	4.2		10.7
Gudauri	1.2	1.1	1.2		3.4
Khaishi	0.9	0.7	1.2		3.7
Khulo	1.9	2.0	1.7	0.0	4.0
Lentekhi	0.3	0.2	0.4		2.1
Mestia	0.5	0.3	0.7		2.2
Pasanauri	1.1	1.1	1.2		2.9
Shovi	1.1	1.0	1.1		2.9
Stepantsminda	1.7	1.8	1.6		6.1
Tianeti	1.2	1.2	1.2		4.6

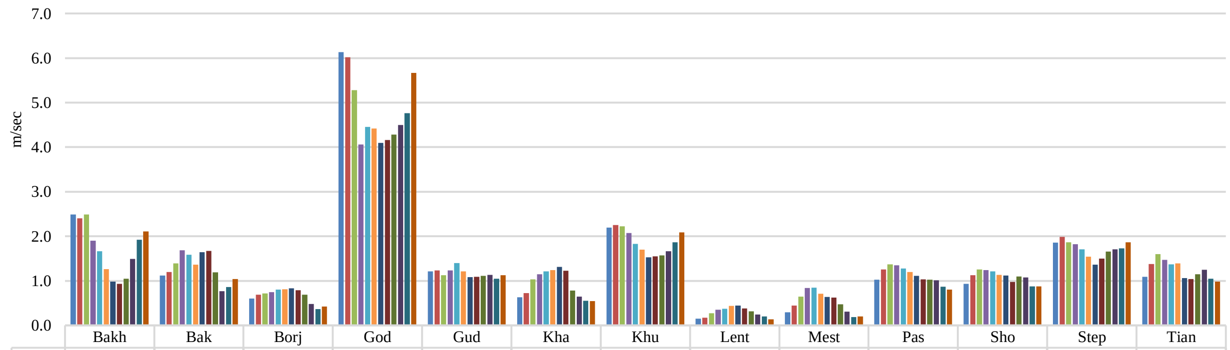

	Bakh	Bak	Borj	God	Gud	Kha	Khu	Lent	Mest	Pas	Sho	Step	Tian
Jan	2.5	1.1	0.6	6.1	1.2	0.6	2.2	0.1	0.3	1.0	0.9	1.9	1.1
Feb	2.4	1.2	0.7	6.0	1.2	0.7	2.3	0.2	0.4	1.3	1.1	2.0	1.4
Mar	2.5	1.4	0.7	5.3	1.1	1.0	2.2	0.3	0.6	1.4	1.3	1.9	1.6
Apr	1.9	1.7	0.7	4.1	1.2	1.1	2.1	0.3	0.8	1.3	1.2	1.8	1.5
May	1.7	1.6	0.8	4.5	1.4	1.2	1.8	0.4	0.8	1.3	1.2	1.7	1.4
Jun	1.3	1.4	0.8	4.4	1.2	1.2	1.7	0.4	0.7	1.2	1.1	1.5	1.4
Jul	1.0	1.6	0.8	4.1	1.1	1.3	1.5	0.4	0.6	1.1	1.1	1.4	1.1
Aug	0.9	1.7	0.8	4.2	1.1	1.2	1.5	0.4	0.6	1.0	1.0	1.5	1.0
Sep	1.0	1.2	0.7	4.3	1.1	0.8	1.6	0.3	0.5	1.0	1.1	1.7	1.1
Oct	1.5	0.8	0.5	4.5	1.1	0.6	1.7	0.2	0.3	1.0	1.1	1.7	1.2
Nov	1.9	0.9	0.4	4.8	1.0	0.5	1.9	0.2	0.2	0.9	0.9	1.7	1.0
Dec	2.1	1.0	0.4	5.7	1.1	0.5	2.1	0.1	0.2	0.8	0.9	1.9	1.0

Fig. 9. Wind speed monthly Mean values in thirteen locations of Georgia in 1956-2015.

The changeability of the ΔV values of in separate points is presented on Fig. 10. The variability of the monthly mean values of wind speed is detected for all 13 investigated points in 145 cases (including 141 cases - a decrease and only for 4 cases, Bakhmaro - an increase of ΔV values).

The changeability of the ΔV values in the separate points is the following: Bakhmaro – increase (January, March, May and June); all another station, except Shovi – decrease (all months, mean annual, cold and warm seasons mean); Shovi - decrease (all months, except April, June and October, mean annual, cold and warm seasons mean).

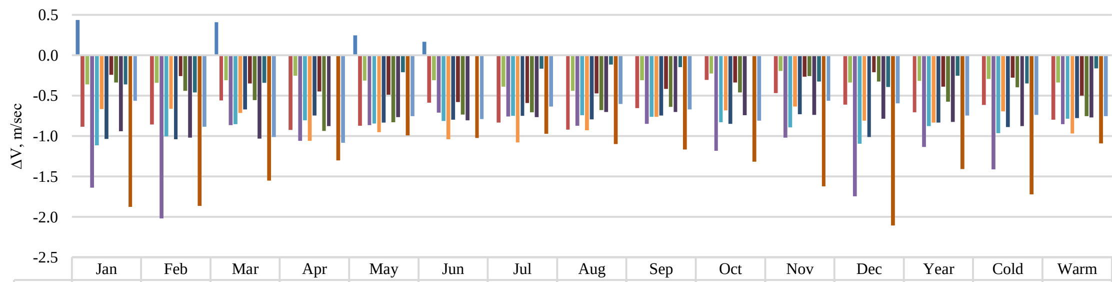

	Jan	Feb	Mar	Apr	May	Jun	Jul	Aug	Sep	Oct	Nov	Dec	Year	Cold	Warm
Bakh	0.4		0.4		0.2	0.2									
Bak	-0.9	-0.9	-0.6	-0.9	-0.9	-0.6	-0.8	-0.9	-0.7	-0.3	-0.5	-0.6	-0.7	-0.6	-0.8
Borj	-0.4	-0.3	-0.3	-0.3	-0.3	-0.3	-0.4	-0.4	-0.3	-0.2	-0.2	-0.3	-0.3	-0.3	-0.3
God	-1.6	-2.0	-0.9	-1.1	-0.9	-0.7	-0.8	-0.9	-0.8	-1.2	-1.0	-1.7	-1.1	-1.4	-0.9
Gud	-1.1	-1.0	-0.9	-0.8	-0.8	-0.8	-0.7	-0.7	-0.8	-0.8	-0.9	-1.1	-0.9	-1.0	-0.8
Kha	-0.7	-0.7	-0.7	-1.1	-0.9	-1.0	-1.1	-0.9	-0.8	-0.7	-0.6	-0.8	-0.8	-0.7	-1.0
Khu	-1.0	-1.0	-0.7	-0.7	-0.8	-0.8	-0.7	-0.8	-0.7	-0.8	-0.7	-1.0	-0.8	-0.9	-0.8
Lent	-0.2	-0.3	-0.3	-0.4	-0.5	-0.6	-0.6	-0.5	-0.4	-0.3	-0.3	-0.2	-0.4	-0.3	-0.5
Mest	-0.3	-0.4	-0.6	-0.9	-0.8	-0.7	-0.7	-0.7	-0.6	-0.5	-0.3	-0.3	-0.6	-0.4	-0.8
Pas	-0.9	-1.0	-1.0	-0.9	-0.8	-0.8	-0.8	-0.7	-0.7	-0.7	-0.7	-0.8	-0.8	-0.9	-0.8
Sho	-0.4	-0.5	-0.3		-0.2		-0.2	-0.1	-0.1		-0.3	-0.4	-0.3	-0.3	-0.2
Step	-1.9	-1.9	-1.6	-1.3	-1.0	-1.0	-1.0	-1.1	-1.2	-1.3	-1.6	-2.1	-1.4	-1.7	-1.1
Tian	-0.6	-0.9	-1.0	-1.1	-0.8	-0.8	-0.6	-0.6	-0.7	-0.8	-0.6	-0.6	-0.7	-0.7	-0.8

Fig. 10. Difference between the V mean values during 1986-2015 and 1956-1985 in thirteen locations of Georgia

Finally, we note that the greatest changes of all other investigated climatic parameters in 1986-2015 compared to 1956 1985 underwent wind speed, the least - atmospheric precipitation. The reasons for such changes are the subject of further research for the studied mountain regions of Georgia.

Data of this work are used in [40].

Conclusion

The analysis confirms once again the earlier obtained results and formulated conclusions on the diversity of climatic conditions of Georgia and their uniqueness. Accordingly, this stimulates the need for the even more detailed study of climatic and associated bioclimatic conditions and their variability in different geographic regions of Georgia, both in terms of impact on public health and in terms of development of various sectors of the national economy of the state, including health resorts - tourism industry.

References

[1] Climate Change 2007: The Physical Science Basis. Summary for Policymakers. Contribution of Working Group I to the Fourth Assessment Report of the Intergovernmental Panel of Climate Change. http://www.ipcc.ch.

[2] Stocker, T.F., Qin D., Plattner G.-K., Tignor M., Allen S.K., Boschung J., Nauels A., Xia Y., Bex V., Midgley P.M. (eds.). IPCC. Summary for Policymakers. In: Climate Change 2013: The Physical Science Basis. Contribution of Working Group I to the Fifth Assessment Report of the Intergovernmental Panel on Climate Change. Cambridge University Press, Cambridge, United Kingdom and New York, NY, USA, 2013, 29 p.

[3] Climate Change 2021: The Physical Science Basis. Summary for Policymakers. Working Group I contribution to the Sixth Assessment Report of the Intergovernmental Panel on Climate Change, 41 p., https://www.ipcc.ch

[4] Barriopedro D, García-Herrera R, Lupo AR et al. A climatology of Northern Hemisphere blocking. Journal of Climate 19, 2006, pp.1042-1063.

[5] Gruza G.V., Meshcherskaya A.V. Izmemenia klimata v Rossii za period instrumentalnih nabliudeni, 2008, http://climate2008.igce.ru/v2008/v1/vI-3.pdf.
[6] Acquaotta F., Fratianni S., Garzena D. Temperature Changes in the North-Western Italian Alps from 1961 to 2010. Theoretical and Applied Climatology, ISSN 0177-798X, Elettronico, 122:3, 2015, pp. 619-634, DOI 10.1007/s00704-014-1316-7
[7] Rybak O. O., Rybak E. A. Changes in the Regime of Air Temperature and Precipitation Rate in the Black Sea Region in the 20th Century. Nauchnyj zhurnal KubGAU . – Krasnodar: KubGAU, - №90 (06), 2013, 21 p., http://ej.kubagro.ru/2013/06/pdf/15.pdf , (in Russian).
[8] Rybak O. O., Rybak E. A. Application of Climatic Indices for Evaluation of Regional Differences in Tourist Attractiveness. Nauchnyy zhurnal KubGAU, №121(07), 2016, 24 p., http://ej.kubagro.ru/2016/07/pdf/16.pdf , (in Russian).
[9] Amiranashvili A., Povolotskaya N., Senik I. Comparative Analysis of the Variability of Monthly and Seasonal Air Temperature in Tbilisi and Kislovodsk in 1931-2020. International Scientific Conference „Natural Disasters in the 21st Century: Monitoring, Prevention, Mitigation“. Proceedings, ISBN 978-9941-491-52-8, Tbilisi, Georgia, December 20-22, 2021. Publish House of Iv. Javakhishvili Tbilisi State University, Tbilisi, 2021, pp. 27 - 30.
[10] Budagashvili T., Karchava J., Gunia G., Inyskirveli L., Kuchava T., Gurgenidze M., Amiranashvili A., Chikhladze T. Inventory of Greenhouze Gas Emissions and Sinks, Georgia's Initial National Communication on Under the United Nations Framework Convection on Climate Change, Project GEO/96/G31, Tbilisi, 1999, 33-45.
[11] Amiranashvili A., Chargazia Kh., Trofimenko L. Dynamics of the thirty-year moving average values of the air temperature in Tbilisi and St.-Petersburg with 1851 to 2010 and their extrapolation to 2051-2080. International Conference "Applied Ecology: Problems, Innovations", ICAE-2015. Proceedings, Tbilisi-Batumi, Georgia, ISBN 978-9941-0-7644-2, 7-10 May, 2015, Tbilisi, 2015, pp. 12-16, http://icae-2015.tsu.ge/
[12] Tavartkiladze K., Begalishvili N., Kharchilava J., Mumladze D., Amiranashvili A., Vachnadze J., Shengelia I., Amiranashvili V. Contemporary climate change in Georgia. Regime of some climate parameters and their variability. Monograph, ISBN 99928-885-4-7, Tbilisi, 2006, 177 p., (in Georgian).
[13] Amiranashvili A., Matcharashvili T., Chelidze T. Climate Change in Georgia: Statistical and Nonlinear Dynamics Predictions, Journ. of Georgian Geophysical Soc., Iss. (A), Physics of Solid Earth, ISSN: 1512-1127, v. 15a, 2011-2012, pp. 67-87.
[14] Elizbarashvili E.E. Climate of Georgia. Monograph, ISBN 978-9941-0-9584-9, Tbilisi, 2017, 360 p., (in Georgian).
[15] Amiranashvili A., Bliadze T., Kartvelishvili L. Statistical Characteristics of Monthly Sums of Atmospheric Precipitations in Tianeti (Georgia) in 1956-2015. Trans. of Mikheil Nodia institute of Geophysics, ISSN 1512-1135, vol. 70, Tb., 2019, pp. 112-118, (in Russian).
[16] Amiranashvili A. Changeability of Air Temperature and Atmospheric Precipitations in Tbilisi for 175 Years. International Scientific Conference "Natural Disasters in Georgia: Monitoring, Prevention, Mitigation". Proceedings, ISBN 978-9941-13-899-7, Publish House of Iv. Javakhishvili Tbilisi State University, December 12-14, Tbilisi, 2019, pp. 86-90.
[17] Fourth National Communication of Georgia. Under the United Nations Framework Convention on Climate Change. Tbilisi, 2021, 425 p.
https://unfccc.int/sites/default/files/resource/4%20Final%20Report%20-%20English%202020%2030.03_0.pdf
[18] Mieczkowski Z. The Tourism Climate Index: A Method for Evaluating World Climates for Tourism. The Canadian Geographer 29, 1985, pp. 220-233.
[19] Scott D., Rutty M., Amelung B., Tang M. An Inter-Comparison of the Holiday Climate Index (HCI) and the Tourism Climate Index (TCI) in Europe. Atmosphere 7, 80, 2016, 17 p., doi:10.3390/atmos7060080www.
[20] Scott D., Mc Boyle G. Using a "Tourism Climate Index" to Examine the Implications of Climate Change for Climate as a Tourism Resource. International Society of Biometeorology, Proceedings of the First International Workshop on Climate, Tourism and Recreation. Retrieved from http://www.mif.uni-freiburg.de/isb/ws/ report.htm, 2001.
[21] Matzarakis A.Climate, thermal comfort and tourism. Climate Change and Tourism-Assessment and Coping Strategies, 2007, pp.139-154.

[22] Amiranashvili A.G., Kartvelishvili L. G. Long-Term Variations of Air Effective Temperature in Tbilisi. Trans. of the Institute of Hydrometeorology, vol. 115, ISSN 1512-0902, Tb., 2008, pp. 214–219, (in Russian).
[23] Amiranashvili A.G., Kartvelishvili L.G., Saakashvili N.M., Chikhladze V.A. Long-Term Variations of Air Effective Temperature in Kutaisi. "Modern Problems of Using of Health Resort Resources", Collection of Scientific Works of International Conference, Sairme, Georgia, June 10-13, 2010, ISBN 978-9941-0-2529-7, Tbilisi, 2010, pp. 152-157, (in Russian).
[24] Ghanbari S., Karimi J. The Review of Changes in Tourism Climate Index (TCI) Isfahan (2005-1976). Journ. of Regional Planning, vol. 3, No 12, Winter 2014, pp. 71 – 82.
[25] Roshan G., Yousefi R., Fitche J.M. Long-Term Trends in Tourism Climate Index Scores for 40 Stations Across Iran: The Role of Climate Change and Influence on Tourism Sustainability. Int. J. Biometeorol., 2015, DOI 10.1007/s00484-015-1003-0
[26] Amiranashvili A., Chargazia Kh., Matzarakis A., Kartvelishvili L. Tourism Climate Index in the Coastal and Mountain Locality of Adjara, Georgia. International Scientific Conference "Sustainable Mountain Regions: Make Them Work". Proceedings, Borovets, Bulgaria, ISBN 978-954-411-220-2, 14-16 May,2015, pp.238-244, http://geography.bg/MountainRegions_Sofia2015
[27] Mihăilă D., Piticar A., Briciu A. E., Bistricean P. I., Lazurca L. G., Puţuntică A. Changs in bioclimatic indices in the Republic of Moldova (1960–2012): consequences for tourism. Boletín de la Asociación de Geógrafos Españoles, 77, 2018, pp. 521–548. doi: 10.21138/bage.2550
[28] Carrillo J., González A., Pérez J. C., Expósito F. J., Díaz, J. P. Impact of Climate Change on the Future of Tourism Areas in the Canary Islands, EGU General Assembly 2021, online, 19–30 Apr 2021, EGU21-11981, https://doi.org/10.5194/egusphere-egu21-11981, 2021.
[29] Araci S.F. S., Demiroglu O. C., Pacal A., Hall C. M., Kurnaz, M. L. Future Holiday Climate Index (HCI) Performances of Urban and Beach Destinations in the Mediterranean. EGU General Assembly 2021, online, 19–30 Apr 2021, EGU21-13217, https://doi.org/10.5194/egusphere-egu21-13217, 2021.
[30] Amiranashvili A., Kartvelishvili L., Matzarakis A. Changeability of the Holiday Climate Index (HCI) in Tbilisi. Trans. of M. Nodia Institute of Geophisics, ISSN 1512-1135, vol. LXXII, Tbilisi, 2020, pp. 129-137.
[31] Landsberg H.E. The Assessment of Human Bioclimate. A Limited Review of Physical Parameters. Technical Note No 123, WMO, No 331, 1972, 37 p.
[32] BSR/ASHRAE Standard 55P, Thermal Environmental Conditions for Human Occupancy 2/24/03 Most Current Draft Standard, 2003, 50 p.
[33] Freitas C. R., Grigorieva E. A. A Comprehensive Catalogue and Classification of Human Thermal Climate Indices. Int. J. Biometeorol, 59, 2015, pp. 109–120, DOI 10.1007/s00484-014-0819-3
[34] Amiranashvili A., Japaridze N., Kartvelishvili L., Megrelidze L., Khazaradze K. Statistical Characteristics of the Monthly Mean Values of Air Effective Temperature on Missenard in the Autonomous Republic of Adjara and Kakheti (Georgia). Transactions of Mikheil Nodia Institute of Geophysics, ISSN 1512-1135, vol. LXIX, 2018, pp. 118-138, (in Russian).
[35] Amiranashvili A.G., Kartvelishvili L.G., Megrelidze L.D. Changeability of the Meteorological Parameters Associated with Some Simple Thermal Indices and Tourism Climate Index in Adjara and Kakheti (Georgia). Journal of the Georgian Geophysical Society, ISSN: 1512-1127, Physics of Solid Earth, Atmosphere, Ocean and Space Plasma, v. 21(2), Tbilisi, 2018, pp. 77-94.
[36] Amiranashvili A., Kartvelishvili L., Matzarakis A. Comparison of the Holiday Climate Index (HCI) and the Tourism Climate Index (TCI) in Tbilisi. Int. Sc. Conf. „Modern Problems of Ecology", Proc., ISSN 1512-1976, v. 7, Tbilisi-Telavi, Georgia, 26-28 September, 2020, pp. 424-427.
[37] Amiranashvili A., Povolotskaya N., Senik I. Comparative Analysis of the Tourism Climate Index and the Holiday Climate Index in the North Caucasus.Transactions of Mikheil Nodia Institute of Geophysics, ISSN 1512-1135, vol. LXXIII, 2021, pp. 96-113, (in Russian).
[38] Amiranashvili A.G., Kartvelishvili L.G. Holiday Climate Index in Kakheti (Georgia). Journal of the Georgian Geophysical Society, e-ISSN: 2667-9973, p-ISSN: 1512-1127, Physics of Solid Earth, Atmosphere, Ocean and Space Plasma, v. 24(1), 2021, pp. 44-62.
[39] Kobisheva N., Narovlianski G. Climatological processing of the meteorological information, Leningrad, Gidrometeoizdat, 1978, 294 p., (in Russian).
[40] Amiranashvili A.G., Kartvelishvili L.G., Kutaladze N.B., Megrelidze L.D., Tatishvili M.R. Holiday Climate Index in Some Mountainous Regions of Georgia. Journal of the Georgian Geophysical Society, e-ISSN: 2667-9973, p-ISSN: 1512-1127, Physics of Solid Earth, Atmosphere, Ocean and Space Plasma, v. 24(2), 2021, pp. 92 – 117.

დასვენების კლიმატურ ინდექსში შემავალი მეტეოროლოგიური პარამეტრების ცვალებადობა საქართველოს სხვადასხვა მთიან რეგიონში 1956-2015 წლებში

ა. ამირანაშვილი, ლ. ქართველიშვიი, ნ. კუტალაძე,
ლ. მეგრელიშვილი, მ. ტატიშვილი

რეზიუმე

წარმოდგენილია საქართველოს ცამეტ მთიან რეგიონში (ბახმარო, ბაკურიანი, ბორჯომი, გოდერძი, გუდაური, ხაიში, ხულო, ლენტეხი, მესტია, ფასანაური, შოვი, სტეფანწმინდა, თიანეთი) დასვენების კლიმატურ ინდექსთან დაკავშირებული მეტეოროლოგიური პარამეტრების სტატისტიკური მონაცემები (ჰაერის საშუალო თვიური მაქსიმალური ტემპერატურა, ჰაერის საშუალო თვიური ფარდობითი ტენიანობა, ღრუბლის საფარი, ატმოსფერულ ნალექთა ჯამი, ქარის სიჩქარე) 1956 წლიდან 2015 წლამდე. კერძოდ, შესწავლილი იქნა მითითებული მეტეოროლოგიური პარამეტრების ცვალებადობა 1986–2015 წლებში 1956 ÷ 1985 წლებთან შედარებით ზემოთ ჩამოთვლილი პუნქტებისთვის.

Изменчивость метеорологических параметров, ассоциированных с климатическим индексом отдыха в различных горных районах Грузии в 1956-2015 гг.

**А.Г. Амиранашвили, Л. Г. Картвелишвили, Н.Б. Куталадзе,
Л.Д. Мегрелидзе, М.Р. Татишвили**

Резюме

Представлены статистические данные о метеорологических параметрах, ассоциированных с климатическим индексом отдыха (среднемесячная максимальная температура воздуха, среднемесячная относительная влажность воздуха, облачный покров, месячная сумма осадков, скорость ветра) в тринадцати горных районах Грузии Грузии (Бахмаро, Бакуриани, Боржоми, Годердзи, Гудаури, Хаиши, Хуло, Лентехи, Местия, Пасанаури, Шови, Степанцминда, Тианети) в период с 1956 по 2015 гг. В частности, изучена изменчивость указанных метеорологических параметров в 1986÷2015 гг. по сравнению с 1956÷1985 гг. для перечисленных выше пунктов.

Journal of the Georgian Geophysical Society, e-ISSN: 2667-9973, p-ISSN: 1512-1127
Physics of Solid Earth, Atmosphere, Ocean and Space Plasma, v. 24(2), 2021, pp. 92 - 117

Holiday Climate Index in Some Mountainous Regions of Georgia

[1]Avtandil G. Amiranashvili, [2]Liana G. Kartvelishvili, [2]Nato B. Kutaladze, [2]Lia D. Megrelidze, [3]Marika R. Tatishvili

[1]Mikheil Nodia Institute of Geophysics of Ivane Javakhishvili Tbilisi State University, Tbilisi, Georgia
1, M. Alexidze Str., 0160, Tbilisi, Georgia, e-mail:avtandilamiranashvili@gmail.com
[2]National Environmental Agency of Georgia
[3]Institute of Hydrometeorology of Georgian Technical University, Tbilisi, Georgia

ABSTRACT

The long-term monthly average values of Holiday Climate Index (HCI) for 13 mountainous locations of Georgia (Bakhmaro, Bakuriani, Borjomi, Goderdzi, Gudauri, Khaishi, Khulo, Lentekhi, Mestia, Pasanauri, Shovi, Stepantsminda, Tianeti) are presented in the article. Detailed analysis of the monthly, seasonal and annual HCIs values over the 60-year period (1956-2015) are carried out. Comparison of HCI and Tourism Climate Index (TCI) monthly values for three locations (Goderdzi, Khulo and Mestia) based on data from 1961 to 2010 are carried out. The variability of the HCI in 1986-2015 compared to 1956-1985 was studied, and the trends of the HCI in 1956-2015 were also investigated. Using Mestia as an example, the expected changes in monthly, seasonal and annual HCI values for 2041-2070 and 2071-2100 year periods has neen assested.

Key Words: *Bioclimate, Tourism Climate Index, Holiday Climate Index*.

Introduction

The formation and development of the resort and tourism industry is directly depended on the geographical location, relief, vegetation, weather and climate of the region. Weather and climate are two main factors that determine the bioclimatic resources of an area. Thus, the study of these resources, which are necessary for the organization and development of the resort and tourism industry, plays a major role and requires significant efforts. Past studies have used a lot of climate indices for tourism [1-7]. The most widely known index, used both in the past and in the present, is the Tourist Climate Index (TCI), proposed by Mechkovsky [9].

In the south Caucasus countries, monthly value of TCI was calculated in Georgia firstly for Tbilisi [10] and then for many other locations of Caucasus (Armenia, Azerbaijan, North Caucasus etc.) [11-18].

From the recent studies of TCI, in particular, the noteable are the works [19, 20]. The study [19] presents the first TCI calculations for Zimbabwe, a country relient on outdoor nature-based tourism for attracting tourists and foreign visitors. The mean annual TCI scores classify Zimbabwe as very good to excellent by climatic suitability for tourism, with scores spanning 75.5–83 (of a maximum 100) for the 1989–2014 period. Monthly TCI scores categorize four locations in the Lowveld region as having a winter-peak suitability; the remaining stations have either summer-peak or bimodal shoulder-peaks. This reveals entire year climatic suitability for tourism in Zimbabwe, and highlights the importance of understanding seasonal variability per destination to maximize tourist satisfaction. The paper [20] evaluates the climate comfortability of Argentina as an intangible resource for tourism. The analysis builds on spatial modelling of the Tourism Climate Index (TCI) calculated for 69 weather stations uniformly distributed throughout the country. The mean annual TCI in Argentina is 73 indicating “very good” climatic-tourist comfort conditions for tourism.

Despite the TCI's wide application, it has been subject to substantial critiques [21]. The four key deficiencies of the TCI include: (1) the subjective rating and weighting system of climatic variables; (2) it neglects the possibility of the overriding influence of physical climatic parameters (e.g., rain, wind); (3) the low temporal resolution of climatic data (i.e., monthly data) has limited relevance for tourist decision-making; and (4) it neglects the varying climatic requirements of major tourism segments and destination types (i.e., beach, urban, winter sports tourism).

To overcome the above noted limitations of the TCI, a Holiday Climate Index (HCI) was developed to more precisely assess the climatic suitability of tourism destinations. The word "holiday" was chosen to better reflect what the index was designed for (i.e., leisure tourism), as the tourism is much broader by definition ("Tourism is a social, cultural and economic phenomenon which entails the movement of people to countries or places outside their usual environment for personal or business/professional purposes") [21-25]. In the same works, comparisons between HCI and TCI were made.

Results of comparison of Holiday Climate Index and Tourism Climate Index at some locations of Georgia and North Caucasus in [26-28] are presented. The article [26] compares the values and categories of TCI and HCI in Tbilisi. The HCI long-term monthly average values for 12 locations of Kakheti (Akhmeta, Dedoplistskaro, Gombori, Gurjaani, Kvareli, Lagodekhi, Omalo, Sagarejo, Shiraki, Telavi, Tsnori and Udabno) are presented in [27]. For 6 stations of this region (Dedoplistskaro, Gurjaani, Kvareli, Lagodekhi, Sagarejo and Telavi) detailed analysis of the monthly, seasonal and annual HCIs values over the 60-year period (1956-2015) are carried out. Comparison of HCI and Tourism Climate Index (TCI) monthly values for four points of Kakheti region (Dedoplistskaro, Kvareli, Sagarejo and Telavi) based on data from 1961 to 2010 are carried out. The results of the comparative analysis of the Tourism Climate Index and the Holiday Climate Index, as well as the ratings of the components of these indices for six points in the North Caucasus (Kislovodsk, Pyatigorsk, Essentuki, Zheleznovodsk, Teberda and Nalchik) are presented in [28].

In particular, it was found out that there is a high degree of correlation between the values of HCI and TCI. However, consider that the TCI is calculated for the so-called "average tourist" (regardless of gender, age, physical condition), the value and category of this index is lower than the HCI values and categories. In general, based on our estimation the HCI more adequately determines the bioclimatic state of the environment for the development of various types of tourism than the TCI [26-28].

Great importance gains the study of variability and prediction of the HCI in relation to the limate change [29-33].

Using the Holiday Climate Index (HCI: Urban) the research [29] examines the long-term tourism climate records in Tokyo between 1964 and 2019. Findings suggest greater climatic variability and the favorability declination of Tokyo's tourism climatic resources in all three summer months. According to these findings the adaptation and mitigation strategies are recommended and a Japanocentric tourism climate index proposed.

The work [30] notes that TCI and HCI are good indicators of the environmental conditions for leisure activities in the Canary Islands. Using the Regional Climate Model, it is shown that by 2030-2059 and 2070-2099, tourism performance is expected to improve significantly in winter and off-season, but deteriorate in the summer months, including October, in the southeast, which is where hotels are currently located.

The aim of study [31] is to assess the future HCI performances of urban and beach destinations in the greater Mediterranean region. For this purpose, HCI scores for the reference (1971-2000) and future (2021-2050, 2070-2099) periods were computed. HCI: Urban results showed that Canary Islands hold suitable conditions for tourism during almost all four seasons and all periods which will have certain implications when other core Mediterranean competitors lose their relative climatic attractiveness. HCI:Beach results for the summer season showed that Las Canteras, Alicate, Pampelonne, Myrtos, Golden Sands and Edremit all pose Very Good to Excellent conditions without any Humidex risks for the extreme future scenario (2070-2099).

The detailed information on the variability of the monthly values of the Holiday Climate Index in Tbilisi in 1956-2015 are presented in [32]. It also presents data on the interval forecast of HCI value variability in Tbilisi for the next few decades.

This study develops the detailed analysis of the monthly, seasonal and annual HCIs values during 60-year period (1956-2015) for 13 mountainous locations of Georgia (Bakhmaro, Bakuriani, Borjomi, Goderdzi, Gudauri, Khaishi, Khulo, Lentekhi, Mestia, Pasanauri, Shovi, Stepantsminda, Tianeti), and comparison HCI and TCI of monthly values for three points of Georgia (Goderdzi, Khulo and Mestia) based on the data from 1961 to 2010. The variability data of HCI in 1986-2015 compared to 1956-1985, and the trends of HCI in 1956-2015 are also presented. Using Mestia as the example the expected changes of monthly, seasonal and annual HCI values of 2041-2070 and 2071-2100 has been assesed. The some results of this work were used in [33]. A more detailed description of these results is given below.

Study Area, Material and Methods

The study area includes 13 mountainous locations in Georgia - Bakhmaro (Bakh): 42.32° N, 41.85° E, 1926 m, a.s.l.; Bakuriani (Bak): 43.52° N, 41.73° E, 1665 m; Borjomi (Borj): 43.40° N, 41.83° E, 789 m; Goderdzi (God): 42.52° N, 41.63° E, 2025 m; Gudauri (Gud): 44.48° N, 42.47° E, 2194 m; Khaishi (Kha): 42.18° N, 42.95° E, 730 m; Khulo (Khu): 42.32° N, 41.65° E, 914 m; Lentekhi (Lent): 42.73° N, 42.78° E, 760 m; Mestia (Mest): 42.75° N, 43.05° E, 1441 m; Pasanauri (Pas): 44.70° N, 42.35° E, 1070 m; Shovi (Sho): 43.68° N, 42.70° E, 1507 m; Stepantsminda (Step): 44.65° N, 42.67° E, 1744 m; Tianeti (Tian): 44.97° N, 42.12° E, 1099 m. The development of the resort and tourism industry takes place in these locations, in particular – the mountain and winter tourism. Fig. 1 depicts the map of the arrangement of the indicated locations.

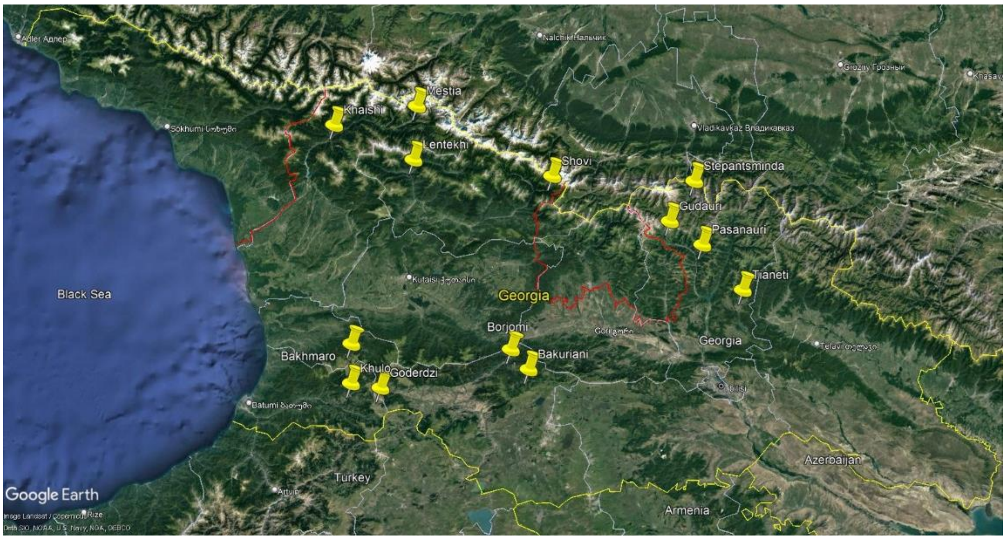

Fig.1. Locations of 13 mountainous meteorological stations in Georgia.

In this work the Holiday Climate Index (HCI) is used. The five climatic variables for the HCI identification are used: air temperature maximum, relative humidity, cloud cover, precipitation and wind [21].

In the Table 1 rating scheme and HCI's category are presented.

Table 1. HCI's Category.

HCI Score	Category (Abbreviation)	HCI Score	Category (Abbreviation)
90÷100	Ideal	**40÷49**	Marginal (Marg.)
80÷89	Excellent (Excell.)	**30÷39**	Unfavorable (Unf.)
70÷79	Very Good (V_Good)	**20÷29**	Very Unfavorable (V_Unf.)
60÷69	Good	**10÷19**	Extremely Unfavorable (Ext_Unf.)
50÷59	Acceptable (Accept.)	**9÷-9; -10÷-20**	Impossible (Impos.)

In this work the monthly mean data of Georgian National Environmental Agency of indicated meteorological parameters during the period from 1956 through 2015 are used [34]. Based on this data the HCI monthly average values were calculated. Comparison of monthly HCI and TCI values for three

locations of Georgia (Goderdzi, Khulo and Mestia) based on the TCI data t from 1961-2010 is performed [12, 17].
Analysis of the HCI data using the standard statistical analysis methods is carried out [35]. The applied following designations are listed below: Mean – average values; Min – minimal values; Max - maximal values; 99%_Low and 99%_Upp - Low and Upper levels of 99% confidence interval of mean values; R^2 - coefficient of determination; R - coefficient of linear correlation; α - level of significance; ΔHCI - the difference between the HCI mean values in 1986-2015 (II period of time) and 1956-1985 (I period of time) using Student's criterion was determined (level of significance not worse than 0.15). Calculation of expected changes in monthly, seasonal and annual HCI values in Mestia by 2041-2070 and 2071-2100 conducted in accordance with the model of expected climate change in Georgia. The expected climate change has been forecast using Representative Concentration Pathway (RCP) 4.5 scenario that stabilizes radiative forcing at 4.5 W/m2 in the year 2100 without ever exceeding that value. Compared to the A1B scenario used in the Third National Communication, the RCP4.5 scenario is less severe. Version 4.6.0 of the RegCM Regional Climate Model has been used to improve the global forecast scale [33].

Results and discussion

Results in Fig. 2-12 and Tables 2-12 and Annexes 1-8 are presented.

1. Basic Information about HCI for 13 Mountainous Regions of Georgia.

The long-term mean HCI real values at 13 locations of Georgia are presented on the Fig. 2.

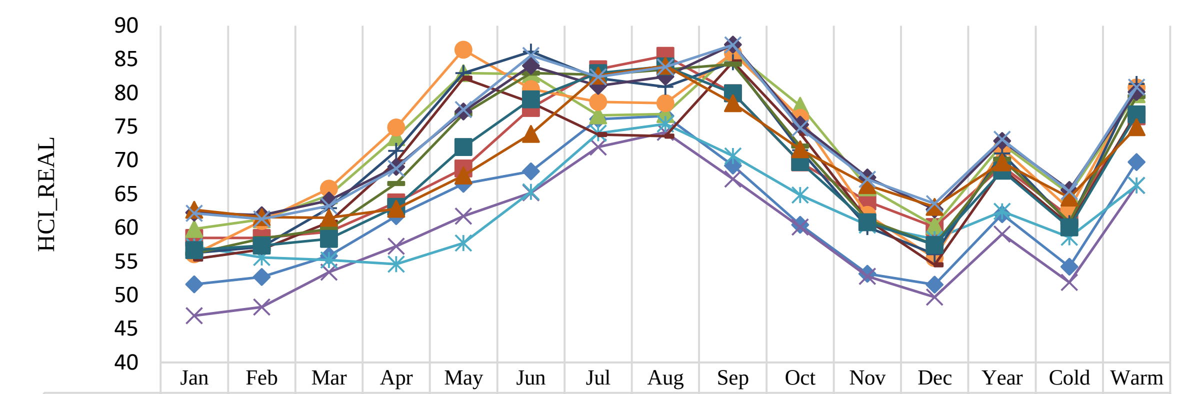

	Jan	Feb	Mar	Apr	May	Jun	Jul	Aug	Sep	Oct	Nov	Dec	Year	Cold	Warm
Bakh	52	53	56	62	67	68	76	77	69	60	53	52	62	54	70
Bak	58	58	59	64	69	78	84	86	80	70	64	60	69	62	77
Borj	60	61	65	73	83	83	77	77	86	78	66	60	72	65	80
God	47	48	53	57	62	65	72	74	67	60	53	50	59	52	66
Gud	57	56	55	55	58	65	74	75	71	65	60	58	62	59	66
Kha	56	61	66	75	86	81	79	78	86	76	62	56	72	63	81
Khu	56	57	63	71	83	86	82	81	85	71	60	56	71	61	81
Lent	55	57	61	70	82	79	74	74	85	74	61	54	69	60	77
Mest	56	58	60	67	77	83	83	84	84	72	61	58	70	61	79
Pas	62	62	64	69	77	84	81	82	87	75	67	63	73	66	80
Sho	57	57	58	63	72	79	83	84	80	70	61	57	68	60	77
Step	63	62	61	63	68	74	83	84	78	72	66	63	70	64	75
Tian	62	61	63	69	78	86	82	84	87	75	67	64	73	65	81

Fig. 2. Mean HCI real values at 13 locations of Georgia.

As it follows from Fig. 2 the HCI mean monthly values change from 47 (Goderdzi, January, Acceptable) to 87 (Pasanauri, Tianeti September, Excellent). The variability of HCI values for individual items is as follows: Bakhmato (52, January, December – 77, August), Bakuriani (58, January, February – 86, August), Borjomi (60, January, December – 86, September), Gooderdzi (47, January – 74, August), Gudauri (55, March, April – 75, August), Khaishi (56, January, December – 86, September), Khulo (56, January, December – 86, June), Lentekhi (54, December – 85, September), Mestia (56, January – 84, August, September), Pasanauri (62, January, February – 87, September), Shovi (57, January, February, December – 84, August), Stepantsminda (61, March – 84, August), Tianeti (61, February – 87, September).

Table 2. Linear correlation coefficient between separated stations of HCI monthly mean values (R min = 0.58, α = 0.04; R max = 1, α = <0.001).

Location	Bakh	Bak	Borj	God	Gud	Kha	Khu	Lent	Mest	Pas	Sho	Step	Tian
Bakh	1	0.95	0.81	0.98	0.83	0.84	0.92	0.81	0.95	0.89	0.96	0.90	0.90
Bak	0.95	1	0.79	0.98	0.94	0.77	0.87	0.78	0.96	0.94	0.99	0.98	0.95
Borj	0.81	0.79	1	0.83	0.62	0.98	0.96	1.00	0.93	0.94	0.86	0.70	0.93
God	0.98	0.98	0.83	1	0.88	0.84	0.91	0.82	0.96	0.93	0.98	0.94	0.93
Gud	0.83	0.94	0.62	0.88	1	0.58	0.69	0.60	0.83	0.82	0.90	0.99	0.83
Kha	0.84	0.77	0.98	0.84	0.58	1	0.97	0.99	0.91	0.90	0.85	0.68	0.89
Khu	0.92	0.87	0.96	0.91	0.69	0.97	1	0.96	0.97	0.96	0.93	0.78	0.96
Lent	0.81	0.78	1.00	0.82	0.60	0.99	0.96	1	0.92	0.93	0.85	0.69	0.91
Mest	0.95	0.96	0.93	0.96	0.83	0.91	0.97	0.92	1	0.99	0.99	0.90	0.99
Pas	0.89	0.94	0.94	0.93	0.82	0.90	0.96	0.93	0.99	1	0.97	0.88	1.00
Sho	0.96	0.99	0.86	0.98	0.90	0.85	0.93	0.85	0.99	0.97	1	0.96	0.97
Step	0.90	0.98	0.70	0.94	0.99	0.68	0.78	0.69	0.90	0.88	0.96	1	0.89
Tian	0.90	0.95	0.93	1	0.83	0.89	0.96	0.91	0.99	1.00	0.97	0.89	1

Linear correlation coefficient between separated station of HCI monthly mean values changes as follows (Table 2) - Bakhmaro: 0.81 (Borjomi, Lentekhi) ÷ 0.98 (Goderdzi); Bakuriani: 0.77 (Khaishi) ÷ 0.99 (Shovi); Borjomi: 0.62 (Gudauri) ÷ 1.00 (Lentekhi); Goderdzi: 0.82 (Lentekhi) ÷ 0.98 (Bakhmaro, Bakuriani, Shovi); Gudauri: 0.58 (Khaishi) ÷ 0.99 (Stepantsminda); Khaishi: 0.58 (Gudauri) ÷ 0.99 (Lentekhi); Khulo: 0.69 (Gudauri) ÷ 0.97 (Khaishi, Mestia); Lentekhi: 0.60 (Gudauri) ÷ 1.00 (Borjomi); Mestia: 0.83 (Gudauri) ÷ 0.99 (Pasanauri, Shovi, Tianeti); Pasanauri: 0.82 (Gudauri) ÷ 1.00 (Tianeti); Shovi: 0.85 (Khaishi, Lentekhi) ÷ 0.99 (Mestia); Stepantsminda: 0.68 (Khaishi) ÷ 0.99 (Gudauri); Tianeti: 0.83 (Gudauri) ÷ 1.00 (Pasanauri).

The intra-annual distribution of TCI monthly mean values for 13 locations of Georgia by the ninth power of polynomial ($R^2 \geq 0.990$) is described. Coefficients of the regression equation of the intra-annual motion of TCI monthly mean values for these points are presented in Table 3.

Table 3. Coefficients of regression equation of the intra-annual motion of TCI monthly mean values for 13 points of Georgia.

Equation of regress., coefficients	$\boldsymbol{HCI = a \cdot X^9 + b \cdot X^8 + c \cdot X^7 + d \cdot X^6 + e \cdot X^5 + f \cdot X^4 + g \cdot X^3 + h \cdot X^2 + i \cdot X + j}$, (X-Month)										
	a	b	c	d	e	f	g	h	i	j	R^2
Bakh	9.76E-05	-0.00591	0.152068	-2.17025	18.76576	-100.966	333.9624	-644.542	648.6272	-201.833	0.994
Bak	1.25E-05	-0.00083	0.022622	-0.33703	2.99689	-16.4553	55.53566	-108.942	110.5176	14.66667	0.999
Borj	-0.00021	0.012368	-0.30315	4.098518	-33.4105	168.8146	-524.14	956.8664	-919.932	408	0.997
God	5.85E-05	-0.00348	0.087734	-1.22078	10.23453	-53.0477	167.8676	-307.733	294.3048	-63.5	0.996
Gud	4.86E-05	-0.00279	0.067503	-0.89662	7.144545	-35.1709	106.5046	-190.103	178.4566	-9	0.999
Kha	-1.56E-04	0.008875	-0.21273	2.797211	-22.0306	106.7157	-315.115	543.5795	-489.079	229.3333	0.990
Khu	-2.43E-04	0.014074	-0.34541	4.688892	-38.5037	196.6584	-619.155	1148.475	-1121.66	485.8333	0.998
Lent	-2.48E-04	0.014261	-0.34608	4.627231	-37.256	185.657	-567.677	1019.447	-963.629	414.1667	0.994
Mest	-1.27E-04	0.007268	-0.17676	2.371367	-19.1728	95.8908	-293.471	525.3931	-492.671	237.8333	0.999
Pas	-0.00023	0.013184	-0.32497	4.435359	-36.6564	188.5303	-597.32	1112.285	-1088.78	479.8333	0.992
Bakh	9.76E-05	-0.00591	0.152068	-2.17025	18.76576	-100.966	333.9624	-644.542	648.6272	-201.833	0.994
Bak	1.25E-05	-0.00083	0.022622	-0.33703	2.99689	-16.4553	55.53566	-108.942	110.5176	14.66667	0.999
Borj	-0.00021	0.012368	-0.30315	4.098518	-33.4105	168.8146	-524.14	956.8664	-919.932	408	0.997

In Table 4the information on the intra-annual distribution types of HCI monthly mean values at 13 locations of Georgia are provided.

As follows from this Table the HCI bimodal distribution type for 6 locations is detected (Borjomi, Khaishi, Khulo, Lentekhi, Pasanauri, Tianeti). At the same time, the first extremum is observed in May (Khaishi, Lentekhi), in May-June (Borjomi) and in June (Khulo, Pasanauri, Tianeti). The second extremum for all points is observed in September. It is notable that all these points are located at the altitude of less than 1100 m above sea level.

For the remaining seven locations, there is the unimodal (or smooth unimodal) type of intra-annual distribution of HCI values with a maximum in the following months: July-August (Bakhmaro, Gudauri, Stepantsminda), August (Bakuriani, Goderdzi), June-September (Mestia), July- September (Shovi). Regarding height, these points are located at an altitude of ≥ 1441 m above sea level.

Table 4. Intra-annual distribution types of HCI monthly mean values at 13 locations of Georgia.

Location	Distribution type	First extremum (Max)	Second extremum
Bakhmaro	Unimodal, flat	Jul, Aug	
Bakuriani	Unimodal	Aug	
Borjomi	Bimodal	May, Jun	Sep
Goderdzi	Unimodal	Aug	
Gudauri	Unimodal, flat	Jul, Aug	
Khaishi	Bimodal	May	Sep
Khulo	Bimodal	Jun	Sep
Lentekhi	Bimodal	May	Sep
Mestia	Unimodal, flat	Jun-Sep	
Pasanauri	Bimodal	Jun	Sep
Shovi	Unimodal, flat	Jul-Sep	
Stepantsminda	Unimodal, flat	Jul, Aug	
Tianeti	Bimodal	Jun	Sep

In Table 5, 6 the categories of HCI monthly mean and seasonal values at 13 locations of Georgia in cold and warm period are presented.

Table 5. Categories of HCI monthly mean and seasonal values at 13 locations of Georgia in cold period.

Location	Jan	Feb	Mar	Oct	Nov	Dec	Cold	Year
Bakhmaro	Accept.	Accept.	Accept.	Good	Accept.	Accept.	Accept.	Good
Bakuriani	Accept.	Accept.	Accept.	V_Good	Good	Good	Good	Good
Borjomi	Good	Good	Good	V_Good	Good	Good	Good	V_Good
Goderdzi	Marg.	Marg.	Accept.	Good	Accept.	Accept.	Accept.	Accept.
Gudauri	Accept.	Accept.	Accept.	Good	Good	Accept.	Accept.	Good
Khaishi	Accept.	Good	Good	V_Good	Good	Accept.	Good	V_Good
Khulo	Accept.	Accept.	Good	V_Good	Good	Accept.	Good	V_Good
Lentekhi	Accept.	Accept.	Good	V_Good	Good	Accept.	Good	Good
Mestia	Accept.	Accept.	Good	V_Good	Good	Accept.	Good	V_Good
Pasanauri	Good	Good	Good	V_Good	Good	Good	Good	V_Good
Shovi	Accept.	Accept.	Accept.	V_Good	Good	Accept.	Good	Good
Stepantsminda	Good	Good	Good	V_Good	Good	Good	Good	V_Good
Tianeti	Good	Good	Good	V_Good	Good	Good	Good	V_Good

As follows from the Table 5 categories of HCI monthly mean and seasonal values at 13 locations of Georgia in year cold period changes from Marginal to Very Good. In warm period of year categories of HCI monthly mean and seasonal values changes from Acceptable to Excellent (Table 6).

Table 6. Categories of HCI monthly mean and seasonal values at 13 locations of Georgia in warm period.

Location	Apr	May	Jun	Jul	Aug	Sep	Warm
Bakhmaro	Good	Good	Good	V_Good	V_Good	Good	V_Good
Bakuriani	Good	Good	V_Good	Excell.	Excell.	Excell.	V_Good
Borjomi	V_Good	Excell.	Excell.	V_Good	V_Good	Excell.	Excell.
Goderdzi	Accept.	Good	Good	V_Good	V_Good	Good	Good
Gudauri	Accept.	Accept.	Good	V_Good	V_Good	V_Good	Good
Khaishi	V_Good	Excell.	Excell.	V_Good	V_Good	Excell.	Excell.
Khulo	V_Good	Excell.	Excell.	Excell.	Excell.	Excell.	Excell.
Lentekhi	V_Good	Excell.	V_Good	V_Good	V_Good	Excell.	V_Good
Mestia	Good	V_Good	Excell.	Excell.	Excell.	Excell.	V_Good
Pasanauri	Good	V_Good	Excell.	Excell.	Excell.	Excell.	Excell.
Shovi	Good	V_Good	V_Good	Excell.	Excell.	Excell.	V_Good
Stepantsminda	Good	Good	V_Good	Excell.	Excell.	V_Good	V_Good
Tianeti	Good	V_Good	Excell.	Excell.	Excell.	Excell.	Excell.

So, as follows from Fig. 2 and Tables 5, 6 in the indicated 13 locations of Georgia there are favorable bioclimatic conditions for the development of tourism and resorts throughout the year in terms of climatic timescale.

In Annexes 1-3 the Min and Max values of HCI and these categories at 13 locations of Georgia in different months and seasons in 1956-2015 are presented. As follows from Annexes values of HCI and these categories in indicated locations changes from 20 (Goderdzi, January, “Very Unfavorable”) to 100 (Stepantsminda, September, “Ideal”; Khaishi, October, “Ideal”). For separated locations Min and Max monthly values of HCI and these categories changes as follows (Annexes 1-3).

Bakhmaro: 21 (January, “Very Unfavorable”) ÷ 91 (July-September, “Ideal”); Bakuriani: 46 (May, “Marginal”) ÷ 95 (August-September, “Ideal”); Borjomi: 48 (February, “Marginal”) ÷ 98 (October, “Ideal”); Goderdzi: 20 (January, “Very Unfavorable”) ÷ 92 (August, “Ideal”); Gudauri: 26 (January and February, “Very Unfavorable”) ÷ 98 (July, “Ideal”); Khaishi: 26 (January, “Very Unfavorable”) ÷ 100 (October, “Ideal”); Khulo: 28 (February, “Very Unfavorable”) ÷ 97 (October, “Ideal”); Lentekhi: 28 (January, “Very Unfavorable”) ÷ 95 (October, “Ideal”); Mestia: 34 (January, “Unfavorable”) ÷ 95 (September-October, “Ideal”); Pasanauri: 44 (April, “Marginal”) ÷ 95 (September, “Ideal”); Shovi: 28 (January, “Very Unfavorable”) ÷ 95 (September, “Ideal”); Stepantsminda: 49 (February and April, “Marginal”) ÷ 100 (September, “Ideal”); Tianeti: 53 (January and April, “Acceptable”) ÷ 95 (September, “Ideal”).

In Annexes 4-6 information about 99%_Low and 99%_Upp levels of mean values of HCI and these categories at 13 locations of Georgia in different months and season in 1956-2015 are presented. As follows from Annexes 4-6 Lower and Upper levels of 99% confidence interval of mean values of HCI changes from 44 (Marginal) to 89 (Excellent). For separated locations 99%_Low and 99%_Upp confidence interval of mean values of HCI and these categories changes as follows (Annexes 4-6).

Bakhmaro: 48 (January, “Marginal”) ÷79 (July-August, “Very Good”); Bakuriani: 57 (January-February, “Acceptable”) ÷ 87 (August, “Excellent”); Borjomi: 59 (January and December, “Acceptable”) ÷ 88 (September, “Excellent”); Goderdzi: 44 (January, “Marginal”) ÷ 77 (August, “Very Good”); Gudauri: 52 (April, “Acceptable”) ÷ 79 (August, “Very Good”); Khaishi: 53 (December, “Acceptable”) ÷ 88 (May and September, “Excellent”); Khulo: 53 (January and December, “Acceptable”) ÷ 87 (June and September, “Excellent”); Lentekhi: 52 (December, “Acceptable”) ÷ 86 (September, “Excellent”); Mestia: 54 (January, “Acceptable”) ÷ 86 (September, “Excellent”); Pasanauri: 60 (February, “Good”) ÷ 89 (September, “Excellent”); Shovi: 55 (January, “Acceptable”) ÷ 86 (August, “Excellent”); Stepantsminda: 60 (February and March, “Good”) ÷ 87 (August, “Excellent”); Tianeti: 60 (February, “Good”) ÷ 89 (September, “Excellent”).

2. Vertical Distribution of HCI in the Mountainous Regions of Georgia.

The vertical distribution of the Tourism Climat Index was studied for 21 points in Georgia and 6 points in the North Caucasus within the height range from 3 m (Anaklia) to 2194 m (Gudauri) above sea level in our early work [14]. Results of the study of the HCI vertical distribution for thirteen mountain locations in Georgia within the height range from 730 m (Khaishi) to 2194 m (Gudauri) above sea level are presented below (Table 7 and Fig. 3-5).

Table 7. Regression equations for the relationship between HCI and terrain height.

Month/Season	**Regression equation**	**R^2**	**α**
Jan	$HCI=19.03 \cdot H^3 - 91.056 \cdot H^2 + 132.83 \cdot H - 0.1852$	0.3596	0.030
Feb	$HCI = -6.362 \cdot H^2 + 13.302 \cdot H + 53.093$	0.4543	0.011
Mar	$HCI = -6.624 \cdot H + 69.492$	0.7689	<0.001
Apr	$HCI= -11.451 \cdot H + 81.671$	0.9334	<0.001
May	$HCI= -16.99 \cdot H + 97.245$	0.957	<0.001
Jun	$HCI = 22.77 \cdot H^3 - 116.94 \cdot H^2 + 173.17 \cdot H + 6.6863$	0.9624	<0.001
Jul	$HCI = -17.581 \cdot H^2 + 47.966 \cdot H + 50.684$	0.7385	<0.001
Aug	$HCI = -18.958 \cdot H^2 + 53.137 \cdot H+ 47.33$	0.7607	<0.001
Sep	$HCI = 16.765 \cdot H^3 - 84.553 \cdot H^2 + 119.68 \cdot H + 35.573$	0.9181	<0.001
Oct	$HCI = -9.5626 \cdot H + 83.802$	0.7359	<0.001
Nov	$HCI = 17.61 \cdot H^3 - 84.639 \cdot H^2 + 122.3 \cdot H + 10.412$	0.4244	0.016
Dec	$HCI = 22.014 \cdot H^3 - 105.32 \cdot H^2 + 155.27x \cdot H- 10.724$	0.3763	0.026
Year	$HCI= 9.3544 \cdot H^3 - 50.088 \cdot H^2 + 74.751 \cdot H + 38.759$	0.8247	<0.001
Cold	$HCI= 12.704 \cdot H^3 - 61.958 \cdot H^2 + 88.966 \cdot H + 24.778$	0.53	0.005
Warm	$HCI = -12.002 \cdot H^2 + 24.754 \cdot H + 67.736$	0.9324	<0.001

For different month the form of this distribution is as follows. Inverse linear regression (decrease of HCI values with increasing altitude H): March, April, May and October; second order polynomial – February, July, August, and warm season mean; third order polynomial – January, June, September, November, December, mean annual and cold season mean.

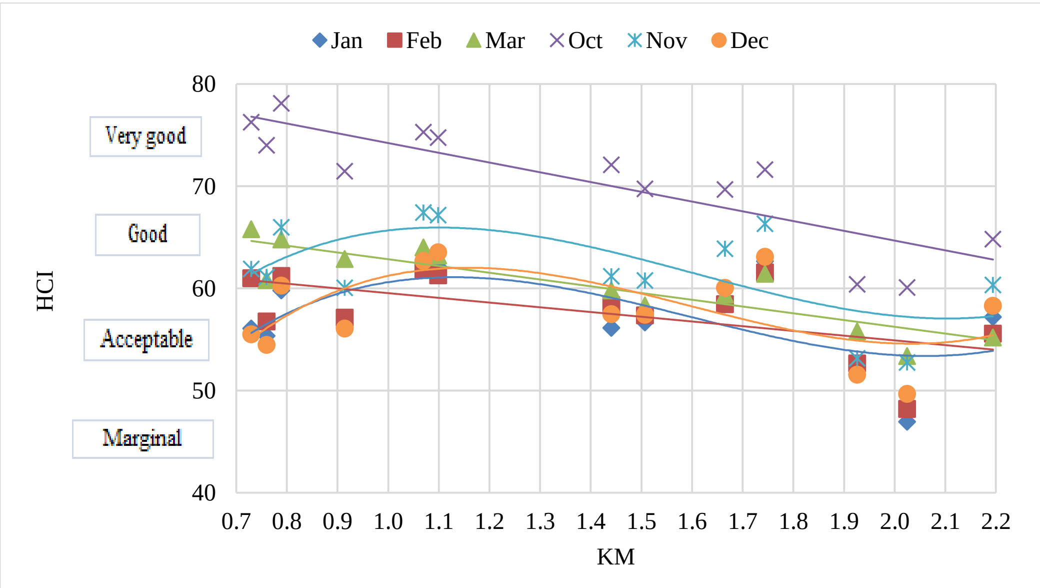

Fig. 3. Vertical distribution of HCI monthly mean values from October to March.

As it follows from Fig. 3 in January and February at level of 1500 m HCI values are weakly dependent on altitude, then there is a slight decrease in their values. In November and December, up to an altitude of 1100 m, HCI values grow, and then slowly decreases.

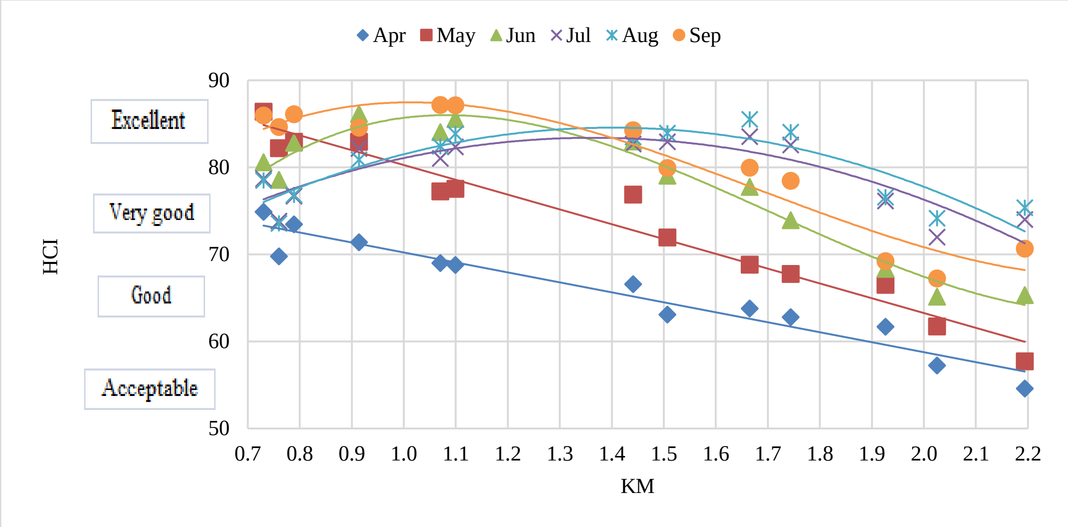

Fig. 4. Vertical distribution of HCI monthly mean from April to September.

In June and September, an increase in HCI values is observed up to an altitude of 1100 m, then a decrease. In July and August, HCI values grow to an altitude of 1400-1500 m with a further decrease (Fig. 4).

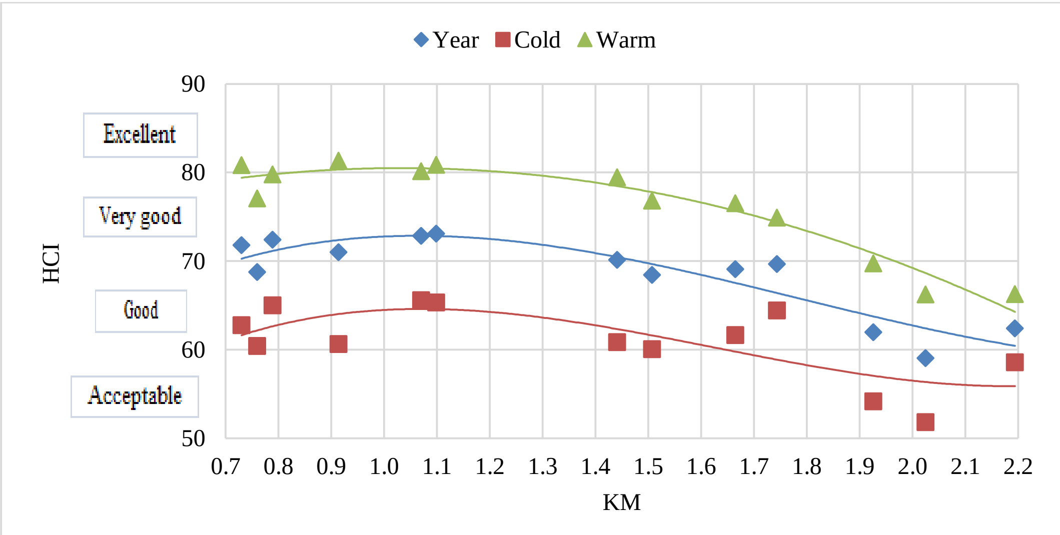

Fig. 5. Vertical distribution of HCI monthly mean and half-year values.

In the warm half of the year, there is a slight increase in the average HCI values up to an altitude of 1100-1200 m with a further decrease in their values. In the cold half of the year and on average over the year, the HCI values grow to an altitude of 1100-1200 m, and then they decrease (Fig. 5).

3. Comparison of TCI and HCI in Goderdzi, Khulo and Mestia in 1961-2010.

Comparison of TCI and HCI values are provided in many investigations [21-25]. In Georgia the analogous study was conducted for Tbilisi [26] and Kakheti region [27], in Russia – for some North Caucasus locations [28].

Comparison of TCI and HCI at three location of Georgia (Goderdzi, Khulo and Mestia) in 1961-2010 is provided below (Fig. 6-9, Table 8).

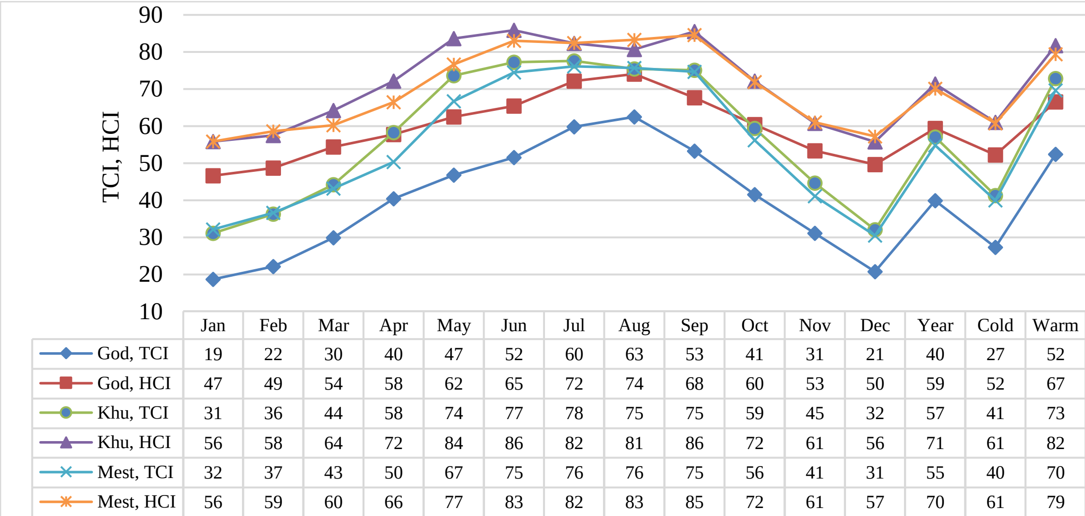

	Jan	Feb	Mar	Apr	May	Jun	Jul	Aug	Sep	Oct	Nov	Dec	Year	Cold	Warm
God, TCI	19	22	30	40	47	52	60	63	53	41	31	21	40	27	52
God, HCI	47	49	54	58	62	65	72	74	68	60	53	50	59	52	67
Khu, TCI	31	36	44	58	74	77	78	75	75	59	45	32	57	41	73
Khu, HCI	56	58	64	72	84	86	82	81	86	72	61	56	71	61	82
Mest, TCI	32	37	43	50	67	75	76	76	75	56	41	31	55	40	70
Mest, HCI	56	59	60	66	77	83	82	83	85	72	61	57	70	61	79

Fig. 6. Monthly and seasonal values of HCI and TCI in Goderdzi, Khulo and Mestia.

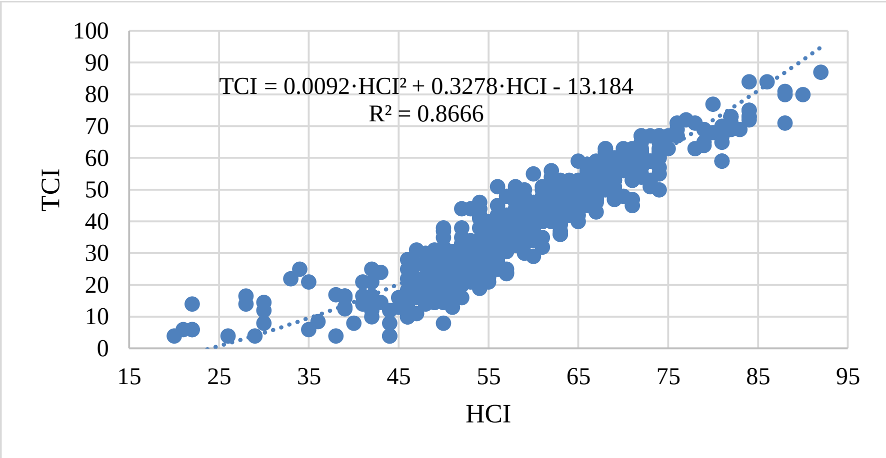

Fig. 7. Correlation and regression between monthly values of HCI and TCI in Goderdzi.

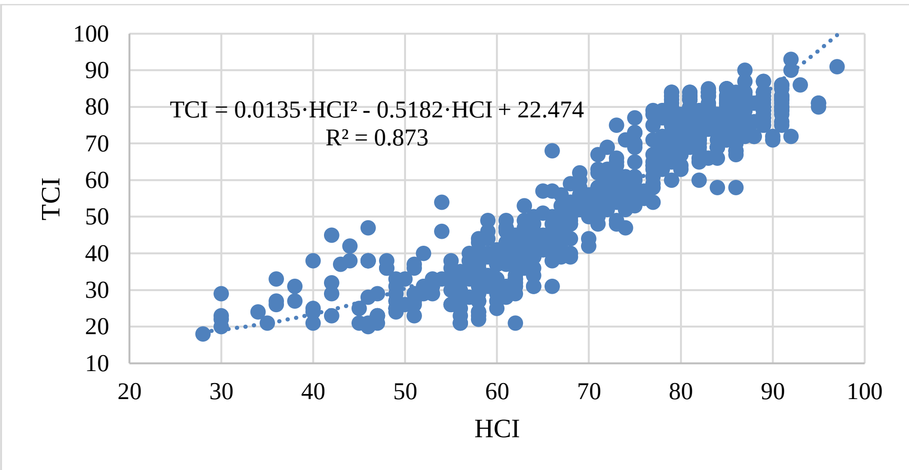

Fig. 8. Correlation and regression between monthly values of HCI and TCI in Khulo.

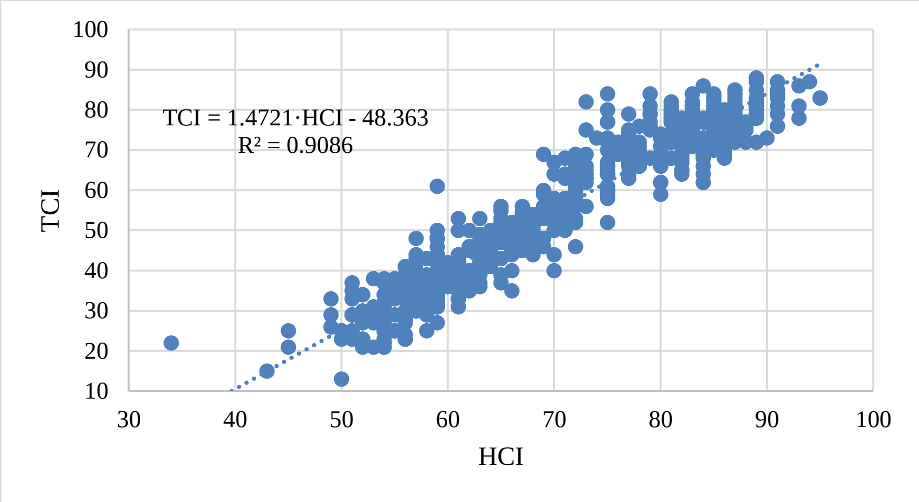

Fig. 9. Linear correlation and regression between HCI and TCI in Mestia.

Table 8. Categories of HCI and TCI monthly mean and seasonal values in Goderdzi, Khulo and Mestia.

Location	**Goderdzi**		**Khulo**		**Mestia**	
Month/Season	**TCI**	**HCI**	**TCI**	**HCI**	**TCI**	**TCI**
Jan	Ext_Unf.	Marg.	Unf.	Accept.	Unf.	Accept.
Feb	V_Unf.	Marg.	Unf.	Accept.	Unf.	Accept.
Mar	Unf.	Accept.	Marg.	Good	Marg.	Good
Apr	Marg.	Accept.	Accept.	V_Good	Accept.	Good
May	Marg.	Good	V_Good	Excell.	Good	V_Good
Jun	Accept.	Good	V_Good	Excell.	V_Good	Excell.
Jul	Good	V_ Good	V_Good	Excell.	V_Good	Excell.
Aug	Good	V_ Good	V_Good	Excell.	V_Good	Excell.
Sep	Accept.	Good	V_Good	Excell.	V_Good	Excell.
Oct	Marg.	Good	Accept.	V_Good	Accept.	V_Good
Nov	Unf.	Accept.	Marg.	Good	Marg.	Good
Dec	V_Unf.	Accept.	Unf.	Accept.	Unf.	Accept.
Year	Marg.	Accept.	Accept.	V_Good	Accept.	V_Good
Cold	V_Unf.	Accept.	Marg.	Good	Marg.	Good
Warm	Accept.	Good	V_Good	Excell.	V_Good	V_Good

In Fig. 6 the HCI and TCI monthly mean and seasonal values of in these locations are presented.

The comparison of the values and categories of the Tourism Climate Index and Holiday Climate Index (Fig. 6, Table 8) shows that the intra-annual distributions of both indices in Goderdzi and Mestia is similar and has a unimodal and flat unimodal forms respectively. In Khulo, this distribution is flat unimodal, for TCI and bimodal for HCI.

The relationship between monthly HCI and TCI values in Goderdzi and Khulo has a second order polynomial form (Figures 7 and 8). In Khulo, this connection is linear (Fig. 9).

Comparison of TCI and HCI categories shows, that in cold months, season and year HCI categories on 0-3 step higher than TCI categories (Table 8).

Difference on 3 step in the following cases are observed: TCI_ Ext_Unf. → HCI_ Marg., in January (Goderdzi); TCI_ V_Unf. → HCI_ Accept., in December and cold season (Goderdzi).

Difference on 2 step: TCI_ V_Unf. → HCI_ Marg., in February (Goderdzi); TCI_ Unf. → HCI_ Accept., in January, February and December (Khulo, Mestia); in March and November (Goderdzi); TCI_Marg. → HCI_Good, in March (Khulo, Mestia); in May and October (Goderdzi); in November and cold season (Khulo, Mestia); TCI_ Accept. → HCI_V_Good, in April, October and mean annual (Khulo, Mestia)

Difference on 1 step: TCI_Marg. → HCI_ Accept., in April and mean annual (Goderdzi); TCI_ Accept. → HCI_Good, in June, September and warm season (Goderdzi); TCI_ Good→HCI_V_Good, in May (Mestia), in July and August (Goderdzi); TCI_ V_Good→ HCI_ Excell., in May (Khulo), from June to September (Khulo, Mestia), warm season (Khulo).

The same category ”Very Good” for TCI and HCI only in warm season mean in Mestia is observed.

So the valuee and categories of TCI is lower than the HCI ones. In general, on our opinions, at least in Georgia HCI more adequately determines the bioclimatic state of the environment for the development of certain types of tourism (mountain tourism, winter tourism, extreme tourism, etc.) than TCI.

4. Changeability of HCI in the Mountainous Regions of Georgia in 1956-2015.

Data on changeability of HCI and its category are presented in Fig. 10-11, Tables 9-11 and Annexes 7-8at the 13 mountainous regions of Georgia in 1956-2015.

On Fig. 10 the information about difference between HCI monthly mean and seasonal values in 1986-2015 and 1956-1985 (ΔHCI) in 13 locations of Georgia are presented.

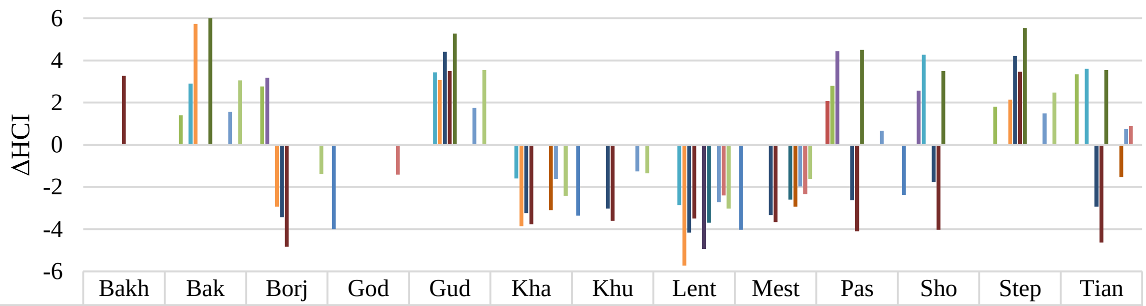

	Bakh	Bak	Borj	God	Gud	Kha	Khu	Lent	Mest	Pas	Sho	Step	Tian
Jan				-4.0			-3.4		-4.0		-2.4		
Feb										2.1			
Mar		1.4	2.8							2.8		1.8	3.3
Apr			3.2							4.4	2.6		
May		2.9			3.4	-1.6		-2.9			4.3		3.6
Jun		5.7	-2.9		3.1	-3.9		-5.7				2.1	
Jul			-3.4		4.4	-3.2	-3.0	-4.2	-3.3	-2.6	-1.8	4.2	-2.9
Aug	3.3		-4.8		3.5	-3.8	-3.6	-3.5	-3.7	-4.1	-4.0	3.5	-4.6
Sep		6.0			5.3					4.5	3.5	5.5	3.5
Oct								-4.9					
Nov								-3.7	-2.6				
Dec						-3.1			-2.9				-1.5
Year		1.6			1.7	-1.6	-1.3	-2.7	-2.0	0.7		1.5	0.7
Cold				-1.4				-2.4	-2.3				0.9
Warm		3.1	-1.4		3.5	-2.4	-1.4	-3.0	-1.6			2.5	

Fig. 10. Difference between HCI monthly mean and seasonal values in 1986-2015 and 1956-1985 in 13 locations of Georgia.

For individual locations, significant values of ΔHCI and their tendencies ($\alpha \leq 0.15$) are observed in the following months and seasons of the year.

Bakhmaro - increase in August. Bakuriani - increase in March, May, June, September, for mean annual and warm season mean. Borjomi - increase in March and April, decrease from June to August and for warm season mean. Goderdzi – decrease in January and for cold season mean. Gudauri – increase from May to September and for mean annual and warm season mean. Khaishi - decrease from May to August, in December and for mean annual and warm season mean. Khulo – decrease in January, July, August, for mean annual and warm season mean. Lentekhi – decrease from May to August, in October, November and for mean annual, cold and warm seasons mean. Mestia - decrease in January, July, August, November, December and for mean annual, cold and warm seasons mean. Pasanauri - increase from February to April, in September and for mean annual; decrease in July and August. Shovi - decrease in January, July and August; increase in April May and September. Stepantsminda – increase in March, from June to September and for mean annual and warm season mean; Tianeti - increase in March, May, September and for for mean annual and cold season mean; decrease in July, August and December.

In Tables 9 and 10 data on the coefficients of the linear trend (α for $R \leq 0.15$) of monthly and seasonal HCI values for 13 points of Georgia in 1956-2015 are presented.

Table 9. Coefficients of the linear trend of monthly and seasonal HCI values for 13 points of Georgia in 1956-2015 (October-March, average for the year, average in the cold half-year). HCI=a·X+b, (X – year).

Location	Parameter	Jan	Feb	Mar	Oct	Nov	Dec	Year	Cold
Bakh	a								
Bakh	b								
Bak	a			0.0546				0.0474	
Bak	b			-49.0				-25.0	
Borj	a			0.1029	0.0812				0.0425
Borj	b			-139.6	-83.0				-19.4
God	a								
God	b								
Gud	a		0.0867					0.0636	
Gud	b		-116.5					-63.9	
Kha	a							-0.0273	
Kha	b							125.9	
Khu	a				-0.1295			-0.0478	
Khu	b				328.6			166.0	
Lent	a				-0.1314			-0.0669	-0.0409
Lent	b				335.0			201.5	141.6
Mest	a	-0.0846					-0.0446	-0.0487	-0.0508
Mest	b	224.1					146.1	166.9	161.7
Pas	a		0.0851	0.091				0.0244	0.0383
Pas	b		-107.1	-116.6				24.5	-10.5
Sho	a								
Sho	b								
Step	a			0.0485				0.0366	
Step	b			-34.7				-2.9	
Tian	a			0.0803					0.0275
Tian	b			-96.2					10.8

Table 10. Coefficients of the linear trend of monthly and seasonal HCI values for 13 points of Georgia in 1956-2015 (April-September, average in the warm half-year). HCI=a·X+b, (X – year).

Location	Parameter	Apr	May	Jun	Jul	Aug	Sep	Warm
Bakh	a					0.089		
Bakh	b					-100.2		
Bak	a		0.0785	0.1868			0.1847	0.0815
Bak	b		-87.0	-293.1			-286.8	-85.3
Borj	a	0.0911		-0.1033	-0.1303	-0.1522	-0.0495	-0.0527
Borj	b	-107.3		287.8	335.4	379.0	184.4	184.4
God	a							
God	b							
Gud	a		0.1058	0.1155	0.1178	0.1119	0.1372	0.0978
Gud	b		-152.4	-164.0	-159.9	-146.9	-201.8	-127.9
Kha	a			-0.1194	-0.0769	-0.0828		-0.0616
Kha	b			317.7	231.3	242.9		203.2
Khu	a				-0.0954	-0.0995		-0.054
Khu	b				271.6	278.5		188.5
Lent	a		-0.0627	-0.1671	-0.1291	-0.1097		-0.0928
Lent	b		206.8	410.4	330.2	291.4		261.4
Mest	a				-0.0958	-0.12		-0.0467
Mest	b				272.9	321.8		172.1
Pas	a	0.0965			-0.0844	-0.1006	0.1205	
Pas	b	-122.6			248.6	282.2	-152.1	
Sho	a	0.0732	0.1916		-0.1178	-0.1628	0.0947	
Sho	b	-82.2	-308.5		316.9	407.2	-108.1	
Step	a				0.0994	0.0896	0.1542	0.0542
Step	b				-114.8	-93.8	-227.7	-32.7
Tian	a		0.0905		-0.1355	-0.1571	0.0912	
Tian	b		-102.2		351.5	395.8	-94.0	

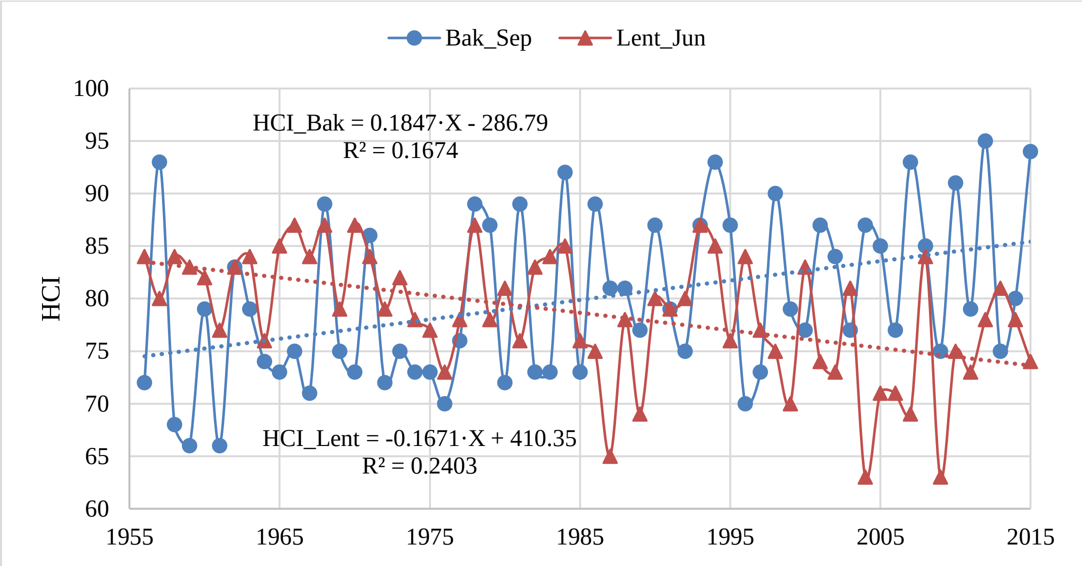

Fig. 11. Example of linear trend of HCI monthly values in Bakuriani (September) and Lentekhi (June) in 1956-2015

Example of linear trend of HCI monthly values in Bakuriani (September) and Lentekhi (June) in 1956-2015 is presented on Fig 11.

In Table 11 data about changeability of monthly mean and seasonal HCI categories in some research locations in 1986-2015 compared with 1956-1985 are presented.

Table 11. Changeability of monthly mean and seasonal HCI categories in some investigation locations in 1986-2015 compared with 1956-1985.

Location	Month	HCI Category, 1956-1985	HCI Category, 1986-2015	Location	Month	HCI Category, 1956-1985	HCI Category, 1986-2015
Bakh	Sep	Good	V_Good	**Khu**	Nov	Good	Accept.
Bak	Mar	Accept.	Good	**Lent**	Apr	V_Good	Good
Bak	May	Good	V_Good	**Lent**	Jun	Excell.	V_Good
Bak	Jun	V_Good	Excell.	**Lent**	Nov	Good	Accept.
Bak	Sep	V_Good	Excell.	**Lent**	Cold	Good	Accept.
Bak	Oct	V_Good	Good	**Lent**	Year	V_Good	Good
Bak	Year	Good	V_Good	**Mest**	Mar	Good	Accept.
Borj	Warm	Excell.	V_Good	**Mest**	Year	V_Good	Good
God	Dec	Accept.	Marg.	**Mest**	Warm	Excell.	V_Good
Gud	Sep	Good	V_Good	**Pas**	Apr	Good	V_Good
Kha	Jun	Excell.	V_Good	**Sho**	Sep	V_Good	Excell.
Kha	Jul	Excell.	V_Good	**Step**	Sep	V_Good	Excell.
Kha	Aug	Excell.	V_Good	**Step**	Year	Good	V_Good
Khu	Aug	Excell.	V_Good	**Tian**	Apr	Good	V_Good

As follows from Table 11, changes in HCI categories occur only by one step downward or an improvement in its rating. However, these changes do not fall outside the 99% confidence interval of mean HCI values (Annexes 4-6).

In Annex 7 information about repetition (%) of monthly values of HCI categories at 13 locations of Georgia in 1956-1985, 1956-2015 and 1986-2015 are presented. In Annex 8 data about number of days in year of various categories of HCI at 13 locations of Georgia in 1956-1985, 1956-2015 and 1986-2015 are presented. As follows from Table 11 and Annexes 7-8 changeability of monthly values of HCI categories and number of days per year of various categories of HCI for separated locations is as follows.

Bakhmaro

In the period from 1956 to 2015 the highest repeatability of HCI values was in the "Good" category (29.7% of cases), the lowest - in the "Ideal" category (0.8% of cases). In the second period, compared to the first in Bakhmaro, there was an increase in the HCI category by one notch in September ("Good" → "Very Good").

Repeatability of HCI category "Very Unfavorable" did not change - 1.1% of cases (respectively, 4 days a year), category "Unfavorable" increased from 2.5% to 4.2% of cases (respectively, 9 and 15 days a year), category "Marginal" decreased from 10.0% to 8.6% of cases (37 and 31 days a year, respectively), category "Acceptable" decreased from 29.7% to 28.1% of cases (109 and 102 days a year, respectively), category "Good" increased from 29.4% to 30.0% of cases (108 and 110 days, respectively) per year), category "Very Good" decreased from 22.5% to 19.2% of cases (82 and 70 days per year, respectively), category "Excellent" increased from 4.2% to 7.8% of cases (15 and 28 days per year, respectively), category " Ideal "grew from 0.6% to 1.1% of cases (2 and 4 days a year, respectively).

Bakuriani

In the period from 1956 to 2015 the highest repeatability of HCI values was in the "Good" category (34.3% of cases), the lowest - in the "Marginal" category (0.8% of cases). In the second period of time, compared to the first in Bakuriani, climate change led to an increase in HCI categories by one level in March ("Acceptable" → "Good"), May and on average per year ("Good" → "Very Good"), June and September ("Very Good" → "Excellent"), decreasing by one notch - in October ("Very Good" → "Good").

Repeatability of HCI category "Marginal" decreased from 1.1% to 0.6% of cases (4 and 2 days per year, respectively), category "Acceptable" remained practically unchanged ≈23.2% of cases (respectively, 85 days per year), category "Good" decreased from 35.6% to 33.1% of cases (respectively 130 and 121 days a year), category "Very Good" decreased from 21.7% to 17.2% (respectively 79 and 63 days a year), category "Excellent" increased from 15.8% to 21.4% of cases (respectively 58 and 78 days a year), the "Ideal" category increased from 2.8% to 4.4% of cases (10 and 16 days a year, respectively).

Borjomi

Over the entire observation period, the highest repeatability of HCI values was in the "Good" category (31.0% of cases), the lowest - in the "Marginal" category (0.1% of cases). In the second period of time, compared to the first in Borjomi, climate change led to an increase in the HCI category by one level only in the warm half of the year ("Excellent" → "Very Good").

The repeatability of the HCI category "Marginal" decreased from 0.3% to 0.0% of cases(respectively 1 and 0 days a year), category "Acceptable" increased from 11.4% to 13.3% of cases(respectively 42 and 49 days a year), category "Good" decreased from 32.8% to 29.2% of cases (respectively 120 and 107 days a year), the "Very Good" category increased from 23.9% to 32.2% of cases (87 and 118 days a year, respectively), the "Excellent" category decreased from 29.7% to 21.9% of cases (109 and 80 days a year respectively), category "Ideal" increased from 1.9% to 3.3% of cases (7 and 12 days a year, respectively).

Goderdzi

In the period from 1956 to 2015 the highest repeatability of HCI values was in the "Acceptable" category (38.2% of cases), the lowest - in the "Ideal" category (0.3% of cases). In the second time period, compared to the first in Goderdzi, climate change led to a decrease in HCI categories by one level only in December ("Acceptable" → "Marginal").

The repeatability of HCI category "Very Unfavorable" increased from 0.8% to 1.9% of cases (3 and 7 days per year, respectively), category "Unfavorable" increased from 2.2% to 2.8% of cases (respectively, 8 and 10 days a year), category "Marginal" increased from 11.7% to 12.8% of cases (43 and 47 days a year, respectively), the "Acceptable" category decreased from 39.4% to 37.2% of cases (144 and 136 days a year, respectively), the "Good" category decreased from 30.3% to 27.8% of cases (respectively 111 and 101 days a year), the "Very Good" category decreased from 12.2% to 11.1% of cases (45 and 41 days a year, respectively), the "Excellent" category increased from 3.3% to 5.8% of cases (12 and 21 days a year, respectively.), the "Ideal" category increased from 0.0% to 0.6% of cases (0 and 2 days a year, respectively).

Gudauri

Over the entire observation period, the highest repeatability of HCI values was in the "Good" category (35.8% of cases), the lowest - in the "Ideal" category (0.1% of cases). In the second period of time, compared to the first in Gudauri, climate change led to an increase in HCI categories by one level only in September ("Good" → "Very Good").

The repeatability of the HCI category “Very Unfavorable” did not change - 0.3% of cases (respectively, 1 day per year), category “Unfavorable” decreased from 1.9% to 0.8% of cases (respectively, 7 and 3 days a year), category “Marginal” increased from 6.9% to 8.6% of cases (25 and 31 days per year, respectively), the “Acceptable” category decreased from 33.3% to 27.8% of cases (122 and 101 days a year, respectively), category “Good” decreased from 37.2% to 34.4% of cases (136 and 126 days per year), category “Very Good” increased from 16.9% to 20.0% of cases (respectively 62 and 73 days per year), category “Excellent” increased from 3.3% to 7.8% of cases (respectively 12 and 28 days per year), category “Ideal” increased from 0.0% to 0.3% of cases (0 and 1 day per year, respectively).

Khaishi

In the period from 1956 to 2015 the highest repeatability of HCI values was in the “Excellent” category (29.3% of cases), the lowest - in the “Very Unfavorable” category (0.1% of cases). In the second period compared to the first in Khaishi, climate change led to a decrease in the HCI category by one notch only in the summer months, from June to August (“Excellent” → “Very Good”).

The repeatability of the HCI category “Very Unfavorable” increased from 0.0% to 0.3% of cases (0 and 1 day per year, respectively), category “Unfavorable” decreased from 1.1% to 0.6% of cases (respectively, 4 and 2 days per year), category “Marginal” decreased from 4.2% to 3.1% of cases (15 and 11 days a year, respectively), the ”Acceptable” category increased from 8.9% to 18.3% of cases (32 and 67 days a year, respectively), the “Good ” category decreased from 27.5% to 22.5% of cases (100 and 82 days a year), the “Very Good” category increased from 22.8% to 24.7% of cases (83 and 90 days a year, respectively), the “Excellent” category decreased from 30.8% to 27.8% of cases (113 and 101 days a year, respectively) , category “Ideal” decreased from 4.7% to 2.8% of cases (17 and 10 days per year, respectively).

Khulo

In the period from 1956 to 2015 the highest repeatability of HCI values was in the “Excellent” category (32.1% of cases), the lowest - in the “Very Unfavorable” category (0.3% of cases). In the second time period compared to the first in Khulo, climate change led to a decrease in the HCI category by one notch in August (“Excellent” → “Very Good”) and November (“Good” → “Acceptable”).

The repeatability of HCI category “Very Unfavorable” did not change - 0.3% of cases (respectively, 1 day per year), category “Unfavorable” increased from 1.4% to 2.5% of cases (respectively, 5 and 9 days per year), category “Marginal” increased from 5.3% to 6.9% of cases (19 and 25 days a year, respectively), the “Acceptable” category decreased from 13.6% to 11.1% of cases (50 and 41 days a year, respectively), the “Good” category increased from 23.6% to 25.0% of cases (86 and 91 days per year respectively), category “Very Good” increased from 17.5% to 19.7% of cases (respectively 64 and 72 days a year), the category “Excellent“ decreased from 34.7% to 29.4% of cases (respectively 127 and 108 days a year), the category “ Ideal “grew from 3.6% to 5.0% of cases (13 and 18 days a year, respectively).

Lentekhi

Over the entire observation period, the highest repeatability of HCI values was in the “Very Good” category (26.5% of cases), the lowest - in the “Very Unfavorable” category (0.1% of cases). In the second period of time, compared to the first in Lentekhi, climate change led to a decrease in the HCI category by one level in April and on average per year (“Very Good” → “Good”), June (“Excellent” → “Very Good”), November and in the cold half of the year (”Good” → “Acceptable”).

The repeatability of the HCI category “Very Unfavorable” increased from 0.0% to 0.3% of cases (0 and 1 day per year, respectively), category “Unfavorable” decreased from 1.9% to 0.8% of cases (respectively, 7 and 3 days per year), category “Marginal” did not changed - 4.4% of cases (16 days a year, respectively), the “Acceptable” category increased from 13.3% to 26.1% of cases (49 and 95 days a year, respectively), the “Good” category decreased from 26.9% to 22.2% of cases (98 and 81 days, respectively per year), category “Very Good” increased from 25.8% to 27.2% of cases (respectively, 94 and 99 days per year), category “Excellent” decreased from 25.8% to 18.6% of cases (respectively, 94 and 68 days per year), category “ Ideal “decreased from 1.7% to 0.3% of cases (6 and 1 days per year, respectively).

Mestia

In the period from 1956 to 2015 the highest repeatability of HCI values was in the “Excellent” category (29.3% of cases), the lowest - in the “Unfavorable” category (0.1% of cases). In the second period of time compared to the first in Mestia, climate change led to a decrease in the HCI category by one level in March (“Good” → “Acceptable”), on average per year (“Very Good” → “Good”) and in the warm half of the year (“Excellent“ → “Very Good).

The repeatability of the HCI category “Unfavorable” increased from 0.0% to 0.3% of cases (0 and 1 day per year, respectively), category “Marginal” increased from 0.6% to 1.4% of cases (respectively, 2 and 5 days per year), category “Acceptable” increased from 21.7% to 30.0% of cases (79 and 110 days a year, respectively), the “Good” category decreased from 29.4% to 19.7% of cases (108 and 72 days a year, respectively), the “Very Good” category increased from 13.9% to 19.2% of cases (respectively 51 and 70 days a year), the “Excellent” category decreased from 30.3% to 28.3% of cases (111 and 103 days a year, respectively), the “Ideal” category decreased from 4.2% to 1.1% of cases (15 and 4 days per year, respectively).

Pasanauri

In the period from 1956 to 2015 the highest repeatability of HCI values was in the “Good” category (36.9% of cases), the lowest - in the “Marginal” category (0.7% of cases). In the second time period compared to the first in Pasanauri, climate change led to an increase in the HCI category by one notch only in April (“Good” → “Very Good”).

The repeatability of the HCI “Marginal” category decreased from 0.8% to 0.6% of cases (3 and 2 days per year, respectively), the “Acceptable” category decreased from 8.9% to 6.4% of cases (32 and 23 days per year, respectively), the “Good” category did not change - 36.9% of cases (135 days a year), category “Very Good” increased from 17.2% to 23.6% of cases (respectively 63 and 86 days a year), category “Excellent” decreased from 31.4% to 25.3% of cases (respectively 115 and 92 days a year), the “Ideal” category increased from 4.7% to 7.2% of cases (17 and 26 days a year, respectively).

Shovi

Over the entire observation period, the highest repeatability of HCI values was in the “Acceptable” category (27.1% of cases), the lowest - in the “Very Unfavorable” and “Unfavorable” categories (0.1% of cases). In the second period of time, compared to the first in Shovi, climate change led to an increase in the HCI category by one notch only in September (“Very Good” → “Excellent”).

The repeatability of HCI categories “Very Unfavorable” and “Unfavorable” increased from 0.0% to 0.3% of cases (0 and 1 day per year, respectively), category “Marginal” decreased from 2.8% to 1.7% of cases (10 and 6 days per year, respectively), category “Acceptable” increased from 24.2% to 30.0% of cases (respectively 88 and 110 days a year), category “Good” decreased from 31.4% to 22.5% of cases (respectively 115 and 82 days a year), category “Very Good” increased from 16.1 % to 18.3% of cases (59 and 67 days a year, respectively), the “Excellent” category increased from 23.3% to 26.7% of cases (85 and 97 days a year, respectively), the “Ideal” category decreased from 2.2% to 0.3% of cases (respectively 8 and 1 days a year).

Stepantsminda

In the period from 1956 to 2015 the highest repeatability of HCI values was in the “Good” category (48.2% of cases), the lowest - in the “Marginal” category (0.3% of cases). In the second period of time, as compared to the first in Stepantsminda, climate change led to an increase in the HCI category by one notch in September (“Very Good” → “Excellent”) and for the whole year (“Good” → “Very Good”).

The repeatability of the HCI category “Marginal” decreased from 0.6% to 0.0% of cases (respectively 2 and 0 days per year), category “Acceptable” increased from 9.2% to 10.3% of cases (respectively, 33 and 38 days per year), category “Good” decreased from 50.6% to 45.8% of cases (185 and 167 days a year, respectively), the “Very Good” category decreased from 24.4% to 23.1% of cases (89 and 84 days a year, respectively), the “Excellent” category increased from 12.8% to 16.4% of cases (47 and 60 days a year, respectively), the “Ideal” category increased from 2.5% to 4.4% of cases (9 and 16 days a year, respectively).

Tianeti

In the period from 1956 to 2015 the highest repeatability of HCI values was in the “Good” category (34.3% of cases), the lowest - in the “Ideal” category (5.8% of cases). In the second time period compared to the first in Tianeti, climate change led to an increase in HCI categories by one notch in April (“Good” → “Very Good”).

The repeatability of the HCI category “Acceptable” decreased from 11.7% to 8.6% of cases (43 and 31 days per year, respectively), category “Good” practically did not change - ≈ 34.3 of cases (respectively, 125 days per year), category “Very Good” increased from 19.7 % to 24.4% of cases (72 and 89 days a year, respectively), the “Excellent” category decreased from 29.2% to 26.1% of cases (107 and 95 days a year, respectively), the “Ideal” category increased from 5.0% to 6.7% of cases(18 and 24 days a year).

In 1956-1985, 1956-2015 and 1986-2015, the number of days in the range of HCI categories “Marginal” - “Ideal” for the studied locations, respectively, is the following: Bakhmaro (352-349-346), Goderdzi (354-351-348), Gudauri (357-359-361), Khaishi (361-362-362), Khulo (359-357-355), Lentekhi (358-360-361), Mestia (365-365-364), Shovi (365-345- 363); Bakuriani, Borjomi, Pasanauri, Stepantsminda and Tianeti (for all three time periods - by 365 days).

5. Expected Changes of HCI by 2041-2070 and 2071-2100 on the Example of Mestia.

Data about expected changes of HCI and its categories by 2041-2070 and 2071-2100 in Mestia according [33] in Fig. 12 and Table 12 are presented.

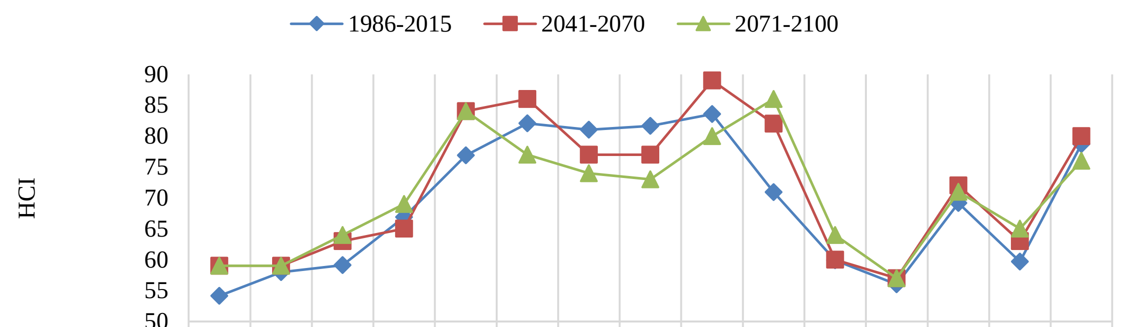

	Jan	Feb	Mar	Apr	May	Jun	Jul	Aug	Sep	Oct	Nov	Dec	Year	Cold	Warm
1986-2015	54	58	59	67	77	82	81	82	84	71	60	56	69	60	79
2041-2070	59	59	63	65	84	86	77	77	89	82	60	57	72	63	80
2071-2100	59	59	64	69	84	77	74	73	80	86	64	57	71	65	76

Fig. 12. Average monthly, annual and seasonal values of HCI in Mestia (1986-2015, 2041-2070 and 2071-2100) [33].

Table 12. Average monthly, average annual and seasonal values of HCI category in Mestia (1986-2015, 2041-2070 and 2071-2100) [33].

Month / Period	**99%_Low**	**99%_Upp**	**1986-2015**	**2041-2070**	**2071-2100**
January	Accept.	Accept.	Acceptable	Acceptable	Acceptable
February	Accept.	Good	Acceptable	Acceptable	Acceptable
March	Accept.	Good	Acceptable	Good	Good
April	Good	Good	Good	Good	Good
May	V_Good	V_Good	Very Good	***Excellent***	***Excellent***
June	Excell.	Excell.	Excellent	Excellent	***Very Good***
July	Excell.	Excell.	Excellent	***Very Good***	***Very Good***
August	Excell.	Excell.	Excellent	***Very Good***	***Very Good***
September	Excell.	Excell.	Excellent	Excellent	Excellent
October	Good	V_Good	Very Good	***Excellent***	***Excellent***
November	Accept.	Good	Good	Good	Good
December	Accept.	Accept.	Acceptable	Acceptable	Acceptable
Year	Good	V_Good	Good	Very Good	Very Good
Cold period	Good	Good	Good	Good	Good
Warm period	V_Good	Excell.	Very Good	Excellent	Very Good

A significant change in HCI values and their categories in 2041-2070 and 2071-2100 compared to the 99% confidence interval of the average HCI values in 1956-2015 is expected in May and October (an increase in HCI values and a corresponding improvement in its category by one level, “Very Good” → “Excellent”), as well as in July and August (a decrease in HCI values and a corresponding deterioration in its category by one notch, “Excellent” → “Very Good”). In June 2071-2100, the HCI category will deteriorate by one notch, “Excellent” → “Very Good” (Fig. 12, Table 12).

Thus, in Mestia, at least until 2100, it is expected to maintain favorable bioclimatic conditions for tourism.

Annexes

Annex 1. Min and Max values of HCI at 13 locations of Georgia in different months and season in 1956-2015.

Parameter	Jan	Feb	Mar	Apr	May	Jun	Jul	Aug	Sep	Oct	Nov	Dec	Year	Cold	Warm
Bakh_Min	21	22	31	45	45	55	51	59	46	34	29	28	55	44	60
Bakh_Max	67	65	63	73	77	83	91	91	91	79	73	65	68	63	77
Bak_Min	50	48	54	49	46	62	70	70	66	60	47	52	65	57	69
Bak_Max	68	66	65	75	85	91	91	95	95	88	78	70	73	66	83
Borj_Min	55	48	56	60	68	70	68	60	78	64	56	52	68	59	74
Borj_Max	69	73	77	89	93	89	87	87	95	98	78	69	75	71	84
God_Min	20	22	37	43	48	52	50	52	48	46	28	21	54	44	59
God_Max	59	58	60	66	74	82	86	92	89	81	67	60	65	60	72
Gud_Min	26	26	30	30	38	46	42	56	55	42	38	34	56	43	57
Gud_Max	72	66	65	68	71	84	98	89	83	79	76	71	69	65	77
Kha_Min	26	47	45	54	72	62	61	69	65	54	42	30	64	55	70
Kha_Max	65	74	75	89	95	91	87	87	97	100	75	66	78	73	86
Khu_Min	30	28	39	44	66	78	66	68	61	42	36	30	63	50	74
Khu_Max	69	71	73	89	95	95	92	95	93	97	82	70	77	72	86
Lent_Min	28	36	32	48	70	63	59	59	71	57	38	34	62	52	71
Lent_Max	68	70	73	89	91	87	85	83	93	95	75	68	74	70	83
Mest_Min	34	45	45	51	66	59	69	74	68	53	49	51	64	55	73
Mest_Max	70	66	68	81	89	93	91	91	95	95	75	66	74	68	85
Pas_Min	45	45	49	44	57	69	62	71	73	65	58	49	68	58	76
Pas_Max	72	72	74	89	93	93	91	91	95	94	80	72	77	70	86
Sho_Min	28	43	43	49	53	61	71	72	62	48	43	36	63	52	72
Sho_Max	70	68	67	83	87	89	91	91	95	91	75	69	72	69	82
Step_Min	55	49	54	49	59	65	63	63	66	61	57	55	65	60	69
Step_Max	72	70	70	74	79	87	95	96	100	84	80	74	74	68	81
Tian_Min	53	54	54	53	57	68	72	69	73	59	54	56	69	60	77
Tian_Max	72	72	76	89	91	94	91	91	95	92	82	76	77	70	86

Annex 2. Categories of HCI Min and Max values at 13 locations of Georgia in cold period in 1956-2015.

Parameter	Jan	Feb	Mar	Oct	Nov	Dec	Year	Cold
Bakh_Min	V_Unf.	V_Unf.	Unf.	Unf.	V_Unf.	V_Unf.	Accept.	Marg.
Bakh_Max	Good	Good	Good	V_Good	V_Good	Good	Good	Good
Bak_Min	Accept.	Marg.	Accept.	Good	Marg.	Accept.	Good	Accept.
Bak_Max	Good	Good	Good	Excell.	V_Good	V_Good	V_Good	Good
Borj_Min	Accept.	Marg.	Accept.	Good	Accept.	Accept.	Good	Accept.
Borj_Max	Good	V_Good	V_Good	Ideal	V_Good	Good	V_Good	V_Good
God_Min	V_Unf.	V_Unf.	Unf.	Marg.	V_Unf.	V_Unf.	Accept.	Marg.
God_Max	Accept.	Accept.	Good	Excell.	Good	Good	Good	Good
Gud_Min	V_Unf.	V_Unf.	Unf.	Marg.	Unf.	Unf.	Accept.	Marg.
Gud_Max	V_Good	Good	Good	V_Good	V_Good	V_Good	Good	Good
Kha_Min	V_Unf.	Marg.	Marg.	Accept.	Marg.	Unf.	Good	Accept.
Kha_Max	Good	V_Good	V_Good	Ideal	V_Good	Good	V_Good	V_Good
Khu_Min	Unf.	V_Unf.	Unf.	Marg.	Unf.	Unf.	Good	Accept.
Khu_Max	Good	V_Good	V_Good	Ideal	Excell.	V_Good	V_Good	V_Good
Lent_Min	V_Unf.	Unf.	Unf.	Accept.	Unf.	Unf.	Good	Accept.
Lent_Max	Good	V_Good	V_Good	Ideal	V_Good	Good	V_Good	V_Good
Mest_Min	Unf.	Marg.	Marg.	Accept.	Marg.	Accept.	Good	Accept.
Mest_Max	V_Good	Good	Good	Ideal	V_Good	Good	V_Good	Good
Pas_Min	Marg.	Marg.	Marg.	Good	Accept.	Marg.	Good	Accept.
Pas_Max	V_Good	V_Good	V_Good	Ideal	Excell.	V_Good	V_Good	V_Good
Sho_Min	V_Unf.	Marg.	Marg.	Marg.	Marg.	Unf.	Good	Accept.
Sho_Max	V_Good	Good	Good	Ideal	V_Good	Good	V_Good	Good
Step_Min	Accept.	Marg.	Accept.	Good	Accept.	Accept.	Good	Good
Step_Max	V_Good	V_Good	V_Good	Excell.	Excell.	V_Good	V_Good	Good
Tian_Min	Accept.	Accept.	Accept.	Accept.	Accept.	Accept.	Good	Good
Tian_Max	V_Good	V_Good	V_Good	Ideal	Excell.	V_Good	V_Good	V_Good

Annex 3. Category of HCI Min and Max values at 13 locations of Georgia in warm period in 1956-2015.

Parameter	Apr	May	Jun	Jul	Aug	Sep	Warm
Bakh_Min	Marg.	Marg.	Accept.	Accept.	Accept.	Marg.	Good
Bakh_Max	V_Good	V_Good	Excell.	Ideal	Ideal	Ideal	V_Good
Bak_Min	Marg.	Marg.	Good	V_Good	V_Good	Good	Good
Bak_Max	V_Good	Excell.	Ideal	Ideal	Ideal	Ideal	Excell.
Borj_Min	Good	Good	V_Good	Good	Good	V_Good	V_Good
Borj_Max	Excell.	Ideal	Excell.	Excell.	Excell.	Ideal	Excell.
God_Min	Marg.	Marg.	Accept.	Accept.	Accept.	Marg.	Accept.
God_Max	Good	V_Good	Excell.	Excell.	Ideal	Excell.	V_Good
Gud_Min	Unf.	Unf.	Marg.	Marg.	Accept.	Accept.	Accept.
Gud_Max	Good	V_Good	Excell.	Ideal	Excell.	Excell.	V_Good
Kha_Min	Accept.	V_Good	Good	Good	Good	Good	V_Good
Kha_Max	Excell.	Ideal	Ideal	Excell.	Excell.	Ideal	Excell.
Khu_Min	Marg.	Good	V_Good	Good	Good	Good	V_Good
Khu_Max	Excell.	Ideal	Ideal	Ideal	Ideal	Ideal	Excell.
Lent_Min	Marg.	V_Good	Good	Accept.	Accept.	V_Good	V_Good
Lent_Max	Excell.	Ideal	Excell.	Excell.	Excell.	Ideal	Excell.
Mest_Min	Accept.	Good	Accept.	Good	V_Good	Good	V_Good
Mest_Max	Excell.	Excell.	Ideal	Ideal	Ideal	Ideal	Excell.
Pas_Min	Marg.	Accept.	Good	Good	V_Good	V_Good	V_Good
Pas_Max	Excell.	Ideal	Ideal	Ideal	Ideal	Ideal	Excell.
Sho_Min	Marg.	Accept.	Good	V_Good	V_Good	Good	V_Good
Sho_Max	Excell.	Excell.	Excell.	Ideal	Ideal	Ideal	Excell.
Step_Min	Marg.	Accept.	Good	Good	Good	Good	Good
Step_Max	V_Good	V_Good	Excell.	Ideal	Ideal	Ideal	Excell.
Tian_Min	Accept.	Accept.	Good	V_Good	Good	V_Good	V_Good
Tian_Max	Excell.	Ideal	Ideal	Ideal	Ideal	Ideal	Excell.

Annex 4. Low and Upper levels of 99% confidence interval of HCI mean values at 13 locations of Georgia in 1956-2015.

Parmeter	Jan	Feb	Mar	Apr	May	Jun	Jul	Aug	Sep	Oct	Nov	Dec	Year	Cold	Warm
Bakh_99%_Low	48	49	54	60	65	66	74	74	66	57	49	49	61	53	69
Bakh_99%_Upp	55	56	58	63	68	70	79	79	72	64	57	54	63	56	71
Bak_99%_Low	57	57	58	62	67	76	82	84	77	68	62	59	69	61	76
Bak_99%_Upp	60	60	60	65	71	80	85	87	83	71	66	61	70	62	78
Borj_99%_Low	59	60	63	71	81	81	75	75	85	76	64	59	72	64	79
Borj_99%_Upp	61	63	66	76	85	84	78	79	88	80	68	61	73	66	81
God_99%_Low	44	46	52	56	60	63	69	71	65	58	50	47	58	51	65
God_99%_Upp	50	51	55	59	64	67	75	77	70	63	56	52	60	53	67
Gud_99%_Low	55	53	53	52	55	63	71	72	68	63	58	56	61	57	65
Gud_99%_Upp	60	58	58	57	60	68	77	79	73	67	63	61	63	60	68
Kha_99%_Low	54	59	64	72	85	79	77	77	84	73	59	53	71	62	80
Kha_99%_Upp	59	63	68	78	88	83	80	80	88	79	65	58	73	64	82
Khu_99%_Low	53	54	61	69	81	85	81	79	83	68	56	53	70	59	81
Khu_99%_Upp	59	60	65	74	85	87	84	83	87	75	64	59	72	62	82
Lent_99%_Low	53	54	59	67	81	77	72	72	83	71	58	52	68	59	76
Lent_99%_Upp	58	59	63	73	84	81	76	75	86	77	64	57	70	62	78
Mest_99%_Low	54	57	58	65	75	81	81	82	82	69	59	56	69	60	79
Mest_99%_Upp	58	60	61	68	79	85	84	85	86	75	63	59	71	62	80
Pas_99%_Low	61	60	62	66	75	82	79	81	85	73	66	61	72	65	79
Pas_99%_Upp	64	63	66	72	80	86	83	84	89	77	69	64	73	66	81
Sho_99%_Low	55	56	57	61	69	77	81	82	78	67	59	56	68	59	76
Sho_99%_Upp	59	59	60	65	74	81	85	86	82	72	63	59	69	61	78
Step_99%_Low	61	60	60	61	66	72	80	82	76	70	65	62	69	64	74
Step_99%_Upp	64	63	63	64	69	76	85	87	81	73	68	64	70	65	76
Tian_99%_Low	61	60	62	67	75	84	81	82	85	73	65	62	73	65	80
Tian_99%_Upp	63	63	65	71	80	87	84	85	89	77	69	65	74	66	82

Annex 5. Category of Low and Upper levels of 99% confidence interval of HCI mean values at 13 locations of Georgia in cold period in 1956-2015.

Parameter	Jan	Feb	Mar	Oct	Nov	Dec	Year	Cold
Bakh_99%_Low	Marg.	Marg.	Accept.	Accept.	Marg.	Marg.	Good	Accept.
Bakh_99%_Upp	Accept.	Accept.	Accept.	Good	Accept.	Accept.	Good	Accept.
Bak_99%_Low	Accept.	Accept.	Accept.	Good	Good	Accept.	Good	Good
Bak_99%_Upp	Good	Good	Good	V_Good	Good	Good	V_Good	Good
Borj_99%_Low	Accept.	Good	Good	V_Good	Good	Accept.	V_Good	Good
Borj_99%_Upp	Good	Good	Good	Excell.	Good	Good	V_Good	Good
God_99%_Low	Marg.	Marg.	Accept.	Accept.	Accept.	Marg.	Accept.	Accept.
God_99%_Upp	Accept.	Accept.	Accept.	Good	Accept.	Accept.	Good	Accept.
Gud_99%_Low	Accept.	Accept.	Accept.	Good	Accept.	Accept.	Good	Accept.
Gud_99%_Upp	Good	Accept.	Accept.	Good	Good	Good	Good	Good
Kha_99%_Low	Accept.	Accept.	Good	V_Good	Accept.	Accept.	V_Good	Good
Kha_99%_Upp	Accept.	Good	Good	V_Good	Good	Accept.	V_Good	Good
Khu_99%_Low	Accept.	Accept.	Good	Good	Accept.	Accept.	V_Good	Accept.
Khu_99%_Upp	Accept.	Good	Good	V_Good	Good	Accept.	V_Good	Good
Lent_99%_Low	Accept.	Accept.	Accept.	V_Good	Accept.	Accept.	Good	Accept.
Lent_99%_Upp	Accept.	Accept.	Good	V_Good	Good	Accept.	V_Good	Good
Mest_99%_Low	Accept.	Accept.	Accept.	Good	Accept.	Accept.	Good	Good
Mest_99%_Upp	Accept.	Good	Good	V_Good	Good	Accept.	V_Good	Good
Pas_99%_Low	Good	Good	Good	V_Good	Good	Good	V_Good	Good
Pas_99%_Upp	Good	Good	Good	V_Good	Good	Good	V_Good	Good
Sho_99%_Low	Accept.	Accept.	Accept.	Good	Accept.	Accept.	Good	Accept.
Sho_99%_Upp	Accept.	Accept.	Good	V_Good	Good	Accept.	Good	Good
Step_99%_Low	Good	Good	Good	V_Good	Good	Good	Good	Good
Step_99%_Upp	Good	Good	Good	V_Good	Good	Good	V_Good	Good
Tian_99%_Low	Good	Good	Good	V_Good	Good	Good	V_Good	Good
Tian_99%_Upp	Good	Good	Good	V_Good	Good	Good	V_Good	Good

Annex 6. Category of Low and Upper levels of 99% confidence interval of HCI mean values at 13 locations of Georgia in warm period in 1956-2015.

Parameter	Apr	May	Jun	Jul	Aug	Sep	Warm
Bakh_99%_Low	Good	Good	Good	V_Good	V_Good	Good	Good
Bakh_99%_Upp	Good	Good	V_Good	V_Good	V_Good	V_Good	V_Good
Bak_99%_Low	Good	Good	V_Good	Excell.	Excell.	V_Good	V_Good
Bak_99%_Upp	Good	V_Good	Excell.	Excell.	Excell.	Excell.	V_Good
Borj_99%_Low	V_Good	Excell.	Excell.	V_Good	V_Good	Excell.	V_Good
Borj_99%_Upp	V_Good	Excell.	Excell.	V_Good	V_Good	Excell.	Excell.
God_99%_Low	Accept.	Good	Good	Good	V_Good	Good	Good
God_99%_Upp	Accept.	Good	Good	V_Good	V_Good	V_Good	Good
Gud_99%_Low	Accept.	Accept.	Good	V_Good	V_Good	Good	Good
Gud_99%_Upp	Accept.	Good	Good	V_Good	V_Good	V_Good	Good
Kha_99%_Low	V_Good	Excell.	V_Good	V_Good	V_Good	Excell.	Excell.
Kha_99%_Upp	V_Good	Excell.	Excell.	Excell.	Excell.	Excell.	Excell.
Khu_99%_Low	Good	Excell.	Excell.	Excell.	V_Good	Excell.	Excell.
Khu_99%_Upp	V_Good	Excell.	Excell.	Excell.	Excell.	Excell.	Excell.
Lent_99%_Low	Good	Excell.	V_Good	V_Good	V_Good	Excell.	V_Good
Lent_99%_Upp	V_Good	Excell.	Excell.	V_Good	V_Good	Excell.	V_Good
Mest_99%_Low	Good	V_Good	Excell.	Excell.	Excell.	Excell.	V_Good
Mest_99%_Upp	Good	V_Good	Excell.	Excell.	Excell.	Excell.	Excell.
Pas_99%_Low	Good	V_Good	Excell.	V_Good	Excell.	Excell.	V_Good
Pas_99%_Upp	V_Good	Excell.	Excell.	Excell.	Excell.	Excell.	Excell.
Sho_99%_Low	Good	Good	V_Good	Excell.	Excell.	V_Good	V_Good
Sho_99%_Upp	Good	V_Good	Excell.	Excell.	Excell.	Excell.	V_Good
Step_99%_Low	Good	Good	V_Good	Excell.	Excell.	V_Good	V_Good
Step_99%_Upp	Good	Good	V_Good	Excell.	Excell.	Excell.	V_Good
Tian_99%_Low	Good	V_Good	Excell.	Excell.	Excell.	Excell.	Excell.
Tian_99%_Upp	V_Good	Excell.	Excell.	Excell.	Excell.	Excell.	Excell.

Annex 7. Repetition of categories of HCI monthly values at 13 locations of Georgia in 1956-1985, 1956-2015 and 1986-2915, (%).

Location	Year	V_Unf.	Unf.	Marg.	Accept.	Good	V_Good	Excell.	Ideal
Bakh	1956-1985	1.1	2.5	10.0	29.7	29.4	22.5	4.2	0.6
Bakh	1956-2015	1.1	3.3	9.3	28.9	29.7	20.8	6.0	0.8
Bakh	1986-2015	1.1	4.2	8.6	28.1	30.0	19.2	7.8	1.1
Bak	1956-1985	0.0	0.0	1.1	23.1	35.6	21.7	15.8	2.8
Bak	1956-2015	0.0	0.0	0.8	23.2	34.3	19.4	18.6	3.6
Bak	1986-2015	0.0	0.0	0.6	23.3	33.1	17.2	21.4	4.4
Borj	1956-1985	0.0	0.0	0.3	11.4	32.8	23.9	29.7	1.9
Borj	1956-2015	0.0	0.0	0.1	12.4	31.0	28.1	25.8	2.6
Borj	1986-2015	0.0	0.0	0.0	13.3	29.2	32.2	21.9	3.3
God	1956-1985	0.8	2.2	11.7	39.4	30.3	12.2	3.3	0.0
God	1956-2015	1.4	2.5	12.2	38.3	29.0	11.7	4.6	0.3
God	1986-2015	1.9	2.8	12.8	37.2	27.8	11.1	5.8	0.6
Gud	1956-1985	0.3	1.9	6.9	33.3	37.2	16.9	3.3	0.0
Gud	1956-2015	0.3	1.4	7.8	30.6	35.8	18.5	5.6	0.1
Gud	1986-2015	0.3	0.8	8.6	27.8	34.4	20.0	7.8	0.3
Kha	1956-1985	0.0	1.1	4.2	8.9	27.5	22.8	30.8	4.7
Kha	1956-2015	0.1	0.8	3.6	13.6	25.0	23.8	29.3	3.8
Kha	1986-2015	0.3	0.6	3.1	18.3	22.5	24.7	27.8	2.8
Khu	1956-1985	0.3	1.4	5.3	13.6	23.6	17.5	34.7	3.6
Khu	1956-2015	0.3	1.9	6.1	12.4	24.3	18.6	32.1	4.3
Khu	1986-2015	0.3	2.5	6.9	11.1	25.0	19.7	29.4	5.0
Lent	1956-1985	0.0	1.9	4.4	13.3	26.9	25.8	25.8	1.7
Lent	1956-2015	0.1	1.4	4.4	19.7	24.6	26.5	22.2	1.0
Lent	1986-2015	0.3	0.8	4.4	26.1	22.2	27.2	18.6	0.3
Mest	1956-1985	0.0	0.0	0.6	21.7	29.4	13.9	30.3	4.2
Mest	1956-2015	0.0	0.1	1.0	25.8	24.6	16.5	29.3	2.6
Mest	1986-2015	0.0	0.3	1.4	30.0	19.7	19.2	28.3	1.1
Pas	1956-1985	0.0	0.0	0.8	8.9	36.9	17.2	31.4	4.7
Pas	1956-2015	0.0	0.0	0.7	7.6	36.9	20.4	28.3	6.0
Pas	1986-2015	0.0	0.0	0.6	6.4	36.9	23.6	25.3	7.2
Sho	1956-1985	0.0	0.0	2.8	24.2	31.4	16.1	23.3	2.2
Sho	1956-2015	0.1	0.1	2.2	27.1	26.9	17.2	25.0	1.3
Sho	1986-2015	0.3	0.3	1.7	30.0	22.5	18.3	26.7	0.3
Step	1956-1985	0.0	0.0	0.6	9.2	50.6	24.4	12.8	2.5
Step	1956-2015	0.0	0.0	0.3	9.7	48.2	23.8	14.6	3.5
Step	1986-2015	0.0	0.0	0.0	10.3	45.8	23.1	16.4	4.4
Tian	1956-1985	0.0	0.0	0.0	11.7	34.4	19.7	29.2	5.0
Tian	1956-2015	0.0	0.0	0.0	10.1	34.3	22.1	27.6	5.8
Tian	1986-2015	0.0	0.0	0.0	8.6	34.2	24.4	26.1	6.7

Annex 8. Year day number of HCI various categories at 13 locations of Georgia in 1956-1985, 1956-2015 and 1986-2015.

Location	Year	V_Unf.	Unf.	Marg.	Accept.	Good	V_Good	Excell.	Ideal	Marg.-Ideal
Bakh	1956-1985	4	9	37	109	108	82	15	2	352
Bakh	1956-2015	4	12	34	106	109	76	22	3	349
Bakh	1986-2015	4	15	31	102	110	70	28	4	346
Bak	1956-1985	0	0	4	84	130	79	58	10	365
Bak	1956-2015	0	0	3	85	125	71	68	13	365
Bak	1986-2015	0	0	2	85	121	63	78	16	365
Borj	1956-1985	0	0	1	42	120	87	109	7	365
Borj	1956-2015	0	0	1	45	113	102	94	10	365
Borj	1986-2015	0	0	0	49	107	118	80	12	365
God	1956-1985	3	8	43	144	111	45	12	0	354
God	1956-2015	5	9	45	140	106	43	17	1	351
God	1986-2015	7	10	47	136	101	41	21	2	348
Gud	1956-1985	1	7	25	122	136	62	12	0	357
Gud	1956-2015	1	5	28	112	131	67	20	1	359
Gud	1986-2015	1	3	31	101	126	73	28	1	361
Kha	1956-1985	0	4	15	32	100	83	113	17	361
Kha	1956-2015	1	3	13	50	91	87	107	14	362
Kha	1986-2015	1	2	11	67	82	90	101	10	362
Khu	1956-1985	1	5	19	50	86	64	127	13	359
Khu	1956-2015	1	7	22	45	89	68	117	16	357
Khu	1986-2015	1	9	25	41	91	72	108	18	355
Lent	1956-1985	0	7	16	49	98	94	94	6	358
Lent	1956-2015	1	5	16	72	90	97	81	4	360
Lent	1986-2015	1	3	16	95	81	99	68	1	361
Mest	1956-1985	0	0	2	79	108	51	111	15	365
Mest	1956-2015	0	1	4	94	90	60	107	10	365
Mest	1986-2015	0	1	5	110	72	70	103	4	364
Pas	1956-1985	0	0	3	32	135	63	115	17	365
Pas	1956-2015	0	0	3	28	135	75	103	22	365
Pas	1986-2015	0	0	2	23	135	86	92	26	365
Sho	1956-1985	0	0	10	88	115	59	85	8	365
Sho	1956-2015	1	1	8	99	98	63	91	5	364
Sho	1986-2015	1	1	6	110	82	67	97	1	363
Step	1956-1985	0	0	2	33	185	89	47	9	365
Step	1956-2015	0	0	1	36	176	87	53	13	365
Step	1986-2015	0	0	0	38	167	84	60	16	365
Tian	1956-1985	0	0	0	43	126	72	107	18	365
Tian	1956-2015	0	0	0	37	125	81	101	21	365
Tian	1986-2015	0	0	0	31	125	89	95	24	365

Conclusion

It is planned in future to continue the climatic resources study of various regions of Georgia for tourism, recreation and treatment (mapping the territory on HCI and TCI, long-term forecasting of HCI and TCI, determining other modern climatic and bioclimatic indicators for tourism, recreation and treatment, assessing the adequacy of bioclimatic indicators scales to human health, etc.).

References

[1] Abegg B. Klimaanderung und Tourismus. Zurich: Schlussbericht NFP 31. vdfHochschulverlag AG ander ETH, 1996.

[2] Matzarakis A. Weather - and Climate-Related Information for Tourism. Tourism and Hospitality Planning & Development, August, 2006, vol. 3, No. 2, pp. 99–115.

[3] Matzarakis A., Cheval S., Lin T.-P., Potchter, O. Challenges in Applied Human Biometeorology. Atmosphere 2021, 12, 296. https://doi.org/10.3390/atmos12030296

[4] Amiranashvili A.G., Chikhladze V.A. Saakashvili N.M., Tabidze M.Sh., Tarkhan-Mouravi I.D. Bioclimatic Characteristics of Recreational Zones – Important Component of the Passport of the Health Resort – Tourist Potential of Georgia. Trans. of the Institute of Hydrometeorology at the Georgian Technical University, vol. 117, ISSN 1512-0902, 2011c, pp. 89-92.

[5] Kartvelishvili L., Matzarakis A., Amiranashvili A., Kutaladze N. Assessment of Touristical-Recreation Potential of Georgia on Background Regional Climate Change. Proc. of IIst Int. Scientific-Practical Conference "Tourism: Economics and Business", June 4-5, Batumi, Georgia, 2011, pp. 250-252.

[6] Rutty M., Steiger R., O. Demiroglu O.C., Perkins D.R. Tourism Climatology: Past, Present, and Future. Int. Journ. of. Biometeorology. Published online: 08 January 2021. https://doi.org/10.1007/s00484-020-02070-0

[7] Matzarakis A., Cheval S., Lin T.-P., Potchter O. Challenges in Applied Human Biometeorology. Atmosphere 2021, *12*, 296. https:// doi.org/10.3390/atmos12030296

[8] Ma S., Craig Ch. A., Feng S. Camping Climate Resources: the Camping Climate Index in the United States. Current Issues in Tourism, 24:18, 2021, 2523-2531, DOI:10.1080/13683500.2020.1846503

[9] Mieczkowski Z. The Tourism Climate Index: A Method for Evaluating World Climates for Tourism. The Canadian Geographer 1985, N 29, pp. 220-233.

[10] Amiranashvili A., Matzarakis A., Kartvelishvili L. Tourism Climate Index in Tbilisi. Trans. of the Institute of Hydrometeorology, ISSN 1512-0902, Tbilisi, 18 – 19 November, 2008, vol. 115, pp. 27 - 30.

[11] Amiranashvili, A., Chargazia, Kh., Matzarakis, A. Comparative Characteristics of the Tourism Climate Index in the South Caucasus Countries Capitals (Baku, Tbilisi, Yerevan). Journal of the Georgian Geophysical Society, ISSN: 1512-1127, Issue (B). Physics of Atmosphere, Ocean, and Space Plasma, 2014, vol.17B, pp. 14-25.

[12] Amiranashvili A., Chargazia Kh., Matzarakis A., Kartvelishvili L. Tourism Climate Index in the Coastal and Mountain Locality of Adjara, Georgia. International Scientific Conference "Sustainable Mountain Regions: Make Them Work". Proceedings, Borovets, Bulgaria, ISBN 978-954-411-220-2, 14-16 May,2015, pp. 238-244, http://geography.bg/MountainRegions_Sofia2015

[13] Rybak O. O., Rybak E. A. Application of Climatic Indices for Evaluation of Regional Differences in Tourist Attractiveness. Nauchnyy zhurnal KubGAU, №121(07), 2016, 24 p., http://ej.kubagro.ru/2016/07/pdf/16.pdf

[14] Amiranashvili A.G., Japaridze N.D., Kartvelishvili L.G., Khazaradze K.R., Matzarakis A., Povolotskaya N.P., Senik I.A. Tourism Climate Index of in the Some Regions of Georgia and North Caucasus. Journal of the Georgian Geophysical Society, ISSN: 1512-1127, Issue (B). Physics of Atmosphere, Ocean, and Space Plasma, 2017, vol.20B, pp. 43-64.

[15] Amiranashvili A.G., Japaridze N.D., Kartvelishvili L.G., Khazaradze K.R., Kurdashvili L.R. Tourism Climate Index in Kutaisi (Georgia). International Scientific Conference „Modern Problems of Ecology", Proceedings, ISSN 1512-1976, v. 6, Kutaisi, Georgia, 21-22 September, 2018, pp. 227-230.

[16] Amiranashvili A.G., Kartvelishvili L.G., Matzarakis A., Megrelidze L.D. The Statistical Characteristics of Tourism Climate Index in Kakheti (Georgia). Journal of the Georgian Geophysical Society, ISSN: 1512-1127, Physics of Solid Earth, Atmosphere, Ocean and Space Plasma, v. 21(2), Tbilisi, 2018, pp. 95-112.

[17] Amiranashvili A., Kartvelishvili L. Statistical Characteristics of the Monthly Mean Values of Tourism Climate Index in Mestia (Georgia) in 1961-2010. Journal of the Georgian Geophysical Society, ISSN: 1512-1127, Physics of Solid Earth, Atmosphere, Ocean and Space Plasma, v. 22(2), 2019, pp. 68–79.

[18] Kartvelishvili L., Amiranashvili A., Megrelidze L., Kurdashvili L. Turistul Rekreaciuli Resursebis Shefaseba Klimatis Cvlilebebis Fonze. Publish Hous "Mtsignobari", ISBN 978-9941-485-01-5, Tbilisi, 2019, 161 p., (in Georgian). http://217.147.235.82/bitstream/1234/293074/1/turistulRekreaciuliResursebisShefasebaKlimatisCvlilebebisFonze.pdf.

[19] Mushawemhuka W.J., Fitchett J.M., Hoogendoorn G. Towards Quantifying Climate Suitability for Zimbabwean Nature-Based Tourism. South African Geographical Journal, 2020, DOI: 10.1080/03736245.2020.1835703

[20] Tanana, A. B. et al. Confort climático en la Argentina: un recurso intangible para el turismo. Cuadernos Geográficos 60*(3)*, 2021, pp. 52-72.

[21] Scott D., Rutty M., Amelung B., Tang M. An Inter-Comparison of the Holiday Climate Index (HCI) and the Tourism Climate Index (TCI) in Europe. Atmosphere 7, 80, 2016, 17 p., doi:10.3390/atmos7060080www.

[22] Javan K. Comparison of Holiday Climate Index (HCI) and Tourism Climate Index (TCI) in Urmia. Physical Geography Research Quarteli. vol. 49, iss. 3, 2017, pp. 423-439.

[23] Yu D. D., Rutty M., Scott D., Li S. A Comparison of the Holiday Climate Index: Beach and the Tourism Climate Index Across Coastal Destinations in China International Journal of Biometeorology, 2020, https://doi.org/10.1007/s00484-020-01979-w, 8 p.

[24] Rutty M., Scott D., Matthews L., Burrowes R., Trotman A., Mahon R., Charles A. An Inter-Comparison of the Holiday Climate Index (HCI: Beach) and the Tourism Climate Index (TCI) to Explain Canadian Tourism Arrivals to the Caribbean. Atmosphere 2020, 11, 412.

[25] Hejazizadeh Z., Karbalaee A., Hosseini S.A., Tabatabaei S.A. Comparison of the Holiday Climate Index (HCI) and the Tourism Climate Index (TCI) in Desert Regions and Makran Coasts of Iran. Arab. J. Geosci. 12, 803, 2019, https://doi.org/10.1007/s12517-019-4997-5

[26] Amiranashvili A., Kartvelishvili L., Matzarakis A. Comparison of the Holiday Climate Index (HCI) and the Tourism Climate Index (TCI) in Tbilisi. Int. Sc. Conf. „Modern Problems of Ecology“, Proc., ISSN 1512-1976, v. 7, Tbilisi-Telavi, Georgia, 26-28 September, 2020, pp. 424-427.

[27] Amiranashvili A.G., Kartvelishvili L.G. Holiday Climate Index in Kakheti (Georgia). Journal of the Georgian Geophysical Society, e-ISSN: 2667-9973, p-ISSN: 1512-1127, Physics of Solid Earth, Atmosphere, Ocean and Space Plasma, v. 24(1), 2021, pp. 44-62.

[28] Amiranashvili A., Povolotskaya N., Senik I. Comparative Analysis of the Tourism Climate Index and the Holiday Climate Index in the North Caucasus.Transactions of Mikheil Nodia Institute of Geophysics, ISSN 1512-1135, vol. LXXIII, 2021, pp. 96-113, (in Russian).

[29] Williams D. An Examination of the Tourism Holiday Climate Index (HCI: Urban) in Tokyo 1964-2019. Josai International University Bulletin, Vol. 29, No. 6, March 2021, p. 1-31. https://www.researchgate.net/publication/352436593

[30] Carrillo J., González A., Pérez J. C., Expósito F. J., Díaz, J. P. Impact of Climate Change on the Future of Tourism Areas in the Canary Islands, EGU General Assembly 2021, online, 19–30 Apr 2021, EGU21-11981, https://doi.org/10.5194/egusphere-egu21-11981, 2021.

[31] Araci S.F. S., Demiroglu O. C., Pacal A., Hall C. M., Kurnaz, M. L. Future Holiday Climate Index (HCI) Performances of Urban and Beach Destinations in the Mediterranean. EGU General Assembly 2021, online, 19–30 Apr 2021, EGU21-13217, https://doi.org/10.5194/egusphere-egu21-13217, 2021.

[32] Amiranashvili A., Kartvelishvili L., Matzarakis A. Changeability of the Holiday Climate Index (HCI) in Tbilisi. Transactions of Mikheil Nodia Institute of Geophysics, ISSN 1512-1135, vol. LXXII, 2020, pp. 131-139.

[33] Fourth National Communication of Georgia. Under the United Nations Framework Convention on Climate Change. Tbilisi, 2021, pp. 333-339. https://unfccc.int/sites/default/files/resource/4%20Final%20Report%20-%20English%202020%2030.03_0.pdf

[34] Amiranashvili A.G., Kartvelishvili L.G., Kutaladze N.B., Megrelidze L.D., Tatishvili M.R. Changeability of the Meteorological Parameters Associated with Holiday Climate Index in Different Mountainous Regions of Georgia in 1956-2915. Journal of the Georgian Geophysical Society, e-ISSN: 2667-9973, p-ISSN: 1512-1127, Physics of Solid Earth, Atmosphere, Ocean and Space Plasma, v. 24(2), 2021, pp. 78-91.

[35] Kobisheva N., Narovlianski G. Climatological Processing of the Meteorological Information, Leningrad, Gidrometeoizdat, 1978, 294 p., (in Russian).

დასვენების კლიმატური ინდექსი საქართველოს ზოგიერთ მთიან რეგიონში

ა. ამირანაშვილი, ლ. ქართველიშვიი, ნ. კუტალაძე,
ლ. მეგრელიშვილი, მ. ტატიშვილი

რეზიუმე

წინამდებარე ნაშრომში წარმოდგენილია მონაცემები დასვენების კლიმატური ინდექსის (დკი) მრავალწლიანი საშუალო თვიური მნიშვნელობების შესახებ საქართველოს 13 მთიანი რეგიონისთვის (ბახმარო, ბაკურიანი, ბორჯომი, გოდერძი, გუდაური, ხაიში, ხულო, ლენტეხი, მესტია, ფასანაური, შოვი, სტეფანწმინდა, თიანეთი). ჩატარდა დკი-ს ყოველთვიური, სეზონური და წლიური მნიშვნელობების დეტალური ანალიზი 60 წლიანი პერიოდისთვის (1956-2015 წწ.). საქართველოს სამი პუნქტისთვის (გოდერძი, ხულო და მესტია) 1961 წ. 2010 წ. მონაცემების მიხედვით, ჩატარდა დკი-ს და ტურიზმის კლიმატური ინდექსის ყოველთვიური მნიშვნელობების შედარება. შესწავლილი იქნა დკი-ს ცვალებადობა 1986-2015 წწ.-ში 1956-1985 წწ.-თან შედარებით და ასევე გამოკვლეულ იქნა დკი-ს ტრენდები 1956-2015 წწ.-ში. მესტიის მაგალითზე შეფასდა დკი-ს ყოველთვიური, სეზონური და წლიური მნიშვნელობების მოსალოდნელი ცვლილებები 2041-2070 და 2071-2100 წწ-ში.

Климатический индекс отдыха в некоторых горных районах Грузии

**А.Г. Амиранашвили, Л. Г. Картвелишвили, Н.Б. Куталадзе,
Л.Д. Мегрелидзе, М.Р. Татишвили**

Резюме

Представлены данные о многолетних среднемесячных значениях климатического индекса отдыха (КИО) для 13 горных районов Грузии (Бахмаро, Бакуриани, Боржоми, Годердзи, Гудаури, Хаиши, Хуло, Лентехи, Местия, Пасанаури, Шови, Степанцминда, Тианети). Проведен подробный анализ месячных, сезонных и годовых значений КИО за 60-летний период (1956-2015 гг.). Проведено сравнение месячных значений КИО и Климатического Индекса Туризма для трех пунктов Грузии (Годердзи, Хуло и Местия) по данным с 1961 по 2010 гг. Изучена изменчивость КИО в 1986-2015 гг. по сравнению с 1956-1985 гг., а также исследованы тренды значений КИО в 1956-2015 гг. На примере Местия сделана оценка ожидаемых изменений месячных, сезонных и годовых значений КИО к 2041-2070 и 2071-2100 гг.

Journal of the Georgian Geophysical Society, e-ISSN: 2667-9973, p-ISSN: 1512-1127
Physics of Solid Earth, Atmosphere, Ocean and Space Plasma, v. 24(2), 2021, pp. 118 - 122

Climatic Features of the Resort

Nana M. Berdzenishvili

Iakob Gogebashvili Telavi State University, Georgia
nana.berdzenishvili@tesau.edu.ge

ABSTRACT

The article considers the resort climatic resources of Imereti. The main climatic characteristics of the Resorts are determined and a map of the resorts and resort areas of Imereti is developed. The thermal characteristics of summer and winter are given in accordance with the classification of Kaygorodov. The spa and curative factors of the main resorts are considered. The physicochemical properties of water, their composition and medicinal properties are indicated. In article resort climatic resources of Imereti are considered. The attention that in the world isn't a lot of places where in rather small territory so many various landscapes are located is focused: from damp subtropics, to the Alpine mountain meadows. It is proved that a relief of mountain landscapes, the coast of the Black Sea, Mineral water and climate – a natural basis of development of resort economy of the region.

Keywords*: Imereti; climate; spa resort; spa climatic resort; national; local; Tskaltubo; Sairme.*

Introduction.

Nature generously endowed Georgia. There are not many places around the world where a relatively small area has so many diverse landscapes - from humid subtropics to alpine meadows. Georgia is a resort country. The relief of mountain landscapes, the Black Sea coast, mineral waters form the basis of a wide resort construction. The basis of the resort factor is its air (climate). Due to the confluence of mountain and sea air, climatic conditions are distinguished by high spa-healing properties and are used for general healing and treatment of various diseases [1,3,5,9,10, etc.].

Due to the unusually diverse climatic and balneological resources of different origin and medical use, more than 100 resorts function in Georgia [1,11-21]. Almost all types of mineral waters are found in Georgia. There are about 2000 sources. The richness of mineral waters and their diversity makes it possible to rehabilitation, as well as the treatment and prevention of cardiovascular and nervous ailments, diseases of the digestive and endocrine systems, musculoskeletal system [1].

The most common are carbon dioxide mineral waters. These waters are used to treat the gastrointestinal tract, liver, and some urological, neurological, and other diseases. Georgian resort resources are redistributed in its various regions, including Imereti [2,3]. Imereti is located in the central part of Georgia (in Western Georgia) at a distance of several tens of kilometers from the Black Sea. Imereti region is rich in resort-climatic resources. Resorts and resort areas are located in different areas of the region. Each of the resorts has its own specialization and features of functioning. This article systematizes the resorts of Imereti.

Brief description of problem statement.

Fig. 1 shows a map of the location of resorts and resort areas of Imereti, which shows that Imereti is a fairly rich region with both resort and climatic resources and resort territories. This creates a sustainable basis for tourism development.

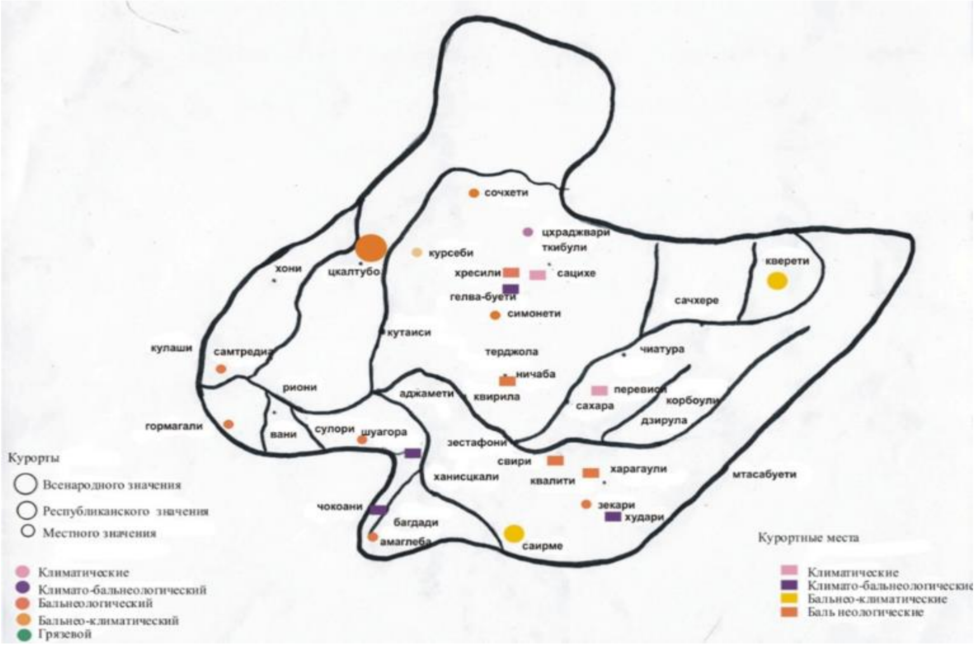

Fig. 1. Resort resources of Imereti.

Table 1 presents a list of Imereti resorts with their status (international, state, local), altitude, profile (balneological, climatic) and basic climate characteristics.

Table 1. Climatic characteristics of the resorts of Imereti [11].

Resorts (status)	Height, a.s.l , m	Profile	Air temperature, ^{0}C			Absolute humidity		Mean annual humidity	Precipitation, mm			Wind, m/s
			Jan	Jul	Year	Jan	Jul		Year	Warm	Cold	
Tskaltubo (international)	120	B	5,3	23,3	73	6,4	22,2	4,7	1818	987	831	1,6
Samtredia (local)	25	B	4,7	23,2	76	6,6	22,3	4,7	1526	746	780	2,8
Gormagala (local)	200	B	4,7	23,2	74	6,5	22,2	4,6	1526	746	780	4,3
Sairme (state)	950	C-B	-0,3	17,4	80	4,8	16,9	3,9	1165	543	629	1,1
Zekari (local)	650	B	1,5	19,0	77	4,5	16,0	4,0	1157	550	608	1,2
Sulori (local)	200	B	3,0	22,0	74	6,5	21,0	4,0	1350	650	700	2,5
Coursevi (local)	350	B-C	2,6	21,0	72	5,4	19,2	4,5	2137	1183	954	2,8
Simoneti (state significance)	300	B	2,5	22,5	73	6,1	20,5	4,2	1185	620	565	2,2
Quereti (local)	750	B-C	0,4	22,3	76	5,6	18,8	4,2	904	454	450	1,8
Nunisi (local)	920	B	-0,3	19,0	75	4,8	17,5	4,3	1185	680	505	2,0
Note	Б: Balneological; C-B: Climatic- Balneological; B-C: Balneo-Climatic											

To characterize the thermal conditions of summer and winter in the resorts, Kaigorodov [8], developed the classification presented in Table 2. This classification was successfully used at the Institute of Balneology and Physiotherapy of Georgia in the medical-climatic classification of resorts [8]. In characterizing the climatic resources of resorts in the Imereti region, we are also based on this classification.

In accordance with tables 1 and 2, we can conclude that in the resorts of Imereti, winters are mostly mild and moderately mild, and summers are warm and very warm.

Table 2. Thermal characteristics of winter and summer according to Kaygorodov [8].

Winter	Temperature gradation, ^0C	Summer	Temperature gradation,^0C
Tough	-38 -31	Moderately cool	10 – 14
Very cold	-31-24	Moderately warm	14 – 18
Cold	-24 -17	Warm	18 – 22
Moderately cold	-17-10	Very warm	22 – 26
Moderately warm	-10 -3	Roast	26 – 30
Soft	3 -4	Very hot	30 – 34
Very soft	4 -10		

Consider the main healing factors of resorts

Tskaltubo is a spa resort in Imereti Region, in west-central Georgia. Tskaltubo holds the status of balneological resort. It is famous for its radon-carbonate mineral springs, whose natural temperature enables the water to be used without preliminary heating.The resort's focus is on balneotherapy for circulatory, nervous, musculo-skeletal, gynaecological and skin diseases. Tskaltubo is a resort of international importance which, functions since 1926. It is rich in unique healing radon-, nitrogen-, chloride-hydrocarbonate-sulfate water, which has fairly stable physico-chemical properties. Mineral water, with a temperature of 33-35 ℃, is used for baths, inhalations and sprays.

Treatment at the resort is indicated for diseases of the musculoskeletal system, neurological, cardiovascular and gynecological diseases. The healing season lasts all year round, which, first of all, is facilitated by the climatic conditions of Tskhaltubo. The healing factor is also the microclimate of karst caves, which has a good effect on the treatment of hypertension, bronchial asthma, neurosis and other diseases.

Sairme is a balneo-climatic resort of national importance. It is located in Baghdat district, 25 km south-west of the district center and 55 km south of Kutaisi, on the northern slope of the Meskhet ridge, at an altitude of 950 m above sea level in the Tsablaritskali gorge. The surrounding slopes are covered with deciduous and coniferous forests. The average annual temperature is + 8,5 ℃. Winter is warm and not snowy. The average January temperature is -10 C. Summer is moderately warm and moderately humid. The average temperature in August is +17 ℃. The average annual rainfall exceeds 900 mm. The average annual humidity is 75-80%. In summer, mountain-valley winds are frequent, which provides sufficient ventilation.

Zekari is a local balneological resort located in Baghdat district, 35 km from the regional center, on the northern slope of the Adzhara-Imereti ridge, at an altitude of 750-780 m above sea level, in the gorge of the Hanitskali River. Therapeutic indicators: chronic arthritis, gynecological diseases, cardiovascular diseases, nephritis and functional diseases of the nervous system.

Kvereti is a low-mountain balneoclimatic resort of local importance in the Sachkhere district. Located at an altitude of 550 m above sea level. It is characterized by moderately warm and mild winters (average January temperature + 2-3 ℃), and warm, moderately humid summers (average July temperature 20 ℃). The amount of average annual precipitation is 1100-1200 mm. The main therapeutic factor of the resort is low-hydrogen sulfide mineral water, the temperature of which is 16 °C. The diseases of the peripheral nervous system, joints and gynecological diseases are treated. It functions during the whole year.

Nunisi is a balneo-climatic resort of local importance. Located 25 km from the railway, in the Kharagaul district at an altitude of 920 m above sea level. The healing factor's mineral water with weakly mineralized warm sulfur and its temperature is 27-28 ℃ and mountain air. It is recommended for the treatment of the following diseases - skin (neurodermatitis, eczema, psoriasis), motor organs, peripheral nervous systems, anemia. The season lasts from May to October.

Samtredia is a local balneological resort. Located in the city of Samtredia. Therapeutic indicators: diseases of the musculoskeletal systems, diseases of the chronically peripheral nervous system, skin ailments (lesions) and hypertension.

Amagleba is a balneological resort. Located near the Van district off the left bank of the Rioni River. Insulated mineral waters contain sodium, chlorine, carbon dioxide and flint. Therapeutic indicators: chronic arthritis.

Sulori is a local balneological resort. Located on the slopes of Adjar-Meskheti ridge, 10 km from Vani. Sulori mineral waters are similar in chemical composition and physical properties to Tskaltubo mineral waters.

At the same time, bromine salt was found in the chemical composition of the resort's water, which has a calming effect on the nervous system. Its best properties are natural radioactivity and natural temperature.

Simoneti is a balneological resort of national importance. Located in Terjol district. Mineral hot water is characteristic. Therapeutic indicators: diseases of the musculoskeletal system, chronic acute arthritis, metabolic disorders, cardiovascular diseases.

Kursebi is a balneological resort. Located 23 km from Tkibuli. The main healing factor of the resort is highly mineralized hydrogen sulfide mineral water, which is used for medicinal purposes in bath of Vani.

Conclusion

Thus, Georgia, however, has not yet fully tapped its potential to promote sustainable tourism in promising regions, such as Imereti, or transform the economy through investment in tourism and agriculture supply chains for both export and import substitution. There is also a need for skills development in order to provide the skilled labor needed for a growing economy and increased productivity. The proposed tourism development vision for the region envisages developing Imereti as a high quality geo-tourism destination throughout the year through attracting domestic and international tourists.

References

[1] Atlas. Resorts and resort resources of Georgia. Moscow, 1989.
[2] Berdzenishvili N. M. “Climatic resources of the Imereti region”, 2012.
[3] Javakhishvili S. Climatography of the Georgian SSR. Tbilisi, 1977 .
[4] Climatic and agroclimatic atlas of Georgia. Tbilisi, 2011.
[5] Climate and climate resources of Georgia. Leningrad, 1971.
[6] Scientific-applied reference on the climate of the USSR. Series 3, parts 1-6, issue 14. Leningrad., 1990.
[7] Handbook of the climate of the USSR. Issue 14. P 1-5. Leningrad., 1967-1972.
[8] Ushveridze G.A., Elizbarashvili E.Sh., Gongladze N.Sh. The scheme of medical and climatic typification of resorts. Tbilisi, 1981.
[9] Elizbarashvili E.Sh. Climatic resources of Georgia. Tbilisi, 2007.
[10] Elizbarashvili E.Sh. The climate of Georgia. Tbilisi, 2017.
[11] Elizbarashvili E.Sh., Gongladze N.Sh. Climatography of Georgian resorts. Tbilisi, 1980.
[12] Saakashvili N.M., Tabidze M.Sh., Tarkhan-Mouravi I.D., Amiranashvili A.G., Melikadze G.I., Chikhladze V.A. To a Question about the Certification of the Health Resort and Tourist Resources of Georgia. “Modern Problems of Using of Health Resort Resources”, Collection of Scientific Works of International Conference, Sairme, Georgia, June 10-13, 2010, ISBN 978-9941-0-2529-7, Tbilisi, 2010, pp. 175-180, (in Russian).
[13] Amiranashvili A.G., Chikhladze V.A. Saakashvili N.M., Tabidze M.Sh., Tarkhan-Mouravi I.D. Bioclimatic Characteristics of Recreational Zones – Important Component of the Passport of the Health Resort – Tourist Potential of Georgia, Pressing Problems in Hydrometeorology and Ecology, Papers of the Int. Conf. Dedicated to the 90th Anniversary of Academician G. Svanidze, September 27-29, Tbilisi, 2011, Trans. of the Institute of Hydrometeorology at the Georgian Technical University, vol. 117, ISSN 1512-0902, Tbilisi, 2011, pp. 89-92.
[14] Amiranashvili A.G., Bliadze T.G., Melikadze G.I., Tarkhan-Mouravi I.D., Chikhladze V.A. Content of Light Aeroions as the Factor of the Air Purity of Some Health Resorts of Georgia. “Modern Problems of Using of Health Resort Resources”, Collection of Scientific Works of International Conference, Sairme, Georgia, June 10-13, 2010, ISBN 978-9941-0-2529-7, Tbilisi, 2010, pp. 145-151, (in Russian).
[15] Kartvelishvili L., Matzarakis A., Amiranashvili A., Kutaladze N. Assessment of touristical-recreation potential of Georgia on background regional climate change, Proc. of IIst International Scientific-Practical Conference “TOURISM: ECONOMICS AND BUSINESS”, June 4-5, Batumi, Georgia, 2011, pp. 250-252.
[16] Amiranashvili A.G., Japaridze N.D., Kartvelishvili L.G., Khazaradze K.R., Matzarakis A., Povolotskaya N.P., Senik I.A. Tourism Climate Index of in the Some Regions of Georgia and North Caucasus. Journal of the Georgian Geophysical Society, Issue B. Physics of Atmosphere, Ocean and Space Plasma, v. 20B, 2017, pp. 43–64.
[17] ქართველიშვილი ლ., ამირანაშვილი ა., მეგრელიძე ლ., ქურდაშვილი ლ. ტურისტულ-რეკრეაციული რესურსების შეფასება კლიმატის ცვლილების ფონზე. გამომცემლობა "მწიგნობარი", ISBN 978-9941-485-01-5, თბილისი, 2019, 161 გვ.

http://dspace.nplg.gov.ge/bitstream/1234/293074/1/turistulRekreaciuliResursebisShefasebaKlimatisCvlilebebisFonze.pdf
[18] Amiranashvili A., Kartvelishvili L., Matzarakis A. Comparison of the Holiday Climate Index (HCI) and the Tourism Climate Index (TCI) in Tbilisi. Int. Sc. Conf. „Modern Problems of Ecology", Proc., ISSN 1512-1976, v. 7, Tbilisi-Telavi, Georgia, 26-28 September, 2020, pp. 424-427.
[19] Amiranashvili A.G., Kartvelishvili L.G. Holiday Climate Index in Kakheti (Georgia). Journal of the Georgian Geophysical Society, e-ISSN: 2667-9973, p-ISSN: 1512-1127, Physics of Solid Earth, Atmosphere, Ocean and Space Plasma, v. 24(1), 2021, pp. 44-62.
[20] Lanchava O. A., Iliashi N., Radu S., Tsikarishvili K., Lezhava Z., Amiranashvili A., Chikhladze V., Asanidze L. წყალტუბოს (დასავლეთი საქართველო) „თეთრა მღვიმის" პრაქტიკული სარგებლიანობის პოტენციალი. GEORGIAN SCIENTISTS, 2021, 15 p.
Retrieved from https://journals.4science.ge/index.php/GS/article/view/285
[21] Amiranashvili A.G., Kartvelishvili L.G., Kutaladze N.B., Megrelidze L.D., Tatishvili M.R. Holiday Climate Index in Some Mountainous Regions of Georgia. Journal of the Georgian Geophysical Society, e-ISSN: 2667-9973, p-ISSN: 1512-1127, Physics of Solid Earth, Atmosphere, Ocean and Space Plasma, v. 24(2), 2021, pp. 92 – 117.

კურორტების კლიმატური თავისებურებანი

ნ. ბერძენიშვილი

რეზიუმე

სტატიაში განხილულია იმერეთის საკურორტო კლიმატური რესურსები. განსაზღვრულია კურორტების ძირითადი კლიმატური მახასიათებლები და შემუშავებულია იმერეთის კურორტებისა და საკურორტო ზონების რუკა. ზაფხულისა და ზამთრის თერმული მახასიათებლები მოცემულია კაიგოროდოვის კლასიფიკაციის მიხედვით. განიხილება ძირითადი კურორტების სპა და სამკურნალო ფაქტორები. მითითებულია წყლის ფიზიკურ-ქიმიური თვისებები, მათი შემადგენლობა და სამკურნალო თვისებები. სტატიაში განხილულია იმერეთის საკურორტო კლიმატური რესურსები. ყურადღება გამახვილებულია იმაზე, რომ მსოფლიოში არც თუ ისე ბევრი ადგილია, სადაც საკმაოდ მცირე ტერიტორიაზეა განლაგებული ამდენი სხვადასხვა პეიზაჟი: ნესტიანი სუბტროპიკებიდან, ალპური მთის მდელოებამდე. დადასტურებულია, რომ მთის ლანდშაფტების რელიეფი, შავი ზღვის სანაპირო, მინერალური წყალი და კლიმატი რეგიონის საკურორტო მეურნეობის განვითარების ბუნებრივი საფუძველია.

Климатические особенности курорта

Н.М. Бердзенишвили

Резюме

В статье рассмотрены курортные климатические ресурсы Имерети. Определены основные климатические характеристики курортов и разработана картосхема курортов и курортных местностей Имерети. Дана термическая характеристика лета и зимы в соответствии с классификацией Кайгородова. Рассмотрены курортные и лечебные факторы главных курортов. Указаны физико-химические свойства вод, их состав и лечебные свойства. Природа щедро одарила Грузию. Во всём мире не так много мест, где сравнительно на небольшой территории расположено столько разнообразных ландшафтов – от влажных субтропиков до альпийских высокогорных лугов. Рельеф горных ландшафтов, побережье Чёрного моря, минеральные воды формируют основу широкого курортного строительства.

Information for contributors

Papers intended for the Journal should be submitted in two copies to the Editor-in-Chief. Papers from countries that have a member on the Editorial Board should normally be submitted through that member. The address will be found on the inside front cover.

1. Papers should be written in the concise form. Occasionally long papers, particularly those of a review nature (not exceeding 16 printed pages), will be accepted. Short reports should be written in the most concise form not exceeding 6 printed pages. It is desirable to submit a copy of paper on a diskette.
2. A brief, concise abstract in English is required at the beginning of all papers in Russian and in Georgian at the end of them.
3. Line drawings should include all relevant details. All lettering, graph lines and points on graphs should be sufficiently large and bold to permit reproduction when the diagram has been reduced to a size suitable for inclusion in the Journal.
4. Each figure must be provided with an adequate caption.
5. Figure Captions and table headings should be provided on a separate sheet.
6. Page should be 20 x 28 cm. Large or long tables should be typed on continuing sheets.
7. References should be given in the standard form to be found in this Journal.
8. All copy (including tables, references and figure captions) must be double spaced with wide margins, and all pages must be numbered consecutively.
9. Both System of units in GGS and SI are permitted in manuscript
10. Each manuscript should include the components, which should be presented in the order following as follows:
    Title, name, affiliation and complete postal address of each author and dateline.
    The text should be divided into sections, each with a separate heading or numbered consecutively.
    Acknowledgements. Appendix. Reference.
11. The editors will supply the date of receipt of the manuscript.

CONTENTS - სარჩევი

საქართველოს გეოფიზიკური საზოგადოების ჟურნალი

მყარი დედამიწის, ატმოსფეროს, ოკეანისა და კოსმოსური პლაზმის ფიზიკა

ტომი 24 , № 2

ჟურნალი იბეჭდება საქართველოს გეოფიზიკური საზოგადოების პრეზიდიუმის დადგენილების საფუძველზე

ტირაჟი 30 ცალი

JOURNAL OF THE GEORGIAN GEOPHYSICAL SOCIETY

Physics of Solid Earth, Atmosphere, Ocean and Space Plasma

Vol. 24, № 2

Printed by the decision of the Georgian Geophysical Society Board

Circulation 30 copies

ЖУРНАЛ ГРУЗИНСКОГО ГЕОФИЗИЧЕСКОГО ОБЩЕСТВА

Физика Твердой Земли, Атмосферы, Океана и Космической Плазмы

Том 24, № 2

Журнал печатается по постановлению президиума Грузинского геофизического общества

Тираж 30 экз

Tbilisi-თბილისი-Тбилиси
2021